UNIVERSITY OF SOUTHAMPTON

FACULTY OF MEDICINE

Cancer Sciences Unit

Integrin αvβ6: Expression and Function in Head and Neck Cancer

By

Karwan A. Moutasim

Thesis for the degree of Doctor of Philosophy

October 2011

UNIVERSITY OF SOUTHAMPTON
ABSTRACT

FACULTY OF MEDICINE
CANCER SCIENCES UNIT

Doctor of Philosophy

Integrin αvβ6: expression and function in head and neck cancer
By Karwan A. Moutasim

αvβ6 integrin is a heterodimeric cell surface receptor expressed exclusively by epithelial cells in humans. It is generally undetectable in healthy tissues, but is upregulated during tissue remodelling, including wound healing. Increasingly, expression of the integrin has been reported in a number of solid tumours and fibrotic disorders. In this thesis, we first examined the expression and function of αvβ6 in a number of pathogenic states of the head and neck. We then attempted to study some of the mechanisms behind the regulation of the integrin's expression.

Oral submucous fibrosis (OSF) is a fibrotic condition of the upper aerodigestive tract with a high malignant potential. We found that αvβ6 was highly expressed in over 50% of OSF cases. *In vitro* studies showed that the betel quid alkaloid arecoline modulated αvβ6 expression through the muscarinic receptor pathway. αvβ6 activated TGF-β1, promoting fibroblast to myofibroblast transdifferentiation and promoting fibrosis. *In vivo*, the majority OSF cases that had transformed to oral squamous cell carcinoma (OSCC) showed high αvβ6 expression.

We next examined αvβ6 expression in nodular and morphoeic basal cell carcinoma (BCC), and found that the integrin was expressed in high levels in the more aggressive morphoeic variant, but at lower levels in nodular BCC. This expression correlated inversely with that of the Sonic Hedgehog signaling molecule Gli1. *In vitro* studies showed that Gli1 significantly down-regulated αvβ6 expression and that αvβ6 may play a role in epithelial to mesenchymal transition (EMT) of skin keratinocytes *in vitro*. These data suggest that morphoeic BCC may represent a form of BCC EMT.

In a large cohort of OSCC samples (282 cases), αvβ6 was strongly expressed in over 50% of cases. We constructed a retrospective clinical database of these cases and examined the utility of αvβ6 as a potential prognostic marker for OSCC disease progression. Although expression of the integrin in itself was a poor marker of prognosis, it correlated significantly with depth of tumour invasion and stromal smooth muscle actin (SMA) expression, correlating with the integrin's functions.

Finally, results from this thesis had suggested several molecules that may potentially regulate αvβ6 expression. Having cloned the ITGB6 promoter, we identified the minimal regulatory sites and carried out pilot studies which showed that TGF-β1 and activated signal transducer and activator of transcription 3 (STAT3) may play a role in modulating αvβ6 expression. Further, more comprehensive studies examining the regulation of αvβ6 expression in health and in disease would be of value in understanding its role in the biology of disease and also in developing more directed therapies.

List of Contents

List of Figures

List of Tables

Author's Declaration

I, Karwan A. Moutasim, declare that the thesis entitled 'Integrin αvβ6: Expression and function in head and neck cancer' and the work presented in the thesis are both my own, and have been generated by me as the result of my own original research. I confirm that:

- this work was done wholly or mainly while in candidature for a research degree at this University;
- where any part of this thesis has previously been submitted for a degree or any other qualification at this University or any other institution, this has been clearly stated;
- where I have consulted the published work of others, this is always clearly attributed;
- where I have quoted from the work of others, the source is always given. With the exception of such quotations, this thesis is entirely my own work;
- I have acknowledged all main sources of help;
- where the thesis is based on work done by myself jointly with others, I have made clear exactly what was done by others and what I have contributed myself;
- parts of this work have been published as:
    - "Betel-derived alkaloid up-regulates keratinocyte alphavbeta6 integrin expression and promotes oral submucous fibrosis" Karwan A Moutasim, Veronika Jenei, Karen Sapienza, Daniel Marsh, Paul H Weinreb, Shelia M Violette, Mark P Lewis, John F Marshall, Farida Fortune, Waninayaka Tilakaratne, Ian R Hart and Gareth J Thomas (2011). *Journal of Pathology* (2011), 223:366-377.
    - "Stromal features are predictive of oral disease mortality in oral cancer patients" Daniel Marsh, Krishna Suchak, Karwan A Moutasim, Sabarinath Vallath, Colin Hopper, Waseem Jerjes, Tahwinder Upile, Nicholas Kalavrezos, Shelia M Violette, Paul H Weinreb, Kerry A Chester, Jagdeep S Chana, John F Marshall, Ian R Hart, Allan K Hackshaw, Kim Piper and Gareth J Thomas (2011). *Journal of Pathology* (2011), 223:470-481.

Signed: ……..

Date:…….

Acknowledgements

Undertaking this PhD has been an incredible experience, and there are so many people to whom I am indebted that I wish to acknowledge.

First and foremost, I must thank my supervisor and mentor Professor Gareth Thomas, for encouraging me to do a PhD and for nurturing my interest in Head and Neck Pathology. His unwavering optimism, his enthusiasm for research and his constant support are much appreciated.

I would also like to acknowledge all members of the Experimental Pathology Group – particularly Dr. Veronika Jenei, Dr. Karen Sapienza, Ms. Marta Chrzan, Dr. Massimiliano Mellone, Dr. Joanne Tod, Dr. Matthew Ward, Dr. Catherine Riley, Dr. Emma Barker, Mr. Toby Mellows, Mr. Chris Hanley and Ms. Samantha Dias – not only for sharing their science secrets with me but also for making this project tremendous fun.

I should also extend my gratitude to Dr. Patrick Duriez (Cancer Sciences Unit), Dr. Susan Wilson (Histochemistry Research Unit) and Dr. David Johnstone (Biomedical Imaging Unit) at the University of Southampton.

Thanks also to our collaborators Dr. John Marshall and Dr. Graham Neill (Queen Mary University of London).

To all my lucky stars at Southampton Cancer Sciences Unit – Yifang, Marta, Nasia, Emma, Breeze, Delphine and Andrew; for putting up with my tantrums and never hanging up on me.

Tanja and Zoi – my best friends & soul mates.

Mum, Dad, Bayan and Avan – for keeping it together in the family.

Finally, I would like to thank Cancer Research UK for funding this project.

Abbreviations

3-D	three dimensional
2-D	two dimensional
AU	arbitrary units
bFGF	basic fibroblast growth factor
BCC	basal cell carcinoma
BM	basement membrane
BSA	bovine serum albumin
CAV	Coxsackie virus
cDNA	complementary deoxyribonucleic acid
CK	cytokeratin
CM	conditioned media
CO_2	carbon dioxide
COX	cyclooxygenase
CSF	colony stimulating factor
d	day
DAB	3,3'-diaminobenzidine
DEPC	diethylpolycarbonate
DMEM	Dulbecco's Modified Eagle's medium
DMSO	dimethyl sulphoxide
dNTP	deoxyribonucleotide triphosphate
ECM	extracellular matrix
EDTA	ethylene diamino tetraacetic acid
EGTA	ethylene glycol tetraacetic acid
EGF	epidermal growth factor
EGFR	epidermal growth factor receptor
ELISA	enzyme-linked immunosorbent assay
EMA	epithelial membrane antigen
EMT	epithelial-to-mesenchymal transition
ERK	extracellular signal-related kinase
FACS	fluorescence activated cell sorting
FAK	focal adhesion kinase
FCS	foetal calf serum
FGM	fibroblast growth medium
FMDV	foot and mouth disease virus
GFP	green fluorescent protein
GM-CSF	granulocyte-macrophage cell stimulating factor
h	hour
H&E	haematoxylin and eosin
HFFF	human foetal foreskin fibroblast
HGF	hepatocyte growth factor (scatter factor)
HH-GLI	hedgehog-gli signalling
HNSCC	head and neck squamous cell carcinoma
HPV	human papilloma virus
HRP	horseradish peroxidase
HSV-TK	herpes simplex virus thymidine kinase
IF	immunofluorescence
IHC	immunohistochemistry
IL	interleukin
IPF	idiopathic pulmonary fibrosis
ISH	in situ hybridisation
JAK	Janus-kinase
JNK	c-Jun N-terminal kinase

kDa	kilodalton
KGM	keratinocyte growth medium
LAP	latency associated peptide
LLC	large latent complex
LTBP	latent TGF-β binding protein
MAPK	mitogen-activated protein kinase
MES	2-(*N*-morpholino)ethanesulfonic acid
min	minute
MLEC	mink lung epithelial cells
MMP	matrix metalloprotease
NSCLC	non-small cell lung cancer
OSCC	oral squamous cell carcinoma
PBS	phosphate-buffered saline
PCR	polymerase chain reaction
PDGF	platelet-derived growth factor
PG	prostaglandin
PKC	protein kinase C
POF	primary oral fibroblast
PTCH	Patched-1
RGD	arginine-glycine-aspartate
RNA	ribonucleic acid
RNAi	ribonucleic acid interference
ROCK	Rho-associated kinase
rpm	revolutions per minute
RTK	receptor tyrosine kinase
RT-PCR	reverse transcriptase polymerase chain reaction
SCC	squamous cell carcinoma
SD	standard deviation
SDS-PAGE	sodium dodecyl sulphate polyacrylamide gel electrophoresis
SE	standard error
SFK	Src-family protein tyrosine kinases
SHC	Src-homology and collagen homology domains (Shc) proteins
SHH	sonic hedgehog homologue
SIP	survival of motor neuron interacting protein 1
siRNA	small interfering ribo nucleic acid
SLC	small latent complex
SMA	smooth muscle actin
SMOH	Smoothened
SS	systemic sclerosis
STAT3	Signal Transducer and Activator of Transcription 3
TBS	tris-buffered saline
TERT	telomerase reverse transcriptase
TGF-β	transforming growth factor β
TGF-βRI	transforming growth factor β type I receptor
TGF-βRII	transforming growth factor β type II receptor
TIMP	tissue inhibitor of matrix metalloproteinases
TN-C	tenascin C
TNF-α	tumour necrosis factor -α
TNM	tumour node metastasis
uPA	urokinase-type plasminogen activator
uPAR	urokinase-type plasminogen activator receptor
VEGF	vascular endothelial growth factor
WASP	Wiskott-Aldrich syndrome protein
WT	wild type

Chapter 1
Introduction

Carcinogenesis is a complex, multi-step process involving at least six essential alterations in cell physiology, collectively defining malignant growth. The 'hallmarks of cancer', originally described by Hanahan and Weinberg in 2000, are: (i) self-sufficiency in growth signals, (ii) insensitivity to growth inhibitory signals, (iii) evasion of programmed cell death, (iv) unlimited replicative potential, (v) sustained angiogenesis and (vi) tissue invasion and metastasis (Hanahan & Weinberg, 2000). Since then, the authors have described two additional, emerging hallmarks: evasion of immune response and altered cellular energetics (Hanahan & Weinberg, 2011)

Cancer cells detach from the primary tumour mass during invasion and breach the basement membrane (BM), invading into the surrounding stroma. This is a fundamental hallmark of malignancy, and the process involves adhesion, directed migration, and proteolysis (Liotta *et al.*, 1980). Integrins are widely considered to be key molecules in these processes (Desgrosellier & Cheresh, 2010).

1.1 Integrins

1.1.1 Background

Integrins were first described as a family of structurally and functionally related heterodimeric cell surface receptors, whose primary role was to "integrate" the extracellular matrix (ECM) with the intracellular cytoskeleton (Tamkun *et al.*, 1986; Hynes, 1987). It is now known that integrins serve as bidirectional signalling molecules, facilitating "outside-in" as well as "inside-out" signalling, and mediating not only interaction between cells and their ECM, but also between cells. Thus, integrins modulate many diverse cellular processes including adhesion, migration, proliferation, differentiation and survival (Desgrosellier & Cheresh, 2010).

Integrins are heterodimers, each consisting of two, non-covalently linked, transmembrane subunits: α and β. Originally, 3 integrin subfamilies were defined on the basis of which β subunits (β1, β2 or β3) were used to form the heterodimer. However, the number of β subunits has now increased to 8 (β1 to β8) and the number of α subunits stands at 18 (α1 to α11, αIIb, αD, αE, αL, αM, αv and αX). These subunits show selectivity in their binding partners and interact in a restricted manner to form the 24 currently identified integrins (Figure 1.1). The "integrin repertoire" present

on a cell surface will determine the extent to which the cell will adhere to and migrate on a particular matrix protein (Hynes, 2004).

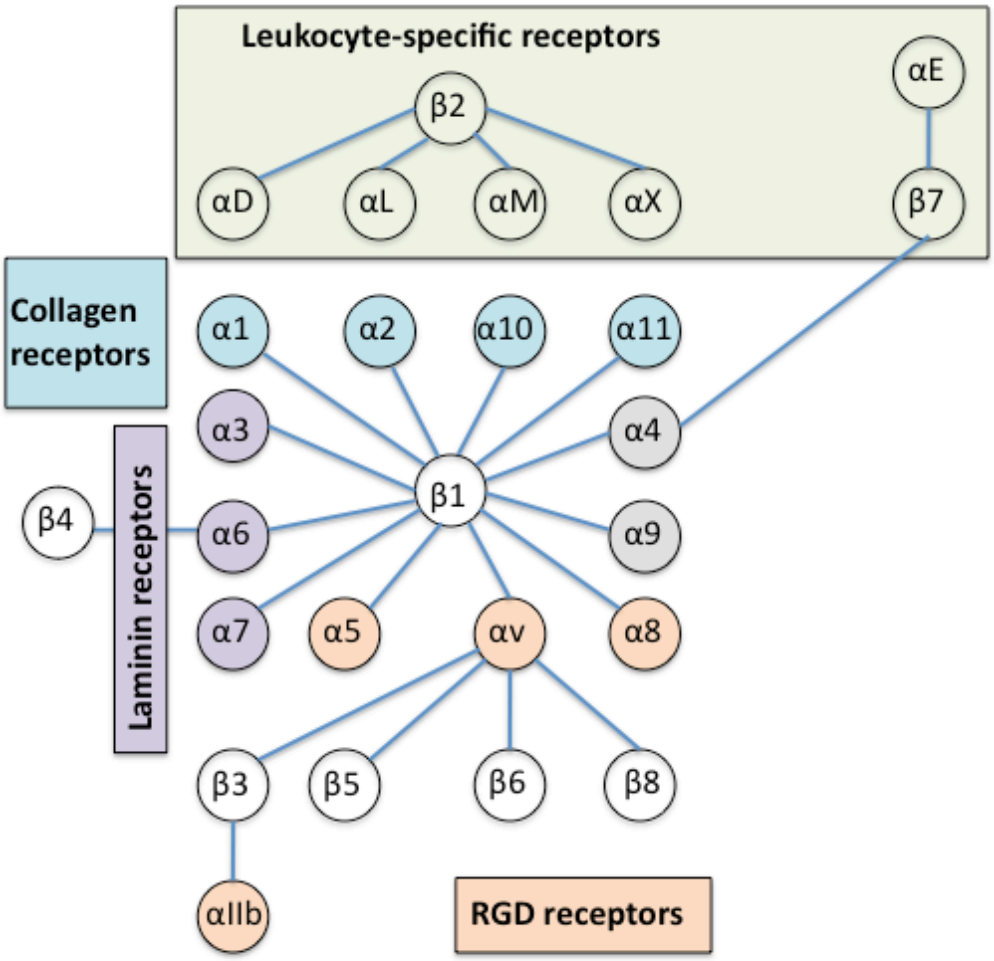

Figure 1.1 The integrin superfamily.
Eighteen α and eight β subunits have been identified, combining to form at least 24 heterodimeric integrins which can be classified into several subfamilies based on ligand specificity and, in the case of β2 and β7 integrins, restricted expression on leukocytes. The different subunits show selectivity in their binding partners; for example, the αv subunit can pair with multiple β subunits (β1, β3, β5, β6 and β8) but the β6 subunit can only bind with αv. Adapted from Thomas *et al.*, 2006.

Integrin α and β subunits are type 1 membrane glycoproteins (spanning the plasma membrane once), composed of a large extracellular domain (700-1,100 amino acids), a transmembrane domain and, generally, a short carboxy (C-) terminal cytoplasmic domain (30-50 amino acids), which interacts with the actin microfilament system (Figure 1.2) and with signalling molecules. The exception is the cytoplasmic tail of integrin β4, with a much larger cytoplasmic domain (approximately 1,000 amino acids), which thus contacts intermediate filaments rather than actin (Hynes, 2002).

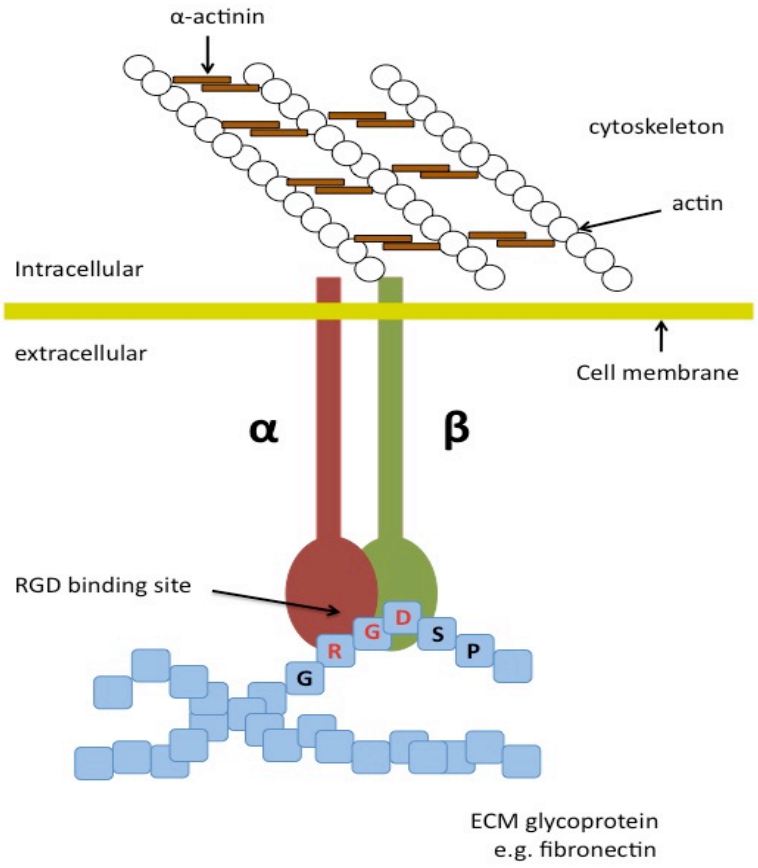

Figure 1.2 Structure of an integrin.
Integrins are αβ heterodimers; each unit crosses the membrane once, with most of each polypeptide (>700 amino acids) in the extracellular space and two short cytoplasmic domains (20-50 amino acids). The extracellular domains interact with ligands (often via the recognition motif RGD) while the intracellular domains are highly conserved and are involved with integrin signalling.

1.1.2 Integrins in cancer

A wide array of integrins is implicated in tumourigenesis. The integrins expressed by epithelial cells (including α6β4, α6β1, αvβ5, αvβ6, α2β1, α3β1) are retained in tumour tissue, although levels are often altered. Most notably, integrins αvβ3, αvβ6, and α5β1 are typically expressed at low or undetectable levels in adult epithelia but can be highly upregulated in some tumours (Thomas *et al.*, 2006). On the other hand, integrins such as α2β1, are downregulated in some tumours (Desgrosellier & Cheresh, 2010). Several studies have attempted to correlate integrin expression levels in cancer with pathological outcomes such as patient survival and metastasis. These have identified several integrins that might have an important role in cancer progression (summarised in Table 1.1).

Tumour type	**Reference(s)**	**Integrin(s) expressed**	**Comments**
Melanoma	Danen *et al.*, 1994 Hsu *et al.*, 1998	αvβ3, α5β1	Vertical growth phase and lymph node metastasis
Breast	Friedrichs *et al.*, 1995 Sloan *et al.*, 2006 Allen and Vaziri *et al.*, 2011	α6β4, αvβ3 α9β1	Increased tumour grade, decreased survival (α6β4), increased bone metastasis (αvβ3) Marker of poor prognosis
Prostate	McCabe *et al.*, 2007 Lamb *et al.*, 2011	αvβ3 α6β1	Increased bone metastasis Promotion of tumour cell survival
Pancreatic	Hosotani *et al.*, 2002 Degrosellier *et al.*, 2009	αvβ3	Lymph node metastasis Mediator of anchorage independence
Ovarian	Slack-Davis *et al.*, 2009 Landen *et al.*, 2008	α4β1 and αvβ3	Increased peritoneal metastasis (α4β1) and tumour proliferation (αvβ3)
Cervical	Gruber *et al*, 2005	αvβ3	Decreased survival
Glio-blastoma	Bello *et al.*, 2001 Cosset *et al.*, 2011	αvβ3 and αvβ5 α5β1	Possible role in invasion Marker of aggressive phenotype; negatively regulated by Caveolin-1
Non-small-cell lung carcinoma	Adachi *et al.*, 2000	α5β1	Decreased survival

Table 1.1 Integrins in cancer.

One of the characteristic features of integrins is the ability of individual family members to recognise multiple ligands whose structures are dissimilar. Conversely, some ligands may be recognised by several integrins (for example, $\alpha 2\beta 1$, $\alpha 3\beta 1$, $\alpha 4\beta 1$, $\alpha 4\beta 7$, $\alpha 5\beta 1$ $\alpha 8\beta 1$, $\alpha v\beta 1$, $\alpha v\beta 3$, $\alpha v\beta 5$, $\alpha v\beta 6$, $\alpha v\beta 8$ and $\alpha IIb\beta 3$ all bind to fibronectin), whereas others may be recognised by only one integrin (for example, plasminogen is bound only by $\alpha IIb\beta 3$).

Many of the ligands recognised by integrins are ECM proteins, such as collagens, fibronectins, laminins and vitronectin, reflecting the primary function of integrins as mediators of cell-cell and cell-ECM adhesion; but also important in defining the roles of integrins in tumourigenesis (Cox *et al.*, 2010). The translation of these adhesive interactions into cellular processes such as proliferation, survival or invasion requires the integrin cytoplasmic tail. These domains do not possess any intrinsic enzyme activity and, as such, must recruit non-receptor tyrosine kinases and phosphatases to initiate signalling cascades (Desgrosellier & Cheresh, 2010; Figure 1.3).

Most integrins activate focal adhesion kinase (FAK), which integrates pro-migratory signals from integrins and receptor tyrosine kinases (RTKs) by recruiting Src family kinases (SFK) to focal adhesions such that they are brought into close proximity to target effectors (Guan & Shalloway, 1992; Desgrosellier & Cheresh, 2010).

Many invasive human cancers over-express FAK, and FAK-SFK signalling regulates cell migration through several pathways (Sood *et al.*, 2004). First, FAK-SFK signalling leads to the recruitment and activation of the small GTPase Rac, which is necessary for extension of lamellopodia (Tilghman *et al.*, 2005). Second, FAK-SFK signalling causes activation of the tyrosine kinase ETK, which is over-expressed in metastatic carcinoma cells and is necessary for their migration (Chen *et al.*, 2001). Third, FAK-SFK signalling promotes disassembly of focal adhesions and this might be important in the detachment of the trailing edge of cells during migration (Webb *et al.*, 2004).

Downstream of Rac and Ras, FAK-SFK signalling leads to activation of extracellular signal-regulated kinase (ERK)/mitogen activated protein kinase (MAPK) (Takeuchi *et al.*, 1997) and Jun amino-terminal kinase (JNK) (Tafolla *et al.*, 2005). ERK/MAPK and JNK regulate cell migration by phosphorylating cytoskeletal proteins as well as by modifying gene expression (Huang *et al.*, 2004). ERK/MAPK and JNK also control cell migration through induction of the activator protein-1 (AP-1)-dependent programme of gene expression (Westwick *et al.*, 1994).

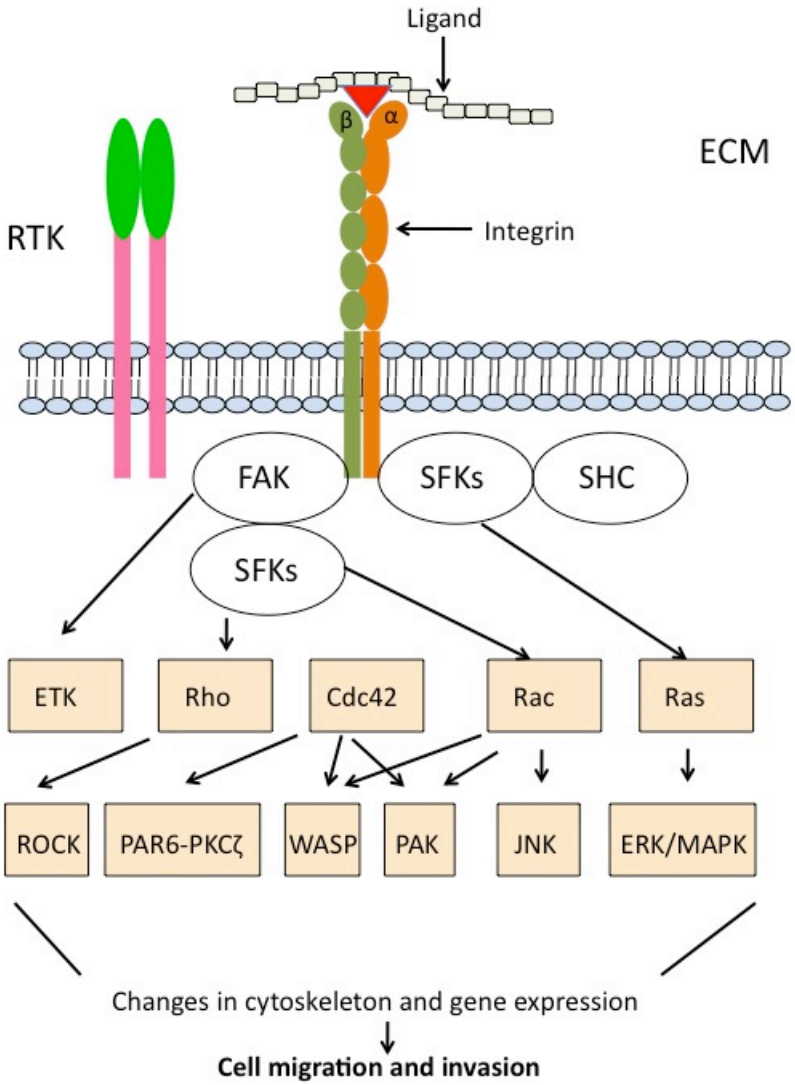

Figure 1.3 Integrin signalling in cell migration and invasion.
Integrins are composed of α and β subunits that span the cell membrane and have a short cytoplasmic tail on the inner side of the plasma membrane and a long extracellular domain extending into the extracellular space. The short cytoplasmic domain of both α and β subunits of integrins interact with a cohort of intracellular proteins, activating several signalling pathways. In this manner, integrin signalling controls critical cell processes such as proliferation, survival and migration. Adapted from Thomas *et al.*, 2006.

The Rho GTPases mediate many integrin-dependent modifications of the actin cytoskeleton necessary for cell migration (Yamazaki *et al.*, 2005). Both Cdc42 and Rac are required for carcinoma migration and invasion (Zhou & Kramer, 2005). They promote actin polymerisation at the cellular leading edge, and thereby the formation of filopodia and lamellopodia. Cdc42 and Rac both induce the assembly of actin filaments through Wiskott-Alkdrich syndrome protein (WASP)-family proteins (Symons *et al.*, 1996). They also activate p21-activated kinase (PAK), which enhances actin polymerisation (Zhang *et al.*, 1995). Finally, Cdc42 may contribute to the establishment of cell polarity by regulating a complex of PAR-6 and protein kinase Cζ (Joberty *et al.*, 2000).

Integrins are thus perceived as central regulators of signal transduction pathways and are the major mechanism by which ECM cues are translated into many diverse cellular functions.

1.2 αvβ6 integrin

1.2.1 Background

αvβ6 is unique amongst integrins in that it is expressed exclusively by epithelial cells (Breuss *et al.*, 1993). It is present at high levels during embryogenesis in the developing lung, skin and kidney epithelia, whilst its expression is downregulated in healthy adult epithelia (Bandyopadhyay & Raghavan, 2009). αvβ6 expression is, however, upregulated during tissue remodelling, including wound healing, carcinogenesis and fibrosis (Breuss *et al.*, 1995; Cass *et al*, 1998; Clark *et al.*, 1996; Haapasalmi *et al.*, 1996; Larjava *et al.*, 1996).

αvβ6 binds to its ligands via the peptide recognition sequence RGDXXL, which is found in various ECM molecules (Kraft *et al.*, 1999). Known ligands of αvβ6 are the ECM proteins (fibronectin, vitronectin, tenascin), latency associated peptide (LAP) of transforming growth factor (TGF-β1 and TGF-β3); and the viral capsid proteins FMDV and CAV9 (Table 1.2).

Ligand	Protein type	Reference
Fibronectin	ECM protein	Busk *et al.*, 1992
Tenascin-C	ECM protein	Prieto *et al.*, 1993
Vitronectin	ECM protein	Huang *et al.*, 1998
LAP of TGFβ-1	Cytokine	Munger *et al.*, 1999
LAP of TGFβ-3	Cytokine	Annes *et al.*, 2002
VP1 coat protein	Foot-and-mouth disease virus (FMDV) capsid	Miller *et al.*, 2001
Coxsackievirus 9 (CAV-9)	Viral capsid	Williams *et al.*, 2004

Table 1.2 Ligands of αvβ6.

1.2.2 αvβ6 structure

Structurally, the β6 subunit of αvβ6 contains three highly conserved cytoplasmic domains (Reszka *et al.*, 1992; Figure 1.4). These regions are involved in the recruitment of integrins to focal adhesions and in modulating integrin affinity. However, the β6 subunit differs from other β subunits in that it has a unique 11-amino acid C-terminus extension (EKQKVDLSTDC), which appears to modulate many of the signalling pathways influencing β6-dependent cellular processes (Morgan *et al.*, 2004).

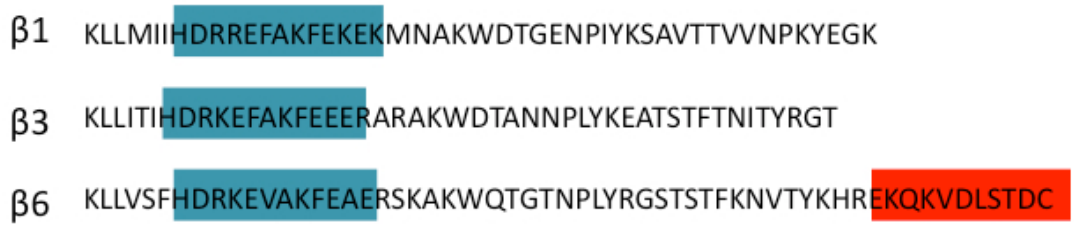

Figure 1.4 Integrin β subunit homology.
Amongst β subunits, there are three highly conserved areas called cytodomains 1, 2 and 3 (shown in blue). However, the β6 subunit differs from the others in that it has a unique C-terminal extension of 11 amino acids – this motif (shown in red) has been shown to be critical for several β6-dependent functions.

1.2.3 αvβ6 signalling

Like many other integrins, αvβ6 can initiate signal transduction through tyrosine kinase phosphorylation of FAK and Fyn, a member of SFKs (Li *et al.*, 2003). Upon ligation of αvβ6 to its ligand fibronectin, Fyn becomes activated as a result of a specific association with αvβ6. The activation of Fyn recruits and activates FAK forming a complex which activates Shc and couples β6 signalling to the ERK/MAPK pathway.

Using a yeast two-hybrid screen, Ramsay and colleagues identified the 35 kDa HS-1 associated protein X1 (HAX1) as a binding partner for the cytoplasmic tail of β6 protein. Direct binding was confirmed by coimmunoprecipitation of the two proteins, and the authors went on to show using siRNA studies that a number of αvβ6-mediated functions such as invasion and migration was regulated by HAX1 (Ramsay *et al.*, 2007).

More recently, the S100 protein Psoriasin (Psor) was identified through a proteomics approach as another binding partner for β6. Morgan and colleagues showed that Psor was capable of binding directly to the C-terminal 11aa sequence of the β6 cytoplasmic unit and modulating β6-dependent tumour cell invasion in oral, breast and lung cancer cells (Morgan & Jazayeri *et al.*, 2011).

1.2.4 Regulation of αvβ6 expression

αvβ6 is highly expressed during wound healing, but this is transient, and its expression is sharply down-regulated at the end of tissue regeneration. In pathogenic fibrosis and carcinogenesis, however, epithelial cells exhibit constitutive expression of the integrin Despite this documented role in many pathogenic states, the regulation of αvβ6 expression is yet to be definitively examined. Since the expression of the αv subunit is ubiquitous in most cell types, *de novo* αvβ6 expression requires exogenous expression of the β6 subunit (Agrez *et al.*, 1994) – thus suggesting that the regulation of the ITGB6 gene is the main mechanism by which αvβ6 expression is regulated. A number of studies have put forward some candidate molecules – namely, transforming growth factor β1 (TGF-β1), tumour necrosis factor-α (TNF-α), Signal Transducer and Activator of Transcription 3 (STAT3) and Ets1 as potential regulators of αvβ6 expression. Below follows a summary of these studies.

Zambruno and colleagues performed one of the initial studies in which potential regulation of β6 expression by the cytokine TGF-β1 was suggested (Zambruno *et al.*, 1995). In this study, the authors examined the role of TGF-β1 in modulating integrin expression in keratinocyte wound healing. Results showed that treatment with TGF-β1 was able to induce the *de novo* expression of the β6 integrin subunit. More recent research has shown that TGF-β1 treatment induced ITGB6 mRNA expression in bile duct epithelial cells (Sullivan *et al.*, 2010). The authors suggested that the mechanism was through p38 MAPK signaling, since pre-treatment of cells with a number of MAPK

inhibitors prevented TGF-β1–modulated ITGB6 mRNA induction. However, more detailed studies with specific inhibition or knock-down of candidate molecules would be imperative in order to fully dissect the mechanism behind TGF-β1 regulation of αvβ6 expression.

TNF-α has also been suggested to influence αvβ6 expression in a single study (Scott *et al.*, 2004). In a skin carcinogenesis model using TNF-$\alpha^{-/-}$ mice, the authors found that expression of both the αv and β6 subunit was lower in comparison with wild type keratinocytes. This reduced level of β6 expression was also reflected functionally, as wild type keratinocytes exhibited higher levels of β6-dependent migration when compared with TNF-$\alpha^{-/-}$ keratinocytes (Scott *et al.*, 2004).

Bates and colleagues examined the transcriptional activation of β6 by the transcription factor Ets1, a member of the Ets transcription factors family, which is involved in development, cell proliferation and had been also shown to have a role in carcinogenesis via modulating EMT (Oikawa & Yamada, 2003; Bates *et al.*, 2005). The authors identified 4 potential Ets consensus binding sites in the 1kb region upstream of the ITGB6 transcription start site, and showed that Ets1 transactivated the ITGB6 promoter by electrophoretic mobility shift assays. However, since chromatin immunoprecipitation (ChIP) assays were not performed in this study, it is not possible to ascertain whether Ets1 physically binds the ITGB6 promoter or not *in vivo*.

Activated or tyrosine phosphorylated signal transducer and activator of transcription (pSTAT3) has been implicated in a variety of solid tumours, including head and neck cancer (Siavash *et al.*, 2004). The persistent activation of pSTAT3 has been reported to influence many of the hallmarks of malignancy, including proliferation, inhibition of apoptosis and neo-angiogenesis (Yu & Jove, 2004). In a recent study, Azare and colleagues over-expressed pSTAT3 in prostate epithelium and then performed Affymetrix array analysis, in which an upregulation of ITGB6 mRNA was seen (Azare *et al.*, 2007). They then went on and identified a series of consensus STAT binding sites in the ITGB6 promoter. Using ChIP assays, the authors found that pSTAT3 was capable of binding to 2 of the consensus binding sites in the ITGB6 promoter.

The above mentioned studies have demonstrated the up-regulation of αvβ6 expression via a number of candidate molecules, but no study has yet suggested a mechanism

through which αvβ6 may be 'switched off', which may represent a novel therapeutic approach in both fibrotic disease and carcinomas.

1.2.5 αvβ6 in wound healing

Several studies on human and animal models have shown that β6 mRNA is detectable in keratinocytes at the wound edge at a relatively early stage of wound development (Breuss *et al.*, 1995). However, protein expression occurs at a later stage, and appears to be maximal when epithelial integrity is restored (Haapasalmi *et al.*, 1996; Clark *et al.*, 1996; Hakkinen *et al.*, 2000). αvβ6 expression correlates with that of TN-C, and this has led to the postulation that the principal functions of αvβ6 in wound healing are modulated through its interaction with TN-C (Haapasalmi *et al.*, 1996; Clark *et al.*, 1996; Hakkinen *et al.*, 2000; Larjava *et al.*, 2011).

TN-C is also a ligand for α9β1 integrin, which is upregulated during the early stages of wound healing (Hakkinen *et al.*, 2000) and downregulated in later stages, coinciding with the induction of αvβ6 expression. Yokosaki and colleagues showed that α9β1 expression in cells plated on TN-C induced proliferation whereas αvβ6 had the opposite effect, suggesting that the switch between α9β1 and αvβ6 in wound epithelium may be a mechanism for regulating cell responses during epithelial regeneration (Yokosaki *et al.*, 1996). These data suggest that the principal role of αvβ6 is not related to initial cell migration, and that factors involving αvβ6 expression are released after the initial movement of wound keratinocytes has occurred (Haapasalmi *et al.*, 1996; Clark *et al.*, 1996).

A similar switch between integrins has been described by Janes and Watt. They demonstrated reciprocal expression of αvβ5 (expressed on stratified squamous epithelia but downregulated in SCC) and αvβ6 (not expressed on normal epithelia but upregulated in SCC). They showed that down-regulation of αvβ5 through up-regulation of αvβ6 may protect SCCs from anoikis by activating an Akt survival signal (Janes & Watt, 2004).

Animal studies have attempted to further dissect the role for αvβ6 in cutaneous wounds. Wound healing does not appear to be impaired in experimentally induced skin wounds in young $\beta6^{-/-}$ mice (Huang *et al.*, 1996; Hakkinen *et al*., 2004). However, old

age and immunosuppression appear to compromise the process in $\beta6^{-/-}$ mice (AlDahlawi *et al.*, 2006).

In a more recent study, $\alpha v\beta6$ integrin appeared to play a role in wound healing in an experimental model of chemically induced type I diabetes in $\beta6^{-/-}$ mice (Jacobsen *et al.*, 2010). The study showed that there was a significant delay in wound healing in the $\beta6^{-/-}$ - diabetic mice. Interestingly, there was also a lack of collagen deposition in the wounds, consistent with the role of $\alpha v\beta6$ in activating TGF-β1 and its subsequent promotion of TGF-β1-dependent fibroblast-to-collagen myofibroblast transdifferentiation, the chief cell type responsible for collagen deposition.

$\alpha v\beta6$ has also been found to play a role in corneal wound healing. Blanco-Mezquita and colleagues studied this process by performing keratectomies in WT and $\beta6^{-/-}$ mice, and monitoring corneal wound healing over a period of 4 months. It was found that $\alpha v\beta6$ was up-regulated in migrating corneal epithelium, and that wound healing was significantly delayed in $\beta6^{-/-}$ mice, which also showed BM defects, leading the authors to hypothesise that $\alpha v\beta6$ also influences laminin function in wound healing (Blanco-Mezquita *et al.*, 2011).

1.2.6 $\alpha v\beta6$ in cancer

Wound healing and carcinogenesis have many biological processes in common; to the extent that carcinogenesis has been described as a misregulated form of wound healing (Dvorak *et al.*, 1986). Consistent with its epithelial specificity, $\alpha v\beta6$ expression has only ever been reported in carcinomas (other cancers, including melanomas, are $\alpha v\beta6$-negative; Ramsay *et al.*, 2007).

1.2.6.1 $\alpha v\beta6$ expression in cancer

$\alpha v\beta6$ upregulation was first described in OSCC but since then it has been shown to be overexpressed in a variety of other carcinomas (mainly, but not exclusively, SCC; Table 1.3).

Using immunohistochemistry, Ahmed and colleagues examined 45 ovarian carcinomas for $\alpha v\beta6$ expression and found that all tumours expressed the integrin. Normal ovarian tissue and benign serous neoplasms had undetectable levels of $\alpha v\beta6$. Staining intensity correlated with tumour grade, suggesting that a gradual increase in the

expression of the molecule may be a correlative index of the progression of this disease (Ahmed *et al.*, 2002a).

Kawashima and colleagues examined 18 gastric carcinomas for β6 mRNA using RT-PCR, and showed that 47% were β6-positive and expression correlated with metastasis to locoregional lymph nodes (Kawashima *et al.*, 2003). Bates and colleagues performed immunohistochemistry on tissue arrays of colorectal cancers with known clinical outcome and showed that 181 of 488 samples (37%) were positive for αvβ6 expression, whilst normal colonic mucosa was αvβ6-negative. Of the αvβ6-positive tumours, 95 (19% of total) exhibited low expression, and 86 (18% of total) exhibited high expression. Expression of αvβ6 correlated with survival; patients whose tumours had no or low expression of αvβ6 had a median survival of 4.8 years and had a 15% lower 5-year survival (46.7% vs. 61.7%). These same authors also showed that αvβ6 was maintained in metastasis, supporting their conclusion that αvβ6 expression in colorectal cancer correlates with progression and poor clinical outcome (Bates *et al.*, 2005).

Arihiro and colleagues immunostained 90 breast carcinoma specimens and showed that 18% of these were positive for αvβ6 but αvβ6 expression did not correlate with prognostic factors such as patient age, tumour size, histological type of tumour or hormone receptor status. With regard to the histological grade of carcinoma, correlation with αvβ6 expression was not statistically significant although it is noteworthy that none of the 14 grade 1 tumours examined were αvβ6 positive (Arihiro *et al.*, 2000). A more recent, larger scale study of over 2,000 study subjects found that αvβ6 was prognostic in a particular cohort of breast cancer patients in the UK (Professor Louise Jones – personal communication).

Carcinoma	Reference	No. of cases	% +ve tumours	Evidence	Comment
Oral SCC	Breuss *et al.*, 1995	30	90	ISH	αvβ6 absent in normal oral mucosa
	Jones *et al.*, 1997	17	100	IHC	41% expression in leukoplakia; dysplastic areas also +ve
	Hamidi *et al.*, 2000	5	80	IHC	Expression maintained in lymph node mets
	Impola *et al.*, 2004	11	100	ISH	
	Regezi *et al.*, 2002	40	100	IHC	Expression co-localised with TN-C
	Marsh *et al.*, 2011	282	100	IHC	
Colon	Bates *et al.*, 2005	488	37	IHC	Poor prognosis
	Yang *et al.*, 2008	358	34	IHC	Liver metastasis
Pancreas	Sipos *et al.*, 2004	34	100	IHC	Expression higher in well-differentiated tumours
Gastric	Kawashima *et al.*, 2003	38	47	IHC, RT-PCR	94% positive had LN mets
NSCLC	Smythe *et al.*, 1995	51	50	IHC	Good prognostic marker?
Breast	Arihiro *et al.*, 2000	90	18	IHC, WB	No Grade 1 +ve tumours
Ovary	Ahmed *et al.,* 2002a	45	100	IHC	Staining correlated with grade
Prostate	Azare *et al.*, 2007	40	23	IHC	No correlation with grade
Basal cell	Marsh *et al.*, 2008	13	77	IHC	αvβ6 promoted invasion via stromal modulation
Cholangio-carcinoma	Patsenker *et al.*, 2010	62	88	IHC	Expression maintained in mets
Endometrial	Hecht *et al.*, 2008	126	42	IHC	Expression maintained in mets
Cervical	Hazelbag *et al.*, 2007	85	59	IHC	Poor prognosis

Table 1.3 Expression of αvβ6 in carcinomas

αvβ6 has been shown to be overexpressed in lung cancers and in the proximal (but not distal) airways of smokers (Weinacker *et al.*, 1995). By contrast, α9β1 (which, like αvβ6, binds to TN-C) was expressed throughout the airway epithelium (but not alveolar epithelium). The same authors showed that αvβ6 was highly expressed on bronchial epithelial cells cultured from resected airways even in patients who did not express the receptor in their airways *in vivo*, suggesting that some component of the *in vitro* environment can induce expression of αvβ6 (Weinacker *et al.*, 1995)

Recently, a role for αvβ6 was demonstrated in a particular subtype of basal cell carcinoma (BCC), where 15 nodular and 13 morphoeic BCCs were examined by immunohistochemistry. This study found that αvβ6 was expressed at low levels in low-risk nodular BCCs but was markedly upregulated in the more infiltrative, aggressive morphoeic variant (Marsh *et al.*, 2008).

Sipos and colleagues showed that αvβ6 expression was restricted to tumour cells in pancreatic ductal adenocarcinoma and gastric carcinomas of the intestinal type. Interestingly, and in contrast to SCCs, αvβ6 expression was poor at the leading edge of the tumours. Furthermore, expression was stronger in well or moderately differentiated tumours, indicating perhaps a role for αvβ6 in carcinoma differentiation in this context (Sipos *et al.*, 2004).

More recently, Hecht and colleagues showed by immunohistochemistry that 42% of endometrial carcinomas expressed αvβ6, with higher expression at the leading edge of the tumour (Hecht *et al.*, 2008). Expression was maintained in nodal metastases at high levels, irrespective of level of expression in the primary tumour. Normal endometrial tissue showed minimal expression of the integrin, as did the majority of premalignant endometrial lesions (Hecht *et al.*, 2008).

In a recent, comprehensive study examining the role of αvβ6 in hepatic neoplasms, αvβ6 was shown by immunohistochemistry to be expressed by the majority of cholangiocarcinomas but not in hepatocellular carcinoma (Patsenker *et al.*, 2010). Hepatomas and fibrolamellar hepatocellular carcinomas were negative for αvβ6. The expression of the integrin was maintained in 83% pancreatic and 13% of colorectal metastases from cholangiocarcinomas. The authors also assessed β6 gene transcript levels by quantitative PCR and showed that there was a 100-fold increase in β6

expression in cholangiocarcinomas in comparison with normal liver (Patsenker *et al.*, 2010).

1.2.6.2 αvβ6 functions in tumour progression

During tumourigenesis, upregulation of αvβ6 promotes tumour progression in several ways (Table 1.4). Tumour invasion requires local degradation of the BM, which is impermeable to cells under normal physiological conditions. The main constituent of BM is type IV collagen that forms a dense network together with other molecules such as laminins, nidogens, fibronectin and heparan sulphate proteoglycans (Yurchenco *et al.*, 2004). Matrix metalloproteases (MMPs) have a pivotal role to play in maintaining the tumour microenvironment by actively remodeling the ECM, which is required for invasion and migration. Type IV collagen is a substrate for a variety of different MMPs (-2, -3, -7, -9, -12 and -19) all of which may facilitate degradation of the BM (Bandyopadhyay & Raghavan, 2009).

In SCC, several studies have shown that αvβ6 has a role in matrix remodelling through upregulation of proteases. Thomas and colleagues created an OSCC cell line with αvβ6 expression (VB6) using β6 cDNA retroviral transfection and showed that VB6 was significantly more invasive through Matrigel® in Transwell® invasion assays than the control C1 cell line (transfected with the empty vector alone) (Thomas *et al.*, 2001a). This was, in part, through αvβ6-dependent upregulation of MMP-9 (a type IV collagenase) and, to a lesser extent, MMP-2. This activity appeared to be modulated through the unique terminal 11 amino acids of the β6 tail (Morgan *et al.*, 2004). In a subsequent study, the authors showed that MMP9 was responsible for the cleavage of fibronectin to produce a 120kDa fragment towards which αvβ6-overepexressing cells migrated. This was accompanied by an increased expression of both MMP-9 and MMP-2, creating a positive feedback loop which may have an important role to play in tumourigenesis (Al-Hazmi *et al.*, 2007).

Similarly, αvβ6 was shown to regulate MMP-9 through ERK binding to the β6 cytoplasmic tail in colon carcinoma cells. MMP-9 secretion was suppressed when β6 expression was down-regulated or when the binding site was lost (Niu *et al.*, 2002; Ahmed *et al.*, 2002b).

αvβ6 has also been shown to upregulate MMP-3 in malignancy. Using retroviral β6 cDNA transduction, Ramos and colleagues showed that αvβ6 promoted OSCC invasion and tumour growth *in vitro* and *in vivo* in the otherwise poorly invasive cell line, SCC9, and that this process was modulated through MMP-3 rather than MMP-9 (Ramos *et al.*, 2002). In a subsequent study, Li and colleagues suggested that the signalling pathway regulating these processes involved β6-dependent activation of Fyn, a tyrosine kinase, which then recruited and activated FAK. Once activated, the FAK-Fyn complex phosphorylated the downstream signalling molecule Shc, which coupled β6 signalling to the Raf-ERK/MAPK pathway. Subsequently, the MMP-3 gene was transcriptionally activated, which promoted OSCC proliferation *in vitro* and metastasis *in vivo* (Li *et al.*, 2003). It thus appears that αvβ6 modulates matrix degradation by signalling mechanisms as well as recruiting proteases to the cell surface.

Additionally, αvβ6 expression regulates serine proteases – namely the urokinase type plasminogen activator (uPA) and its receptor uPAR, which are major players in tumour invasion and metastasis. In one study, overexpression of αvβ6 in OSCC cells modulated transcriptional reduction of uPAR through the C-terminal 11 amino acids of β6. Interestingly, αvβ6-overexpressing cells were significantly more invasive than control cells (with higher uPAR levels), suggesting that the receptor is not critical for regulating invasive potential in this model (Dalvi *et al.*, 2004). Another study, however, showed that αvβ6 expression correlated with levels of uPAR, uPA and MMP-9 (Ahmed *et al.*, 2002c).

Function	Comment	Cell type	Reference
Promotion of migration and invasion	Promotion of invasion through upregulation of MMP-9	OSCC	Thomas *et al.*, 2001(a,b)
	Promotion of invasion through upregulation of MMP-3	OSCC	Li *et al.*, 2003
	Promotion of migration over FN, VN, LAP	OSCC, mouse keratinocytes	Thomas *et al.*, 2002
	Upregulation of uPA	Ovarian carcinoma	Ahmed *et al.*, 2002c
	TNFα-dependent upregulation of αvβ6 and promotion of migration through MMP-9	Mouse keratinocytes	Scott *et al.*, 2004
Activation of TGF-β	Binds & activates latent TGF-β1	Colon carcinoma cells Keratinocytes	Munger *et al.*, 1999 Shi *et al.*, 2011
	Binding & activating TGF-β3	Colon carcinoma cells	Annes *et al.*, 2002
	Promotion of TGF-β1-dependent EMT	Colon carcinoma cells	Bates *et al.*, 2005
	Promotion of TGF-β1-dependent myofibroblast differentiation	Keratinocytes	Marsh *et al.*, 2008
Promotion of proliferation & generation of survival signals	Protective action on OSCC from anoikis via downregulating αvβ5	OSCC	Janes & Watt, 2004
	Proliferation through 11-amino-acid C-terminus of β6 subunit	Colon carcinoma cells	Agrez *et al.*, 1994

Table 1.4 Functions of αvβ6.

1.2.7 αvβ6 in fibrosis

Fibrosis can be defined as an abnormal tissue response to injury, typically characterised by the deposition of collagen and other ECM components. Although collagen deposition is a normal part of wound healing, in pathogenic fibrosis the process is chronic. The chief cell type involved in fibrosis is the myofibroblast: defined as a contractile, smooth muscle-like collagen-secreting cell (De Wever *et al.*, 2008; Margadant & Sonnenberg, 2010).

Pathogenic organ fibrosis is a major public health issue, and can lead ultimately to major organ failure or even death. Fibrotic disorders include liver cirrhosis, systemic sclerosis (scleroderma) and pulmonary fibrosis. The pleiotropic cytokine transforming growth factor β1 (TGF-β1), is invariably involved in fibrotic disorders, and there is a wealth of evidence to support integrin crosstalk with TGF-β1 as one of the key mechanisms behind organ fibrosis – particularly integrins α3β1, αvβ5 and, most notably, αvβ6 (Margadant & Sonnenberg, 2010; Worthington *et al.*, 2011; summarised in Table 1.5).

The first evidence for the role of αvβ6 in experimental fibrosis was provided in a study by Munger and colleagues, in which they demonstrated that the activation of TGF-β1 by αvβ6 was crucial to the development of pulmonary fibrosis. The study employed mice lacking the β6 subunit, which were protected from bleomycin-induced pulmonary fibrosis (Munger *et al.*, 1999). Constitutive expression of αvβ6 in the basal epidermal layer in transgenic mice led to the development of chronic, fibrotic ulcers (Hakkinen *et al.*, 2004). In contrast, $\beta6^{-/-}$ mice are partially or completely protected from pulmonary, tubulointerstitial or acute biliary fibrosis (Margadant & Stonnenberg, 2010). Recently, Jenkins and colleagues performed a series of studies showing that injury induced αvβ6 activation of TGF-β1 in epithelial cells via G protein coupled receptors and a RhoA mediated pathway, which contributed to pulmonary fibrosis (Jenkins *et al.*, 2006; Xu *et al.*, 2009).

αvβ6 is also implicated in the fibrosis of other organs, including the liver and kidney (studies summarised in Table 1.5). In the oral cavity, αvβ6 has recently been shown to be involved in a study of phenytoin-induced gingival fibrosis (Sume *et al.*, 2010). The integrin was found to be highly expressed in fibrotic gingiva but only present at minimal tissues in healthy gums. Interestingly, E-cadherin levels were down-regulated in fibrotic

gingival tissue. Thus, the authors proposed that αvβ6 promoted epithelial-to-mesenchymal transition (EMT) in this context, chiefly through its activation of TGF-β1, a known inducer of EMT (Sume *et al.*, 2010).

Several studies have shown that fibrosis can be equally inhibited in wild-type mice with TGF-β signalling pathway antagonists or with αvβ6 antibody blockade (Ma *et al.*, 2003; Hahm *et al.*, 2007; Wang *et al.*, 2007; Patsenker *et al.*, 2008; Table 1.5). These studies are particularly of interest given that blocking the TGF-β1 pathway can have severe adverse affects – including the development of autoimmune disease. Thus, the inhibition of αvβ6-dependent TGF-β1 activation at injury sites is emerging as a potential therapeutic modality against TGF-β1-mediated fibrosis (Margadant and Sonnenberg, 2010).

Organ/ tissue involved	Reference	Main finding
Lung	Munger *et al.*, 1999	αvβ6 binds to LAP and activates TGF-β1; $\beta6^{-/-}$ mice protected from bleomycin induced pulmonary fibrosis
	Puthawala *et al.*, 2008	$\beta6^{-/-}$ mice protected from radiation induced pulmonary fibrosis
	Horan *et al.*, 2008	100% positive αvβ6 expression in 21 clinical IPF cases and 11 SS cases by IHC; inhibition of αvβ6 blocked murine pulmonary fibrosis
Liver	Wang *et al.*, 2007	Induction of αvβ6 expression in mouse cholangiocytes after bile duct ligation and development of acute biliary fibrosis
	Popov *et al.*, 2008	β6 mRNA upregulated in 79 Hepatitis C patients with progression of fibrosis (qRT-PCR); αvβ6 protein absent in normal human liver
	Nadler *et al.*, 2009	αvβ6 protein upregulated in human clinical samples and experimental biliary atresia in mice by IHC
	Sullivan *et al.*, 2010	αvβ6 up-regulation and subsequent activation of TGF-β1 dependent on thrombin generation and PAR-1. Fibrosis diminished in $PAR\text{-}1^{-/-}$ mice.
Kidney	Ma *et al.*, 2003	Experimentally obstructed kidneys in $\beta6^{-/-}$ mice showed significantly less tubulointerstitial fibrosis than WT mice. Activated pSmad2 levels significantly lower in $\beta6^{-/-}$ mice
	Hahm *et al.*, 2007	αvβ6 highly expressed in glomerulonephritis, diabetes mellitus, IgA nephropathy, Goodpasture's syndrome, Alport syndrome and lupus (IHC and IF).
	Gewin *et al.*, 2010	Paradoxical induction of αvβ6 expression and progression of fibrosis in $TGF\beta RII^{-/-}$ mice
Skin	Hakkinen *et al.*, 2004	High αvβ6 expression in 5 chronic diabetic wounds (100%, IHC). Minimal αvβ6 expression in fibrotic skin disorders and keloid scars.
Oral cavity	Sume *et al.*, 2010	αvβ6 up-regulated in phenytoin induced gingival fibrosis

Table 1.5 Expression and function of αvβ6 in fibrotic disease.

1.2.8 αvβ6 activation of TGF-β1

The TGF-β superfamily is a group of highly conserved, pleiotropic cytokines consisting of 33 different members that includes TGF-βs, bone morphogenetic proteins (BMPS), activins and inhibins (Shi *et al.*, 2011). TGF-βs are vital in regulating a number of cellular processes including inflammation, ECM production, proliferation, adhesion and differentiation in a tissue- and context-specific manner (Gordon & Blobe, 2008' Worthington *et al.*, 2011). There are 3 TGF-β isoforms in mammals: TGF-β1, TGF-β2 and TGF-β3, each encoded by a different gene and each with distinct functions. In order for TGF-β to exert its biological effects, it must be activated (Goodwin & Jenkins, 2009).

Each TGF-β is synthesised as a homodimer (pro-TGF-β), comprised of TGF-β covalently linked to its latency associated peptide (LAP) at its N-terminus. Pro-TGF-β is then cleaved intracellularly by furin-like enzymes, still attached to LAP in a non-covalent state forming the small latent complex (SLC), from which it must be released to be activated. Secreted TGF-βs are usually in the form of large latent complexes (LLCs), formed by the association of latent TGF-β binding proteins (LTBPs) to the SLCs (TGF-β/LAP) by disulphide covalent bonds (Wipff & Hinz, 2008). LTBPs are members of a fibrillin-like ECM protein superfamily that bind other ECM proteins such as vitronectin and fibronectin. There are 4 LTBP isoforms: LTBP1 through LTBP4, all of which can bind to all isoforms of TGF-β except for LTBP3. Thus, the LLCs can be seen as a large pool of inactive, latent TGF-β. This represents an important safeguard against inadvertent activation of TGF-β (Bandyopadhyay & Raghavan, 2009).

All of the αv integrins, in addition to α8β1, bind to the RGD motif within LAP-1 but only αvβ6 and αvβ8 have been shown to activate TGF-β1 *in vivo*, whilst the role of αvβ1 is still unclear (Munger *et al.*, 1999; Annes *et al.*, 2004; Margadant & Sonnenberg, 2010). The activation of TGF-β1 by αvβ8 is different from αvβ6 in that it is protease-dependent and occurs by recruitment of MMP14 (Mu *et al.*, 2002).

The LAP of TGF-βs contains RGD motifs that render them possible ligands for integrins. Munger and colleagues were first to show that LAP-1 is a high affinity ligand for αvβ6 and proposed that this was a potential mechanism for the activation of TGF-β1 (Munger *et al.*, 1999). The binding of αvβ6 to the RGD sequence in LAP and αvβ6

connecting to the cytoskeleton triggers a conformational change in the LLC (TGF-β1-LAP-LTBP1 complex; Figure 1.5). Mice in which the aspartic acid has been replaced with glutamic acid in this sequence recapitulate the phenotype of TGF-β knock-out mice, thus highlighting the importance of this mechanism of TGF-β activation (Yang *et al.*, 2007)

Thus, TGF-β1 is released from the LLC, and binds to a heterodimeric serine/threonine kinase receptor complex (consisting of TGF-βRI and TGF-βRII), leading to the recruitment and phosphorylation of the intracellular effector proteins Smad2 and Smad3 (Wipff and Hinz, 2008; Margadant and Sonnenberg, 2010). Subsequently, phosphorylated Smad2 and Smad3 bind to Smad4 and translocate to the nucleus to initiate transcription of TGF-β target genes. αvβ6 is only capable of activating TGF-β bound to LTBP1, as each LTBP isoform has significant differences in the hinge region sequence, which implies that this region may have a significant role in the specific association with and activation of TGF-β by integrins (Bandyopadhyay & Raghavan, 2009).

However, binding of αvβ6 to TGF-β1 is insufficient to activate the cytokine. In fact, the integrin is constitutively bound to TGF-β1, thus being 'primed' for activation. For TGF-β1 activation to occur, the actin cytoskeleton must be intact. Jenkins and colleagues have performed a series of elegant studies demonstrating the importance of tissue injury mediators in αvβ6-mediated TGF-β1 activation in the context of pulmonary fibrosis, thus further dissecting the mechanisms behind αvβ6-dependent TGF-β1 activation (Jenkins *et al.*, 2006; Xu *et al.*, 2009; Jenkins and Goodwin, 2009; Figure 1.5). The authors first showed that the serine protease thrombin, a mediator of haemostasis released during injurious processes, mediated αvβ6-dependent TGF-β1 activation *in vitro* and *in vivo* via acting as a ligand for the G-protein coupled receptor (GPCR) protease activated receptor 1 (PAR-1), which then signalled to αvβ6 through RhoA and Rho kinase. This then resulted in changes in actin cytoskeleton and thus modulation of αvβ6-dependent TGF-β1 activation through 'inside-out' signalling (Jenkins *et al.*, 2006; Figure 1.5). In a subsequent study, the group went on to show that the bioactive phospholipid lysophosphatidic acid (LPA), released from platelets during wound healing, was also implicated αvβ6-dependent TGF-β1 activation in human lung epithelial cells (Xu *et al.*, 2009; Figure 1.5). This process was also modulated through the RhoA and Rho Kinase pathway. To validate the *in vitro* findings,

Xu and colleagues then showed that, alongside αvβ6, the LPA2 receptor was also highly expressed both in an experimental model of bleomycin-induced fibrosis and *in vivo* in IPF (Xu *et al.*, 2009).

Since αvβ6 is also implicated in the process of tumour progression, its activation of TGF-β1 may seem contradictory, given the growth inhibitory effects of this cytokine (Elliott & Blobe, 2005). However, TGF-β has a complex role in tumourigenesis, inhibiting cancer cell proliferation in some contexts and promoting it in others (Ikushima & Miyazono, 2010) – as such it seems to have a "biphasic effect", initially suppressing epithelial cell proliferation but later actually stimulating cancer progression (Prime *et al.*, 2004). Thus, it appears that αvβ6 activation of TGF-β can promote tumourigenesis by releasing MMPs and contributing to matrix degradation (Thomas *et al.*, 2001b), or by modulating the surrounding stroma. Activated TGF-β can promote the transdifferentiation of fibroblasts into myofibroblasts, which in turn have been shown to promote SCC invasion via the secretion of hepatocyte growth factor (HGF) (Lewis *et al.*, 2004; Marsh *et al.*, 2008).

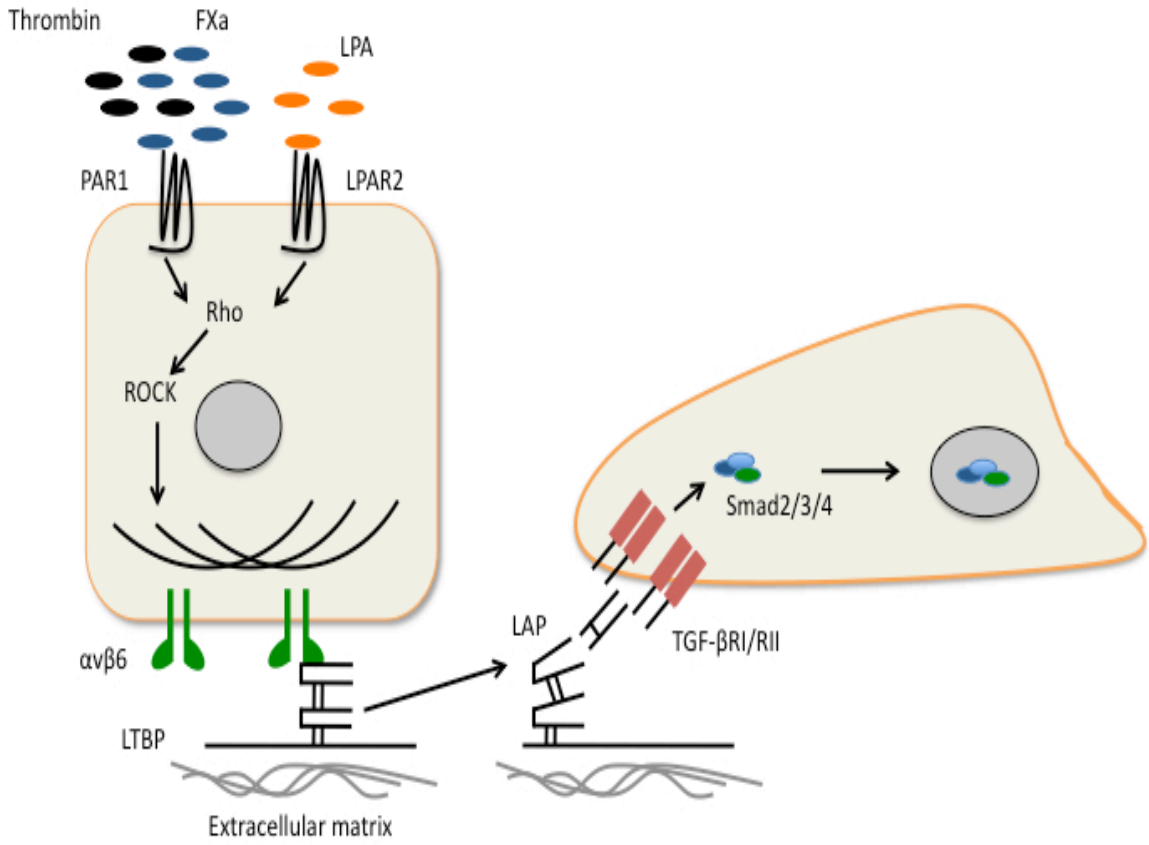

Figure 1.5 TGF-β1 activation by αvβ6.
αvβ6-dependent activation of TGF-β1 is protease-independent and is induced by cell traction forces. FXa, coagulation factor X; LAP, latency associated peptide; LPA, lysophosphatidic acid; LPAR2, lysophosphatidic acid receptor 2; LTBP, latent TGF-β binding protein; PAR1, protease-activated receptor 1; ROCK, Rho-associated kinase. Adapted from Margadant & Sonnenberg, 2010.

1.2.9 αvβ6 in epithelial to mesenchymal transition (EMT)

The epithelial to mesenchymal transition (EMT) is a fundamental, evolutionarily conserved process in embryology (Thiery, 2003). During EMT, epithelial cells lose their characteristic apico-basal polarity and close intercellular contacts, acquiring a more invasive, mesenchymal phenotype. Sequential 'rounds' of EMT and, conversely, mesenchymal to epithelial transition (MET) orchestrate the process of gastrulation in metazoa (Thiery *et al.*, 2009). Increasingly, EMT has been described in human disease, particularly organ fibrosis and cancer (Hanahan and Weinberg, 2011). As mentioned earlier, the hallmark cell type in pathological fibrosis is the myofibroblast, also implicated in EMT by virtue of its somewhat controversial potential source of origin (Thiery *et al.*, 2009). Whilst fibroblasts can transdifferentiate readily into myofibroblasts under the influence of TGF-β, lineage tracing studies have demonstrated that myofibroblasts may also originate from epithelial cells, circulating pericytes or hepatocytes (de Wever *et al.*, 2008).

The molecular pathways involved in pathological EMT are remarkably similar to those involved in physiological EMT. The downregulation of E-cadherin via its transcriptional repression is one of the key features of EMT, and several factors contribute to this phenomenon. The transcription factors Snail and Zeb bind the E-cadherin promoter directly, whilst Goosecoid and Twist downregulate E-cadherin indirectly (Peinado *et al.*, 2007; Figure 1.6). E-cadherin downregulation is frequently accompanied by the up-regulation of mesenchymal markers such as Vimentin and N-cadherin (Thiery *et al.*, 2009; Figure 1.6).

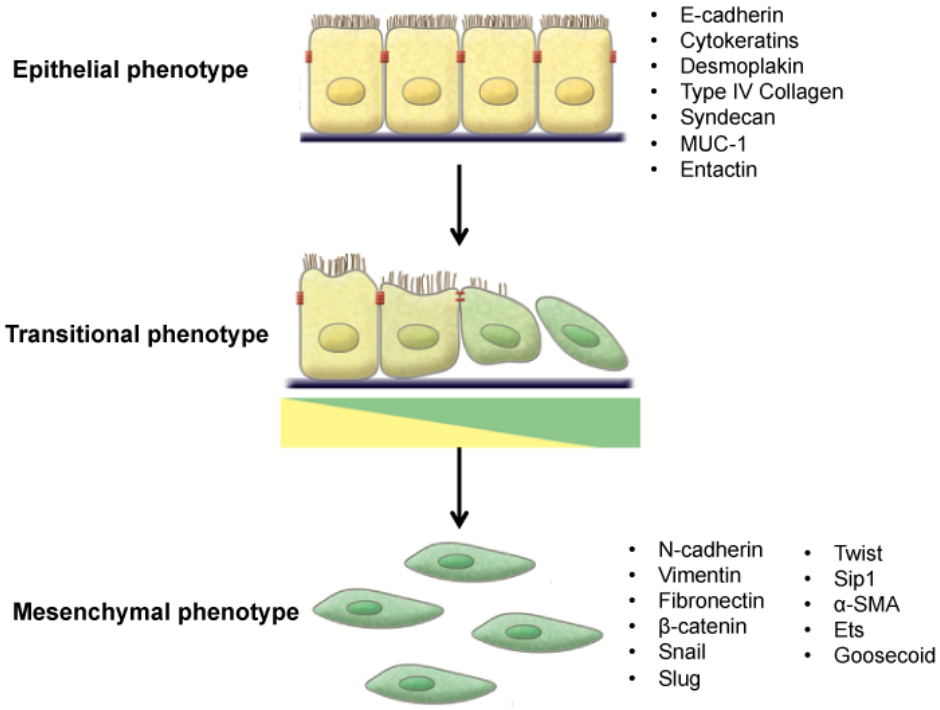

Figure 1.6 Epithelial to mesenchymal transition. During EMT, epithelial cells down-regulate characteristic proteins defining the epithelial phenotype and acquire mesenchymal proteins as they transition into more motile, invasive cells. Diagram adapted from Kalluri & Weinberg, 2009.

TGF-β signalling plays a central role in regulating EMT, both in normal physiology and in disease (Thiery *et al.*, 2009). Notably, the TGF-β Smad effector proteins associate with Zeb transcription factors to repress E-cadherin transcription (Singh and Settleman, 2010). Additionally, TGF-β1 is the main activator of Snail1, key in the EMT process (Kalluri & Weinberg, 2009). The importance of TGF-β1 in the EMT of organ fibrosis has been elegantly demonstrated in mouse studies using BMP-7, a TGF-β antagonist, whereby the inhibitor restored E-cadherin expression and resulted in epithelial repair (Zeisberg *et al.*, 2003).

Given that αvβ6 is a major means through which TGF-β1 is activated, it is hardly surprising that several recent studies have now attempted to identify the potential role of this integrin in pathological EMT. Bates and colleagues investigated a possible role for αvβ6 in the EMT of colorectal cancer, where they attempted to correlate αvβ6 expression in the more invasive fronts of colorectal cancer to a loss of E-cadherin expression (Bates *et al.*, 2005). A subsequent study by Sume and colleagues also showed E-cadherin loss in conjunction with upregulation of αvβ6 expression in the

context of gingival fibrosis (Sume *et al.*, 2010). However, more detailed examination of the molecular pathways involved in EMT and a clearer definition of what constitutes the EMT in pathogenic processes involving αvβ6 remains to be seen. Given that αvβ6 expression is epithelial-specific, it may be that it plays an as yet undefined role within the heterogeneous environment of a tumour, in which the EMT phenomenon is very much a complex, dynamic process.

1.2.10 αvβ6 as a therapeutic target

The fact that αvβ6 is exclusively expressed by epithelia and is mainly upregulated during disease processes makes it an attractive therapeutic target. αvβ6-specific probes are required for effective targeting of αvβ6-expressing lesions and potential biopharmaceutical compounds which would fulfil such a purpose include monoclonal antibodies, single chain variable fragment antibodies (scFv), peptides or peptide mimetics and viral vectors, each of which has its advantages and disadvantages as targeting agents.

Monoclonal antibodies inhibiting human and mouse αvβ6 with high affinity have been developed and are divided into two biochemical classes (Weinreb *et al.*, 2004). One class of antibodies was cation-dependent, internalised by αvβ6-expressing cells and despite containing an RGD motif, was specific for αvβ6, not binding to other αv integrins (Weinreb *et al.*, 2004). The other class of antibodies was cation-independent; class members were not internalised and did not contain an RGD sequence (Weinreb *et al.*, 2004). The two classes were unable to bind to αvβ6 simultaneously suggesting that they may have overlapping epitopes (Weinreb *et al.*, 2004). Such antibodies could be used therapeutically to deliver radionuclides, cytotoxic drugs; or biological toxins to αvβ6-expressing cells; clinical trials are needed to test whether αvβ6 inhibition can effectively block SCC and fibrosis progression *in vivo.* Currently, the αvβ6 function blocking antibody 6.3G9 is in clinical trials for the treatment of pulmonary fibrosis (Biogen Idec., unpublished data.)

Xue and colleagues (2001), co-injected OSCC HSC-3 cells and anti-αvβ6 antibody into the floor of the mouth of nude mice. Ten days after injection, 100% of control animals (18/18) had formed tumours but only 40% of the αvβ6-treated mice (8/20) had developed these lesions. These same authors also investigated systemic

administration of an αv inhibitory antibody (which inhibited all αv integrins and was not specific to αvβ6) and found that although the antibody was inefficient at inhibiting early tumour growth at 10 days, after 38 days the tumours in the treated animals were 40% smaller than in the control group (Xue *et al.*, 2001). More recently, it has been shown that incorporating the specific high-affinity peptide A20FMDV20 to αvβ6 into an adenoviral vector resulted in improved tumour uptake *in vivo* and reduced hepatotoxicity, further validating αvβ6 as a potential tumour target and highlighting the potential for using adenoviral vectors in αvβ6-expressing tumours (DiCara *et al.*, 2008; Coughlan *et al.*, 2009).

1.3 Oral cancer

1.3.1 Background

1.3.1.1 Classification of oral neoplasms

The oral cavity extends from the skin of the lips to the junction of the hard and soft palate. The oropharynx extends from the hard palate superiorly to the plane of the hyoid bone inferiorly, and is continuous with the oral cavity through the faucial isthmus. The junction of the hard and soft palate separates between the oral cavity and the pharynx (Figure 1.6).

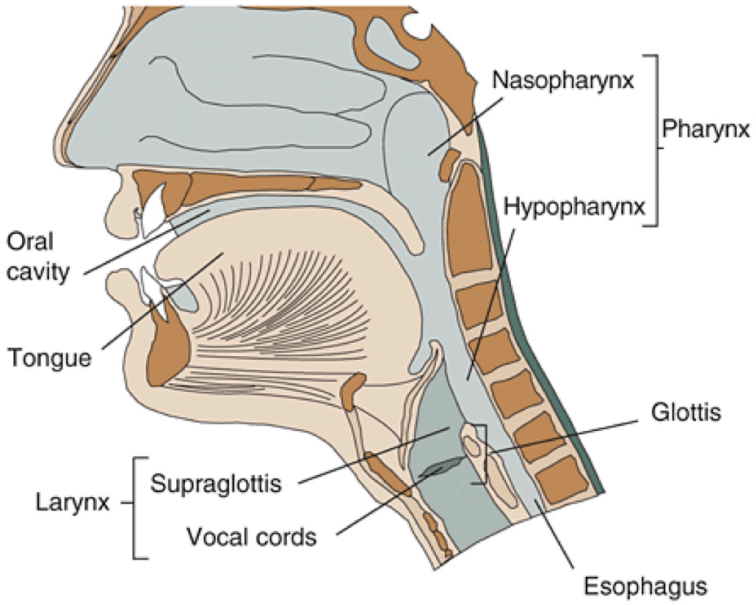

Figure 1.7 Anatomy of the upper aerodigestive tract. Image taken from the National Institute of Alcohol Abuse and Alcoholism website (http://www.niaaa.nih.gov/)

The most common cancer arising in the oral cavity and pharynx is squamous cell carcinoma (SCC), which is estimated to comprise over 90% of all oral malignancies (Warnakulasuriya, 2009); hence, the term “oral cancer” is used synonymously with OSCC. Oral cancers arise at different anatomic sites and they vary considerably in their epidemiologic, demographic, pathologic and clinical features. Thus, OSCCs can be categorised as SCCs of the lip; buccal mucosa; floor of the mouth (FOM) and oral tongue; gingival and alveolar mucosa; hard palate; and retromolar trigone. SCCs of the pharynx are categorised as: soft palate and uvula; oropharyngeal wall and tonsils and base of tongue. Histologically, keratinising squamous cell carcinoma (KSCC) is the most common SCC, with a broad range of morphologic variants that are of clinical significance. These variants include nonkeratinising squamous cell carcinoma (NKCa), basaloid squamous carcinoma (BSC), adenosquamous carcinoma (ASC), adenoid

squamous carcinoma, verrucous carcinoma (VC), papillary squamous carcinoma and spindle cell (sarcomatoid) carcinoma (Mao *et al.*, 2004).

1.3.1.2 Epidemiology of oral cancer

Oral cancer is an important global health problem in many parts of the world. Cancer of the oral cavity and pharynx is the sixth most common cancer worldwide, with an annual estimated incidence of over 400,000 (Warnakulasuriya, 2009). The incidence of oral cancer has a wide geographic variation, with nearly two-thirds of all cases diagnosed in the developing world. In the United Kingdom, 5410 new cases of oral and pharyngeal cancer were diagnosed in 2007, accounting for 2% of all new cancers; whilst 1882 cancer deaths from oral cancer were reported in 2008 (Cancer Research UK, 2010). Men are affected twice as often as women, but the incidence is rising in women. Most oral cancers arise between the fifth and eighth decades of life (Mao *et al.*, 2004). Oral cancer is associated with severe morbidity, due both to the disease itself and to treatment, which is chiefly by surgery with or without chemoradiotherapy; and the 5-year survival rate of approximately 50% has not improved in more than 2 decades (Marur & Forastiere, 2010).

1.3.1.3 Risk factors for oral cancer

Risk factors for oral and pharyngeal cancer can be classified into several categories, including: chemical carcinogens, oncogenic viruses, sunlight, oral hygiene, nutritional factors, genetic predisposition and immunocompromise (Warnakulasuriya, 2009).

Tobacco (smoked or chewed) and alcohol abuse are the chief chemical carcinogens related to oral cancer. Several epidemiological studies have demonstrated a strong link between tobacco use and the development of OSCC. Whilst alcohol is an independent risk factor, it appears to have a synergistic effect when combined with tobacco (Mao *et al.*, 2004). The risk of developing oral cancer is three to nine times greater in those who smoke or drink, and about 100 times higher in those who smoke and drink heavily, than nonsmokers and nondrinkers (Neville *et al.*, 2002). In total, around 75% of all oral cancers have been attributed to tobacco use and alcohol abuse (Warnakulasuriya, 2009). However, it is the widespread habit of chewing betel quid or paan that accounts for the very high incidence in oral cancer in South Asia.

Over the past two decades, overwhelming evidence has linked high-risk human papillomavirus (HPV), notably type 16, with tonsillar and base of tongue carcinomas

(D'Souza *et al.*, 2007). This is mainly in a distinct, nonkeratinising subtype of SCCs, and is found in patients with or without tobacco and alcohol use. Histopathology shows predominantly basaloid tumour islands. This subtype of head and neck cancers tends to present with better prognosis than the 'classic' OSCC cases, and tumours are generally responsive to chemo- and radiotherapy (Marur *et al.*, 2010).

1.3.1.4 Genetics and molecular biology of oral cancer

Like most epithelial cancers, OSCC is a multi-step process that develops as a result of multiple genetic and epigenetic alterations (Mao *et al.*, 2004; Hunter *et al.*, 2005). These changes commonly include loss of heterozygosity (LOH), mutations or promoter methylation of tumour suppressor genes; overexpression of oncogenes and changes in DNA repair gene expression (Figure 1.8; Argiris *et al.*, 2008). LOH is commonly observed at 3p, 9p and 17p. OSCCs frequently show deletions or mutations in the tumour suppressor gene P16INK4a (p16), a member of the retinoblastoma pathway (Jefferies *et al.*, 2001). TP53 (p53), a tumour suppressor gene located on the short arm of chromosome 17, is frequently mutated or deleted in OSCC (Brennan *et al.*, 1995).

Several genes or proteins have been shown to be upregulated in OSCC, including Cyclin D1, p63, cyclooxygenase-2 (COX-2) and epidermal growth factor receptor (EGFR), the latter of which has received attention as a possible therapeutic target (Hunter *et al.*, 2005; Nystrom *et al.*, 2006).

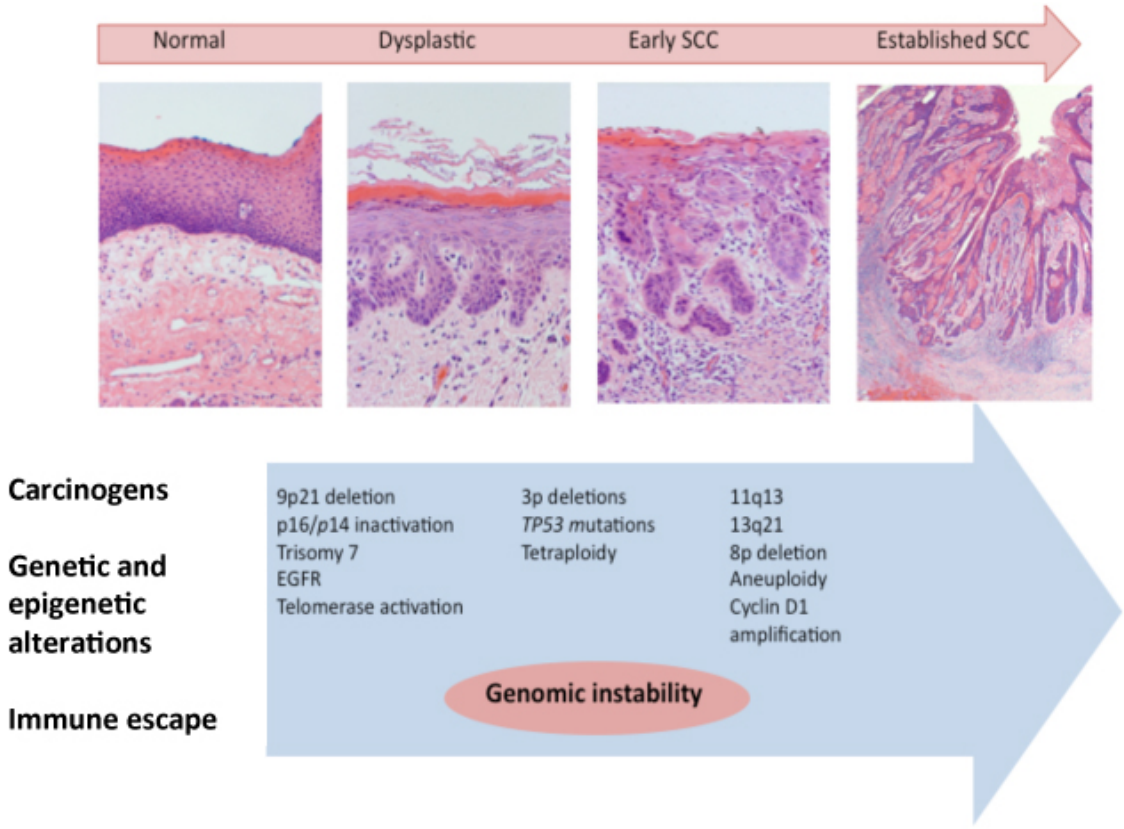

Figure 1.8 Phenotypical progression and accumulation of molecular alterations in oral cancer. Adapted from Arigiris *et al.*, 2008.

1.3.2 αvβ6 in oral cancer

High levels of αvβ6 expression have been described most consistently in OSCC, and this was first shown by Breuss and colleagues, who demonstrated high levels of αvβ6 in 27 out of 30 OSCC specimens examined. However, there was absent expression in normal oral mucosa specimens from the same patients. αvβ6 was found in both the primary tumour and in lymph node metastases buts its level did not correlate with the degree of tumour differentiation (Breuss *et al.,* 1995). Interestingly, αvβ6 expression was often localised to the host-stroma interface, i.e. the invasive front. In a similar study, strong expression of αvβ6 was detected in 90% of OSCC specimens but not in normal oral mucosa (Hamidi *et al.*, 2000).

Ragezi and colleagues examined floor-of-mouth *in situ* carcinomas and OSCC specimens and showed that they were also positive for αvβ6 expression in all cases, whereas normal oral epithelium was negative for αvβ6 (Ragezi *et al.*, 2002). More recently, Impola and colleagues examined αvβ6 expression in OSCC using *in situ* hybridisation and found that β6 mRNA was detectable in 100% of tumours (Impola *et al.*, 2004).

αvβ6 has now been shown to be of prognostic significance in several carcinoma types (Table 1.3). Given its consistent expression in OSCC, it would seem logical that a large study examining its potential role for prognosticating OSCC would of value.

1.4 Oral premalignancy

1.4.1 Background

Premalignant disorders of the oral and oropharyngeal mucosa can be defined as conditions of the epithelial lining that carry an increased risk of OSCC development in that area. These are a mixture of lesions defined by clinical appearance, histology or aetiology (summarised in Table 1.6). Given that OSCC can and does arise *de novo*, that not all premalignant lesions progress to OSCC and that, indeed, some regress spontaneously, it is expected that the term "potentially malignant disorders" would become more widely used to describe these conditions (van der Waal, 2010).

Disease name	Reference	Comment
Leukoplakia	Holmstrup *et al.*, 2006	Annual malignant transformation rate of 1%. Risk varies between different subtypes (homogenous; non-homogenous; verrucous)
Erythroplakia	Reichart & Philipsen, 2005	50% of erythroplakias showed OSCC histologically, 40% *in situ* cancer and 10% were dysplastic.
Oral lichen planus	Gonzalez-Moles *et al.*, 2008	Malignant potential debatable. Annual transformation rate of <1% has been quoted.
Oral submucous fibrosis	Tilakaratne *et al.*, 2006	Association with habitual betel quid chewing. 7-13% rate of malignant transformation.
Actinic cheilitis	van der Waal, 2009	Association with sun exposure, particularly in elderly men. No reliable figures for malignant transformation rate.
Immunodeficiency states	van der Waal, 2009	Increased incidence of oral cancers (particularly of the lip) in patients on long-term immunosuppressive therapy. Oral cancers in HIV patients have also been reported.

Table 1.6 Potentially malignant disorders of the oral cavity.

1.4.1.2 Oral submucous fibrosis

Oral submucous fibrosis (OSF) is a chronic, premalignant disease characterised by progressive submucosal fibrosis of the oral cavity, pharynx and occasionally, the upper oesophagus (Pindborg & Sirsat, 1966; Tilakaratne *et al.*, 2006). It is especially common in people of South Asian origin, with an estimated 5 million patients affected worldwide (Hazarey *et al.*, 2007). The main aetiological factor associated with the disease is the chewing of areca (betel) nut, practised by approximately 10-20% of the world's population, particularly in the Indian Subcontinent and Far East (Gupta & Warnakulasuriya, 2002), and recent studies have demonstrated a clear dose-dependent relationship between the use of areca nut and the development of OSF (Tilakaratne *et al.*, 2006). The chemical constituents of areca nut appear to play a major role in the pathogenesis of OSF, particularly the alkaloids arecoline, arecaidine, guvacine and guvacoline (Tilakaratne *et al.*, 2006). Approximately 7-13% of OSF cases have been reported to progress to oral squamous cell carcinoma (OSCC) (Tilakaratne *et al.*, 2006), and there is accumulating evidence that implicates areca nut in the development of other gastrointestinal malignancies, including oesophageal and liver carcinoma (Secretan *et al.*, 2009).

The progression of OSF involves fibrosis and hyalinisation of the sub-epithelial oral tissues, which accounts for most of the clinical features of the disease (trismus, dysguesia, dysphagia and dysarthria). The mechanisms initiating OSF development and progression, however, have yet to be determined: Research has focused primarily on fibroblasts, examining mechanisms regulating ECM synthesis and degradation (Tilakaratne *et al.*, 2006). It appears that the main pathological change in OSF is increased accumulation of type I collagen within the sub-epithelial tissues. This is thought to result from an imbalance between matrix deposition and degradation, and studies have found increased levels of fibrogenic cytokines such as bFGF, PDGF and TGF-β1 in OSF tissues (Haque *et al.*, 1998). Additionally, decreased proteolytic activity has been described, both as a result of downregulation of matrix metalloproteinases and up-regulation of protease inhibitors such as TIMPs (Tilakaratne *et al.*, 2006).

1.4.2 $\alpha v\beta 6$ in oral premalignancy

Several studies have demonstrated $\alpha v\beta 6$ expression in oral premalignancy. Hamidi and colleagues found that 41% of oral leukoplakia specimens were $\alpha v\beta 6$-positive, and that expression correlated with progression to malignant disease, suggesting that $\alpha v\beta 6$

expression may not only be useful in predicting malignant transformation but may actually promote this process. However, in the same study, αvβ6 expression was also seen in 85% of specimens of lichen planus, which has a much lower rate of malignant transformation, suggesting that expression of αvβ6 *per se* is not enough to drive malignant progression (Hamidi *et al.*, 2000).

In their study examining αvβ6 expression in OSCC, Ragezi and colleagues also detected αvβ6 in dysplastic areas adjacent to carcinomas, suggesting that changes in the expression of αvβ6 occur prior to acquisition of the invasive phenotype (Ragezi *et al.*, 2002). The authors concluded that transgression of the BM required additional molecular changes. The same authors also showed that αvβ6 and TN-C were variably expressed in oral dysplastic warts in men infected with human immunodeficiency virus (HIV) (Ragezi *et al.*, 2002).

1.5 Skin cancer

Malignancies of the skin are broadly classified into melanoma and non-melanoma cancers. Non-melanoma cancers of the skin are either squamous or basal cell carcinomas of the epidermis. Grouped together, nearly 100,000 cases were reported in the UK in 2008 (Cancer Research UK, 2008). Ultraviolet (UV) radiation is the chief risk factor for both types, and the management is primarily surgical.

1.5.1 Basal cell carcinoma

Basal cell carcinoma (BCC) is the most common malignancy in humans, and its incidence is increasing worldwide by 10% a year (Wong *et al.*, 2003; Crowson, 2006). The overwhelming majority of BCCs present clinically as slow-growing, indolent tumours that very rarely metastasise. Patient mortality is low, but the disease can present with significant morbidity thus forming a substantial burden on healthcare services. Approximately 80% of BCCs arise in the head and neck region (Scrivener *et al.*, 2002).

Although the major risk factor for BCC is exposure to UV radiation through prolonged exposure to sunlight, lesions can arise both on sun-exposed and non-exposed skin (Crowson, 2006). BCC is essentially a tumour of the light-skinned population and it usually arises in the 4^{th} to 5^{th} decade of life. Tumours can also arise in the context of genodermatoses such as xeroderma pigmentosum. Gorlin-Goltz syndrome (naevoid

basal cell carcinoma syndrome) is a condition in which BCCs arise alongside other abnormalities including keratocystic odontogenic tumours, skeletal abnormalities, and intracranial calcifications. In contrast to the isolated BCCs, which are mostly sporadic in nature, Gorlin-Goltz syndrome has an autosomal dominant pattern of inheritance (Scully *et al.*, 2010).

BCCs are morphologically diverse tumours, with several different histologic subtypes (Table 1.7). However, it is not uncommon for a single tumour to exhibit areas of several different patterns. Nodular (nodulocystic) BCC is by far the most common presentation, accounting for approximately 80% of all BCCs (Christenson *et al.*, 2005). Clinically, nodular BCCs present as small, pearly nodules with rolled, telangiectatic edges and an often ulcerated centre (hence the term 'rodent ulcer'). Histopathology shows well-defined tumour islands with peripherally palisaded nuclei and an occasionally retracted stroma (Marsh *et al.*, 2008). Nodular BCC is typically regarded as 'low-risk' owing to its inert clinical behaviour (Crowson, 2006).

In contrast to nodular BCC, morphoeic (morpheaform; sclerosing) BCC exhibit a more aggressive clinical presentation. They often present in the form of a fibrotic scar in sun-exposed areas. Histologically, the tumours are comprised of poorly circumscribed, thin, elongated nests of neoplastic cells in a dense, fibrotic stroma with plentiful myofibroblasts (Crowson, 2006). Morphoeic BCC can cause significant tissue destruction, and are prone to recurrence (Marsh *et al.*, 2008).

Type	% of BCCs	Histomorphology	Clinical Behaviour	Reference
Superficial	~ 7%	Atypical basaloid cells parallel to epidermis; occasional lymphocytic infiltrate	Indolent	Crowson, 2006
Nodular	~ 80%	Basaloid nodules of tumour cells with peripherally palisaded nuclei; slit-like retraction from stroma; may be pigmented	Indolent	Marsh *et al.*, 2008 Christensen *et al.*, 2005
Morphoeic	1-5%	Columns of basaloid cells in dense, collagenous, desmoplastic stroma	Aggressive; prone to recurrence	Crowson, 2006 Marsh *et al.*, 2008
Infiltrative	~ 7%	Irregular nests of tumour cells; frequently fibrotic stroma; risk of perineural infiltration	Aggressive	Crowson, 2006

Table 1.7 BCC subtypes.

1.5.2 Hedgehog signaling in the pathogenesis of BCC

Much of the understanding of the pathogenesis of BCC is derived from advances made in the aetiopathogenesis of Gorlin-Goltz syndrome. The majority of patients diagnosed with the syndrome harbour mutations in the human homologue of the Patched 1 (PTCH) tumour suppressor gene, a key component of the Hedgehog-Gli (HH-GLI) signaling pathway (Crowson, 2006). The importance of HH-GLI signalling has been confirmed in transgenic mouse models, where PTCH mutations in the basal keratinocytes was sufficient to induce BCC-like tumours in mice (Adolphe *et al.*, 2006). The overexpression of HH-GLI signaling mediators has also been shown to lead to the development of BCC-like tumours (Grachtchouk *et al.*, 2000; Nilsson *et al.*, 2000).

The HH-GLI pathway plays a particular role in pattern formation in embryonal development (Stecca & Ruiz i Altaba, 2010). Over the past few years, an emerging role

for HH-GLI has been identified in several cancers, including those of the skin, brain, colon, lungs, prostate, blood and pancreas (Neill *et al.*, 2004; Stecca *et al.*, 2007; Marsh *et al.*, 2008; Stecca *et al.*, 2009; Stecca & Ruiz i Altaba, 2010).

The Sonic Hedgehog Homolog (SHH) is the best studied ligand of the hedgehog signalling family, which also comprises desert hedgehog (DHH) and Indian hedgehog (IH) (Beachy *et al.*, 2004). SHH signal transduction involves binding of the SHH protein to its receptor, the 12-transmembrane protein Patched 1 (PTCH), which in the absence of its ligand normally represses pathway activity by inhibiting another protein, the 7-span transmembrane Smoothened (SMOH). Binding of the HH protein to PTCH removes this inhibition, thereby activating SMOH, which in turn triggers an intracellular signalling cascade enabling the activation of the Glioma associated family of transcription factors (Gli), Gli1 through Gli3 (Stecca & Ruiz i Altaba, 2010).

The three Gli proteins (Gli1, Gli2 and Gli3) are transcription factors of >1000 amino acids that encode both activator and repressor functions. In responding cells, they act together to integrate HH and other signalling inputs to determine tissue pattern, size and shape during organ morphogenesis (Ruiz i Altaba *et al.*, 2007). Gli1 lacks a repressor domain, and is thus primarily a transcriptional activator; whereas Gli2 has both activator and repressor domain and Gli3 is predominantly a transcriptional repressor (Neill *et al.*, 2003). In the absence of HH ligands, the zinc finger transcription factor Gli1 is normally transcriptionally repressed (Stecca & Ruiz i Altaba, 2010). When the pathway is active, its function is reinforced by a positive feedback loop, making it the best read-out of an active HH pathway (Bai *et al.*, 2004). Gli targets include a variety of genes that regulate cellular processes such as proliferation and differentiation (FoM1, CyclinD1, Wnts), survival (Bcl2), angiogenesis (Vegf) and EMT (Snail1, Sip1, Elk1 and Msx2).

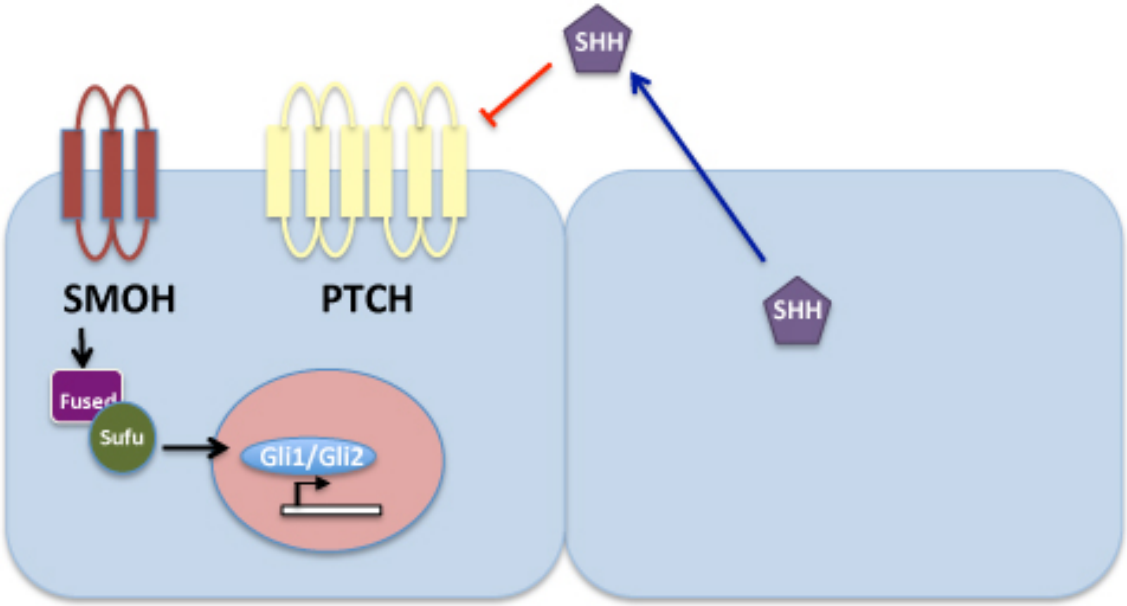

Figure 1.9 Sonic Hedgehog signalling pathway.
PTCH receptor normally has an inhibitory action on SMOH. This is removed in the presence of SHH, which inhibits PTCH. SMOH then facilitates the nuclear translocation of the Gli family of transcription factors, which mediate the transcription of various target genes implicated in cancer. PTCH, Patched-1; SMOH, Smoothened; SHH, Sonic Hedgehog Homologue; SUFU, Suppressor of Fused Homologue.

Gli1 was originally identified as an oncogene amplified in glioblastoma, where its ability to transform primary cells was described (Kinzler *et al.*, 1987). *In situ* hybridisation studies on fresh patient-derived tissues have shown that tumour cells express Gli1 and other HH-GLI components in BCC, melanomas, gliomas, medulloblastomas, prostate and colon cancers (Stecca & Ruiz i Altaba, 2010).

1.5.2.1 Hedgehog signalling and integrins

One of the earliest studies examining integrin signalling interactions with the HH-GLI pathway was carried out by Goh and colleagues, in which they examined mesodermal defects in $\alpha5\beta1$ deficient mice (Goh *et al.*, 1997). The authors found an interruption in SHH expression in the developing notochord of $\alpha5^{-/-}$ mice, suggesting a modulation of the SHH pathway by $\alpha5$ integrin signalling. In another study, SHH was found to have an inhibitory effect on αv-, α1- and α4-mediated adhesion and migration of neural crest cells *in vitro* (Testaz *et al.*, 2001).

Recently, work from our laboratory described a potential role for αvβ6 in the pathogenesis of morphoeic BCC (Marsh *et al.*, 2008). By immunohistochemistry, we found that αvβ6 was highly expressed in this variant of BCC, but was weakly present in the low-risk nodular subtype. In the study, it was shown that αvβ6 promoted BCC tumour cell invasion indirectly, by activating TGF-β1 and promoting myofibroblastic transdifferentiation *in vitro*; findings which were recapitulated *in vivo*, where morphoeic BCC displayed a prominent desmoplastic stroma. SHH pathway components, particularly Gli1, have been shown to be expressed at high levels in nodular BCC, but the potential interaction with αvβ6 has not been investigated as yet.

1.6 Aims of the Study

The epithelial-specific integrin αvβ6 is not normally detectable in healthy adult epithelia but is overexpressed in OSCC (Breuss *et al.*, 1995; Renkonen *et al.*, 2002) and in pathogenic organ fibrosis (Hahm *et al.*, 2007; Wang *et al.*, 2007; Popov *et al.*, 2008; Horan *et al.*, 2008). The integrin has been shown to promote tumour cell invasion both directly and indirectly. However, the exact mechanisms regulating its expression and function are yet to be elucidated.

αvβ6 has also been shown to promote disease progression both in cancer and fibrosis via activating TGF-β1 and thus promoting fibroblast-to-myofibroblast transdifferentiation (Marsh *et al*. 2008). Furthermore, it has been shown to be implicated in the EMT of colorectal cancer (Bates *et al.*, 2005) and in gingival fibrosis (Sume *et al.*, 2010). It is plausible that the integrin is implicated in similar processes in other pathologies.

The overall aim of this project was to identify how expression of β6 expression is upregulated in pathogenic disease states of the head and neck; namely, carcinoma, premalignancy and fibrosis, and to use this knowledge to try to prevent the development of disease and to develop novel treatment modalities.

The specific objectives of this project were to:

- Study the role of αvβ6 integrin in the potentially malignant disorder oral submucous fibrosis.
- Dissect the interaction between αvβ6 integrin and Sonic Hedgehog Signaling pathway components in the context of basal cell carcinoma.
- Examine the potential utility of αvβ6 integrin as a prognostic marker for OSCC.
- Develop the relevant tools to study the mechanisms regulating the expression of αvβ6 integrin both in health and in disease.

Chapter 2
Materials and Methods

2.1 Tissue culture

2.1.1 General principles of cell culture

Routine cell culture was carried out in a laminar flow hood. All tissue culture reagents were sterilised using 0.22 μm filter (Millipore, Watford, UK), using either a syringe or a vacuum driven filter, and stored in sterile containers at 4° C. Prior to use, media and reagents were placed in a water-bath at 37° C. Cells were grown in a humidified environment of 5-10% CO_2 in incubators maintained at 37° C. Media and solutions are listed in Appendix 9.1

2.1.2 Keratinocyte cell lines and growth requirements

Keratinocyte cell lines used in this study are listed in Table 2.1.

Cell lines	Origin	Level of αvβ6 expression
CA1	Oral keratinocytes derived from an SCC of the tongue (Mackenzie, 2004)	Moderate
BICR6	Oral keratinocytes derived from an SCC (Forsyth *et al*., 2002)	High
Detroit 562	Oropharyngeal keratinocytes derived from SCC of the pharynx (Bartelt & Duncan, 1978)	High
SCC25	Oral keratinocytes derived from an SCC of the tongue (Vermeer *et al*., 1986	High
H400	Oral keratinocytes derived from SCC of the alveolar process (Prime *et al*., 1990)	High
VB6	Oral keratinocytes from an SCC of the tongue transfected with β6 cDNA (Thomas *et al*., 2001a)	High
C1	Oral keratinocytes from an SCC of the tongue transfected with αv cDNA (Thomas *et al*., 2001a)	Low
IC6pr	Oral keratinocytes from an SCC of the tongue retrovirally infected with pBABE empty vector (generated in this study)	Nil
OKF6/Tert1	Immortalised oral keratinocytes derived from normal oral mucosa (Dickson *et al*., 2000)	Low
N/Tert-puro	Immortalised epidermal keratinocytes derived from normal skin retrovirally infected with pBABE empty vector (Dickson *et al*., 2000; Marsh *et al*., 2008)	High
NTGli1	N/Tert cells retrovirally infected with Gli1 cDNA (Regl *et al*., 2002)	Low
HaCaT-puro	Spontaneously immortalised skin keratinocytes derived from normal skin of the back (Boukamp *et al*., 1988), retrovirally infected with pBABE empty vector (generated in this study)	High
HaCaT-Gli1	HaCaT cells retrovirally infected with Gli1 cDNA (generated in this study)	Low

Table 2.1 Keratinocyte cell lines used in the study.

CA1, H400 and BICR6 are OSCC cell lines which express varying levels of endogenous β6 protein; they were kindly provided by I. Mackenzie (Queen Mary University of London), S. Prime (University of Bristol) and K. Parkinson (Queen Mary University of London), respectively. OKF6/TERT-1 is an immortalised oral keratinocyte cell line obtained from the Rheinwald Laboratory (Harvard Institute of Medicine). N/Tert and N/Tert-Gli1 are skin keratinocyte cell lines that were kindly provided by Dr. Graham Neill (Queen Mary University of London). Detroit 562 and HaCaT are derived from a carcinoma of the oropharynx and normal epidermis, respectively, and were both obtained from the European Collection of Cell Cultures. Unless otherwise indicated, all oral and epidermal keratinocyte cell lines were cultured in oral or epidermal keratinocyte growth medium, respectively (O-KGM and E-KGM; Appendix 9.1).

2.1.2.1 Generation of the HaCaT-Gli1 and H400-Gli1 cell lines

The pBABE-Gli1 retroviral vector containing Gli1 coding cDNA, pBABE-puro empty vector and the Phoenix packaging cell line were all generous gifts from Dr. Graham Neill (Queen Mary University of London). Amphotropic retrovirus was produced using the Phoenix packaging cell line. 1.5 x 10^6 Phoenix cells were plated in a 6-cm dish 18 hours (h) prior to transfection (~ 80% confluency), following which 10 μg of plasmid DNA (pBABE-Gli1 or pBABE-puro) was introduced using Fugene (Roche, UK) at a ratio of 1:3 (μg DNA : μl Fugene). 24 h post-transfection cells were selected in Puromycin (2 μg/ml) for 48 h (at least). The drug selection was then removed, cells were fed fresh medium and incubated for 24 h at 32° C prior to harvesting retroviral supernatant. The supernatant was filtered through a 0.45 μm filter and stored at -80° C until use.

HaCaT and H400 cells were plated at a density of 1 x 10^6 18 h prior to retroviral transduction. Post-transduction, cells were incubated for 24 h and then selected in Puromycin (2 μg/ml) for 48 hours at least. The drug selection was then removed, cells were fed fresh medium and cultured routinely. Gli1 expression in HaCaT-Gli1 and H400-Gli1 cells was confirmed by Western blotting.

2.1.3 Fibroblast cell lines and growth requirements

Fibroblast cell lines used in this study were human foetal foreskin fibroblasts (HFFF2), grown in fibroblast growth medium (FGM) without antibiotics (Appendix 9.1). They were obtained from the European Collection of Cell Cultures.

2.1.4 Primary fibroblast culture

Tissue surplus to diagnosis from patients undergoing routine oral biopsies at the Department of Oral and Maxillofacial Surgery, Southampton University Hospitals NHS Trust was taken after obtaining written, informed consent. Appropriate ethical approval was in place (REC No. 09/H050/50). The tissue was harvested and transported in phosphate-buffered saline (PBS) supplemented with 250 ng/ml amphotericin, 100 IU/l penicillin and 100 mg/l streptomycin. The tissue was washed twice in PBS and left in PBS supplemented with antifungals and antibiotics until further treatment. To isolate fibroblasts, the tissue was cut into $2mm^3$ pieces and a single piece was placed in a well of a six-well plate and placed in an incubator. The explants were cultured in primary fibroblast growth medium (Appendix 9.1).

2.1.5 Routine cell culture

Cells were grown as adherent monolayers in sterile tissue culture flasks (BD Falcon™ or Corning) in a humidified atmosphere (5-10% CO_2) at 37° C in incubators. When the cells were approaching confluency (80-90%) they were subcultured (usually 2-3 times per week) at a ratio of 1:3 to 1:10 depending upon the growth rate. After aspiration of the existing medium, the cell layer was rinsed briefly with PBS to remove traces of serum, which contains trypsin inhibitors. Trypsin/EDTA (0.05% trypsin (w/v)/5mM EDTA, Invitrogen) was then added to the cells for 5-10 minutes (min) at 37° C. Once the cells had been detached from the plastic, the trypsin was inactivated by the addition of serum-containing medium. Aliquots of cell suspension were then added to new tissue culture flasks containing fresh medium.

2.1.6 Storage and recovery of liquid nitrogen stocks

2.1.6.1 Cryopreservation of cells

Cells growing in log phase growth were pelleted and resuspended in pre-filtered foetal calf serum containing 10% DMSO (Sigma-Aldrich®) at a concentration of 1-2 x 10^6 cells/ml and kept on ice. One ml of cell suspension was pipetted into labelled Nunc cryotubes in an insulated polycarbonate freezing container (“Mr Frosty”, Nalgene®) and placed at −80° C overnight, before transfer to −196° liquid nitrogen for long-term storage.

2.1.6.2 Thawing cell stocks

Vials removed from liquid nitrogen were immediately placed in a water bath at 37° C. Following complete thawing, the contents of the vial were pipetted into 15 ml tubes (BD Falcon™) containing pre-warmed serum-containing medium and centrifuged at 1,200 rpm for 3 min. The supernatant was discarded and the cell pellet was resuspended in growth medium and transferred to a 25cm^2 flask containing fresh medium. Cells retrieved from long-term storage were cultured routinely for 1 week prior to experimental use.

2.1.7 Cell counting

Cells were counted using a CASY automated cell counter (Shärfe System, Reutlingen, Germany). This process involves suspending cells in filtered isotonic buffer ("Isoton", Coulter Euro Diagnostics, GMBH, Buckinghamshire, UK) and passage through a fine gauge tube. The cells elicit a change in the direction of current flow, producing a series of pulses, which are sorted and counted.

2.2 Antibodies and reagents

Antibodies and reagents (including inhibitors) used in this study are summarised in Appendix 9.2.

2.3 Analysis of cellular proteins

Western blotting, flow cytometry and ELISA (enzyme linked immunosorbent assay) are common methods of analysing cellular proteins. Each of these will be discussed in turn.

2.3.1 Western blotting

2.3.1.1 Cell lysis

Cells that were nearing confluency were washed with ice-cold PBS, being careful to remove all remaining fluid with a 200 μl pipette. A 100 μl solution of NP40 buffer (Appendix 9.1) with freshly added protease inhibitor cocktail at a dilution of 1:100 (Calbiochem, Darnstadt, Germany) was added to each well or plate and the cells were scraped on ice using a cell scraper. The lysates were then cleared by centrifugation at 4° C for 10 min at 13,300 rpm in a microcentrifuge tube. The supernatant was carefully pipetted into a fresh microcentrifuge tube, aliquoted and stored at –20° C until use.

2.3.1.2 Estimation of protein concentration

Protein concentration was determined by using the BIO-Rad DC Protein Assay (Bio-Rad Laboratories, Hercules, Hertfordshire, UK) according to the manufacturer's instructions. This is a colourimetric assay based on the Lowry assay and depends upon the reaction between protein and copper in an alkaline medium, and the subsequent reduction of Folin reagent by the copper-treated protein. A blue colour develops, which is read on a spectrophotometer at 650 nm absorbance.

Bovine serum albumin [(BSA); Sigma-Aldrich ®] protein standards were set up at protein concentrations of 0, 125, 250, 500, 750, 1500, 2000, 4000 and 5000 μg/ml. Firstly, 5 μl of standard solution (in duplicates) and lysate samples were added into each well of a 96-well plate. 1 ml of reagent A was added to 25 μl reagent S to form Reagent A', 25 μl of which was then pipetted into each well. 200 μl Reagent B was then added to the wells and the plate incubated at RT for 15 minutes. The plate was read at OD 650 nm on a spectrophotometer (BD Biosciences). The concentration of the unknown proteins was determined against the standard curve using Microsoft Excel.

2.3.1.3 Sodium dodecyl sulphate polyacrylamide gel electrophoresis (SDS-PAGE)

Cellular proteins were separated using a polyacrylamide gel mounted on a vertical gel electrophoresis apparatus system (Xcell SureLock™ Novex Mini-Cell system, Invitrogen Ltd.), and the 1 or 1.5 mm thick gels assembled according to the manufacturer's instructions. The desired percentage of acrylamide gel (Appendix 9.1) was poured into the gel cassette and covered with propan-2-ol to eliminate the air interface (which inhibits acrylamide polymerisation). The gel was allowed to polymerise for about 30 min, the propan-2-ol poured off and a 4% stacking gel (Appendix 9.1) was poured onto the resolving gel, and allowed to polymerise for a further 30 min. The gel was then placed into the electrophoresis tank and the chamber filled with SDS-running buffer (Appendix 9.1). Lysate samples were diluted in loading buffer (Appendix 9.1), boiled for 10 min, the contents spun down by centrifugation and loaded using capillary disposable pipette tips. The gel was run for 10 min at 100 Volts, then 120 Volts for 1 h, until sufficient protein migration had occurred, as evidenced by migration of the loaded molecular weight markers (Fermentas, UK) and the dye in the loading buffer. After

running, the apparatus was dismantled carefully, the gel removed and equilibrated in transfer buffer (Appendix 9.1).

2.3.1.4 Immunoblotting

After separation of the proteins on the polyacrylamide gel, they were transferred to a polyvinylidene fluoride (PVDF) membrane (ImmunoBlon™; Amersham Life Science). The membrane was laid on the gel and sandwiched two 3 mm Whatman Chromotography papers (Whatman Int, Maidstone, UK). Using a transfer cassette, the sandwiched gel was compressed in the cassette and assembled according to the manufacturer's instructions (XCell II™ Blo Module; Invitrogen Ltd.). The cassette was immersed in transfer buffer (Appendix 9.1). Proteins were transferred at 30 Volts for 75 min at RT or at 12 Volts overnight at 4° C. After completion of protein transfer, the membrane was incubated in blocking solution (Appendix 9.1), to minimise non-specific antibody binding, for 1 hr at RT with gentle agitation. Depending on the primary antibody, the membrane was then incubated with the primary antibody diluted in blocking solution overnight at 4° C or 1-2 hr at RT. The blot was then washed 3 times (5 min each) in washing buffer (Appendix 9.1) before incubation with 1:1,000 HRP-conjugated secondary antibody (Dako, UK) for 1 hr at RT with agitation. The membrane was washed again 3 times (5 min each) in washing buffer and bound antibody was detected using chemiluminescence (SuperSignal West Pico, ThermoScientific) or enhanced chemiluminescence (SuperSignal West Femto, ThermoScientific). Images were visualised using an automated imager (QuantityOne). Blots were probed for Hsc-70 or β-actin as a loading control (Appendix 9.2). Exposures of blots in the linear ranged were quantified by densitometry software (ImageJ, National Institute of Health, USA).

2.3.2 Flow cytometry (FACS analysis)

Adherent cells to be labelled with anti-αvβ6 monoclonal antibody (620.w, Appendix 9.2) were allowed to approach confluence and were trypsinised, washed twice in 0.1% BSA in DMEM (0.1% DMEM) and re-suspended in 200 μl 0.1% DMEM in a FACS tube (BD Biosciences™). Cells were then incubated with 620.w for 45 minutes on ice. After incubation, the cells were pelleted by centrifugation at 1,200 rpm for 3 min and washed twice in 0.1% DMEM. The pellet was re-suspended in 0.1% DMEM containing Alexa 488-conjugated IgG secondary antibody (Appendix 9.2). The cells were mixed and incubated with the secondary antibody for 30 minutes at on ice. Control samples were labelled with mouse IgG class-matched negative control (Dako). Unlabelled controls

used secondary antibody only. Cells were then washed 3 times in 0.1% DMEM, twice in FACS buffer (Appendix 9.1), re-suspended in 100 μl FACS buffer and kept on ice until flow cytometric acquisition. Labelled cells were scanned on a FACSCalibur or FACSCanto II cytometer (BD Biosciences™) and analysed using FACSDiva software (BD Biosciences™). With each cell line, the same settings were used for each experiment.

For E-cadherin flow cytometry, adherent cells to be labelled with anti-E-cadherin monoclonal antibody (HECD1, Appendix 9.2) were allowed to approach confluence and were trypsinised in EDTA-free trypsin (Invitrogen), and the rest of the experiment was carried out as described.

2.3.3 Enzyme linked immunosorbent assay (ELISA)

Acid-activated TGF-β1 was measured using an ELISA kit (Quantikine®, R&D Systems). One ml aliquots of cell-conditioned media were snap frozen and the adherent cells detached and counted. Prior to analysis, samples were centrifuged at 2,000 rpm for 3 min to remove cell debris. The TGF-β1 ELISA was performed according to the manufacturer's instructions. Experiments were carried out in quadruplicate and all measurements were performed in duplicate.

2.4 Functional assays

2.4.1 Transwell® invasion assay

Cell invasion assays were performed using Transwells® (Costar®, Corning Inc. Life Sciences, Corning, NY, USA) in which an upper and lower chamber are divided by a polyethylene tetraphthallate membrane 6.5 mm in diameter with 8 μm pore size (Figure 2.2). 5 x 10^4 keratinocytes/well were plated in the upper chamber, incubated for 72 h and allowed to invade through the membrane into the lower chamber towards a chemo-attractant (KGM; Appendix 9.1).

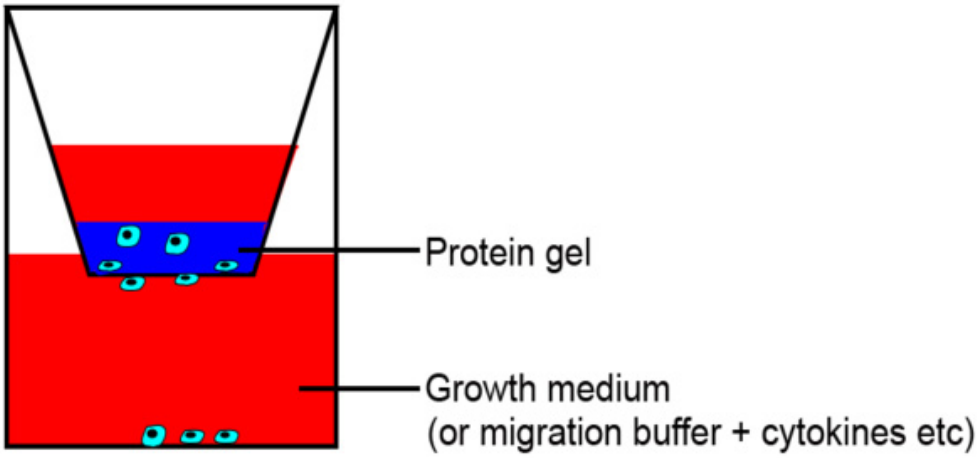

Figure 2.1 Transwell® invasion assay.

Inserts were coated with 70 μl Matrigel® (BD Biosciences, Bedford, MA, USA), diluted 1:2 in α-MEM, and allowed to polymerise at 37º C for 1 h. To act as a chemo-attractant, 500 μl of KGM was placed in the lower chamber. Cells grown on tissue culture plastic were trypsinised and added to a 50 ml Falcon tube, which was filled completely with α-MEM. Cells were centrifuged at 1,200 rpm for 3 min and the pellet re-suspended in α-MEM. Cells were plated in the upper chamber of quadruplicate wells at a density of 5 x 10^4 in 200 μl α-MEM and incubated 37º C for 72 h.

After incubating for 72 h at 37º C, the KGM in the lower chamber was aspirated off with a 1 ml pipette and the chamber washed with PBS. Cells attached to the floor of the lower chamber, and those still on the undersurface of the Transwell® insert were harvested by the addition of 500 μl trypsin/EDTA into the lower chamber. With the insert still in place, the Transwells® were incubated at 37º C for 1 h following which the undersurface of the insert was washed twice, carefully, with trypsin from the lower chamber to rinse off any remaining adherent cells. The total volume of trypsin (500 μl) containing the detached cells was pipetted into 9.5 ml filtered Isoton and counted using a CASY counter as described in section 2.1.7.

For blocking experiments, anti-αvβ6 antibody (6.3G9, 10 μg/ml) was added to the cells for 30 min prior to plating and was present during the entire experiment.

2.4.2 Transwell® migration assay

Haptotactic migration assays were also performed using Transwell® inserts. The undersurface of the polycarbonate filters were coated with LAP (0.5 μg/ml) and cells were plated into the upper chamber and allowed to migrate for 24 hours (Figure 2.2). Cells migrating to the lower chamber were trypsinised and counted on a CASY counter. Keratinocyte treatments were carried out prior to the migration assays and blocking antibodies were added to the cells for 30 minutes (on ice) before plating and were present throughout the assay, as described in section 2.5.1.

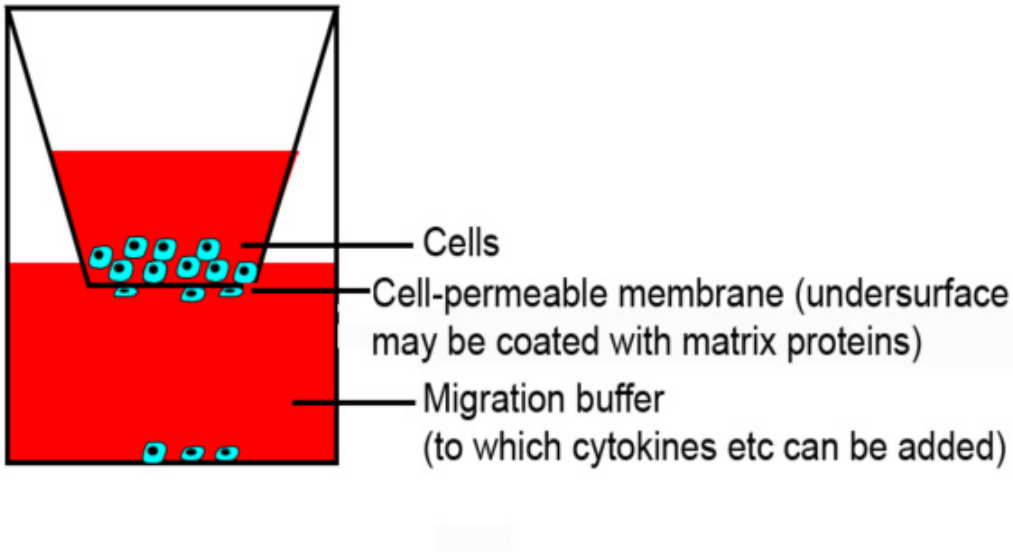

Figure 2.2 Transwell® migration assay.

2.4.3 Organotypic culture

2.4.3.1 General principles of organotypic culture

Tumour cell invasion is not easily studied *in vitro*, and whilst techniques such as Transwell® assays represent a simple approach to studying invasion, it is recognised that these fail to re-establish the *in vivo*-like tumour environment, and trade physiological relevance for ease of repetition. However, advances in tissue culture techniques have allowed the development of "organotypic" culture models that better replicate *in vivo* patterns of cell behaviour and differentiation. In organotypic culture, epithelial cells are grown at an air/liquid interface on collagen matrices populated with fibroblasts. Such models have allowed study of cell interactions, whether in the context of normal epithelial growth and differentiation, or between tumour cells and stromal components.

2.4.3.2 Preparation of organotypic cultures

To prepare organotypic gels, 3.5 volumes of Type I rat-tail collagen (Millipore) and 3.5 volumes of Matrigel were mixed on ice with 1 volume 10x DMEM (Gibco®), 1 volume FCS and 1 volume 10% DMEM in which fibroblasts had been suspended at a concentration of 0.5 x 10^6 /ml (final collagen concentration was 2 mg/ml). The solution was neutralised as necessary by drop-wise addition of 0.1 M sterile-filtered sodium hydroxide, and mixed gently by pipetting up and down (taking care to prevent the introduction of air bubbles). Then, 1 ml of this solution was pipetted into each well of a 24-well plate and allowed to polymerise at for 30 min at 37° C. After polymerisation, 1 ml of FGM was then added to each well and the gels were left for 18 hours at 37° C to equilibrate. Concurrently, a fibroblast-free collagen gel mix (made as above but with 1 volume of FGM in which no fibroblasts were suspended) was used to coat sterile (autoclaved) nylon discs (100 μm pore size, Tetko Inc; New York, USA).

After polymerization at 37° C for 10 minutes, gels were fixed in 1% glutaraldehyde (Sigma-Aldrich®) then washed 4 times in PBS and twice in 10% DMEM. They were then left at 4° C until required. Twenty-four hours later, the medium covering the gels was aspirated from the wells and 0.5-1 x 10^6 keratinocytes (suspended in α-MEM supplemented with 10% FCS and L-glutamine) were added to each well. Next day, the medium covering the gels was aspirated, thus allowing the gels to be removed from the 24-well plate using a sterile spatula, and these were placed onto individual collagen-coated nylon discs resting on steel grids. These steel grids were made from 2.5 cm^2 squares of stainless steel mesh with the edges bent down to form 4-5 mm high “legs”. This initial time point was defined as day 1 of the organotypic culture. The steel grids were placed in 6-well plates and sufficient growth medium was added to reach the undersurface of the grid, allowing the epithelial layer to grow at an air-liquid interface. The growth medium used for organotypic culture was KGM, and the medium was changed every 2-3 days. Treatments (including siRNA) were present throughout the experiment(s). After 7-14 days, the gels were bisected, fixed in 10% formol saline and processed to paraffin. Figure 2.3 demonstrates a typical organotypic experiment.

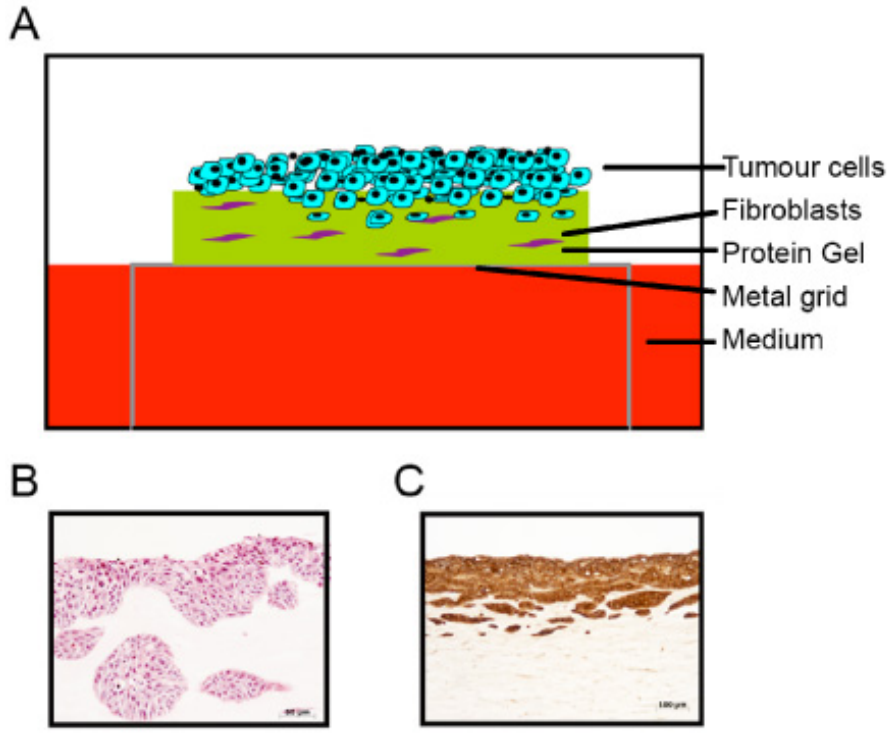

Figure 2.3 Organotypic cultures.
2.3(A) Schematic representation of an organotypic culture.
2.3(B) H&E-stained section of basal cell carcinoma organotypic culture demonstrating surface epithelium and invading islands of tumour.
2.3(C) A squamous cell carcinoma organotypic culture immunostained for cytokeratins to highlight the tumour cells.

To assess the effect of gene silencing on SCC invasion, keratinocytes transfected with siRNA were counted and incorporated into organotypic culture 24 h after transfection.

In some experiments, arecoline (5-10 μg/ml) and/or tropicamide (350 μM) were added to the keratinocytes 48 h prior to plating and were added to the growth medium whenever the cultures were fed such that the supplements were present throughout the entire experiment.

2.4.4 Collagen gel contraction assays

Fibroblasts were cocultured with keratinocytes with or without αvβ6-blocking antibodies (6.3G9, 10 μg/ml) prior to seeding in type I collagen at a final concentration of 1 x 10^6 cells/ml and 2 mg collagen/ml. The mixture was poured into 24-well tissue culture plates (1 ml per well) and allowed to polymerise at 37° C for 1 h. 1 ml of 10% DMEM was then added and the gels manually detached from the wells. Gel contraction was measured at 24 h by weighing the gels.

2.5 Generation of tissue microarrays

Basal cell carcinoma specimens derived from 20 nodular and 20 morphoeic cases of patients presenting to Southampton General Hospital from January 2010 to February 2011 were selected for the study. Two tissue microarrays were constructed, for each tumour subtype, containing 20 specimens. Triplicate cylindrical cores (1 μm in diameter) were taken from representative areas of each tumour, as determined by a consultant pathologist (Professor Gareth Thomas) and arrayed onto a new recipient paraffin block using a tissue microarrayer (Alphelys MiniCore® 3)

2.6 Immunohistochemistry

Paraffin sections from OSCC, OSF and BCC specimens derived from archival material were de-waxed in xylene, brought to absolute ethanol and endogenous peroxidase neutralised with 0.5% hydrogen peroxide in methanol for 15 min. After 2 washes in TBS, an Immedge™ Pen (Vector Laboratories Inc., Burlingame, CA, USA) was used to delineate the specimen on the slide, surrounding it with a hydrophobic barrier in order to minimise the volume of reagents required to coat the samples.

Antigen retrieval varied according to the primary antibody: Digest-All Pepsin solution (Invitrogen) for 5-7 minutes at 37° C (6.2G2; 6.2A1); microwaving for 30 minutes in 0.01 mol/L pH 6.00 citrate buffer (Smad4, pSmad2); whilst for certain antibodies, no antigen retrieval was required (α-SMA, Gli1). Sections were then washed twice in PBS and treated with an Avidin/Biotin block (Vector Laboratories Inc.) according to the manufacturer's instructions. Non-specific protein binding was blocked with a solution of 5% normal serum (from the species in which the secondary antibodies was raised in) in TBS. Negative control antibody was a class-matched immunoglobulin used at the same concentration (Dako). Primary antibody was applied and the samples left overnight at 4° C. The next day samples were washed twice in TBS and secondary biotinylated secondary antibody (Vectastain Elite, Vector Laboratories Inc.) applied for 30 min. Sections were washed in PBS and peroxidase-labelled streptavidin (Vectastain Elite ABC Reagent; Vector Laboratories Inc.) was applied for 30 min. Peroxidase was visualised using DAB+ (Dako Cytomation, Carpinteria, CA, USA) for 5-7 min following which samples were washed in running tap water for 2 min, counterstained in Mayer's haematoxylin (Sigma-Aldrich®) for 1 min, washed in running tap water for a further 1 min, and immersed in TBS as a blueing agent for 1 min. The sections were then dehydrated (using the dewaxing protocol described above in reverse order) and then mounted using DPX Mounting Medium (Sigma-Aldrich®).

Staining was scored by two consultant pathologists (Professor Gareth Thomas and Dr Kim Piper), using the Quickscore method. For immunohistochemical analysis of αvβ6, the staining intensity was scored on a scale of 1 to 3 (1, weak; 2, moderate and 3, strong), and the proportion of cells staining positively was scored on a scale of 1 to 4 (1, focal staining confined to basal layer; 2, diffuse staining confined to basal layer; 3, diffuse staining of basal and suprabasal layers; and 4, diffuse staining of full thickness of epithelium). The score for intensity was added to the score for proportion to give a score in the range of 0 to 7 and grouped as negative (score = 0), low (score = 1-4) or high (score = 5-7). For Gli1, nuclear staining intensity was scored on a scale of 1 to 3 (1, focal; 2, patchy; 3, diffuse)

2.7 Immunofluorescence

2.7.1 Staining cells cultured on coverslips

2-5 x 10^4 cells were counted and plated on 13mm coverslips and allowed to grow from 24-72 h depending on the experiment. Cells were then fixed for 10 minutes in 4% formaldehyde in cytoskeletal buffer (10 mmol/L MES, 3 mmol/L $MgCl_2$, 138 mmol/L KCl, 2 mmol/L EGTA; pH 6.1) with 0.32 mol/L of sucrose. Cells were permeabilised for 5 min with 0.2% Triton X-100 and incubated for 30 min in 0.1% DMEM. Nonspecific staining was blocked by incubation in 5% normal serum from the animal species in which the secondary antibody was raised in for 1 hr at RT. Cells were then incubated for 1 h at RT with primary antibody (Appendix 9.2). Three washes in 0.1% Triton-X/PBS were performed, and binding detected by incubation with secondary antibodies conjugated with Alexa 488 or 546 (Molecular Probes, Invitrogen) for 45 min at RT. Nuclei were visualised using 4',6-diamidino-2-phenylindole (DAPI) or To-Pro3 (Invitrogen) for 10 min at RT (both diluted 1:5,000 in PBS/0.1% Triton-X100). Coverslips were mounted onto glass slides using Fluorescent Anti-Fade mountant (Dako) or Pro-Long Anti-Fade (Invitrogen). All antibody dilutions were in PBS/0.1% Triton-X100, except for αvβ6 (0.1% DMEM). Negative controls were with isotype-specific immunoglobulins at matching concentrations.

2.7.2 Staining paraffin embedded tissue and organotypic cultures

For immunofluorescent staining of paraffin embedded patient tissue and organotypic gels, sections were dewaxed and rehydrated and antigens were retrieved (as described in Section 2.7). Sections were then permeabilised in 0.2% Triton-X100, blocked with 2% BSA/0.02% Fish Skin Gelatin (Sigma-Aldrich®)/10% FCS in PBS and

incubated with primary antibody overnight. After three washes in PBS/0.1% Triton-X100, secondary antibody was applied and the experiment was completed as outlined in section 2.7.1

2.7.3 Fluorescence and confocal microscopy

Immunofluorescent cells and sections were visualised (x630 or x400 magnification) with a Confocal laser scanning microscopy (Zeiss LSM 5100, Carl Zeiss Inc. or Leica SP5) or a fluorescent microscope (Olympus), using Immersol 518 TF oil (Zeiss) as an imaging medium. Images were then recorded, processed and organised in ImageJ.

2.8 PCR

2.8.1 RNA extraction

Total RNA was extracted using an RNeasy Mini Kit (Qiagen). Cells were disrupted by adding 350 μl RLT buffer (high salt content) to the tissue culture plate, after adding 1% β-mercaptoethanol for further ribonuclease inhibition. To optimise column binding conditions, 350 μl 70% ethanol was then added and mixed. Up to 700 μl of the lysate was then transferred to a spin column and centrifuged at maximum speed (13,300 rpm) for 30-60 seconds at room temperature to allow binding of RNA to the silica column. 350 μl buffer RW1 (high salt) was then added to wash the column, and the centrifugation step was repeated. Next, the column was washed with 500 μl buffer RPE. The column was then transferred to a new 1.5 ml Eppendorf tube and the RNA was eluted with 30 μl ribonuclease-free DEPC water. RNA was quantified by photospectroscopic absorbance at 260 nm using a Nanodrop 1000 Spectrophotometer (Thermo Scientific), using the 260:280 nm absorbance ratio to confirm purity. Samples were stored at -80° C for long-term use.

2.8.2 RT-PCR

Template complementary DNA (cDNA) was obtained by reverse transcription of 1 μg total RNA using a High Capacity cDNA Reverse Transcription Kit (Applied Biosystems). PCR reactions were set up in 20 μl volumes containing: 100-200 ng of template DNA, forward and reverse primers at 0.5-1 μM each (primer sequences listed in Appendix 9.3), 1 mM dNTPs, 1X buffer and 1U *Taq* DNA polymerase (Promega). A control lacking DNA was run in parallel. PCR was performed in a Thermal Cycler. PCR products were confirmed by gel electrophoresis analysis.

2.8.3 Quantitative real time PCR (q-PCR)

Q-PCR allows the quantification of a specific cDNA as it is amplified by PCR in real time. Values are normalised to a control gene expressed at equal levels in all cells to correct for variations in the original amount of total mRNA. The probes used hybridise with the cDNA of a chosen gene and contain a fluorescent label and a quencher molecule. The quencher is cleaved from the probe by the exonuclease activity of the polymerase when the chosen cDNA is copied during the PCR cycle, allowing an increase in fluorescent signal. The fluorescence change proportional to the number of copies of cDNA present and is measured at each cycle of the PCR.

To determine the levels of β6 cDNA or control gene GAPDH cDNA in cells, q-PCR was performed and the results analysed according to the standard curve method. Log cDNA was concentration was plotted against Ct values for known amounts of cDNA (Universal Human Reference RNA, Stratagene, UK) and the equation of this standard curve used to calculate the amount of β6 or GAPDH cDNA present in cells. C values represent the cycle number when the fluorescence of a sample increases above baseline fluorescence. At this point the reaction enters log phase, and it is during this log phase when the quantity of the PCR product (hence, fluorescence) is directly proportional to the input amount of input cDNA (e.g. β6 or GAPDH cDNA). Hence, the Ct value measures input cDNA, as it marks the number of cycles it took to reach this point.

Commercially available β6 and GAPDH primers (β6: Hs00168458_m1, GAPDH: Hs02758991_g1 from Applied Biosystems, California, USA) were used to assess β6 and GAPDH cDNA levels in cells. Samples of 5 μl cDNA, 10 μl Universal PCR master mix (Applied Biosystems), 1 μl probes and primers and 4 μl dH_2O were run in duplicate on a 7500 Realtime PCR System (Applied Biosystems). Average values were normalised to GAPDH expression.

2.9 Recombinant DNA and cloning techniques

2.9.1 PCR amplification of ITGB6 promoter

Genomic DNA (BD Biosciences) was amplified by PCR using high fidelity *LongAmp* DNA polymerase (New England Biolabs). All cloning PCR primers and sequencing primers used were supplied by Sigma-Aldrich® (primer sequences are listed in

Appendix 9.3.) The PCR product was cloned into the promoterless luciferase reporter vector, pGL3-Basic (Promega).

2.9.2 DNA analysis by gel electrophoresis

Gel electrophoresis analysis was used to confirm successful cloning, ligation or PCR steps. 5-10 μl of restriction digests or PCR products were run on a 1-2% (w/v) agarose gel (1-2g agarose in 1X Tris-Borate-EDTA (TBE) buffer with 5 μl ethidium bromide (EtBr) at 0.5 μg/ml) for 30 minutes at 120 V. Samples were run alongside a 100bp, 1kb or 10kb DNA ladder (Promega). Visualisation of the gel under UV light ensured that inserts were present or that PCR products were the expected size. Digested fragments, or PCR bands required for further cloning and ligation steps, were excised from the gel under UV light using a sterile blade and DNA purified using QIAquick Gel Extraction Kit 50 (Qiagen).

2.9.3 Restriction Digestions

All restriction enzymes were provided by Promega. Restriction enzyme digestions were set up in 10 μl volumes. Samples were digested with 1.0 U/μg DNA with the required restriction enzyme(s) in 1X buffer supplied by the manufacturer, as directed. 1X Bovine Serum Albumin (BSA) was added.

2.9.4 Ligations

20 μl reactions using 1 μl T4 DNA *Ligase* (New England Biolabs), 1X T4 *Ligase* buffer and a ratio of 1:3 of insert:vector were used. Controls included were: vector-no insert and insert-only (no vector). Ligation reactions were incubated overnight at 16 °C prior to transformation into competent *E.coli* bacteria.

2.9.5 Transformations

JM109 *E.coli* were made competent by $CaCl_2$ treatment by standard method (Cohen *et al*, 1972). They were kindly provided by Dr Patrick Duriez. Chemically competent JM109 *E.coli* were transformed using 5 μl of standard ligation reactions. Cells were kept on ice for 5 minutes or until thawed before addition of DNA and gentle mixing. The cell-DNA suspension was incubated for a further 20 minutes on ice. Bacteria were subjected to heat shock at 42° C for 45 seconds and transferred immediately to ice for 2 minutes. Cells were resuscitated in 400 μl lyosgeny broth (LB) medium, and cultures incubated for 45 minutes at 37° C with aeration. Approximately 200 μl of culture was spread onto pre-warmed selective agar and plates incubated overnight at 37° C.

2.9.6 Plasmid DNA extraction

Colonies were picked from overnight selective medium plates, inoculated into 2 ml antibiotic selective LB broth, and were incubated in a shaking 37° C incubator overnight. Bacterial cultures were harvested by centrifugation at 13,000 rpm and plasmid DNA extracted from pellet by standard protocol, using QIAprep Spin Miniprep Kit 250 (Qiagen). Constructs confirmed by sequencing analysis were amplified by QIAprep Maxiprep kit. DNA concentration was determined using a NanoDrop.

2.9.7 Sequencing and analysis

Plasmid DNA for sequencing was prepared from overnight cultures using the QIAprep spin miniprep kit (Qiagen). Following alkaline lysis of bacteria, DNA adsorbs to the silica membranes in the spin columns in high salt conditions, which were then washed and the DNA eluted in low-salt, nuclease free water. Plasmids were then sent for sequencing at Source Bioscience (Oxford, UK). Sequence analysis was performed using CLCDNA Workbench software (Aarhus, Denmark) and the Jusbio.com website (http://www.justbio.com) was used for sequence alignment.

2.10 Transfections

2.10.1 siRNA transfection

Oligofectamine™ reagent (Invitrogen Ltd.) interacts efficiently with oligonucleotides to form transfection complexes and was used to transfect cells growing in 6-well plates.

Custom *SMART*pool siRNA reagents targeting β6 integrin or random (non-targeting siRNA) and GeneSolution siRNA reagents targeting Gli1 were purchased from Dharmacon RNA Technologies (Chicago, IL, USA) and Qiagen (Crawley, West Sussex, UK), respectively and were re-suspended in siRNA buffer (100 mM KCl, 30 mM HEPES – pH 7.5, 1.0 mM $MgCl_2$) to a 20 μM stock solution and then stored at -20° C until use.

Keratinocytes were seeded into 6-well plates (5 x 10^4 cells/well) in standard KGM such that after 24 h the cells were approximately 30% confluent (which is optimal for transfection). For each well in a 6-well plate, the following solutions were prepared: 10 μl of *SMART*pool or GeneSolution stock solution was diluted in 175 μl of Opti-MEM® reduced-serum medium (GIBCO™ , Invitrogen Ltd.) to form 185 μl duplex solution

(solution A). 3 μl Oligofectamine™ reagent was diluted in 12 μl Opti-MEM® forming 15 μl transfection solution (solution B). Both solutions A and B were incubated for 10 minutes at RT after which the solutions were combined, mixed gently (total volume 200 μl – solution C) and incubated at RT for a further 20 min. During this incubation, the adherent cells were washed once with Opti-MEM® (1 ml/well) and 800 μl Opti-MEM® was added to each well. After 20 min, 200 μl of solution C was added drop-wise onto each well and the contents of each well (1 ml total volume) mixed gently by rocking the 6-well plate back and forth. Cells were incubated at 37° C in a humidified incubator (5-10% CO_2) for 4 h. Transfection was terminated by adding 500 μl 30% FCS KGM into each well and mixing gently as above. At 24 h post-transfection, cells were trypsinised, counted and incorporated into functional assays while protein expression was determined at 48-96 h post-transfection by lysing cells in replicate wells and performing Western blotting.

2.10.2 Plasmid transfections

The day before transfection, keratinocytes were plated into 24-well tissue culture plated at a density that allowed the cells to reach 80-90% confluency by the time of transfection. Transfections were performed with LipofectAMINE™ 2000 (Invitrogen Ltd.). Plasmids were combined with 50 μl Opti-MEM® reduced serum medium (Gibco) per well (solution A), after which 50 μl Opti-MEM® was combined with 2 μl LipofectAMINE™ 2000 per well (solution B) and incubated for 5 minutes at room temperature. The two solutions were then combined (solution C) and incubated at room temperature for 20 minutes. During this incubation the adherent cells were washed with KGM and 500 μl KGM was added to each well. After 20 minutes, 100 μl of the transfection mix was added drop-wise onto each well and the contents mixed gently by rocking the plate back and forth. Cells were incubated at 37° C for 6-18 h. To evaluate transfection efficiencies, cells were cotransfected with a reporter vector containing the *Renilla* luciferase gene driven by the herpes simplex virus thymidine kinase (HSV-TK) promoter pRL-TK (Promega). Each transfection was carried out in triplicate using 1.0 μg luciferase reporter construct DNA and 10 ng pRL-TK.

2.11 Luciferase reporter assays

2.11.1 TGF-β1 reporter assay

Mink lung epithelial reporter cells (MLEC) stably expressing a TGF-β1-responsive luciferase reporter construct (Abe *et al.*, 1994) were plated overnight in 96-well plate in DMEM, 10% FCS (5 x 10^4 cells/well). The medium was changed to serum-free α-MEM and keratinocytes (2.5 x 10^4 cells/well) were added to each well in serum-free α-MEM (with or without antibodies or siRNA). The cells were co-cultured overnight, washed once in PBS and lysed in reporter lysis buffer (Promega). Luciferase assay substrate (Promega) was added to the supernatant and luminescence was measured using a Wallac plate reader.

2.11.2 Dual Luciferase Reporter Assays

At 18 h post-transfection, cells were lysed and the firefly and *Renilla* luciferase activities were sequentially measured using the Dual-Luciferase Reporter Assay System (Promega). Firefly luciferase activity was normalised against the *Renilla* luciferase activity in each well.

2.12 Statistical analysis

Statistical analysis was performed using GraphPad Prism software Version 5.0 or Microsoft Excel (2011 edition). Analysis of variance (ANOVA) was used for multiple group comparisons and Student's *t*-test (two-tailed) was used for pair-wise comparisons. Significance was defined as a *p* value of <0.05

Chapter 3

The role of αvβ6 integrin in oral submucous fibrosis.

3.1 Introduction

Oral submucous fibrosis (OSF) is a chronic, premalignant disorder of the oral cavity, pharynx and upper oesophagus characterised by progressive fibrosis of the submucosa and a predilection for transformation to OSCC upon long-term follow-up (Tilakaratne *et al.*, 2006). The disease is associated with the habitual chewing of betel quid (*paan*; areca nut). Historically, αvβ6 integrin was first described in OSCC, but has since also been shown to be present in dysplastic oral tissues (Ragezi *et al.*, 2002), oral lichen planus (Hamidi *et al.*, 2000) and oral leukoplakia (Hamidi *et al.*, 2002). Additionally, αvβ6 also plays a major role in pathogenic pulmonary fibrosis (Munger *et al.*, 1999; Jenkins *et al.*, 2006; Xiu *et al.*, 2009).

The aim of the work described in this chapter is to investigate the potential role of αvβ6 integrin in the pathogenesis of OSF, given its role both in tumourigenesis and pathogenic fibrosis of other organs. We will first examine αvβ6 expression in OSF samples, followed by *in vitro* studies to delineate the potential mechanisms that may be involved in αvβ6-dependent processes.

3.2 αvβ6 expression in oral submucous fibrosis

Forty-one OSF and 14 cases of fibro-epithelial hyperplasia of oral mucosa (representing normal tissue) were selected from archival material and stained for αvβ6 by immunohistochemistry. Expression of αvβ6 in clinical specimens of normal oral mucosa (fibroepithelial hyperplasia) and OSF is summarised is summarised in Table 3.1.

	Cases	Negative	Low	High
Fibro-epithelial hyperplasia	14	3	11	0
Oral submucous fibrosis	41	9	10	22 (54%)

TABLE 3.1 αvβ6 expression in OSF. Forty-one OSF and 14 oral fibroepithelial hyperplasia cases were selected from archival material and stained for αvβ6. Staining was scored according to the Quickscore method, as described in Section 2.6. No strong expression was detected in hyperplastic oral mucosa; however, there was significantly higher expression in OSF with high expression seen in 22 cases (54%; *p<0.001*).

Of 41 OSF cases examined, strong expression (+++) of αvβ6 was present in 54% of cases (Figure 3.1, *B-F*). In contrast, no strong αvβ6 staining was observed in hyperplastic oral epithelium (Figure 3.1*A;* Fisher's exact test, *p<0.001*).

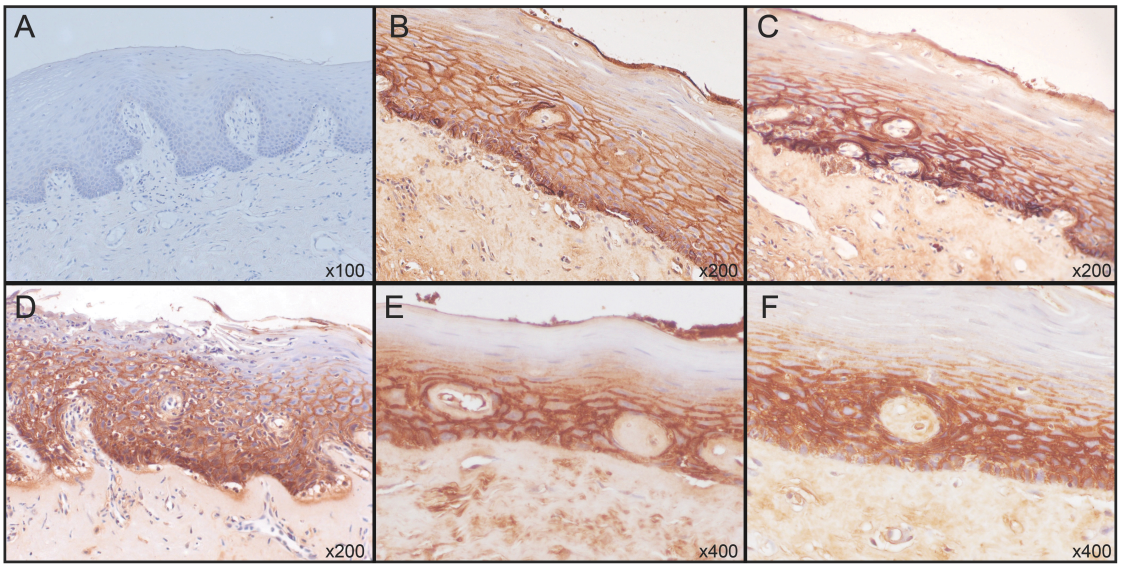

Figure 3.1 αvβ6 is significantly upregulated in OSF.
Tissue sections from OSF and fibro-epithelial hyperplasia cases were stained αvβ6 (6.2G2, 0.5 μg/ml) after antigen retrieval in pepsin for 5 minutes at 37° C. Figure shows representative αvβ6 expression in fibro-epithelial hyperplasia (A) and individual cases of OSF (B-F). αvβ6 expression was significantly higher in OSF (Fisher's exact test, *p<0.001*) than fibro-epithelial hyperplasia.

3.3 αvβ6 expression in keratinocyte cell lines

In order to determine the functional role of αvβ6 in OSF, keratinocyte cell lines were screened for β6 expression to carry out *in vitro* studies. The TERT-immortalised oral keratinocyte cell line OKF6/TERT-1 was first examined for αvβ6 expression. Although normal oral keratinocytes express αvβ6 *in vitro* (Thomas *et al.*, 2001a), OKF6/TERT-1 cells expressed αvβ6 at relatively low levels (Figure 3.2). Using cDNA transfection and retroviral infection, our laboratory had previously generated the VB6 cell line, which expresses high levels of αvβ6 (Thomas *et al.*, 2001a). To generate an αvβ6 negative control cell line, IC6pr control cells, which are αvβ6 negative, were retrovirally infected with the empty pBABE vector (encoding the puromycin resistance gene alone) to generate the IC6pr cell line (Chapter 5; Figure 2.1). αvβ6 expression was significantly higher in VB6 cells compared with OKF6/TERT-1 and IC6pr cells, as shown by flow cytometry, Western blotting and confocal microscopy (Figure 3.2). Thus, VB6 was used as a model for the high αvβ6-expressing keratinocytes identified in the OSF clinical samples and IC6pr was used as the negative control cell line. OKF6/TERT-1 was used as it expresses low levels of αvβ6.

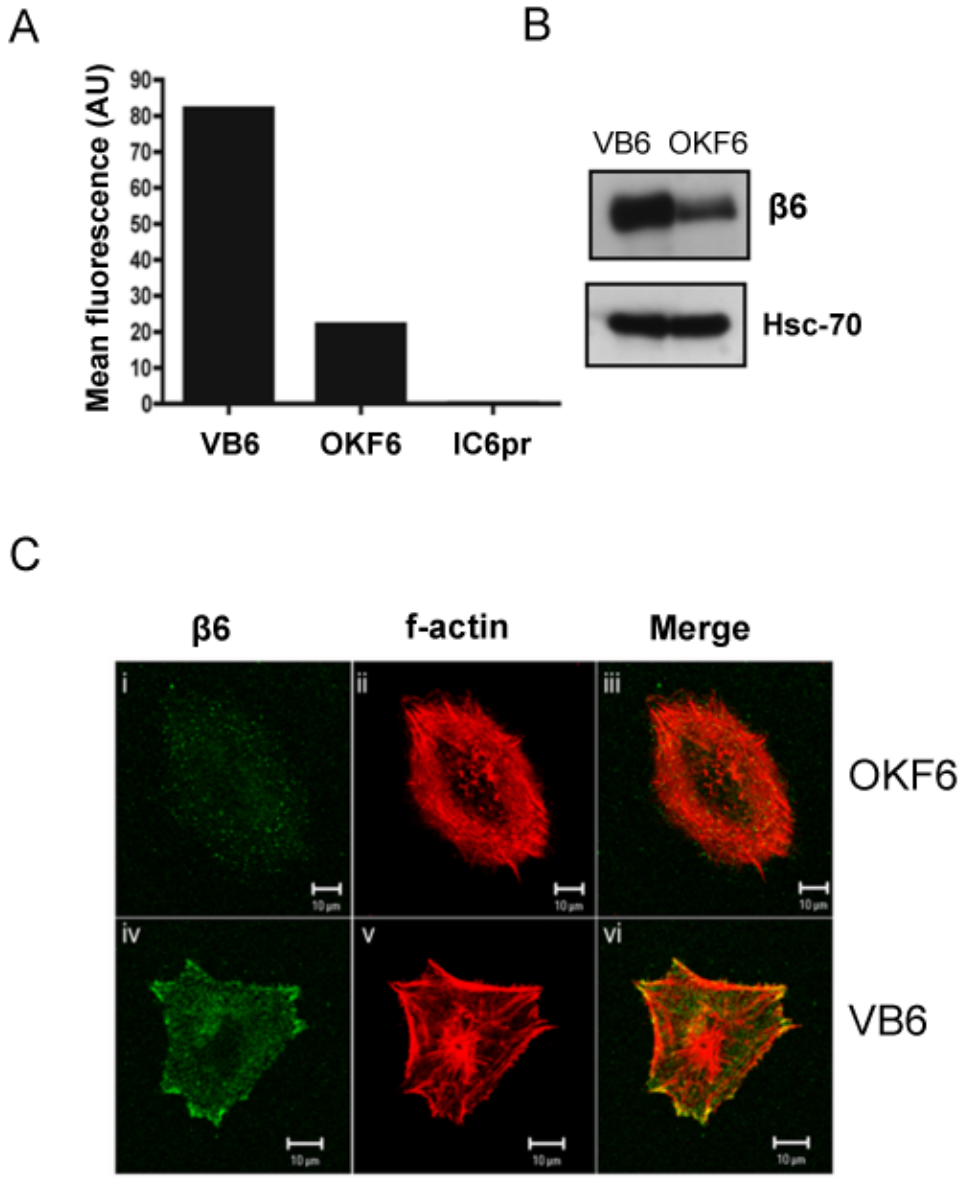

Figure 3.2 αvβ6 expression is significantly higher in VB6 cells than OKF6 cells.
3.2(A) Flow cytometry for VB6, OKF6-TERT1 and IC6pr cells was performed and the geometric mean (arbitrary units) of cells labelled with anti-αvβ6 (*620.w*) antibody is shown. Negative control had secondary antibody only and has been subtracted from the results. Flow cytometry confirmed high αvβ6 expression by VB6 cells and that the IC6pr null transfectant cell line expressed non-detectable levels of αvβ6. OKF6/TERT-1 had lower αvβ6 surface level in comparison to VB6.
3.2(B) Western blotting was carried out after cells had been lysed at 80-90% confluency levels, and shows higher αvβ6 protein level in VB6 than OKF6/TERT-1. Hsc-70 was used as a loading control.
3.3(C) Confocal microscopy demonstrating higher αvβ6 expression in VB6 than OKF6/TERT-1, particularly in focal adhesions and the leading edge of the cell. Cells were plated on fibronectin-coated 13 μm coverslips at a density of $4x10^4$ and allowed to adhere for 24 h. Cells were then fixed, stained and images were taken on a Zeiss confocal microscope. Scale bar = 10 μm. Figure shows a representative experiment.

3.4 αvβ6 activation of TGF-β1

αvβ6 modulates several cell functions, including activation of TGF-β1. To investigate whether activation of the cytokine by oral keratinocytes was αvβ6-dependent, we carried out TGF-β1 reporter assays. Keratinocyte cell lines were cocultured with mink lung epithelial reporter cells (MLEC), which have been stably transfected with a TGF-β1 promoter. Consistent with their lower level of αvβ6 expression, TGF-β1 activation by OKF6-TERT1 cells was significantly lower than VB6 cells (*p=0.0006*; Figure 3.3), and similar to the αvβ6-negative IC6pr cells (Figure 3.3). Inhibition of αvβ6 reduced TGF-β1 activation by VB6 cells (41% reduction, *p<0.005*; Figure 3.3), but had little effect on low αvβ6-expressing OKF6/TERT-1 or IC6pr cells.

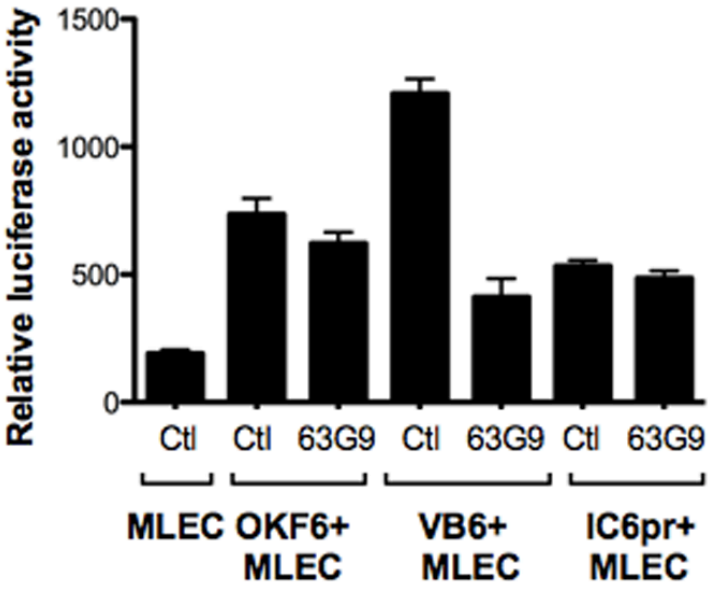

Figure 3.3 αvβ6 activates TGF-β1.
Mink lung epithelial reporter cells stably expressing a TGF-β1-responsive luciferase reporter construct were plated overnight in 96-well plates in DMEM, with 10% FCS and 400 μg/ml G418 (5 x 10^4 cells/well). The medium was changed to serum-free α-MEM and VB6, OKF6/TERT-1 or IC6pr cells (2.5 x 10^4 cells/well) were added to each well in serum-free α-MEM containing anti-αvβ6 antibody (10 μg/ml, *6.3G9*) or control anti-α4 antibody (10 μg/ml,*7.2*, produced in-house). Cells were cocultured overnight and lysed in Luciferase assay buffer, after which luminescence was measured on a Wallac plate reader. TGF-β1 activation was significantly higher in VB6 cells than OKF6/TERT-1 (*p*=0.0006). Error bars represent standard deviation (SD). Experiments were carried out in triplicate.

3.5 TGF-β1 effect on myofibroblast transdifferentiation

The activation of stromal fibroblasts into contractile myofibroblasts is commonly seen in tissue fibrosis (Wynn, 2008) and TGF-β1 is considered to be a major cytokine in inducing this myofibroblastic phenotype (Powell *et al.*, 1999). To confirm that TGF-β1 induced myofibroblast transdifferentiation, primary oral fibroblasts and HFFF2 cells were treated with TGF-β1 at 5 ng/ml for 48 hours. Smooth muscle actin (α-SMA), a myofibroblast marker, was significantly upregulated upon TGF-β1 treatment (Figure 3.4A and B), confirming myofibroblastic transdifferentiation.

Since OSF is characterised clinically by the dense deposition of collagen in the submucosal tissue, we investigated whether TGF-β1-mediated myofibroblast transdifferentiation also upregulated fibrosis-associated genes. We found by RT-PCR that collagen I (Col1A1) and TIMP1 were both upregulated in myofibroblasts (Figure 3.4*C*).

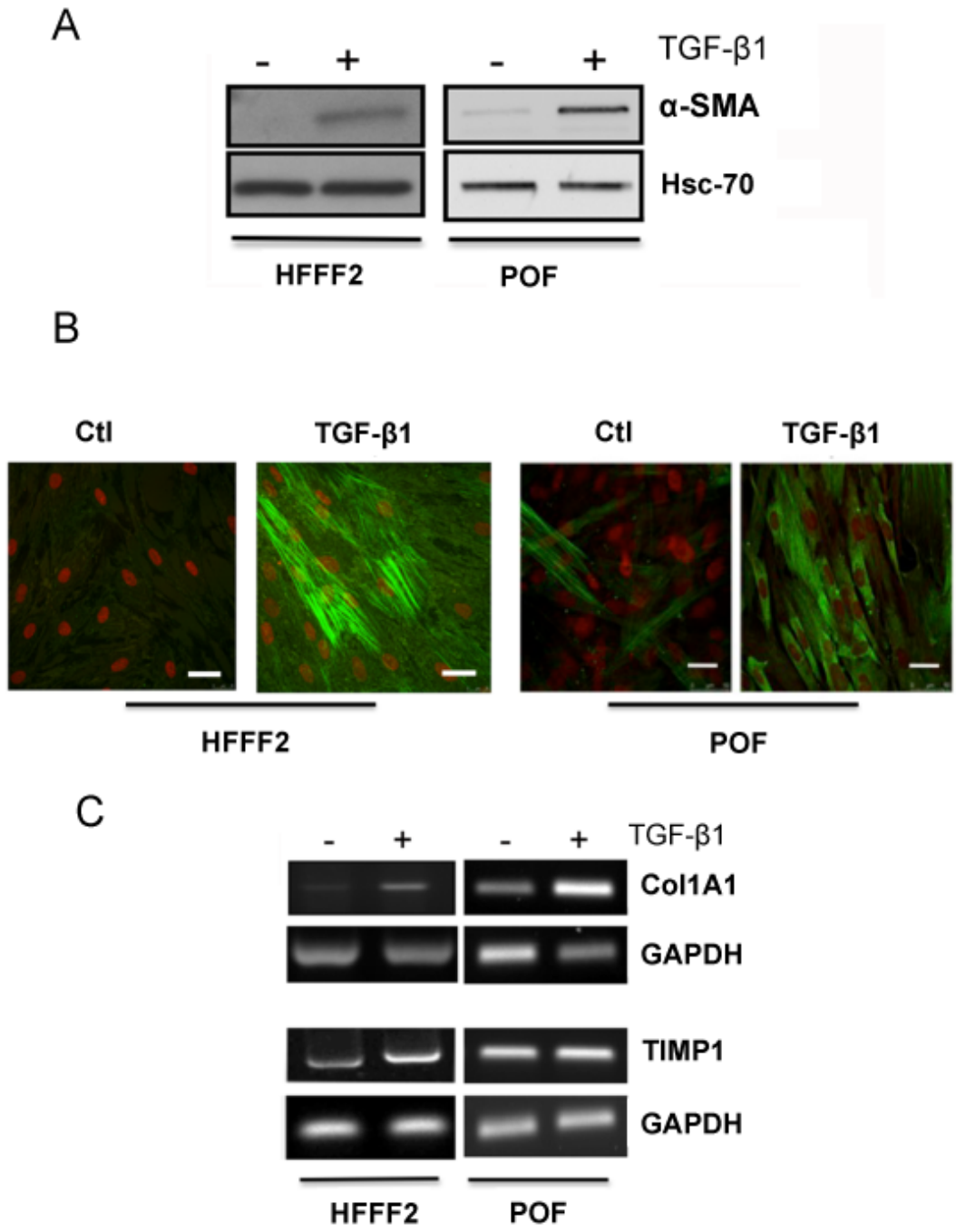

Figure 3.4 TGF-β1 promotes myofibroblastic transdifferentiation.
3.4(A) Western blotting confirmed that treatment of HFFF2 cells and primary oral fibroblasts (POF) with TGFβ1 at 5 ng/ml for 48 hours resulted in myofibroblastic transdifferentiation, shown by upregulation of α-SMA. A representative experiment is shown.
3.4(B) Confocal micrograph demonstrates an upregulation of α-SMA (green) in TGF-β1-treated POF and HFFF2 cells. Nuclei were visualised by TO-PRO3 (red). A representative experiment is shown. Scale bar = 10 μm.
3.4(C) Myofibroblastic transdifferentiation was associated with upregulation of genes associated with tissue fibrosis, including collagen 1 and TIMP1, shown by RT-PCR. A representative experiment is shown.

3.6 αvβ6 modulation of myofibroblast transdifferentiation

To determine whether VB6 cells could induce myofibroblast differentiation, we carried out co-culture experiments with POF and HFFF2 fibroblasts. Co-culture of fibroblasts with VB6 cells induced myofibroblast transdifferentiation, producing a significant increase in SMA expression (Figure 3.5 and Figure 3.6), forming cytoplasmic stress fibres. Co-cultures of IC6pr and POF or HFFF2 fibroblasts showed significantly less SMA expression (Figure 3.6A; p=0.003 and p=0.002, respectively). To show that myofibroblast generation was modulated via αvβ6, the assays were repeated in the presence of 6.3G9, an αvβ6-inhibitory antibody (Figure 3.6B). When the αvβ6 antibody was included, SMA expression was inhibited significantly. This was confirmed by Western blotting (Figure 3.6B; p=0.003 and p=0.006). All experiments were performed in triplicate or quadruplicate.

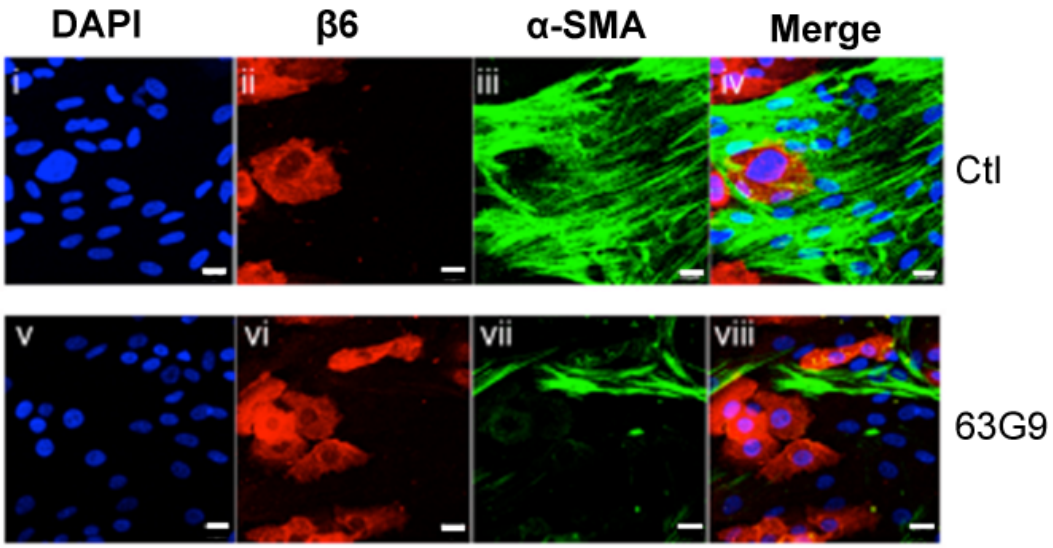

Figure 3.5 Keratinocyte and fibroblast co-culture experiments.
HFFF2 cells and VB6 cells were co-cultured on glass coverslips and treated with control (*7.2*; i-iv) or anti-αvβ6 (*6.3G9*; v-viii) antibodies. Confocal micrograph shows cell nuclei (blue; i and v), αvβ6-positive VB6 cells (red; ii and vi), SMA-positive myofibroblasts (green; iii and vii), or the combined images (right; iv and viii). When co-cultured with VB6, HFFF2 cells up-regulated SMA indicating myofibroblastic transdifferentiation (i-iv). The transdifferentiation was suppressed by inhibiting αvβ6 (v-viii). Results shown are from a representative experiment. Scale bar = 10 μm.

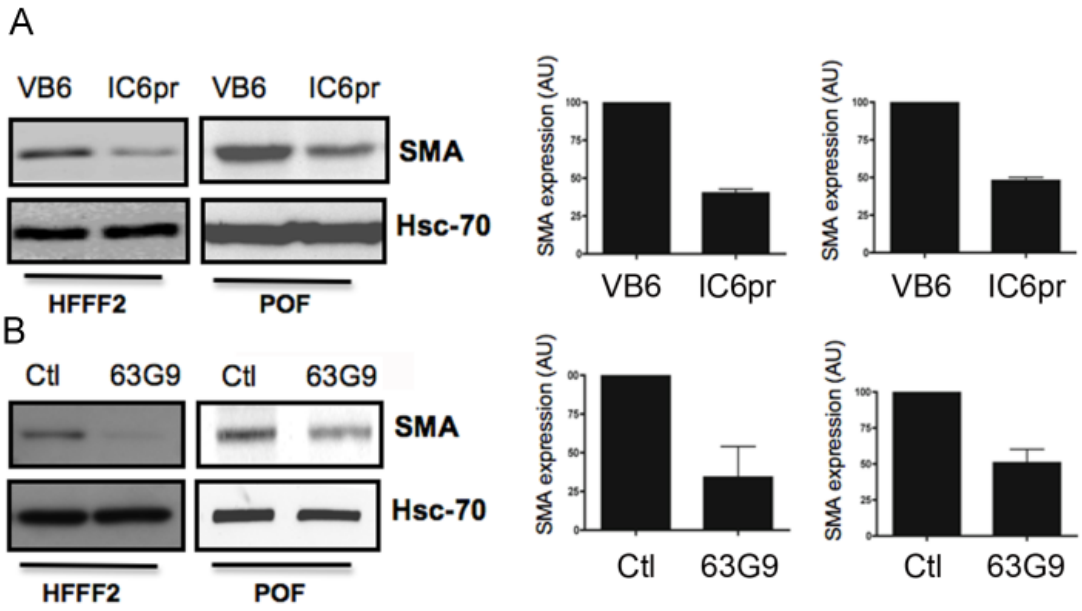

Figure 3.6 Myofibroblast transdifferentiation in co-cultures is possibly mediated through αvβ6-dependent TGF-β1.
3.6(A) 2.5 x 10^5 keratinocytes (VB6 or IC6pr) were co-cultured with an equal number of fibroblasts (POF or HFFF2) in serum-free medium for 48 hours. Western blotting showing that high-αvβ6 expressing VB6 cells induced myofibroblast transdifferentiation significantly more than IC6pr control cells, which are αvβ6 negative in both HFFF2 and POF cells (*p*=0.003 and *p*=0.002, respectively). Figure shows a representative experiment. Histograms represent the combined densitometric analyses from four sets of experiments. Error bars represent SD.
3.6(B) 2.5 x 10^5 keratinocytes (VB6 or IC6pr) were co-cultured with an equal number of fibroblasts (POF or HFFF2) in serum-free medium for 48 hours. To inhibit αvβ6, the inhibitory antibody 6.3G9 was used. Control antibody (anti-α4, *7.2*) was used in the control condition. VB6-dependent myofibroblastic transdifferentiation was significantly suppressed by *6.3G9* in both HFFF2 and POF co-cultures (*p*=0.003 and *p*=0.006, respectively). Figure shows a representative experiment. Histograms represent the combined densitometric analyses from four sets of experiments. Error bars represent SD.

To address whether αvβ6-dependent myofibroblastic transdifferentiation produced a functional effect, collagen gel contraction assays using co-cultures of VB6 cells and POFs were carried out. These assays were based on the established organotypic model generated previously by our laboratory (Nystrom *et al.*, 2005). This was achieved by modifying the components of the protein gel, essentially substituting Matrigel with collagen.

Inhibition of keratinocyte αvβ6 significantly inhibited gel contraction, demonstrating that this myofibroblast-dependent process can be modulated by epithelial cells (Figure 3.7; *p*=0.02). Initial experiments with HFFF2 showed similar results. Thus, we subsequently focused on POF since they represent a more physiologically relevant model.

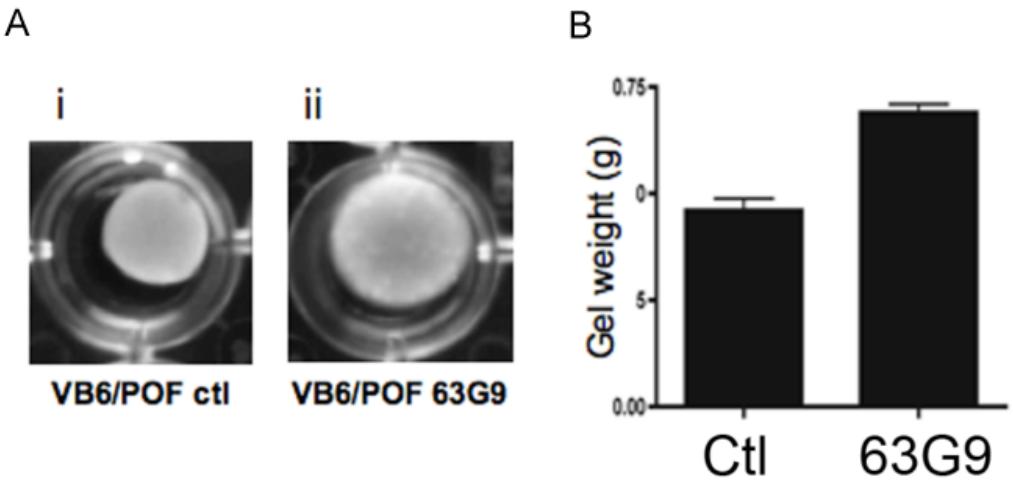

Figure 3.7 Myofibroblasts derived from co-cultures are contractile.
3.7(A) 5x10^5 VB6 cells were cocultured with an equal number of POFs with control (*7.2*; Fig. 3.7A(i) or αvβ6-blocking (*6.3G9*; Fig. 3.7A(ii)). Cells were then trypsinised and placed in a collagen gel. All experimental conditions were carried out in duplicates. Gels were left to polymerise and photographs were taken 18 h later (i and ii). Co-culture of VB6 cells and POF promoted myofibroblast-dependent gel contraction (i). This was αvβ6-dependent, and was suppressed by *6.3G9* (ii).
3.7(B) Histograms representing the combined gel weights from 4 independent experiments. Collagen gels in which αvβ6 had been inhibited by *6.3G9* were significantly heavier (*p*=0.02) than control gels. Error bars represent SD.

3.7 Stromal features of OSF

The preceding *in vitro* data suggested that the stroma of OSF would contain collagen-producing myofibroblasts, modulating the fibrosis that characterises the disease. To determine whether the lamina propria contained myofibroblasts, OSF samples were immunostained for SMA expression (Figure 3.8ii and 3.8iii). To further show that the TGF-β1 signalling pathway is potentially activated in OSF, samples were stained for pSmad2 and Smad4, where pSmad2- and Smad4-positive nuclei in both myofibroblasts and basal and suprabasal keratinocytes were seen (Figure 3.8v and 3.8vi).

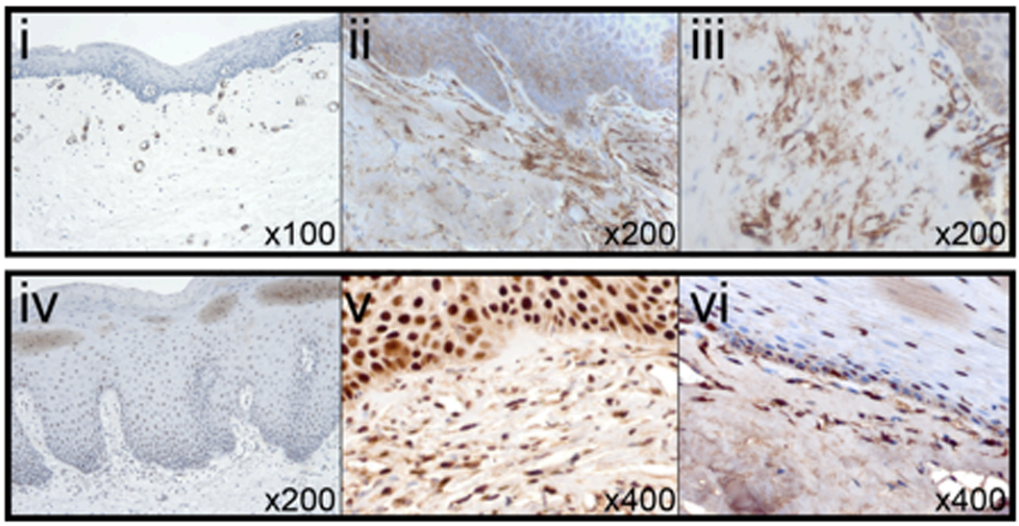

Figure 3.8 SMA-positive myofibroblasts are present in OSF.
Tissue sections from OSF and fibro-epithelial hyperplasia cases were stained SMA, pSmad2 and Smad4 after antigen retrieval in citrate buffer pH 6.00 (for pSmad2 and Smad4). Figure shows representative expression in fibro-epithelial hyperplasia and individual cases of OSF. SMA-positive myofibroblasts were not detectable in fibroepithelial hyperplasia (i), but were prominent within the lamina propria of OSF cases (ii, iii). pSmad2- and Smad4-positive nuclei (v and vi respectively) were prominent in both keratinocytes and myofibroblasts in OSF, compared with fibroepithelial hyperplasia (iv, pSmad2), suggesting activated TGF-β1 signalling.

3.8 Effect of the betel quid constituent arecoline on αvβ6 expression in keratinocytes

The alkaloid arecoline is a potentially carcinogenic constituent of areca nut (Tilakaratne *et al.*, 2006) and concentrations as high as 100 μg/ml of the alkaloid have been reported in saliva isolated from OSF patients (Nair *et al.*, 1985). To determine whether arecoline had an effect on αvβ6 expression, OKF6/Tert1 cells which express low levels of αvβ6, were treated with arecoline at varying, physiologically relevant concentrations for 48 hours (Xia *et al.*, 2009), and αvβ6 expression was assessed. Initial experiments showed upregulation of αvβ6 expression at a concentration range of 5-15 μg/ml of arecoline (Figure 3.9). At these concentrations, arecoline had no discernible effect on cell proliferation and viability.

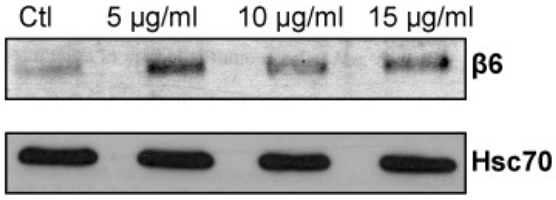

Figure 3.9 Arecoline upregulates αvβ6 expression in keratinocytes.
2.5 x 10^5 OKF6/Tert-1 cells were treated with 5-15 µg/ml arecoline for 48 hours, after which cells were lysed and proteins were analysed by Western blotting. Figure shows an upregulation of αvβ6 integrin expression upon arecoline treatment at the concentration range of 5-15 µg/ml. A representative experiment is shown.

More detailed studies were then carried out, and a significant increase in αvβ6 expression was observed at the physiologically relevant concentration of 5 µg/ml (p = 0.006; Figure 3.10A) RT-PCR showed increased levels of β6 mRNA following arecoline treatment, indicating possible transcriptional regulation (Figure 3.10A).

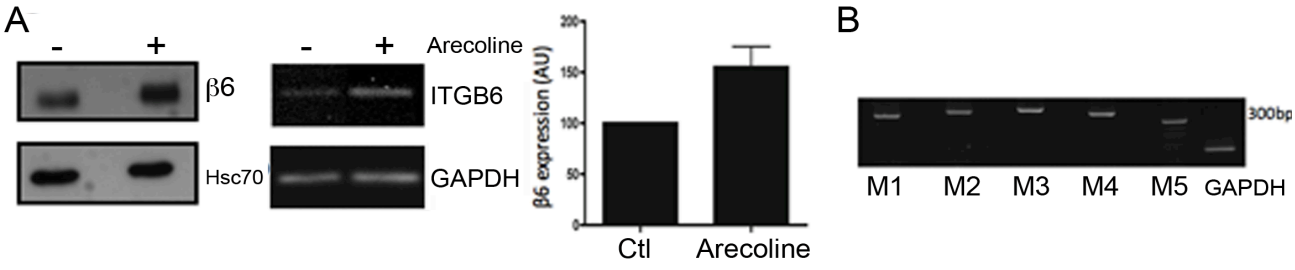

Figure 3.10 Arecoline significantly up-regulates αvβ6 protein and gene expression in keratinocytes.
3.10(A) 2.5 x 10^5 OKF6/Tert-1 cells were treated with 5 µg/ml arecoline for 48 hours. Cells well then lysed for protein analysis or RNA was extracted for RT-PCR. Western blotting and RT-PCR show upregulation of αvβ6 upon arecoline treatment (p=0.006). Histogram represents the combined results of Western blot densitometric analysis from three individual experiments. Error bars represent SD.
3.10(B) RT-PCR showing that OKF6/TERT-1 cells express $M_{1\text{-}5}$ receptors. Negative controls contained no cDNA template.

Arecoline is a known agonist of acetylcholine muscarinic receptors (McKinney *et al.*, 1991), and it has been shown previously that overexpression of the M_4 muscarinic receptor is associated with upregulation of keratinocyte migratory integrins (Chernyavsky *et al.*, 2004). RT-PCR was used to confirm that OKF6/TERT-1 cells expressed M_4 (Figure 3.10B).

We used the M_4 antagonist tropicamide to examine whether arecoline-dependent upregulation of $\alpha v\beta 6$ was modulated through this receptor (Chernyavsky *et al.*, 2004). Culture of OKF6/TERT-1 cells with tropicamide suppressed arecoline-induced upregulation of $\alpha v\beta 6$ (Figure 3.11A; $p = 0.04$). This finding was confirmed by confocal microscopy (Figure 3.11B).

Since OKF6/TERT-1 cells express low levels of $\alpha v\beta 6$, they spread poorly on the $\alpha v\beta 6$ ligand LAP, producing a spindled morphology (Figure 3.11B; top panel). Treatment of cells with arecoline promoted cell spreading and formation of ruffling membranes, with cells having a more rounded, epithelioid appearance, while tropicamide suppressed this morphological change (Figure 3.11B; middle and bottom panels, respectively).

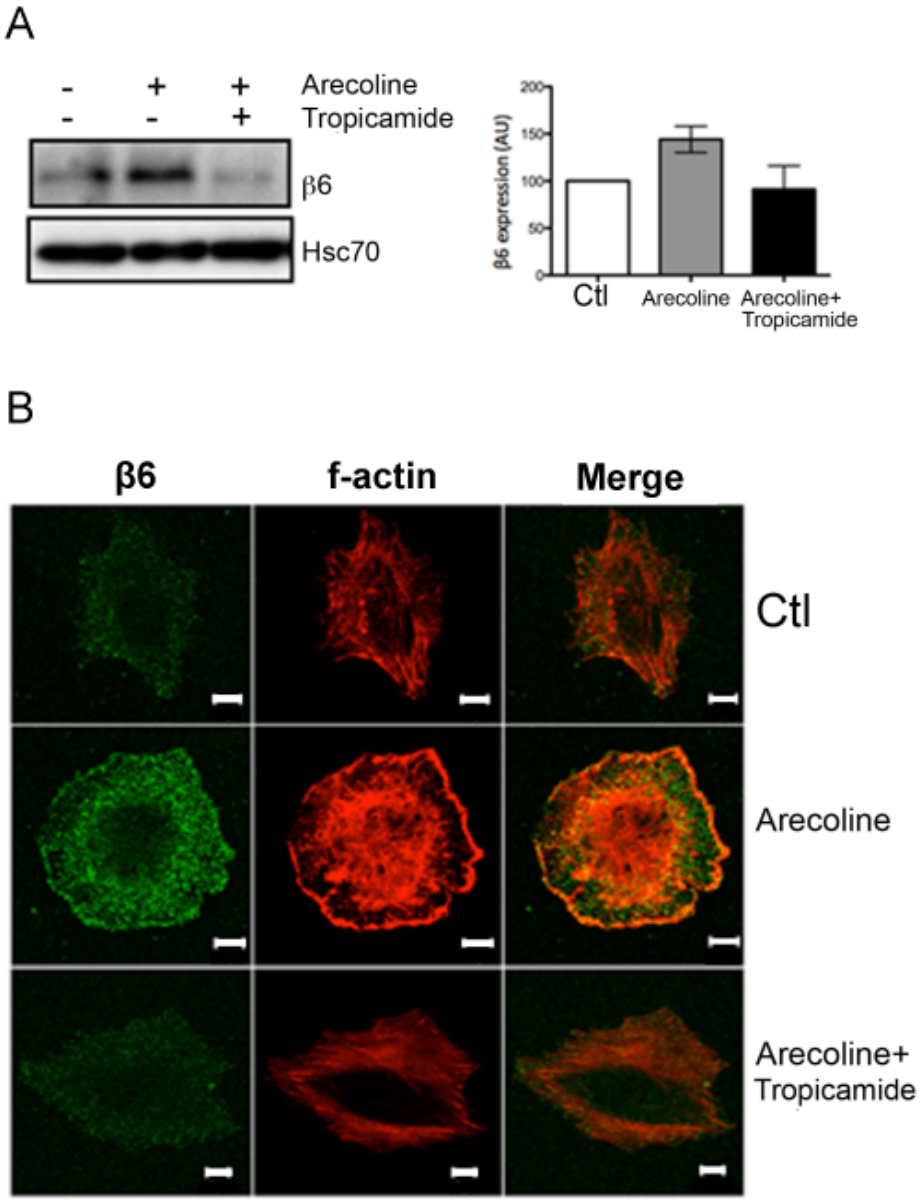

Figure 3.11 Arecoline-mediated up-regulation of αvβ6 expression in keratinocytes is modulated through the M_4 muscarinic acetylcholine receptor.
3.11(A) 2.5 x 10^5 OKF6/Tert 1 cells were plated per each condition and treated with arecoline (5 μg/ml) and/or tropicamide (350 μM) for 48 hours. Control wells were treated with ethanol diluted in tissue culture medium. Western blotting shows that arecoline-dependent upregulation αvβ6 expression in OKF6/TERT-1 cells is suppressed by the selective M_4 receptor antagonist tropicamide (p=0.04). Histogram represents the combined results of Western blot densitometric analysis from four individual experiments. Error bars represent SD.
3.11(B) Confocal microscopy of OKF6/TERT-1 cells plated on TGF-β1 LAP. Upregulation of αvβ6 expression was seen in arecoline-treated cells (green; middle panel). This allowed the cells to spread more effectively on LAP, resulting in a rounded, more epithelioid appearance. The arecoline-dependent upregulation of αvβ6 was suppressed by tropicamide, with cell morphology reverting to a more spindled phenotype (lower panel). Scale bar = 10 μm.

3.9 Effect of arecoline on αvβ6-dependent cellular functions.

We next wanted to determine whether the observed arecoline-dependent upregulation of αvβ6 produced any functional effects in these cells. OKF6/TERT-1 cells treated with arecoline with or without tropicamide inhibition were co-cultured with oral fibroblasts and α-SMA expression was examined. We found that arecoline-dependent upregulation of αvβ6 in OKF6/TERT-1 cells promoted the transdifferentiation oral fibroblasts into myofibroblasts, and that this was inhibited by tropicamide (Figure 3.12; *p*=0.005 and *p*=0.027).

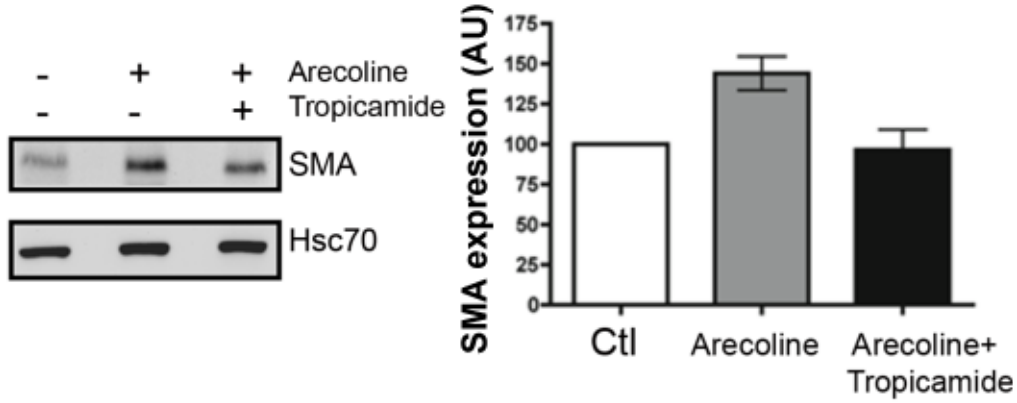

Figure 3.12 Arecoline-dependent upregulation of αvβ6 promotes myofibroblast transdifferentiation.
Co-cultures were carried out with 2.5 x 10^5 OKF6/Tert-1 cells and an equal number of fibroblasts with arecoline and/or tropicamide treatment. Western blotting shows that tropicamide suppresses POF SMA upregulation in co-cultures with arecoline-treated OKF6/TERT-1 cells (*p*=0.005 and *p*=0.027). Histogram represents the combined results of Western blot densitometric analysis from three individual experiments. Error bars represent SD.

Additionally, and given that approximately 7-13% of OSF patients develop invasive malignancies, the effect of arecoline on keratinocyte motility was examined next. Although OKF6/TERT-1 cells migrated poorly towards the latency associated peptide (LAP) of TGF-β1, an αvβ6 substrate, migration was promoted significantly by arecoline (*p*<0.01). This was αvβ6-dependent, and was also suppressed by tropicamide (Figure 3.13; *p*<0.01).

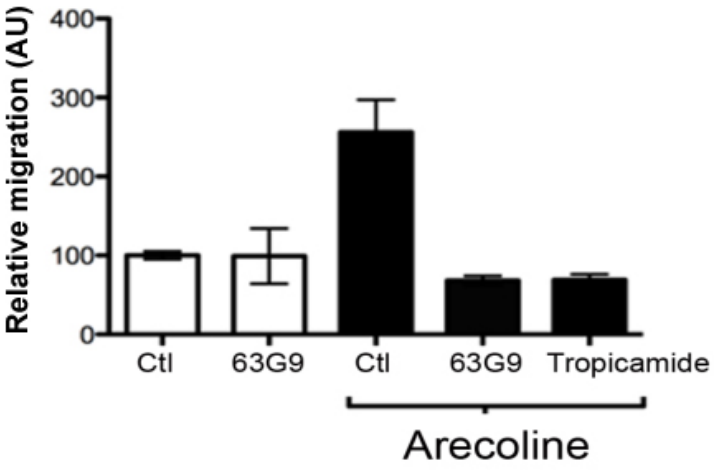

3.13 Arecoline-dependent upregulation of αvβ6 promotes keratinocyte migration. $2.5x10^5$ OKF6/TERT-1 cells were treated first with arecoline with or without tropicamide for 48 h prior to the assay. Transwell migration assays were carried out using LAP-coated (0.5 μg/ml) polycarbonate filters. $5x10^4$ OKF6 cells were plated in quadruplicate in the upper chamber of a Transwell. Cells that had migrated to the lower chamber were trypsinised and counted 18 h later. For blocking experiments, anti-αvβ6 blocking antibody (*6.3G9*, 10 μg/ml) was added to the cells for 30 min prior to plating and was present throughout the experiment. Results showed enhanced migration of OKF6/TERT-1 cells towards the αvβ6 ligand LAP, when treated with arecoline ($p<0.01$ when compared with controls). This was inhibited by *6.3G9* and tropicamide ($p<0.01$). Results are collated from three independent experiments.

In order to investigate a direct effect of arecoline on fibroblasts, endogenous TGF-β1 secretion was examined by ELISA after treating keratinocytes and fibroblasts with arecoline (Figure 3.14A). Arecoline did not significantly increase endogenous TGF-β1 secretion by keratinocytes or fibroblasts ($p>0.05$). There was a suggestion of increased TGF-β1 secretion upon arecoline treatment in HFFF2, potentially indicating a cell-line dependent effect. HFFF2 fibroblasts were also treated with arecoline at 5 μg/ml and 10 μg/ml and Western blotting showed no change in α-SMA expression (Figure 3.14B). These experiments suggested that the myofibroblastic transdifferentiation was possibly modulated through αvβ6-mediated activation of TGF-β rather than a direct effect of arecoline on fibroblasts.

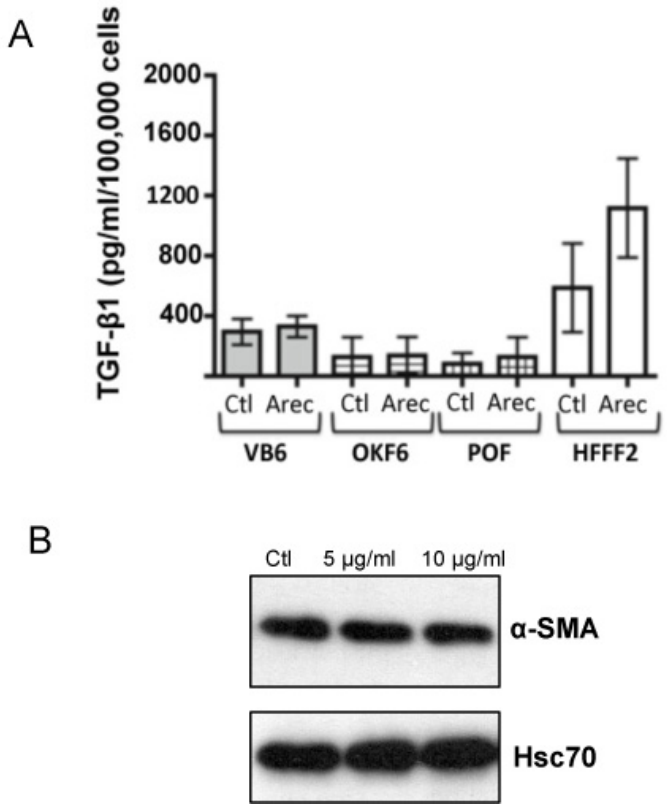

Figure 3.14 TGF-β1 ELISA and arecoline effect on fibroblast α-SMA.
3.14(A) Cells were cultured in 6-well plates and treated with arecoline as described for 48 h. Prior to analysis, samples were centrifuged at 2,000 rpm for 3 min to remove cell debris. TGF-β1 ELISA was performed according to the manufacturer's instructions. Figure shows combined results from 4 independent experiments. There was no significant difference in TGF-β1 secretion by keratinocytes. TGF-β1 secretion by fibroblasts may be cell-line dependent.(*p*>0.05).
3.14(B) $2.5x10^5$ fibroblasts were treated with arecoline as described for 48 h, then lysed for analysis by Western blotting. There was no significant upregulation of α-SMA in HFFF2 fibroblasts upon arecoline treatment. Figure shows a representative experiment.

To investigate the effect of arecoline on keratinocyte invasion, an organotypic culture model was used, which had been shown previously to be a physiologically relevant method for studying tumour cell invasion (Nystrom *et al.*, 2006; Marsh *et al.*, 2008). Preliminary experiments were first performed to test whether OKF6/TERT-1 cells were viable in this setting, and to investigate the effect of arecoline on αvβ6 expression and function in organotypic cultures (Figure 3.15)

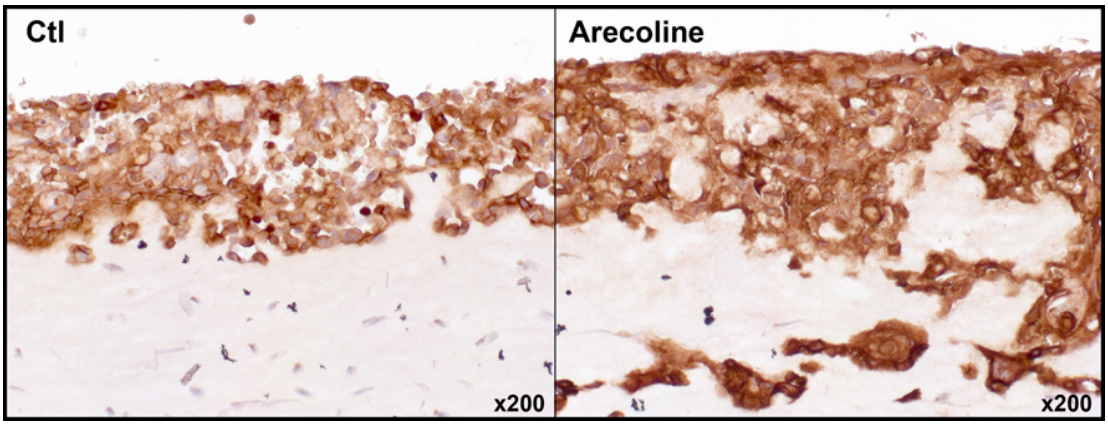

Figure 3.15 Arecoline-dependent upregulation of αvβ6 promotes keratinocyte invasion in organotypic cultures.
Organotypic cultures with an air-tissue interface were performed by preparing gels comprising a 50:50 mixture of Matrigel and type I collagen containing 5 x 10^5 per ml of fibroblasts, to which 1 x 10^6 OKF6/TERT-1 cells were added. The cell suspension was treated with arecoline 5 μg/ml for 48 hours prior to seeding onto organotypic cultures in duplicate, and was present throughout the experiment. The medium was changed every 2 d, and after 10 d, the gels were bisected, fixed in formal saline and processed to paraffin. The figure shows that arecoline-treated OKF6/TERT1 invaded into organotypic cultures. The invasive islands also appeared to have higher αvβ6 expression. Experiments were carried out in duplicate. Photo-micrographs are from a representative section of an individual organotypic gel.

Once the experimental conditions had been optimised, further organotypic studies were carried out, with tropicamide included to test αvβ6 inhibition. αvβ6 expression was also silenced by small interfering RNA (siRNA), in order to compare the effect of tropicamide inhibition on αvβ6 function with β6 gene knockdown. Results showed that arecoline similarly promoted αvβ6-dependent OKF6/TERT-1 invasion, and this was suppressed by tropicamide and by β6 siRNA (Figure 3.16).

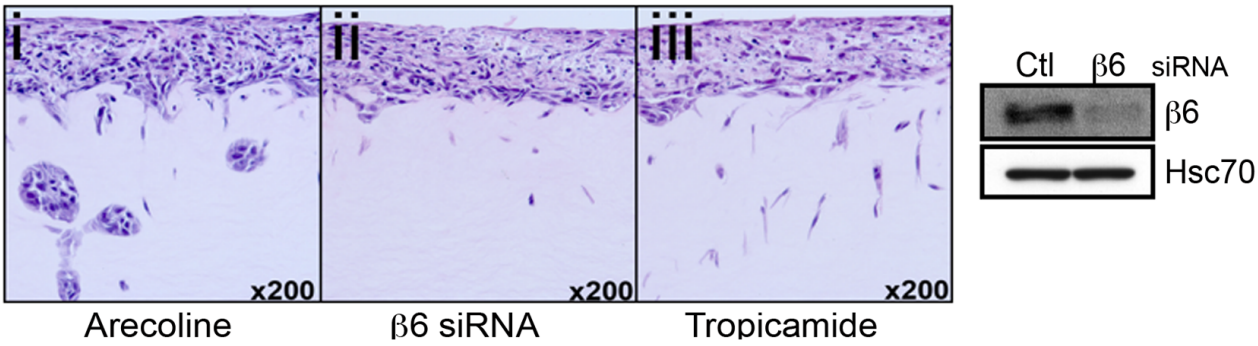

Figure 3.16 Arecoline-mediated keratinocyte invasion is αvβ6-dependent.
Organotypic culture was carried out by plating $1x10^6$ OKF6/Tert-1 cells onto a protein gel in which 0.5 x 10^6 fibroblasts were seeded. All conditions were treated with arecoline at 5-10 μg/ml, which was present throughout the experiment. Western blotting was done to confirm knock-down of β6. The figure shows that arecoline-treated OKF6/TERT-1 invaded into organotypic cultures (i). Invasion was suppressed by siRNA knockdown of β6 (ii) and tropicamide treatment (iii). Experiments were carried out in duplicate. Photo-micrographs show results from a representative section of an organotypic gel.

3.10 αvβ6 expression in OSF-associated OSCC.

Since upregulated αvβ6 expression promoted keratinocyte invasion, we examined the expression of the integrin in six cases of OSCC arising on a background of OSF. Five of 6 cases (83%) showed moderate/strong expression of the integrin (Figure 3.17). Four biopsies from OSF patients that subsequently developed SCC were also immunostained. Three of the 4 cases of OSF expressed the integrin at moderate/high levels.

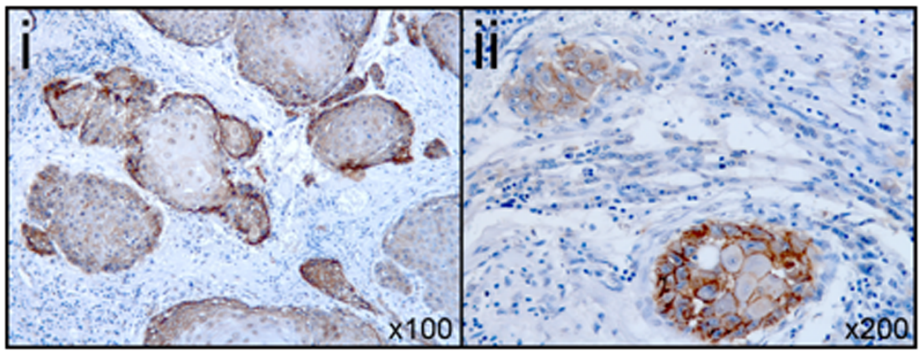

Figure 3.17 αvβ6 is up-regulated in OSF-associated OSCC.
Immunohistochemistry shows representative αvβ6 expression in OSCC arising from OSF (i and ii). 83% of cases (5 of 6) showed moderate/strong αvβ6 expression.

3.11 Discussion

OSF is a debilitating disease of the oral cavity and oropharynx with substantial morbidity and a potential for malignant transformation into OSCC (Tilakaratne *et al.*, 2006). Given its close association with betel quid chewing, the condition is prevalent within the Indian Subcontinent and Far East, but it is now also being increasingly seen in the Western world in Asian immigrant communities. Furthermore, the incidence is rising amongst young individuals, which is of particular concern given the chronic course of the disease. The pathogenesis of the disease involves increased accumulation of collagen within the lamina propria of the oral mucosa, eventually leading to scarring of underlying muscle (Tilakaratne *et al.*, 2006; Isaac *et al.*, 2008). Research has focused primarily on the role of fibroblasts in regulating ECM turnover, examining levels of fibrogenic cytokines, proteases and protease inhibitors (Tilakaratne *et al.*, 2006). However, the mechanisms initiating and promoting OSF remain to be elucidated.

The expression of αvβ6 has been increasingly described in numerous carcinoma types, including oral cancer (Thomas *et al.*, 2006), and also several fibrotic conditions (Munger *et al.*, 1999; Patsenker *et al.*, 2008). However, the mechanisms regulating its expression are yet to be fully determined. In this chapter, we have shown that treatment of immortalised normal oral keratinocytes with the areca nut alkaloid arecoline induced upregulation of the integrin, and had a role in modulating some αvβ6-dependent cell functions, including motility. Keratinocytes express muscarinic acetylcholine receptors M_1-M_5 (Ndoye *et al.*, 1998), for which arecoline is an agonist, particularly of the M_4 receptor (McKinney *et al.*, 1991). Interestingly, Chernyavsky and colleagues found that M_4 receptor expression in keratinocytes upregulated expression of migratory integrins, and promoted cell migration (Chernyavsky *et al.*, 2004). Consistent with these findings we have found here that treatment of OKF6/TERT-1 keratinocytes with a selective M_4 receptor antagonist, prevented arecoline-dependent αvβ6 upregulation. Arecoline has also been shown to upregulate TNF-α production by keratinocytes; indeed, polymorphisms of the TNF-α gene have been reported as a significant risk factor for OSF (Jeng *et al.*, 2003; Chiu *et al.*, 2001). Since this cytokine has been shown to modulate αvβ6 expression (Scott *et al.*, 2004), it is possible then that TNF-α may form part of the downstream arecoline/M_4 signalling pathway.

TGF-β1 is regarded as the principal modulator of tissue fibrosis, as it is considered to have a central role in inducing myofibroblast transdifferentiation (De Wever *et al.*,

2008). Although increased levels of TGF-β1 in OSF have been reported previously, the mechanism by which the latent cytokine is activated has not been investigated (Haque *et al.*, 1998). Since latent TGF-β1 is concentrated at high levels within the ECM, activation rather than increased production often regulates this cytokine's function (Saharinen *et al.*, 1999; Sheppard, 2006). Our co-culture experiments showed that VB6 cells modulated fibroblast-to-myofibroblast transdifferentiation, possibly through αvβ6-dependent activation of TGF-β1. Myofibroblasts are the principal modulators of tissue fibrosis facilitating matrix accumulation both by increasing the deposition and decreasing the degradation of matrix proteins (De Wever *et al.*, 2008). We confirmed that myofibroblasts upregulated collagen I, the principal matrix protein deposited in OSF, and also the matrix metalloproteinase inhibitor, TIMP-1. We also carried out immunochemistry on human OSF samples, and demonstrated that the fibrosing lamina propria contained SMA-positive myofibroblasts, which showed nuclear positivity for phosphorylated Smad2 and Smad4, suggesting TGF-β1 signalling. Myofibroblasts were most obvious in the earlier stages of OSF and, as the disease progressed, the lamina propria became increasingly acellular. TGF-β1 is also a potent inhibitor of epithelial growth. A characteristic feature of advanced OSF is pronounced epithelial atrophy, and it is possible that this also is mediated through TGF-β1, since pSmad2 nuclear positivity likewise was detected in lesional keratinocytes.

Areca nut is implicated in the development of oesophageal and liver carcinoma, as well as OSCC (Secretan *et al.*, 2009). Consistent with the fact that αvβ6 promotes migration and invasion in several cancers, the data here demonstrate that arecoline up-regulated αvβ6-dependent keratinocyte migration. A useful experiment would be to test the effect of arecoline on keratinocyte TGF-β1 activation. Additionally, arecoline-treated OKF6/TERT-1 cells invaded organotypic cultures. Given that 7-13% of OSF patients develop OSCC, it is possible that expression of αvβ6 may contribute, in part, to this malignant transformation. Interestingly, TGF-β1 and *Ras* may modulate epithelial-to-mesenchymal transition, a process that contributes to tumour cell invasion (Janda *et al.*, 2002). In OSCC, *Ras* mutations show great geographical variation, being rare in the Western world, but relatively common in India and South East Asia, with a similar distribution to areca nut chewing (Paterson *et al.*, 1996). Indeed, OSCC in OSF patients have a higher incidence of *Ras* mutations (Saranath *et al.*, 1991; Kuo *et al.*, 1994). Thus it may be interesting to examine whether αvβ6-expressing OSF lesions transform on acquiring mutated *Ras* and then undergo EMT.

3.12 Summary

In summary, the results of this chapter show that αvβ6 is strongly expressed in over 50% of OSF cases examined, and that it may have a role in the malignant transformation of the condition to OSCC. αvβ6 expression appears to be upregulated by the areca nut constituent, arecoline, through the muscarinic receptor M_4, and it may exert its pro-fibrotic and pro-malignant effect via activating TGF-β1, which promotes the transdifferentiation of fibroblasts into myofibroblasts, a cell type implicated in pathogenic organ fibrosis and in malignancy (De Wever *et al.*, 2008). Interestingly, the M_4 receptor antagonist tropicamide down-regulated the expression of αvβ6. However, the exact mechanisms behind the regulation of αvβ6 are still unknown. Given that αvβ6 is implicated in the development and progression of a number of carcinoma types, as well as fibrotic disease, understanding the mechanisms regulating expression of the integrin may lead to the development of directed therapies.

Chapter 4

αvβ6 interaction with Sonic Hedgehog pathway in basal cell carcinoma

4.1 Introduction

Basal cell carcinoma (BCC) is the most common malignancy in the Western world, with an incidence that is rising by 10% yearly (Wong *et al*., 2003). BCCs rarely metastasise, but although patient mortality is low, these tumours are locally invasive and may cause significant tissue destruction and morbidity, with approximately 80% of tumours occurring in the head and neck (Scrivener *et al.*, 2002). The pathogenesis of BCC involves deregulated Sonic Hedgehog (SHH) signalling, leading to activation of the glioma-associated (Gli) family of zinc finger transcription factors (Stecca & Ruiz i Altaba, 2010).

BCCs display diverse morphology and a number of different histologic subtypes have been described. The most common BCC variant is the nodular subtype, which accounts for ~80% of tumours and is typically regarded as "low-risk" (Scrivener *et al*., 2002) In contrast, ~6% of BCCs comprise the "high risk" morphoeic variant, which displays a more aggressive clinical behaviour. Data from our laboratory had previously demonstrated a role for αvβ6 integrin in the pathogenesis of morphoeic BCC (Marsh *et al.*, 2008). For this study, Gli1 was transfected into TERT-immortalised skin keratinocytes to generate a BCC model. Using this cell line, it was found that αvβ6 could promote tumour invasion indirectly, through activating TGF-β1 and modulating the tumour stroma.

Given the importance of αvβ6 in cancer and fibrotic disease, and the paucity of data regarding the regulation of the integrin (particularly how expression may be down-regulated), the aim of the work described in this chapter was to further investigate the potential regulation of αvβ6 integrin expression by Gli1, using BCC as the disease model.

4.2 Molecular profile of nodular and morphoeic BCCs

To study the molecular profile of BCC, tissue micro-arrays of 20 representative cases of nodular and morphoeic BCCs were generated from archival tissue, and immunostained for a panel of molecular markers (Figure 4.1). General levels of cytokeratin 5 (CK5), CK7, CK8, Ber-EP4, Vimentin, β-catenin and Epithelial Membrane Antigen (EMA) displayed no difference between the two subtypes. As reported previously in our laboratory, α-SMA was strongly expressed in morphoeic BCC stroma (Marsh *et al.*, 2008).

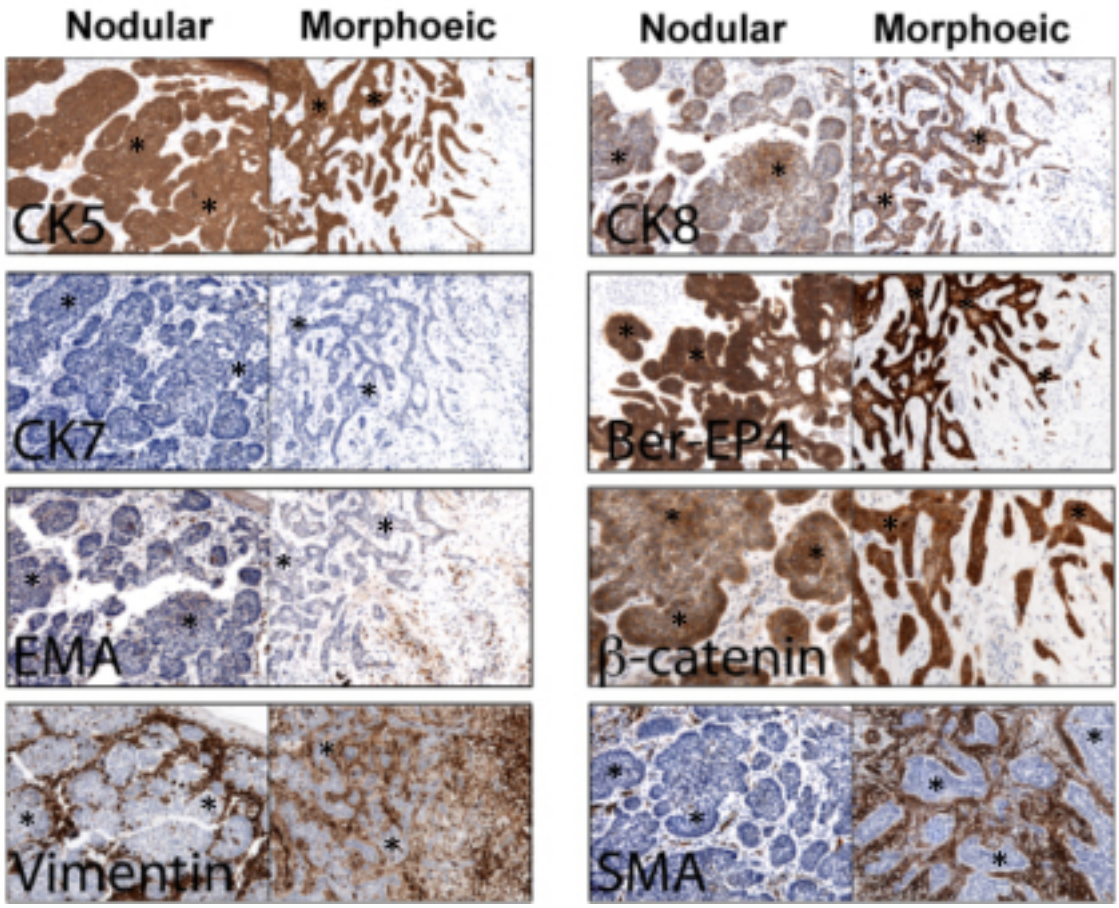

Figure 4.1 Immunohistochemical profile of nodular and morphoeic BCCs. Twenty nodular and 20 morphoeic BCC cases were selected from archival tissue and micro-arrayed. Immunohistochemical analysis was carried out for a panel of molecular markers. Results show no differences in cytokeratin (CK) expression profile. Similarly, total Vimentin and β-catenin levels were were not significantly different. Ber-EP4, a BCC marker, displayed a similar expression pattern in both subtypes, as did Epihelial Membrane Antigen (EMA). α-SMA was strongly expressed in the morphoeic variant of BCC. Tumour islands are astericked (*).

4.3 αvβ6 expression in basal cell carcinoma

Next, we examined αvβ6 expression in 20 nodular and morphoeic BCCs. Although nodular BCCs showed weak αvβ6 expression, the integrin was strongly expressed in the more aggressive morphoeic subtype (Figure 4.2).

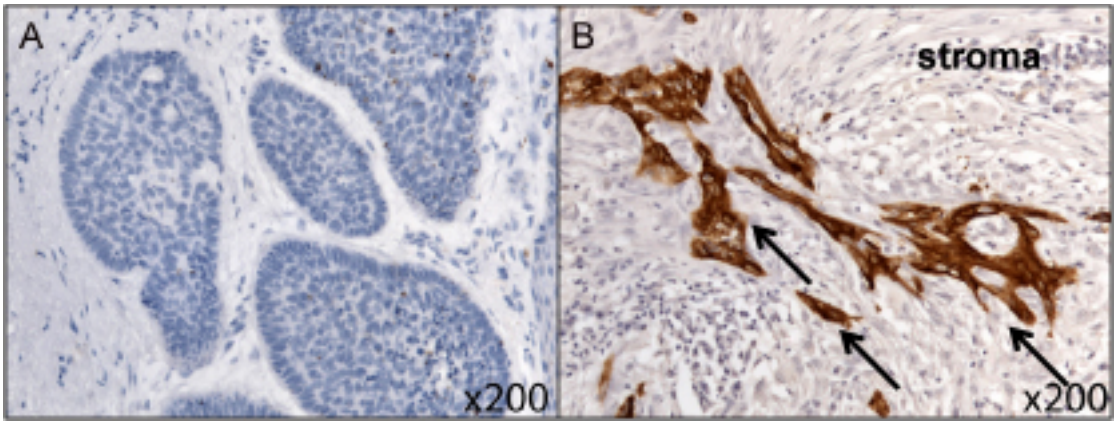

Figure 4.2 αvβ6 is strongly expressed in morphoeic basal cell carcinoma.
Tissue sections from nodular and morphoeic basal cell carcinoma were stained for αvβ6 (*6.2G2*, 0.5 μg/ml) after antigen retrieval in pepsin for 5 min at 37° C. Figure shows representative αvβ6 expression in nodular (A) and morphoeic (B; arrowed) individual cases of BCC. αvβ6 expression was stronger in morphoeic BCC.

4.4 Generation of Gli1 keratinocyte cell lines

To study the role of αvβ6 in BCC, an *in vitro* model of the disease was used. cDNA encoding the SHH transcription factor Gli1 had been previously introduced into NTert-1 skin keratinocytes by retroviral transduction (Marsh *et al*., 2008). Gli1 was next retrovirally introduced into HaCaT skin keratinocytes and H400 SCC cells in this study. Expression of Gli1 was confirmed using Western blotting (Figure 4.3A) and fluorescence microscopy (Figure 4.3B).

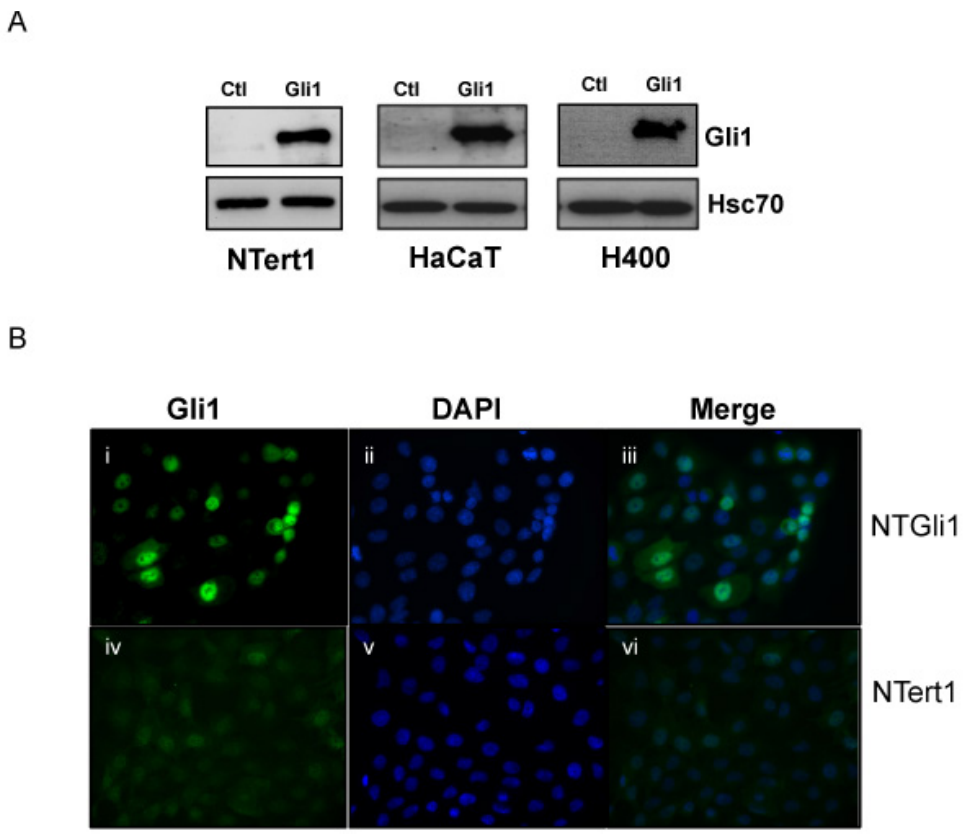

Figure 4.3 Generation of Gli1 keratinocyte cell lines.
Phoenix packaging cell lines were transfected with 10 μg pBABE-Gli1 or pBABE-puro plasmid using Fugene. Keratinocyte cell lines were then retrovirally infected overnight at 37° C and subsequently put into Puromycin selection (2 μg/ml). Hexadimethrine bromide (polybrene) was used in order to increase retroviral infection efficiency.
4.3(A) Western blotting confirmed Gli1 expression in NTert-1, HaCaT and H400 cell lines transduced with pBABE-Gli1 in comparison with pBABE-puro. Blots from representative experiments are shown.
4.3(B) Fluorescence microscopy showing nuclear Gli1 expression in NTGli1 cells (green). A representative experiment is shown.

4.5 Effect of Gli1 on αvβ6 expression in keratinocytes

αvβ6 expression *in vitro* was assessed using the keratinocyte Gli1 cell lines generated as described in the previous section. Transfection of NTert1 keratinocytes with Gli1 significantly down-regulated total and surface αvβ6 protein expression (p=0.001 and p=0.032, respectively), assessed by Western blotting and flow cytometry, respectively (Figure 4.4A). Transfection of HaCaT keratinocytes with Gli1 similarly down-regulated total and surface αvβ6 expression (p=0.003 and p=0.01, respectively; Figure 4.4B). To assess whether Gli1 also down-regulated β6 gene expression, real-time PCR studies were carried out, which showed significant down-regulation of β6 mRNA in NTGli1 and HaCaTGli1 cells (p=0.009 and p=0.001, respectively; Figure 4.4C)

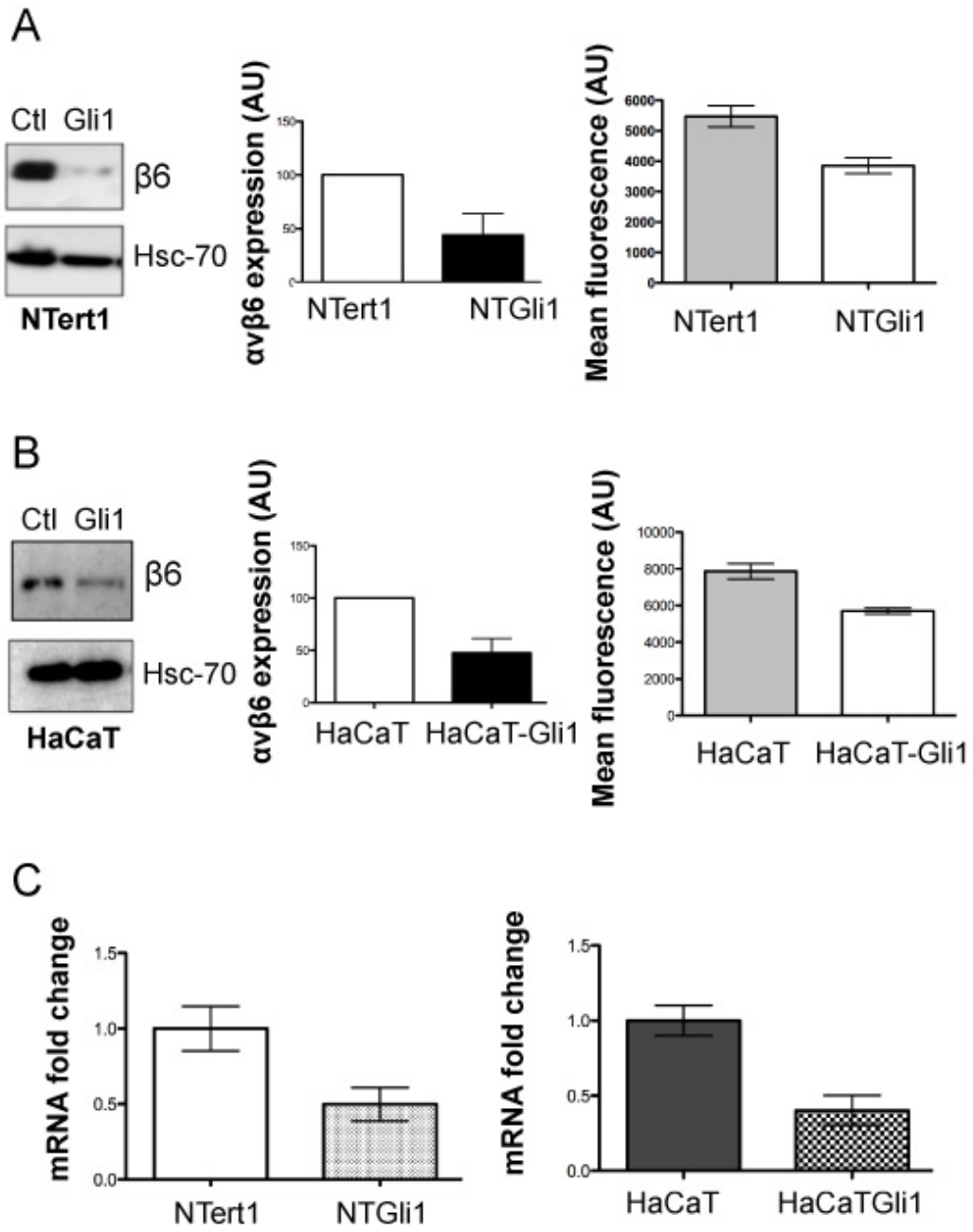

Figure 4.4 Gli1 downregulates αvβ6 expression.
Gli1 was introduced into NTert1 and HaCaT cells by retroviral infection as described.
4.4(A) Western blot showing β6 expression in NTert1 control cells and NTGli1 cells. β6 was significantly down-regulated (*p*=0.001). Flow cytometry also showed significant down-regulation of surface levels of β6 (*p*=0.032). Histogram shows combined results from three independent experiments. Error bars represent SD.
4.4(B) Western blot showing β6 expression in HaCaT control cells and HaCaT-Gli1 cells. β6 was significantly downregulated (*p*=0.003). Flow cytometry also showed significant down-regulation of surface levels of αvβ6 (*p*=0.001). Histogram shows combined results from three independent experiments. Error bars represent SD.
4.4(C) qRT-PCR showing significant down-regulation of β6 mRNA in NTGli1 and HaCaTGli1 cells (*p*=0.009 and *p*= 0.001, respectively). Histograms show combined results from three independent experiments. Error bars represent SD.

4.6 Gli1 expression pattern in nodular and morphoeic BCC

Nuclear Gli1 is classically expressed in the nodular variant of BCC, which had shown low αvβ6 expression. Since αvβ6 was highly expressed in the more invasive morphoeic variant of BCC, we wondered whether Gli1 expression is lost in this variant of BCC. Immunohistochemical analysis for Gli1 in our tissue micro-arrays showed that, whilst nuclear Gli1 was strongly present in nodular BCCs (Figure 4.5A and Figure 4.5B), it was absent or weakly expressed in morphoeic BCCs (Figure 4.5C and Figure 4.5D). This inverse pattern of Gli1 and αvβ6 expression *in vivo* and the suppressive effect of Gli1 on αvβ6 expression *in vitro* led us to investigate whether Gli1 had any suppressive effects on αvβ6-dependent cellular functions.

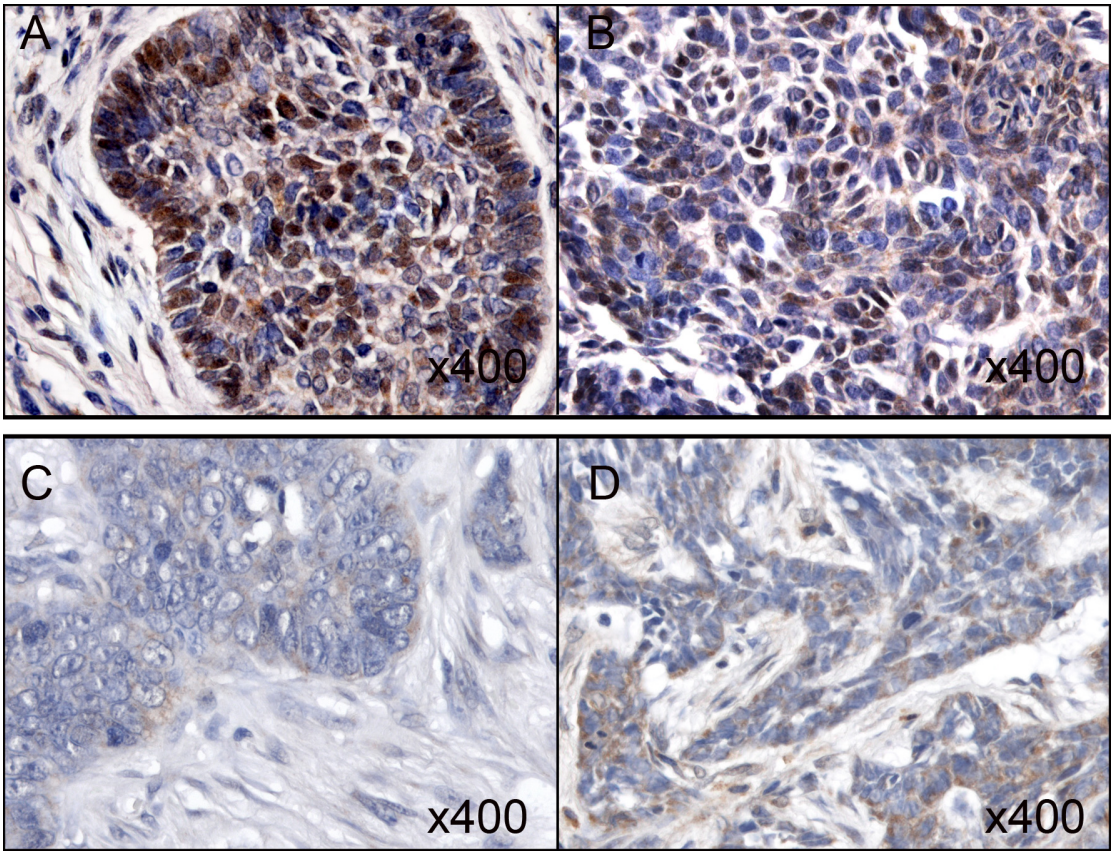

Figure 4.5 Gli1 is weakly expressed in morphoeic basal cell carcinoma.
Tissue sections from 20 nodular and 20 morphoeic basal cell carcinoma were stained for Gli1 (H300, 1:50). Figure shows representative Gli1 expression in nodular (A and B) and morphoeic (C and D) individual cases of BCC. Nuclear Gli1 was strongly expressed in nodular BCC and weak or absent in morphoeic BCC, thus showing an inverse pattern to αvβ6 expression in the two different BCC subtypes. Nuclear Gli1 staining intensity was scored as outlined in Section 2.6.

4.7 Effect of Gli1 on αvβ6-dependent TGF-β1 activation

The inverse expression pattern of αvβ6 and Gli1 *in vivo*, coupled with Gli1's suppressive effect on αvβ6 *in vitro* next led us to investigate whether Gli1 had any suppressive effect on αvβ6-dependent cellular functions. αvβ6 is a pro-invasive integrin, being one of the main mechanisms by which TGF-β1 is activated (Munger *et al*., 1999). In order to investigate whether Gli1 had an effect on αvβ6-dependent activation of TGF-β1, Luciferase reporter assays were carried out (as described in Chapter 3) using NTGli1 and HaCaT-Gli1 cells (and their respective empty vector control cell lines). NTert1 cells activated TGF-β1, which was significantly blocked when αvβ6 was inhibited by the blocking antibody 10D5 (p<0.0001; Figure 4.6A). TGF-β1 activation was significantly reduced in NTGli1 cells, suggesting that the down-regulation of αvβ6 expression by Gli1 also affects αvβ6-dependent cellular functions (p<0.0001; Figure 4.6A). Similarly, HaCaT cells activated TGF-β1, which was significantly inhibited by the αvβ6-blocking antibody 63G9 (Figure 4.6B; p=0.0015). Gli1 similarly suppressed TGF-β1 activation in HaCaT-Gli1 cells (Figure 4.6B; p=0.0001)

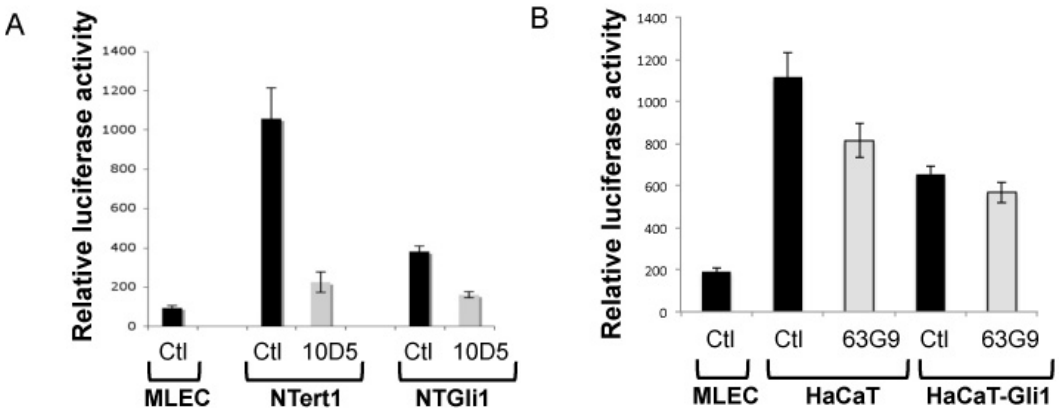

Figure 4.6 Gli1 suppresses αvβ6-dependent TGF-β1 activation.
Keratinocyte cell lines were co-cultured with mink lung epithelial reporter cells (MLEC), as described in Chapter 3.
4.6(A) Co-culture of NTert1 cells with MLEC promoted TGF-β1 activation, which was suppressed by antibody blockade of αvβ6 integrin (*10D5*; p<0.0001). TGF-β1 activation was significantly higher in NTert1 cells than NTGli1 cells. Error bars represent SD. Experiments were carried out in triplicate.
4.6(B) Co-culture of HaCaT cells with MLEC promoted TGF-β1 activation, which was suppressed by antibody blockade of αvβ6 integrin (*63G9*; p=0.0015). TGF-β1 activation was significantly higher in HaCaT cells than HaCaT-Gli1 cells (p=0.0001). Error bars represent SD. Experiments were carried out in triplicate.

4.8 Optimisation of Gli1 siRNA

In order to ascertain that the observed suppression of αvβ6 expression and function was due to Gli1 overexpression rather than a non-specific transfection artefact, we silenced Gli1 using RNAi technology. To determine the best level of knock-down, several concentrations were assessed, and 30 nM was the lowest concentration for optimal knock-down. Gli1 protein knock-down was then examined at several time points by Western blotting (Figure 4.7A) in NTGli1 cell lines. Maximal Gli1 knockdown was observed after 2 d (92% reduction). However, a 53% reduction in Gli1 protein was still observable after 7 d, a sufficiently long time period over which to perform an organotypic culture. Similarly, the best knock-down level in HaCaTGli1 cells was observed at 2 d (Figure 4.7B).

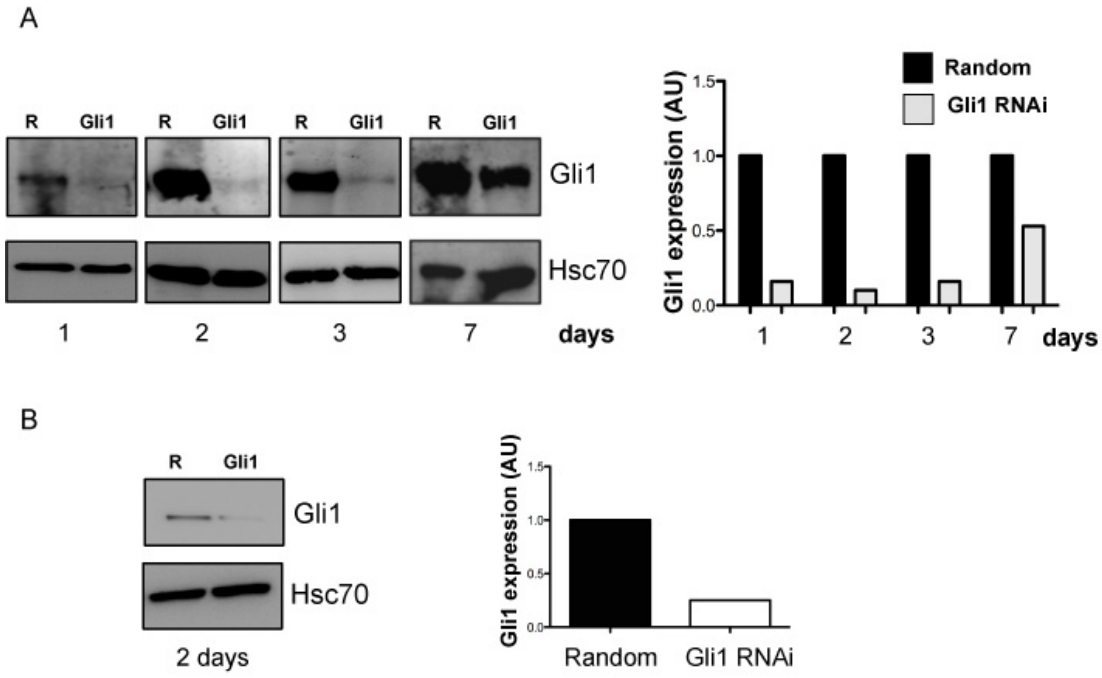

Figure 4.7 Gli1 expression and RNAi knockdown in NTGli1 and HaCaT-Gli1 cells
4.7(A) Western blotting of Gli1 RNAi time-course in NTGli1 cells. Maximal reduction was seen on day 2, however a reduction of 53% was still present after 7 d. Histograms show densitometric analysis.
4.7(B) Western blotting showing 80% Gli1 knockdown in HaCaT-Gli1 cells at 30 nM at 48 hours. Histogram shows densitometric analysis.

4.9 Effect of Gli1 knockdown on αvβ6 expression

Having optimised the time and concentration conditions for silencing Gli1, we next re-examined αvβ6 expression in NTGli1 and HaCaT-Gli1 cell lines in which Gli1 had been silenced. As described earlier, αvβ6 protein was significantly down-regulated upon Gli1 transfection in NTert1 cells. The suppressive effect of Gli1 on αvβ6 was significantly reversed and αvβ6 expression returned to levels similar to basal expression when Gli1 was silenced (p=0.03; Figure 4.8A). Surface levels of αvβ6 were similarly suppressed in NTGli1, and this was suppression was reversed upon Gli1 knockdown (p=0.003; Figure 4.8B). To further validate these results in a second cell line, the same experiments were carried out in the HaCaT-Gli1 cell line, and similar results were obtained for total and surface αvβ6 expression (p=0.02 and p=0.03, respectively; Figure 4.8C). qRT-PCR studies were performed, and similarly showed a significant restoration of β6 mRNA re-expression upon Gli1 RNAi in NTGli1 cells (p=0.02, Figure 4.8D).

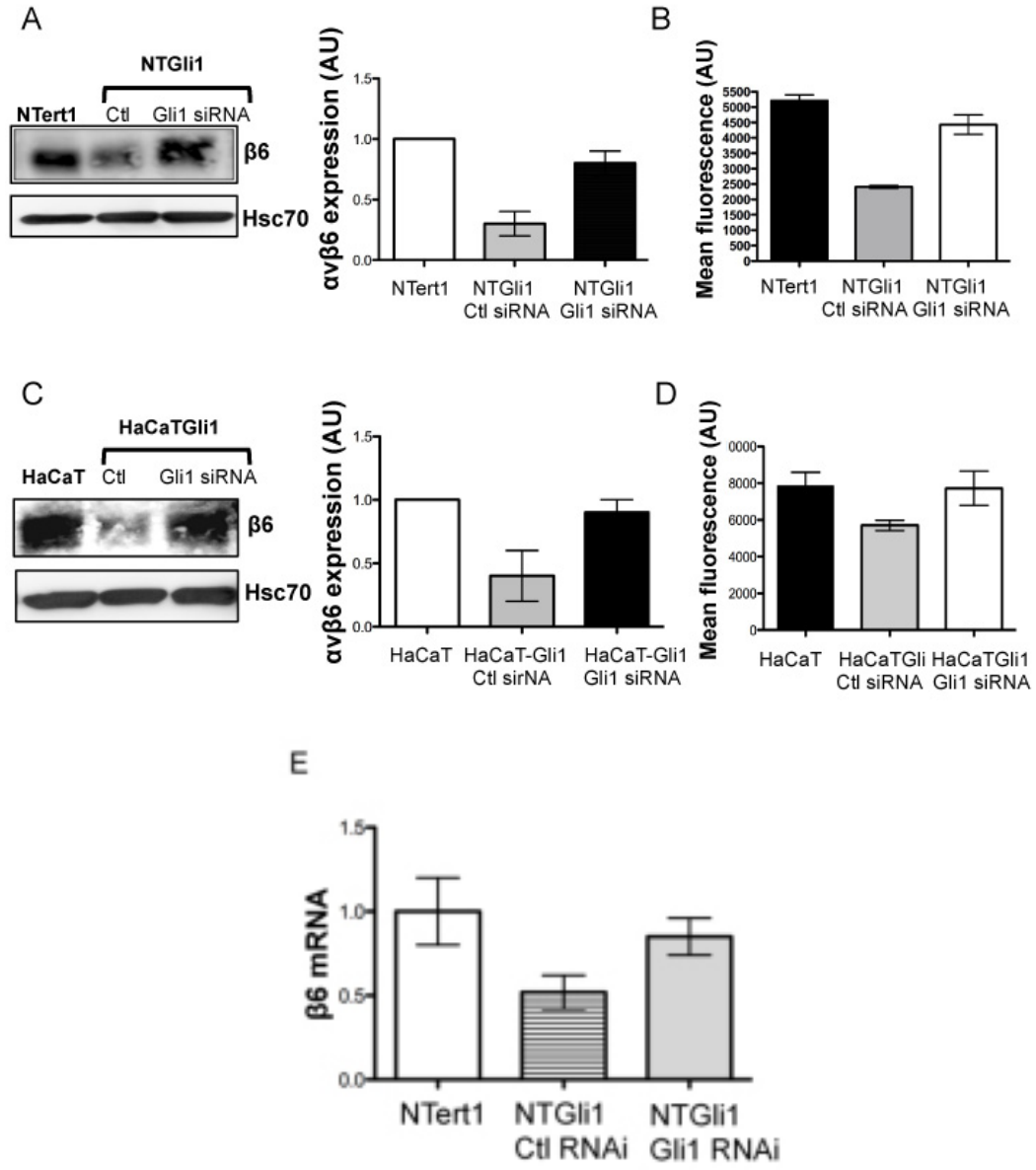

Figure 4.8 Silencing Gli1 reverses its suppressive effect on αvβ6 expression

4.8(A) Western blotting showing αvβ6 expression in NTert1 cells, NTGli1 cells transfected with random siRNA and NTGli1 cells transfected with Gli1 siRNA. αvβ6 protein expression was significantly down-regulated in NTGli1 cells, and this down-regulation was reversed when Gli1 was silenced (*p*=0.03). Error bars represent SD. Experiments were carried out in triplicate.

4.8(B) Flow cytometry showing relative surface level αvβ6 expression showing, similarly, that surface αvβ6 was significantly down-regulated in NTGli1 cells, and this effect being reversed upon treatment with Gli1 siRNA (*p*=0.02) Error bars represent SD. Experiments were carried out in triplicate.

4.8(C) Western blotting showing αvβ6 expression in HaCaT cells, αvβ6 protein expression was significantly down-regulated in HaCaT-Gli1 cells, and this down-regulation was reversed when Gli1 was silenced (*p*=0.02).

4.8(D) Flow cytometry showing relative surface level αvβ6 expression showing, similarly, that surface αvβ6 was significantly down-regulated in HaCaTGli1 cells, and this effect being reversed upon treatment with Gli1 siRNA (*p*=0.03)

4.8(E) qRT-PCR showing re-expression of β6 mRNA upon Gli1 RNAi treatment in NTGli1 cells (*p*=0.02).

4.10 Effect of Gli1 knockdown on αvβ6-dependent cellular functions

As described in Section 4.7, Gli1 overexpression significantly inhibited αvβ6-dependent cellular functions, namely TGF-β1 activation. Since Gli1 knock-down resulted in a reversal of its suppressive effect on αvβ6 expression, we next wanted to investigate whether this also resulted in a restoration of αvβ6-dependent TGF-β1 activation. TGF-β1 activation assays were carried out as described. Results showed that NTert1 cells activated TGF-β1 in a β6-dependent manner, which was significantly inhibited upon β6 RNAi treatment (*p*<0.0001; Figure 4.9). Upon Gli1 knock-down in NTGli1 cells, TGF-β1 activation was restored to a similar level to NTert1 cells, demonstrating a restoration of αvβ6-dependent TGF-β1 activation (*p*=0.0002; Figure 4.9).

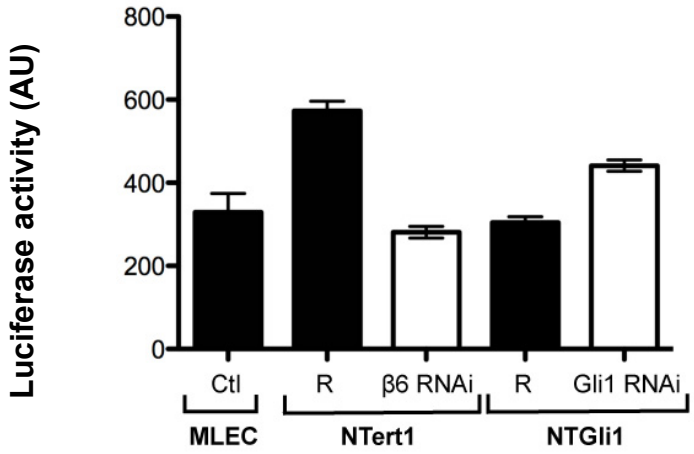

Figure 4.9 Gli1 knockdown restores αvβ6-dependent TGF-β1 activation.
NTert1 and NTGli1 keratinocytes were co-cultured with MLEC cells as described and Luciferase assays carried out. NTert1 cells treated with random (R) non-targeting RNAi activated TGF-β1, which was significantly suppressed with β6 RNAi (*p*<0.0001). NTGli1 cells showed minimal TGF-β1 activation, comparable to NTert1 cells in which β6 had been silenced. Gli1 knock-down restored TGF-β1 activation in NTGli1 cells to levels comparable with NTert1 (*p*=0.0002). Error bars represent SD. Experiments were carried out in duplicate.

To investigate the effect of Gli1 on keratinocyte invasion, organotypic experiments were performed next. Results showed, surprisingly, that NTert1 cells were more invasive in organotypic cultures than NTGli1 cells (Figure 4.10). Furthermore, silencing Gli1 in organotypic cultures resulted in a restoration of invasion comparable to NTert1 control cells (Figure 4.10).

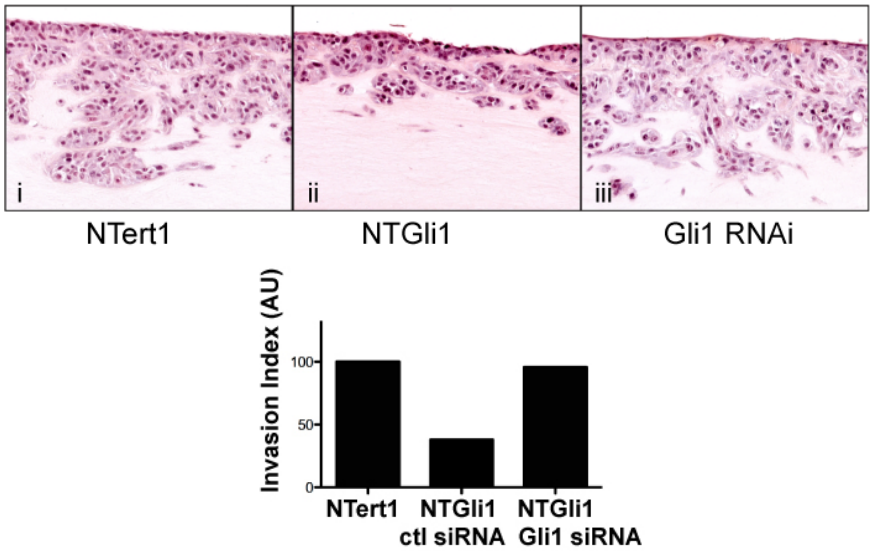

Figure 4.10 NTGli1 cells are less invasive in organotypic cultures than NTert1.
24 h after transfection with random or Gli1 siRNA, cells were plated onto organotypic gels as described in Chapter 3. After 6 d of organotypic cultures (7 d post-transfection) gels were harvested and processed for histology. NTGli1 were less invasive in organotypic gels than NTert1 control cells (ii and i, respectively). When treated with Gli1 RNAi, invasion levels in NTGli1 were restored to NTert1 control levels (iii). Experiments were performed in duplicate. Results from a representative experiment are shown. Histogram shows relative invasion index of an organotypic experiment.

Since NTert1 cells express higher levels of αvβ6 than NTGli1 cells, we wanted to investigate if their invasion in organotypic gels was αvβ6-dependent. To examine this hypothesis, organotypic experiments were carried out next with β6 RNAi, which showed abrogation of invasion upon silencing αvβ6 (Figure 4.11).

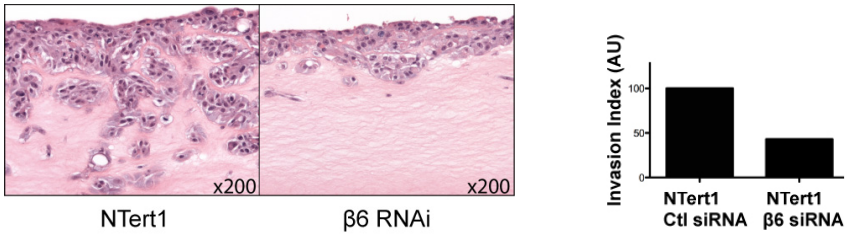

Figure 4.11 NTert1 cells invade in organotypic gels in a β6-dependent manner.
24 h after transfection with random or β6 siRNA, cells were plated onto organotypic gels as described in Chapter 3. After 6 d of organotypic cultures (7 d post-transfection) gels were harvested and processed for histology. NTert1 cells invaded into organotypic gels. When treated with β6 RNAi, invasion was inhibited. Experiments were performed in duplicate. Results from a representative experiment are shown.

4.11 EMT marker studies in BCC *in vitro* model

The epithelial-to-mesenchymal transition (EMT) is a process in developmental biology in which epithelial cells lose cell-cell contacts and acquire a migratory phenotype (Kalluri & Weinberg, 2009). There is accumulating evidence over the past decade describing EMT (or EMT-like processes) in cancer and fibrotic disease (Thiery, 2003; Kalluri & Weinberg, 2009). Several markers for EMT have been described, the most consistent of which is generally considered to be the loss of E-cadherin expression (Gumbiner, 2005). Interestingly, several recent studies have recently described αvβ6 integrin as a marker of EMT (Bates *et al.*, 2005; Ramos *et al.*, 2009; Sume *et al.*, 2010).

Since the organotypic experiments in the previous section showed that NTert1 cells were highly invasive in an αvβ6-dependent manner, we next tested the hypothesis that the high αvβ6-expressing morphoeic BCCs may represent an EMT in BCC. We examined total levels of E-cadherin, N-cadherin and Vimentin by Western blotting in NTert1 cells, NTGli1 cells and NTGli1 cells in which Gli1 had been silenced by RNAi. Results showed that there was no obvious difference in total levels of these markers (Figure 4.12).

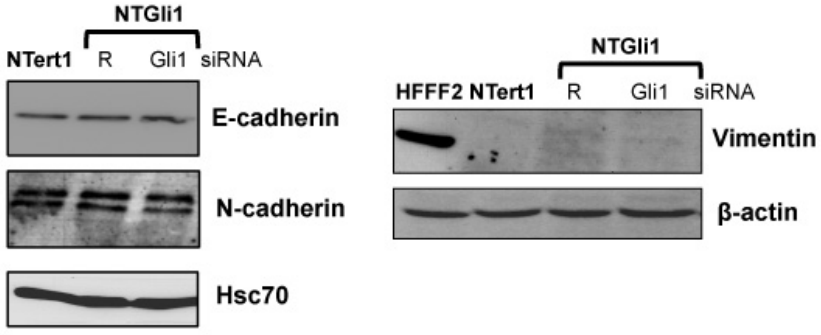

Figure 4.12 Total levels of EMT markers are not different in NTert1 and NTGli1 cells. Western blotting showing no differences in total levels of E-cadherin and N-cadherin and Vimentin between NTert1 cells and NTGli1 cells treated with random or Gli1 RNAi. Vimentin expression was below the detection level by Western blotting. Lysates from the fibroblast cell line HFFF2 were used as a positive control for Vimentin.

Several studies have shown that TGF-β1 and EGFR/Ras signalling co-operate in modulating EMT (Wednt *et al.*, 2010; Ohashi *et al.*, 2010; Freytag *et al.*, 2010; Natsuizaka *et al.*, 2010). Therefore, we speculated that NTert1 cells (which show higher levels of αvβ6-dependent TGF-β1 activation) may show a greater ability to undergo EMT following EGF treatment, and that this may account for their increased invasiveness in organotypic culture (where EGF is included in the growth medium). We therefore treated the cells with EGF (100 ng/ml) for 48 hours to induce EMT, as described in the literature (Davies *et al.*, 2005). Having first confirmed that NTert1 and NTGli1 cells expressed EGFR (Figure 4.13A), we next examined E-cadherin expression with and without EGF treatment. We found that, whilst EGF treatment did not alter the total levels of E-cadherin expressed by the cells (Figure 4.13B), it produced a more significant downregulation of cell surface E-cadherin in NTert cells by flow cytometry (Figure 4.13A). Fluorescence microscopy confirmed these findings, showing that EGF treatment had a more profound effect on the redistribution of E-cadherin from the membrane to the cytoplasm in NTert1 cells compared with NTGli1 cells (Figure 4.13C).

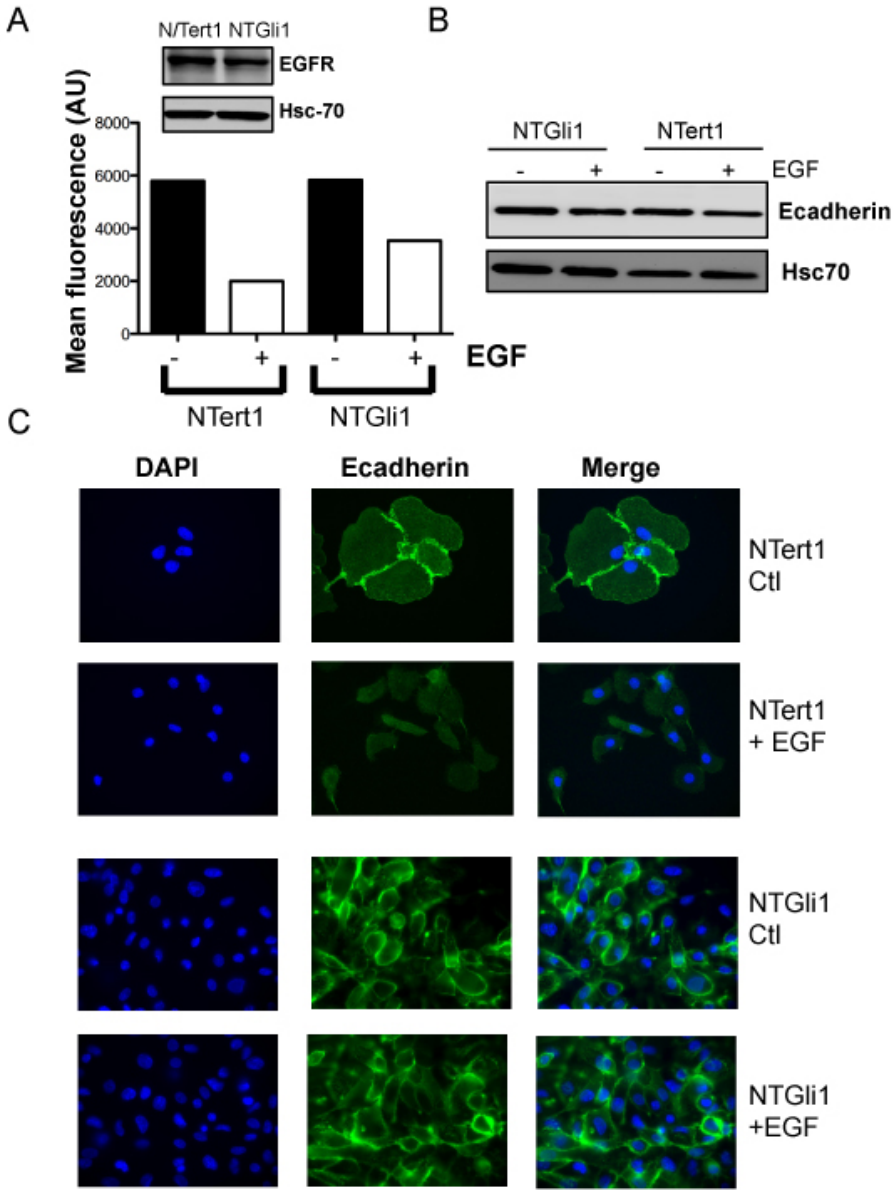

Figure 4.13 EMT induction in skin keratinocytes.
Keratinocytes were plated in 6-well plates and on coverslips, respectively, in serum-free E-KGM and treated with EGF (100 ng/ml) for 48 hours. All experiments were carried out in duplicate.
4.13(A) Western blotting confirming EGFR expression in N/Tert1 and NTGli1 cells. Flow cytometry showing that EGF stimulation inhibits surface levels of E-cadherin in both NTert1 and NTGli1 cells. However, this inhibition was more pronounced in NTert1 cells. A representative experiment is shown.
4.13(B) Western blotting showing minimal reduction in total E-cadherin levels on EGF stimulation in both NTert1 and NTGli1 cells. A representative experiment is shown.
4.13(C) Immunofluorescence for E-cadherin showing loss of membraneous E-cadherin and disruption of cell-cell contacts in NTert1 cells upon EGF stimulation compared with minimal effect on NTGli1 cells. A representative experiment is shown.

To assess the functional relevance of these findings, organotypic experiments were carried out, and E-cadherin expression was assessed by fluorescent microscopy (Figure 4.14). Whilst E-cadherin expression was membraneous in the surface epithelium in NTert1 cells (Figure 4.14), its expression was generally down-regulated and delocalised to the cytoplasm in the more invasive islands, suggesting an EMT-like phenomenon (Figure 4.14).

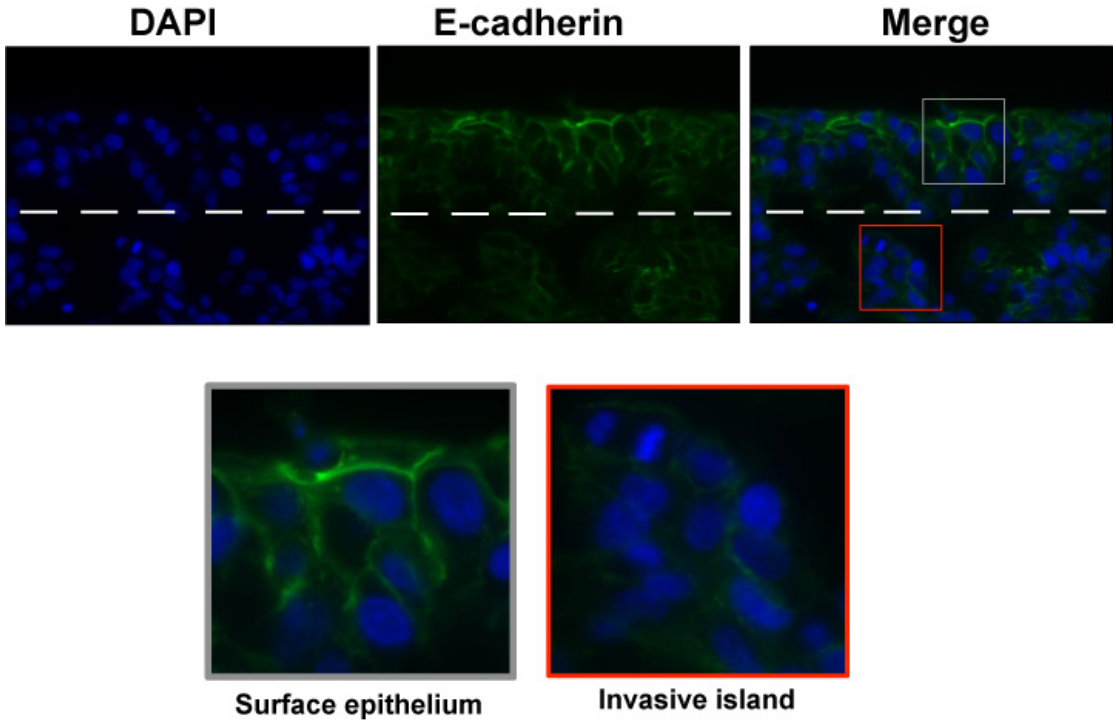

Figure 4.14 E-cadherin expression is delocalised from membraneous to cytoplasmic in the invasive islands in NTert1 cells.
Organotypic cutures were carried out by plating $1x10^6$ keratinocytes onto a protein gel in which $5x10^5$ fibroblasts was seeded. Gels were fixed and processed to histology 6 d later (7 d post-transfection). Fluorescent microscgraph shows cell nuclei (blue) and E-cadherin expressing cells (green) or the combined images in a representative section of the organotypic gel. Dashed white line represents approximate location of basement mebrane. E-cadherin expression is down-regulated in the invasive islands in NTert1 cells (red square) whereas the surface epithelium displays more uniform membraneous expression (grey square). Experiments were carried out in duplicate. Results from a representative experiment are shown.

Next, we assessed the expression of another EMT marker, Vimentin, where we found that, inversely to E-cadherin, expression was generally low in the surface epithelium in organotypic gels, but it was up-regulated in invasive islands (Figure 4.15).

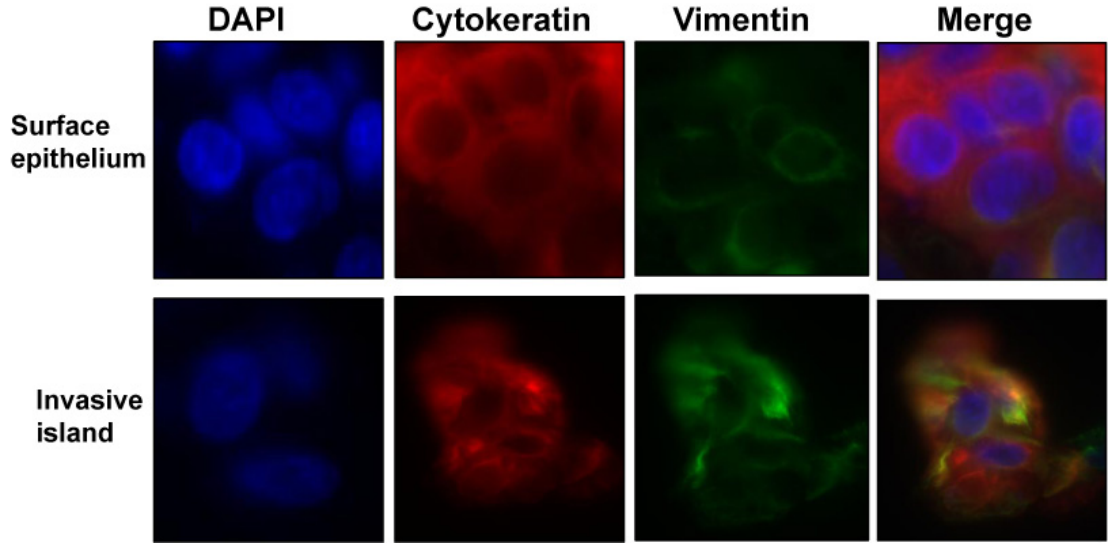

Figure 4.15 Vimentin expression is up-regulated in invasive NTert1 islands in organotypic gels.
Organotypic cutures were carried out by plating $1x10^6$ keratinocytes onto a protein gel in which $5x10^5$ fibroblasts was seeded.Gels were fixed and processed to histology 6 d later. Fluorescent microscgraph shows cell nuclei (blue), pan-cytokeratin (red), Vimentin (green) or the combined images. Vimentin expression appears to be up-regulated in the invasive islands in NTert1 cells. Experiments were carried out in duplicate. Results from a representative experiment are shown.

4.12 Morphoeic BCCs display aberrant E-cadherin expression *in vivo*

To confirm our *in vitro* findings from the previous section, we next returned to clinical BCC samples and examined E-cadherin expression by fluorescence microscopy in 10 nodular and 10 morphoeic BCCs. Results showed that normal surface epidermis and nodular BCC displayed membraneous E-cadherin, whilst this was delocalised to the cytoplasm in the invasive morphoeic BCC islands (representative samples are shown in Figure 4.16), confirming our *in vitro* findings from the organotypic experiments and providing further evidence that morphoeic BCCs may represent a form of tumour cell EMT, and that αvβ6 is potentially implicated in this process.

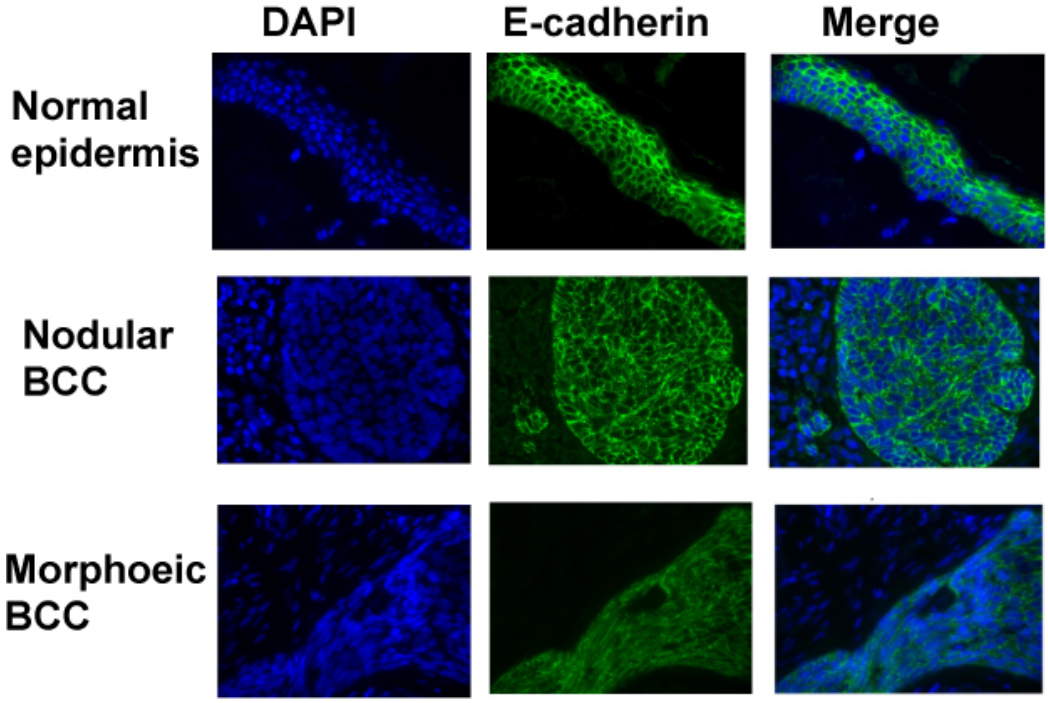

Figure 4.16 E-cadherin displays a more cytoplasmic than membraneous expression in morphoeic BCC. Immunofluorescence studies were carried out on nodular and morphoeic tissue sections. Photomicrographs from representative clinical specimens show uniform membraneous E-cadherin expression in nodular BCC, similar to normal epidermis. Morphoeic BCC, on the other hand, shows a less uniform pattern of E-cadherin expression.

4.13 Discussion

BCC is the most common human cancer worldwide and its incidence is increasing (Armstrong & Kricker, 2001). Although most BCCs are indolent and slow growing, several aggressive histologic variants exist, some of which can cause significant morbidity (Marsh *et al.*, 2008). Sonic Hedgehog signalling is a major developmental pathway important in organ patterning and morphogenesis. Aberrant SHH signalling, principally mediated by the Gli zinc finger transcription factors, has been reported in a variety of carcinomas, including those of the skin, prostate, colon, breast, lung and pancreas, where it has been shown to regulate an array of diverse cell functions, including proliferation, differentiation, migration and invasion (Stecca & Ruiz i Altaba, 2010).

αvβ6 integrin expression has been reported in many carcinoma types, where it has been shown to promote an invasive phenotype (Bates *et al.*, 2005; Nystrom *et al*., 2006). Previous work from our laboratory on the role of αvβ6 in BCC showed that the integrin modulated the invasion of morphoeic BCC indirectly, via its role in activating TGF-β1 and promoting stromal fibroblast-to-myofibroblast transdifferentiation (Marsh *et al.*, 2008).

In this chapter, we show that αvβ6 and Gli1 have an inverse pattern of expression in two different BCC histological subtypes *in vivo* – with nuclear Gli1 being strongly expressed in the 'classic', benign, nodular subtype of BCCs, which showed low αvβ6 expression. Conversely, αvβ6 was highly expressed in the highly invasive, morphoeic BCC, which in turn, showed minimal nuclear Gli1 expression. Using Gli-transfected skin keratinocytes as a BCC model, we examined the interactions of αvβ6 and Gli1 *in vitro*, where we found that Gli1 significantly down-regulated αvβ6 expression. αvβ6-dependent cellular functions such as TGF-β1 activation and keratinocyte invasion were also inhibited by Gli1, suggesting that the inverse pattern of αvβ6 and Gli1 expression in BCCs may also have a functional implication.

Previous studies have shown co-operation between TGF-β1 and EGF/Ras signalling in the induction of EMT (Murillo *et al.*, 2005; Wendt *et al.*, 2010). We showed that NTert1 cells show increased αvβ6-dependent TGF-β1 activation, and since EGF is present in keratinocyte growth medium, we speculated that the increased αvβ6-dependent invasion observed in NTert organotypic cultures may be due to EMT. Consistent with

this, invasive NTert islands displayed features consistent with EMT, with a loss of membraneous E-cadherin expression and an upregulation of Vimentin. Morphoic BCCs *in vivo* also showed deregulation of E-cadherin localisation. Interestingly, a very recent study has shown similar findings in the context of drug-induced gingival overgrowth, in which *de novo* αvβ6 expression was coupled with a down-regulation of E-cadherin and an induction of Slug expression, another EMT marker (Sume *et al.*, 2010).

A potential caveat in this hypothesis is the inverse correlation between αvβ6 and Gli1, which itself has also been the subject of recent studies suggesting a pro-EMT role for the transcription factor in oesophageal, gastric, prostate and colorectal carcinomas (Ohta *et al*., 2009; Isohata *et al.*, 2009; Varnat *et al*., 2010). A possible explanation for this dichotomy is that the action of Gli1 is cell-type and context-specific. So, whilst Gli1 has been shown to transcriptionally activate Snail, a known EMT inducer, in colorectal carcinoma cells (Varnat *et al.*, 2009); our results here suggest that Gli1 imparts a less migratory phenotype to keratinocytes in the context of basal cell carcinoma. This is, in fact, in line with previous work in this area, which has shown that Gli1 transfection was asssociated with reduced pathway activation downstream of EGFR, repression of Vimentin and the induction of a more compact, epithelial phenotype in epidermal keratinocytes (Neill *et al*., 2008).

Of particular interest is the finding that Gli1 transfection in skin keratinocytes significantly down-regulated αvβ6 expression and function. Transfection of Gli1 into the OSCC cell line H400 produced a similar effect on αvβ6 expression, suggesting this effect may be relevant in different cell types and contexts. αvβ6 is not expressed in normal epithelia but is up-regulated during tissue remodeling, and in pathogenic states such as cancer and fibrosis (Thomas *et al.*, 2006). The mechanisms regulating its expression, however, remain to be fully described. The cytokines TGF-β1 and TNF-α have been shown to up-regulate αvβ6 expression (Munger *et al.*, 1999; Scott *et al.*, 2004); and more recently, the transcription factors Ets1 and Stat3 have been shown to interact with the β6 promoter (Bates *et al*., 2005; Azare *et al*., 2007). Gli1 is traditionally regarded as a transcriptional activator, suggesting that this observed inhibitory action on αvβ6 transcription is possibly via an indirect mechanism. Further studies attempting to dissect the potential mechanisms regulating the expression of αvβ6 are carried out in Chapter 6 of this thesis.

4.14 Summary

In summary, the results of this chapter showed that αvβ6 integrin was strongly expressed in the aggressive morphoeic variant of BCC. Conversely, the Sonic Hedgehog transcription factor Gli1, traditionally expressed in the majority of nodular BCCs, was weakly expressed or lost in the morphoeic variant. We showed that transfection of skin keratinocytes with Gli1 significantly down-regulated αvβ6 expression and function *in vitro*, suggesting that Gli1 may regulate BCC αvβ6 expression. Morphologically, morphoeic BCCs *in vivo*, showed features suggestive of EMT, with cells often appearing elongated and spindled. Although total levels of E-cadherin were unaltered in our 2-D experiments, EGF treatment induced a more pronounced effect on keratinocyte discohesion in NTert1 than NTGli1 cells. We also found that NTert1 cells (which have high αvβ6 expression) were more invasive in organotypic cultures, and the invasive islands showed EMT features, which were EGF-dependent. Moreover, E-cadherin expression was delocalised to the cytoplasm in morphoeic BCC *in vivo*. Since Gli1 signalling appeared to be weakened or lost in morphoeic BCC, our data suggest that Gli1 is possibly a negative regulator of EMT in the majority of BCC cases, *viz-a-viz* its inhibitory effect on αvβ6 expression and function. When Gli1 signaling is down-regulated, as is the case in morphoeic BCC, αvβ6 can then exert its pro-invasive effects, via promoting an EMT phenotype in this disease context. The exact mechanism of Gli1 regulating the expression of αvβ6 remains to be elucidated, but it is likely to be an indirect effect on the transcription of β6 gene. Given the paucity of data on the regulation of αvβ6 expression both in health and in disease, dissecting the mechanism behind Gli1 regulation of αvβ6 expression will be of immense value both in the context of disease pathophysiology, but also in the development of directed therapies.

Chapter 5
αvβ6 in oral squamous cell carcinoma prognosis

5.1 Introduction

Oral squamous cell carcinoma (OSCC) is the eleventh most common solid tumour worldwide, representing about 5% of all malignancies (WHO World Cancer Report, 2003), with over 5,500 new cases in the UK annually. Grouped with oropharyngeal cancer, OSCC is the 6th most common cancer worldwide (Warnakulasuriya, 2009). Despite improvements in surgery and radiotherapy, the mainstay of OSCC treatment, the mortality rate for the disease has remained largely unchanged for decades, with 5-year survival rates of less than 50% (Parkin, 2001).

Many attempts have been made to identify biological and molecular markers to tailor treatment and predict OSCC prognosis, but as it stands, management of the OSCC patient is determined primarily by thorough pathological examination of the tumour resection specimen. The tumour, node and metastasis (TNM) classification underpins this management, staging the disease according to the size of the tumour and the presence or absence of loco-regional and/or distant metastasis (Woolgar, 2006).

Additional information routinely collected by histopathologists and clinicians involved in OSCC patient management include tumour depth, grade, surgical margin status, pattern of invasion (tumour cohesiveness) and the presence of lymphovascular and/or perineural invasion. Attempts have been made to combine some of these parameters and use them in defined clinical scoring systems, but these have been largely unsuccessful owing to unsatisfactory inter-observer agreement (Woolgar, 2006).

αvβ6 integrin is strongly expressed in OSCC (Thomas *et al.*, 2006) and it promotes tumour cell invasion by several mechanisms (Nystrom *et al.,* 2006; Marsh *et al.*, 2008; Yap & Jenei *et al.*, 2009). Several studies have shown that αvβ6 is prognostic in numerous tumour types, including colorectal, gastric, lung and breast cancer (Bates *et al.*, 2005; Elayadi *et al.*, 2007; Hazelbag *et al.*, 2007; Professor Louise Jones – personal communication). In this chapter, we aimed to investigate αvβ6 integrin as a potential prognostic marker in OSCC. We conducted a retrospective clinico-pathological study based on 282 cases of OSCC, and developed a prognostic model using Cox regression analysis with backward elimination.

5.2 OSCC cell line construction

To study αvβ6 in OSCC invasion *in vitro*, we used a panel of cell lines derived from the H357 tongue cancer cell line, kindly provided by Professor S. Prime, University of Bristol (Prime *et al.*, 1990). Derivatives of H357 that vary in their expression of αvβ6 have been generated in our laboratory, and are shown schematically in Figure 5.1A. H357 (αv negative) was retrovirally infected with αv cDNA to form V3 (expressing low levels of αvβ6; Jones *et al.*, 1996). V3 was then retrovirally infected with wild type human β6 cDNA to form VB6 (expressing high levels of αvβ6; Thomas *et al.*, 2001a). In this study, we retrovirally infected the IC6 cell line with the empty pBABE vector (encoding the puromycin resistance gene alone) to form IC6pr, not expressing αvβ6 (Figure 5.1). This cell line represents the appropriate αv-negative control cell line for VB6.

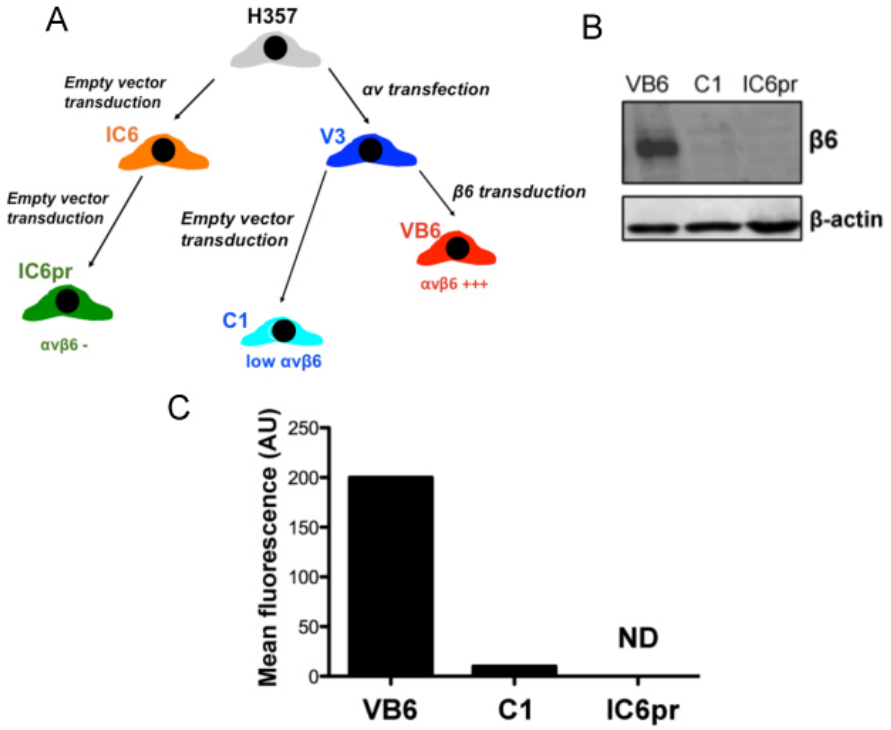

Figure 5.1: SCC cell line construction and β6 expression
5.1(A) Diagrammatic representation of SCC cell line construction. The αv negative SCC cell line H357 was retrovirally transfected with αv cDNA to form V3 (expressing low levels of αvβ6). This was then retrovirally infected with β6 cDNA to form VB6 (expressing high levels of αvβ6; Thomas *et al.*, 2001a). IC6 was retrovirally infected in this study with the empty vector to form IC6pr, which do not express αvβ6
5.1(B) Western blot showing strong expression of αvβ6 in VB6 and undetectable expression in C1 and IC6pr. A representative experiment is shown.
5.1(C) Flow cytometry confirmed high αvβ6 expression in VB6. C1 null transfectants had low αvβ6; whilst IC6pr were αvβ6 negative. ND = not detectable. A representative experiment is shown.

5.3 αvβ6 directly promotes OSCC invasion in Transwell® assays

To confirm that SCC cell lines are capable of invasion in an αvβ6-dependent manner, Transwell® invasion assays were carried out utilising the cell lines described in Section 5.2. Results showed that the high-β6 expressing VB6 cell line was significantly more invasive than the β6 negative cell line IC6pr (Figure 5.2A; *p*=0.0002). These assays were then repeated in the VB6 cell line in the presence of the αvβ6-blocking antibody (*63G9*), which significantly blocked αvβ6-dependent SCC cell line invasion (Figure 5.2B; *p*=0.009), confirming that the observed invasion was β6-dependent.

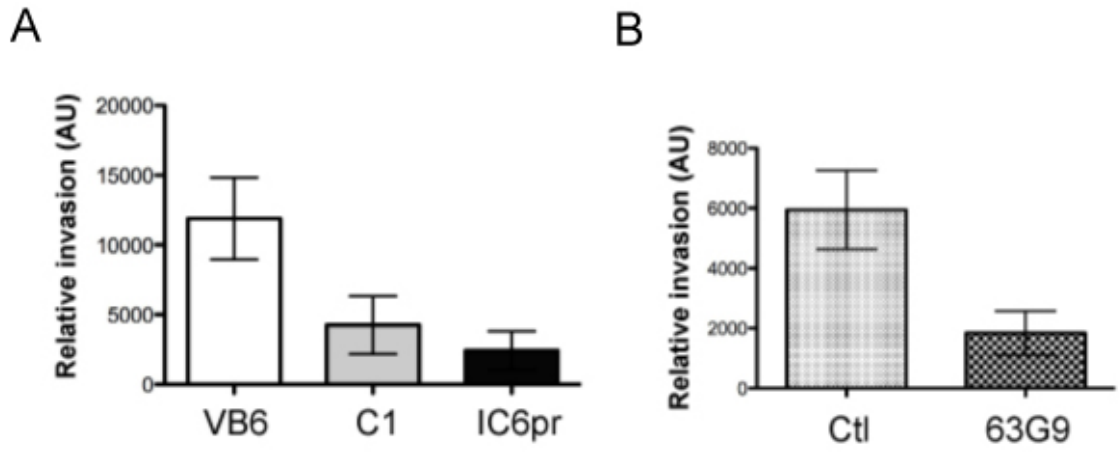

Figure 5.2 αvβ6 promotes OSCC invasion in Transwell® assays *in vitro*.
5.2(A) Invasion assays were performed using Matrigel®-coated polycarbonate filters. VB6 cells were significantly more invasive than both C1 and IC6pr cell lines (*p*=0.001 and *p*=0.0002, respectively). Figure shows combined results from three experiments. Error bars represent SD.
5.3(B) Invasion assays were carried out in VB6 cells in the presence or absence of a function-blocking antibody (63G9). Controls were treated with control antibody (7.2). Blocking αvβ6 significantly inhibited OSCC cell line invasion in Matrigel® (*p*=0.009). Figure shows combined results from three experiments. Error bars represent SD.

5.4 αvβ6 promotes invasion in organotypic cultures

Next, we examined the ability of αvβ6 to promote invasion in organotypic cultures, a more physiologically relevant method of studying cancer. Results showed that VB6 cells were highly invasive in organotypic cultures (Figure 5.4). To confirm that the observed invasion was β6-dependent, we transfected cells with RNAi targeting the β6 integrin. Results showed that silencing β6 by RNAi inhibited OSCC invasion in organotypic cultures, confirming that the observed invasive ability of OSCC cells was β6-dependent. (Figure 5.4)

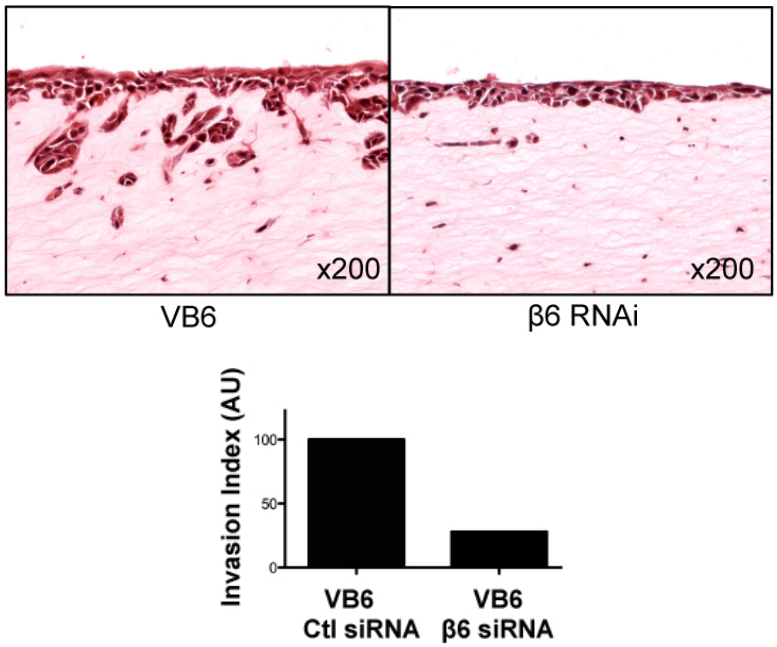

Figure 5.3 αvβ6 promotes OSCC invasion in organotypic cultures.
Organotypic cultures with an air-tissue interface were performed by preparing gels comprising a 50:50 mixture of Matrigel and type I collagen containing 5 x 10 per ml of fibroblasts, to which 1 x 10 VB6 cells were added. The figure shows that VB6 invaded into organotypic cultures and that invasion was inhibited when β6 was silenced by RNAi. Experiments were carried out in duplicate. Photo-micrographs are from a representative section of an individual organotypic gel. Relative quantification of invasion from a representative experiment is shown.

5.5 αvβ6 is highly expressed in OSCC

Having established that αvβ6 promoted OSCC invasion *in vitro,* we next examined its expression in clinical OSCC specimens. 282 OSCC cases were obtained from archival material and stained for αvβ6. Appropriate ethical approval was in place. Expression of αvβ6 in OSCC is summarised in Table 5.1

αvβ6 expression	No.of patients (%), n = 282	No. dead from OSCC (%), n = 120
Low / medium	144 (51)	50
High	138 (49)	70

Table 5.1 αvβ6 expression in OSCC. Two hundred and eighty-two OSCC cases were selected from archival material and stained for αvβ6. Staining was scored according to the Quickscore method, as described in Section 2.3. 49% of OSCC cases expressed αvβ6 at high levels.

Of 282 OSCC cases, strong expression of αvβ6 was present in 49% of cases (Figure 5.4). In contrast, no strong staining was observed in normal oral epithelium (Figure 5.4)

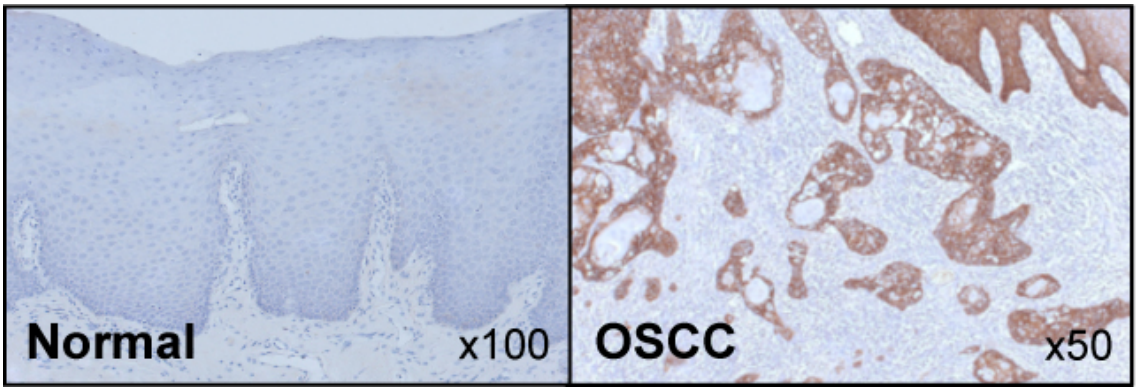

Figure 5.4 αvβ6 expression in OSCC. Tissue sections from 282 OSCC cases were stained αvβ6 (*6.2G2*, 0.5 μg/ml) after antigen retrieval in pepsin for 5 minutes at 37º C. Figure shows representative αvβ6 expression in d individual cases of OSCC. αvβ6 expression was expressed at high levels in 49% of OSCC cases.

5.6 Construction of clinicopathological OSCC database

Having confirmed that αvβ6 was expressed in OSCC *in vivo*, and that it promoted OSCC invasion *in vitro*, we next wanted to examine whether it may be used as a potential prognostic marker for OSCC. A retrospective database was constructed based on 282 consecutive OSCC patients (1992-2005) identified from medical records at two teaching hospitals. The median follow-up was 6.4 years. Of 282 patients, 120 were known to have died from OSCC. Tumour histology was reviewed blindly by two histopathologists (Professor Gareth Thomas and Dr Kim Piper), and a suitable paraffin block was selected. Data were obtained on age, sex, tumour stage (I-IV), lymph node (LN) metastasis (yes or no) with or without extranodal spread, grade (well, moderately, poorly differentiated), surgical margins, (positive = <1mm; close =>1 to <5 mm, clear = > 5mm), tumour depth (in mm) (Woolgar, 2006) and pattern of invasion (cohesive or discohesive). Pattern of invasion was used to classify tumours as cohesive (Bryne patterns 1 and 2) or discohesive (Bryne patterns 3 or 4) (Bryne *et al.*, 1992). The inflammatory infiltrate was scored as high (diffuse), moderate (patchy) or low (weak/absent). The complete database is shown in Table 5.2.

Characteristic		No. of patients (%) N=282	No. dead from OSCC N=120
Age	<50 years	49(17)	16
	50-59	75 (27)	36
	60-69	78 (28)	32
	70+	79 (28)	36
Sex	Male	179 (63)	77
	Female	103 (37)	43
Cancer site	Tongue	106 (38)	44
	Floor of mouth	39 (14)	17
	Buccal mucosa	30 (11)	13
	Gingiva/alveolar mucosa	26 (9)	12
	Lip	24 (9)	5
	Tonsil/base of tongue	21 (7)	12
	Maxilla/palate	16 (6)	6
	Retromolar	13 (5)	7
	Mandible	7 (2)	4
Disease stage	I	98 (35)	21
	II	43 (15)	20
	III	15 (5)	8
	IV	125 (44)	70
Radiotherapy	Yes	166 (59)	56
	No	113 (41)	63
Grade	Well differentiated	53 (19)	14
	Moderately differentiated	169 (6)	72
	Poorly differentiated	59 (21)	34
Surgical margins	Clear (>5 mm)	85 (30)	23
	Close (1-5 mm)	82 (29)	36
	Involved (<1 mm)	113 (40)	61
Metastases	No	190 (67)	66
	Yes	92 (33)	54
Extranodal spread	No	242 (86)	94
	Yes	39 (14)	25
Pattern of invasion	Cohesive	162 (57)	51
	Discohesive	120 (43)	69
Depth of invasion	<3.0 mm	43 (15)	8
	3.0-3.9 mm	17 (6)	7
	4.0-4.9 mm	23 (8)	6
	5.0-9.9 mm	95 (34)	36
	10.0+ mm	104 (37)	63
Inflammation	Low	138 (49)	74
	Medium	85 (30)	32
	High	59 (21)	14

Table 5.2 Complete clinico-pathological OSCC database. Database was based on 282 retrospective cases of OSCC from two teaching hospitals.

5.7 Association of risk factors with mortality

Next, we examined the hazard ratios for OSCC mortality for each factor in the clinico-pathological database separately (Table 5.3). The death rate was associated with advanced disease stage, close or involved surgical margins, prior radiotherapy, moderately or poorly differentiated tumour grade, metastatic disease, extranodal spread, discohesive pattern of invasion, increasing depth of invasion and low inflammation. There was a suggestion of an effect for age. There was insufficient evidence of an association with age and cancer site. αvβ6 integrin was significantly associated with death rate (Figure 5.5 and Table 5.3; *p*=0.037). Given this promising initial result, we next wanted to further investigate the potential use of αvβ6 integrin as a possible prognostic marker for OSCC by examining its role as a potential predictor for patient mortality.

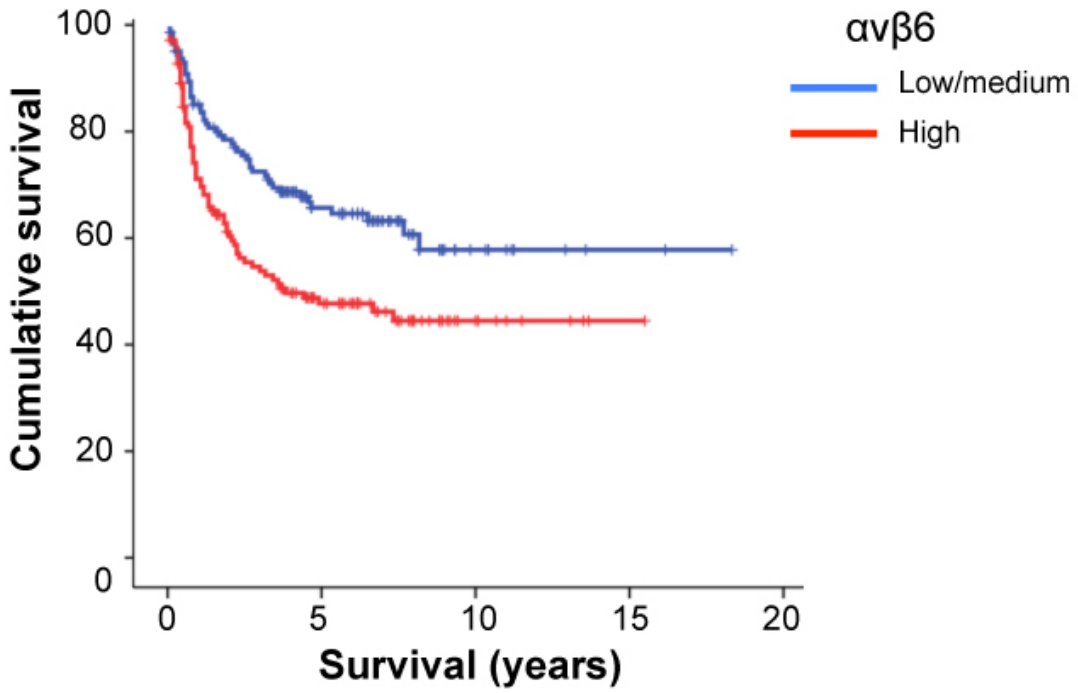

Figure 5.5 αvβ6 Kaplan Meier survival curve for OSCC mortality. Survival analysis was performed using Statistical Package for Social Sciences (SPSS) v. 18. Figure shows Kaplan Meier survival curves for OSCC mortality according to αvβ6 expression (log-rank text, *p*=0.037)

Characteristic	Unadjusted hazard ratio (95% CI)	Adjusted hazard ratio (95% CI)	*p* value (adjusted model)
Age			
For increase of 5 years	1.04 (0.97-1.11)	1.08 (0.99-1.16)	0.07
Sex			
Male	1.0	1.0	
Female	0.96 (0.66-1.40)	1.43 (0.94-2.18)	0.10
Cancer site			
Buccal	1.0	1.0	0.93
Floor of mouth	0.95 (0.46-1.95)	0.83 (0.38-1.80)	
Tongue	1.01 (0.55-1.88)	0.99 (0.50-1.94)	
Lip	0.48 (0.18-1.26)	0.71 (0.26-1.93)	
Other	1.30 (0.68-2.35)	0.98 (0.50-1.94)	
Disease stage			
I	1.0	1.0	0.20
II	2.61 (1.41-4.82)	1.90 (0.99-3.66)	
III	3.02 (1.34-6.82)	1.62 (0.65-4.03)	
IV	3.64 (2.24-5.94)	1.21 (0.62-2.33)	
Radiotherapy			
Yes	1.0	1.0	0.41
No	1.94 (1.35-2.78)	1.18 (0.80-1.75)	
Grade			
Well differentiated	1.0	1.0	0.94
Moderately differentiated	1.82 (1.03-3.22)	1.07 (0.51-2.21)	
Poorly differentiated	2.96 (1.59-5.52)	1.11 (0.58-2.12)	
Surgical margins			
Clear (>5 mm)	1.0	1.0	0.04
Close (1-5 mm)	1.81 (1.07-3.05)	1.98 (1.16-3.38)	
Involved (<1 mm)	2.58 (1.60-4.17)	1.68 (0.97-2.93)	
Metastases			
No	1.0	1.0	0.05
Yes	2.31 (1.61-3.32)	1.76 (1.00-3.11)	
Extranodal spread			
No	1.0	1.0	0.70
Yes	2.54 (1.63-3.96)	1.12 (0.63-1.98)	
Pattern of invasion			
Cohesive	1.0	1.0	0.001
Discohesive	2.46 (1.71-3.54)	2.07 (1.33-3.24)	
Depth of invasion			
For increase of 5 mm	1.40 (1.23-1.59)	0.96 (0.78-1.19)	0.71
Inflammation			
Low	1.0	1.0	0.55
Medium	0.58 (0.38-0.88)	0.88 (0.55-1.42)	
High	0.32 (0.18-0.57)	0.69 (0.36-1.35)	
αvβ6 integrin			
Low/medium	**1.0**	**1.0**	**0.037**
High	**1.71 (1.19-2.46)**	**1.486 (1.024-2.157)**	

Table 5.3 Association of risk factors with mortality (univariate analysis). There was a significant association for high αvβ6 expression with mortality (*p*=0.037)

5.8 Prognostic performance of each factor individually

Given that high αvβ6 expression was shown to be significantly associated with mortality from OSCC (p<0.05) in the previous section, we next wanted to evaluate the prognostic performance of each factor in the database (i.e., the 1- and 3-year OSCC death rates). We did so by calculating the detection rate (DR; also known as sensitivity) and the false-positive rate (FPR; also known as 1-minus specificity). DR was the proportion of patients who died from OSCC with marker-positive results; FPR was the proportion of patients who did not die from OSCC with marker-positive ratios. Likelihood ratios (DR/FPR) were obtained, which indicate the strength of a marker (i.e. maximizing the DR whilst minimizing the FPR). Table 5.4 shows the prognostic performance of each factor using DR and FPR. Upon consultation with a statistician (Dr. Alan Hackshaw, University College London), a likelihood ratio value of '3' was set as highly predictive. Further analysis showed that the likelihood ratio for 3-year mortality only exceeded 3 for extranodal spread (3.4). Although several factors on their own could identify a high proportion of patients who died from OSCC by 3 years (high DR), they also identified too many patients who did not die from OSCC (high FPR). When we performed this type of detailed analysis, αvβ6 expression proved to be a poor predictor of patient mortality, with a likelihood detection ratio of 1.5.

5.9 αvβ6 expression correlation studies

A series of correlation studies to examine whether αvβ6 expression correlated negatively or positively with any other factors in the clinico-pathological database were performed (Marsh *et al.*, 2011). Of all factors examined, αvβ6 expression correlated significantly positively (p<0.05) only with depth of invasion and stromal SMA expression. The utility of SMA as a prognostic marker for OSCC was further examined in a parallel, in-depth study from our laboratory (Marsh *et al.*, 2011).

	1-year status			*3-year status*		
Characteristic and definition of test-positive	**DR % (60 deaths)**	**FPR % (214 alive)**	**Likeli-hood ratio**	**DR % (99 deaths)**	**FPR % (164 alive)**	**Likeli-hood ratio**
Age, years						
≥45	95	90	1.05	95	88	1.1
≥50	85	82	1.04	87	79	1.1
≥55	73	69	1.06	74	67	1.1
≥60	57	56	1.02	58	55	1.05
Sex						
Male	68	63	1.1	64	64	1.0
Disease stage						
≥ II, III, IV	93	57	1.6	88	52	1.7
≥ III, IV	75	43	1.7	69	39	1.8
IV	71	37	1.9	62	34	1.8
Radiotherapy						
Yes	50	39	1.3	53	35	1.5
Grade						
Moderate	88	79	1.1	90	76	1.2
Poor	33	17	1.9	31	15	2.1
Surgical margins						
Close; involved	87	66	1.3	83	62	1.3
Involved	62	35	1.8	54	32	1.7
Metastases						
Yes	55	36	1.5	48	23	2.1
Extranodal spread						
Yes	27	10	2.7	24	7	3.4
Pattern of invasion						
Discohesive	72	35	2.1	66	30	2.2
Depth of invasion						
≥ 4.0 mm	88	75	1.2	89	71	1.2
≥ 5.0 mm	85	65	1.3	85	60	1.4
≥ 6.0 mm	73	59	1.2	76	52	1.5
≥ 10.0 mm	60	30	2.0	49	23	2.6
Inflammation						
Low; medium	92	75	1.2	90	71	1.3
Low	63	43	1.5	65	37	1.8
αvβ6 integrin						
High	**12**	**60**	**1.4**	**20**	**52**	**1.5**

Table 5.4 Prognostic value of each factor from the OSCC clinico-pathological database (multivariate analysis)

5.10 Expression pattern of αvβ6 in different OSCC subtypes

The results of this chapter thus far and the analysis of αvβ6 in OSCC showed that the integrin is expressed at medium to high levels in the majority of OSCC cases, In order to investigate its role in prognosticating OSCC in more detail, we assessed its expression in different histopathological subtypes of OSCC. First, we examined αvβ6 expression pattern across the three major OSCC grades (poor, moderately and well differentiated OSCC). We found that the different OSCC tumour grades showed roughly an equal expression pattern of αvβ6 (Table 5.5).

αvβ6 expression	Poorly differentiated OSCC (60)	Moderately differentiated OSCC (169)	Well differentiated OSCC (51)
Low / moderate	31 (52%)	81 (48%)	30 (59%)
High	29 (48%)	88 (52%)	21 (41%)

Table 5.5 αvβ6 expression in different OSCC grades.

Interestingly, however, when we examined the expression of αvβ6 in verrucous and basaloid SCC (which are regarded as well- and poorly-differentiated respectively), we found that the integrin was either weakly expressed or not present at all (Figure 5.6)

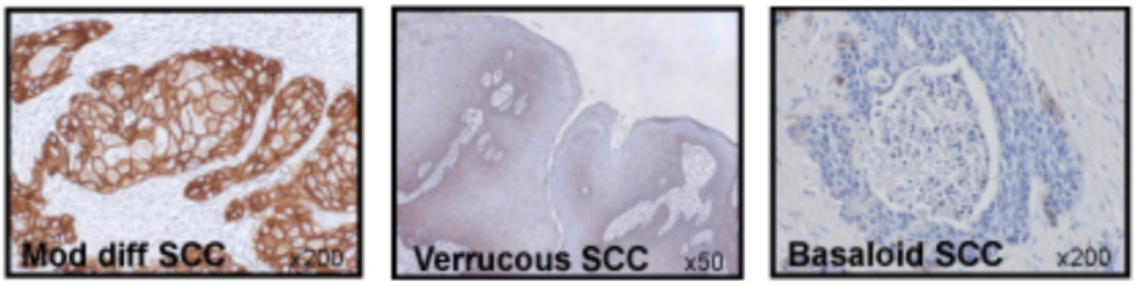

Figure 5.6 αvβ6 expression pattern in different cancer subtypes. . Tissue sections were stained αvβ6 (6.2G2, 0.5 μg/ml) after antigen retrieval in pepsin for 5 minutes at 37º C, as described. Whilst moderately differentiated OSCC expressed the integrin at high levels (as described), both verrucous and basaloid SCC showed minimal to no expression of β6.

5.11 Discussion

The management of oral cancer patients is presently based primarily on the tumour-node-metastasis (TNM) system in conjunction with additional clinico-pathological features (Woolgar, 2006). In this heterogeneous type of cancer, the classification and prognostication of the disease is generally based on tumour morphology. Patients presenting with advanced disease progression typically show poor survival rates. However, there is as yet no single pathological or molecular feature that can identify aggressive tumours at an early stage.

In this chapter, we constructed a retrospective clinico-pathological database of 282 OSCC cases. We found that the pathology features were typical of those generally seen in OSCC patients. Tumour stage, grade, depth, pattern of invasion, positive surgical margins, metastatic disease and extranodal spread were all statistically significant risk factors for OSCC mortality. These findings were in line with other, similar studies (Shah, 1990; Chen *et al.*, 1999; Woolgar, 2006; Rogers *et al.*, 2009). The likelihood ratio for 3-year mortality (DR/FPR) exceeded 3 only for extranodal spread (3.4); a rather expected result given that it is usually a feature of advanced disease.

We thus examined αvβ6 as a potential molecular marker for oral cancer prognosis. Several studies have investigated the utility of the integrin to prognosticate other cancers. It has been shown to correlate with poor prognosis in colorectal, cervical and gastric carcinomas (Bates *et al.*, 2005; Hazelbag *et al.*, 2007; Zhang *et al.*, 2008) It also appears to be a marker of poor prognosis in a specific subset of breast cancers (Professor Louise Jones – personal communication).

αvβ6 has been shown to be expressed in a high percentage of OSCC cases. In spite of the statistically significant correlation of high αvβ6 expression with patient survival in our initial Kaplan Meier analysis, when a more detailed analysis of the data set was performed, we found that the prognostic performance of αvβ6 expression was relatively poor. Indeed, in this study we found that the integrin was expressed at some level in all of the 282 OSCC cases we examined, making it difficult to use it as a marker to distinguish tumour behaviour. Furthermore, when we examined the expression of the integrin within different grades of OSCC (low, moderate to highly differentiated OSCC),

we found similar patterns of expression across different subtypes. These data suggest that αvβ6 is a relatively poor prognostic marker in the classical OSCC presentations.

Interestingly, αvβ6 expression correlated significantly with two factors in our database: depth of invasion and stromal SMA expression. These are of particular interest given the direct and indirect roles of αvβ6 in tumourigenesis. The integrin is known to have a pro-invasive role in carcinogenesis (Thomas *et al.*, 2006), and as such, its significant positive correlation with the depth of invasion in tumours is to be expected. Additionally, we have previously shown that αvβ6 promotes tumour invasion indirectly via activating TGF-β1 and promoting stromal fibroblast-to-myofibroblast transdifferentiation (Marsh *et al.*, 2008). Since SMA is one of the major markers of myofibroblasts, it is not entirely unexpected that αvβ6 expression correlated significantly with a strong stromal SMA signature.

Next, we examined αvβ6 in some other pathological subtypes of OSCC. We found that, interestingly, the integrin was only weakly present in verrucous SCC. Given the different aetiopathogenesis of verrucous SCC in comparison to 'classic' OSCC, it may be that αvβ6 plays a limited role in this particular SCC subtype. Further studies performed on larger cohorts of verrucous SCC may be of value. Indeed, examining αvβ6 expression in proliferative verrucous leukoplakia (PVL) may yield interesting results, given that the integrin has been shown to be expressed in some other potentially malignant disorders.

We also examined basaloid SCC for αvβ6 expression and found that, similarly to verrucous SCC, they, too, were negative for αvβ6 expression. Again, since the aetiology of these cancers is mostly HPV-associated, they may also represent an OSCC subtype in which the role of αvβ6 is yet to be defined. These data generally suggest that a more detailed study of αvβ6 expression in different HNSCC subtypes may be useful in shedding light on which particular subtype the integrin may be useful as a potential prognostic marker.

In terms of study limitations, several factors must be considered in interpreting our findings from a general database point of view. Firstly, patients lost to follow-up were excluded from the study, as were cases with insufficient archival material for full immunochemical analysis; if these were characteristically different to those who were

included, there may have been some bias. Additionally, although the Barts & The London NHS Trust cohort (one of the two teaching hospitals from which the cases were collected) contained a significant number of patients of South-East Asian extraction, both cohorts in this study came from the same city, and these findings may not be generalisable to other settings with different genetic or ethnic influences. Another limitation to our study is the inherent subjectivity to tissue immunohistochemistry scoring, which has a high probability of inter- and intra-observer variability.

Our findings did highlight the limited predictive value of the TNM system, which is used currently to stage OSCC and plan patient therapy. We identified three prognostic factors that together had a good performance in identifying OSCC mortality: metastasis, tumour cohesion and age. Of these, only metastatic disease is included in the current TNM classification. Prospective analysis of this prognostic model will be informative and allow detailed observation of the natural disease progression in this patient group, perhaps suggesting how treatment may be altered to improve survival.

5.12 Summary

In this chapter, we constructed a retrospective clinico-pathological database of OSCC cases and then examined the potential use of αvβ6 integrin expression in OSCC disease prognosis. Results showed that αvβ6 was strongly expressed in the majority of OSCC cases and that its expression was a poor predictor of patient mortality, thus making it unsuitable as a prognostic marker for the disease. High αvβ6 expression correlated significantly with depth of tumour invasion and stromal SMA expression, consistent with its direct and indirect roles in promoting tumour cell invasion. Although the prognostic performance of αvβ6 was relatively poor, the high expression in nearly 50% of OSCC suggests that it may represent a therapeutic target.

Chapter 6
The regulation of αvβ6 expression

6.1 Introduction

The epithelial-specific integrin αvβ6 is not expressed in normal tissues, but is up-regulated during tissue remodeling, including wound healing, fibrosis and carcinogenesis (Thomas *et al.*, 2006). Expression during wound healing and tissue regeneration is transient, whereas in fibrosis and cancer, epithelial cells exhibit constitutive expression of the integrin. The regulation of αvβ6 expression is yet to be definitively examined. As most cells express the αv subunit of the integrin, *de novo* expression of αvβ6 usually only requires exogenous expression of the β6 subunit (Agrez *et al.*, 1994), suggesting that expression of the heterodimer αvβ6 is controlled through regulation of the β6 gene, ITGB6.

Studies have reported increased β6 mRNA expression following treatment of cells with cytokines TGF-β1 and TNF-α (Zambruno *et al.*, 1995; Scott *et al.*, 2004; Sullivan *et al.*, 2011), and Bates and colleagues used ITGB6 promoter constructs (-926/+208) to show that expression may be modulated by the transcription factor (TF) Ets1 (Bates *et al.*, 2005). More recently, Signal Transducer and Activator of Transcription 3 (STAT3) has been shown to bind to the β6 promoter (Azare *et al.*, 2007). No study has yet suggested a mechanism through which αvβ6 may be 'switched off', which may represent a novel therapeutic approach in both fibrotic disease and carcinomas.

In the previous chapters of this thesis, we showed that the areca nut alkaloid arecoline up-regulated β6 expression in the context of oral submucous fibrosis via the muscarinic receptor pathway. We also showed that the Sonic Hedgehog transcription factor Gli1 down-regulated αvβ6 expression and function *in vitro*.

The aim of the work described in this chapter was to investigate the regulation of αvβ6 expression in greater detail. Since all the candidate molecules implicated in regulating β6 expression thus far have been TFs, we set out to study the transcriptional regulation of β6 by first identifying and then cloning the ITGB6 promoter into a luciferase reporter vector and then generating a number of deletion constructs to identify the key regulatory sites. We then investigated the effect of a number of chemical inhibitors on β6 expression.

6.2 *In silico* study of the promoter region of the human ITGB6 gene

The proximal promoter sequence of the ITGB6 gene was obtained from the Cold Spring Harbour Laboratory Homo sapiens Promoter Database (http://rulai.cshl.edu/cgi-bin/CSHLmpd2/hspd.pl). The DNA sequence located 1325 bp 5' and 208 3' of the transcription start site (TSS) was first analysed using the MatInspector tool (Quandt *et al.*, 1995; www.genomatix.de/products/MatInspector). Figure 6.1 shows a diagrammatic representation of the ITGB6 promoter, with reported consensus sites for ETS (Bates *et al.*, 2005) and STAT (Azare *et al.*, 2007) and a potential site for Gli1 binding.

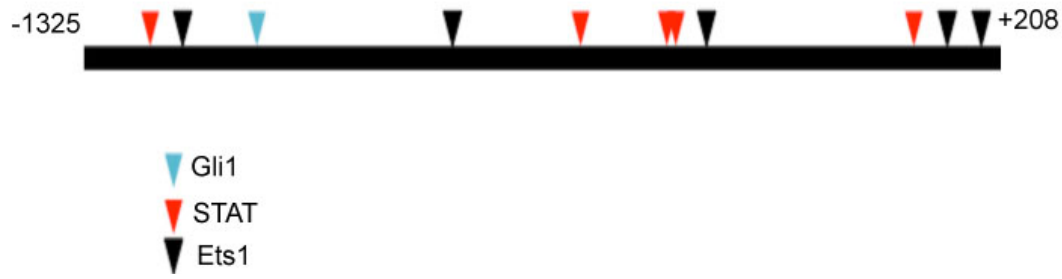

Figure 6.1 Diagrammatic representation of the ITGB6 promoter. ~1,533 bp sequence upstream of the transcription start site (TSS) was identified on Genbank. Inverted triangles show published or potential binding sites for candidate transcription factors (ETS, STAT and GLI).

6.3 Cloning the ITGB6 promoter

The 1,533bp sequence described in Section 6.2 was then amplified from genomic DNA and subcloned into the pGL3-Basic luciferase reporter vector (Promega). The pGL3-Basic vector was a 4,818 bp vector containing a synthetic firefly luciferase gene and lacking any additional promoter or enhancer elements (Figure 6.2).

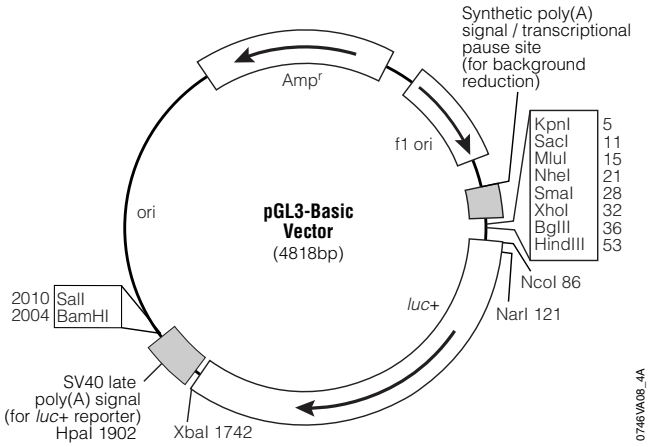

Figure 6.2 pGL3-Basic vector. Plasmid map of the pGL3-Basic vector (Promega), showing restriction enzyme sites and key constructs.

To amplify DNA using PCR, forward and reverse primers were designed using Primer3 software (http://frodo.wi.mit.edu/primer3/; SDS Biology Workbench), with restriction sites for MluI and XhoI added to the end of the forward and reverse primers, respectively (primer sequences are listed in Appendix 9.3). To confirm successful cloning of the ITGB6 promoter insert, double digests with MluI and XhoI followed by PCR were carried out (Figure 6.3).

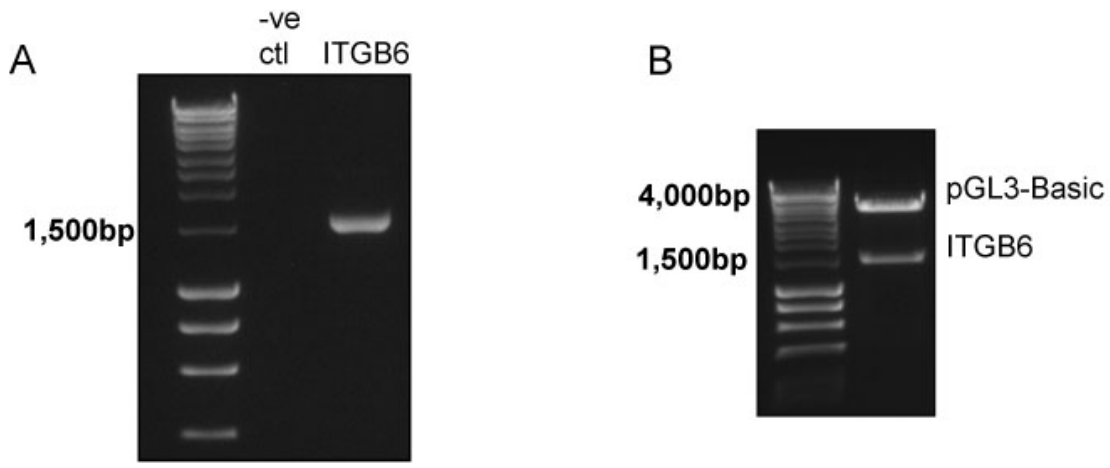

Figure 6.3 Cloning the ITGB6 promoter.
3.6(A) Successful amplification of the 1533bp ITGB6 promoter DNA sequence. 1 μg of genomic DNA was amplified using *LongAmp* high-fidelity polymerase (New England Biolabs). PCR conditions used were: 94° C for 30 seconds, followed by 32 cycles of 94° C for 10 seconds, 60° C for 30 seconds and 65° C for 75 seconds and a final elongation at 65° C for 10 minutes. Sequences were confirmed at Source BioScience (Oxford).
3.6(B) Confirmatory double digest (MluI and XhoI) showing representative bands for the pGL3-Basic and the released ITGB6 promoter insert at approximately 4,000bp and 1,500 bp, respectively.

In addition to the full-length promoter, two smaller constructs lacking potential TF binding sites were also generated and subcloned into the pGL3-Basic vector (Figure 6.4), and correct sequencing was also confirmed (Source BioScience, Oxford). Cloning primer sequences are provided in Appendix 9.3.

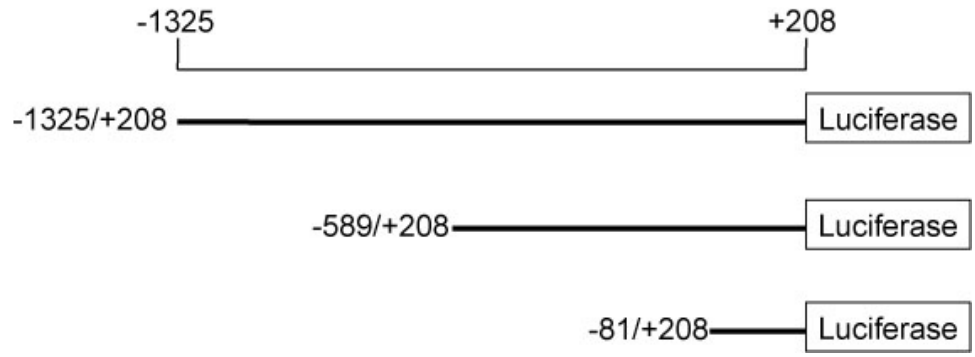

Figure 6.4 Generation of ITGB6 promoter deletion constructs. In addition to the full-length promoter (-1325/+208), two smaller constructs (-589/+208 and -81/+208) were generated by PCR as described in Section 6.3.

6.4 Screening OSCC cell lines for β6 expression

In order to study the regulation of β6 expression, we first screened a panel of OSCC cell lines for β6 protein and gene expression by Western blotting, flow cytometry and RT-PCR (Figure 6.5). Results showed varying levels of endogenous β6 expression. The cell lines SCC25, H400 and BICR6 showed high levels of β6 expression; CA1 and Detroit showed moderate levels of β6 expression and H376 was β6 negative (Figure 6.5). VB6 served as a positive control for high exogenous β6 expression, whilst IC6pr and H357 were negative controls (Figure 6.5).

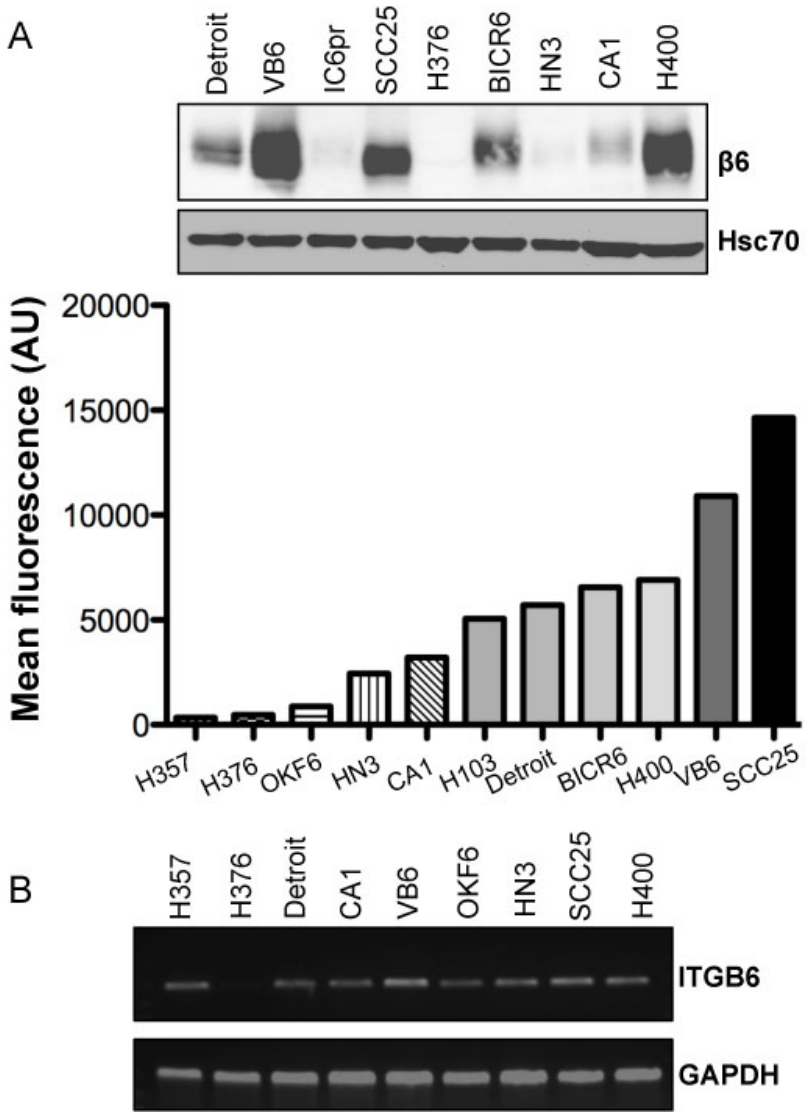

Figure 6.5 Keratinocyte cell line expression of β6.
6.5(A) Western blotting and flow cytometry showing total and surface levels of β6 expression in a panel of keratinocyte cell lines, respectively. Cells were lysed or processed for flow cytometric acquisition at 80-90% confluency. A representative experiment is shown.
6.5(B) RT-PCR showing ITGB6 mRNA expression in a panel of keratinocyte cell lines. RNA was extracted at 80-90% confluency. A representative experiment is shown.

6.5 ITGB6 promoter Dual Luciferase reporter assays

In order to study β6 promoter activity, promoter Dual Luciferase assays were carried out (Figure 6.6) using the SCC25 and CA1 cell lines as examples of high- and low-β6 expressing cell lines, respectively, as shown in Section 6.4. Results showed higher transcriptional activity of the ITGB6 promoter in the high-β6 expressing cell line SCC25 when compared with CA1. Promoter activity gradually diminished in the shorter constructs in which the binding sites for STAT3 and Ets1 had been eliminated.

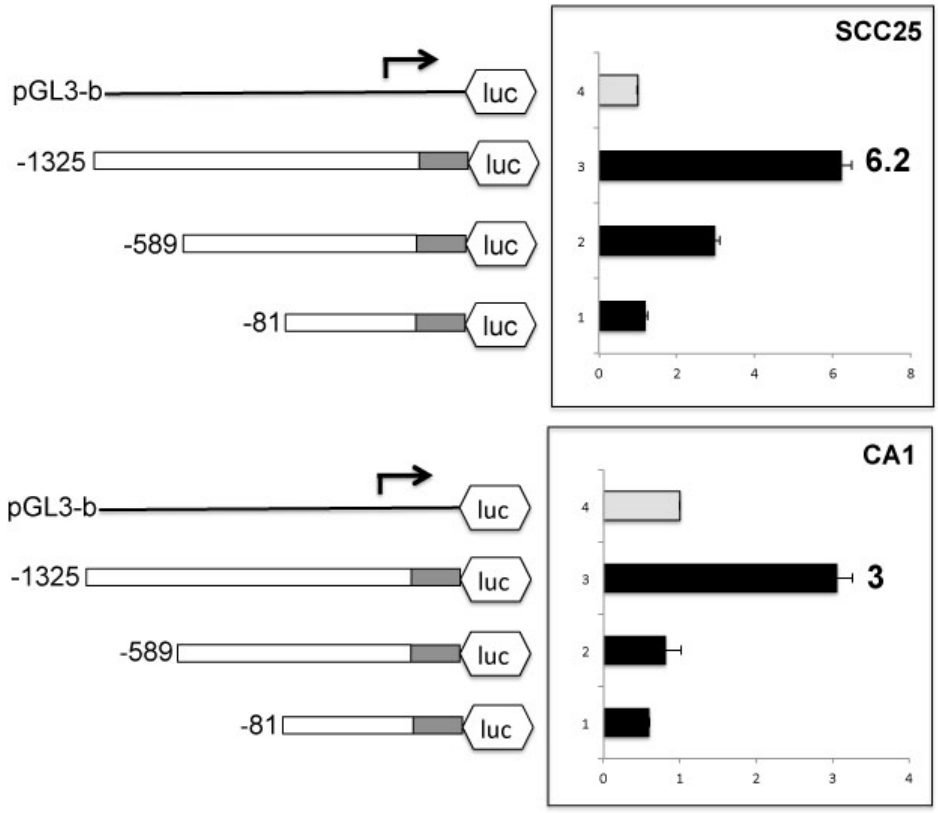

Figure 6.6 ITGB6 promoter luciferase assays. SCC25 and CA1 were transfected with sequentially deleted constructs of the ITGB6 promoter (cloned into pGL3-Basic Luciferase vector). 80,000 cells were plated in each well of a 24-well plate in triplicate. Plasmid transfections were carried out the next day using LipofectAMINE 2000 reagent. 18 hours later, cells transfection complexes were removed and cells were re-fed. Firefly luciferase activity was read on a Wallac plate reader and was normalised with *Renilla* luciferase activity. These values were then normalised to those of pGL3-Basic vector without any insert. The high β6-expressing OSCC cell line SCC25 shows 6-fold induction of ITGB6 promoter activity, compared with 3-fold induction in the low-β6 expressing CA1 cell line. Promoter activity gradually diminished in the shorter constructs. Combined results from two independent experiments are shown. Error bars represent SD.

6.6 pSTAT3 as a potential regulator of β6 expression

The JAK/STAT pathway is vital in modulating the responses of cytokines to the haematopoietic system in normal physiology. Aberrant activation of the pathway has been described in several solid tumours – including head and neck cancer (Lai & Johnson, 2010). Activated (or tyrosine phosphorylated) pSTAT3 expression in HNSCC has been reported in several studies and attempts have been made to correlate nuclear expression with cancer prognosis (Macha *et al.*, 2011).

Given that the results of the previous section showed that β6 promoter activity diminished when the published STAT binding sites for STAT had been eliminated (Azare *et al.*, 2007), we thus attempted to examine whether pSTAT3 may have a role in the regulation of β6 expression in the context of OSCC. We started by screening OSCC cell lines for pSTAT3 expression (Figure 6.7A), where we found that OSCC cell lines expressed the activated TF at varying levels. Next, we screened a number of STAT3 chemical inhibitors to test whether pSTAT3 expression can be down-regulated in OSCC cell lines.

The RTK inhibitor Sunitinib is widely used as a targeted therapy modality in renal cell carcinoma, where it has been shown to inhibit pSTAT3 (Powles *et al.*, 2011). We treated the Detroit and SCC25 OSCC cell lines with Sunitinib at two concentrations and found no discernible inhibition of pSTAT3 in both cell lines (Figure 6.7B).

Next, we tested the STAT3 inhibitor VI (S31-201) at a concentration of 200 μM on four different OSCC cell lines, and found that pSTAT3 expression was successfully inhibited upon overnight treatment in CA1, Detroit, SCC25 and BICR6 cells.

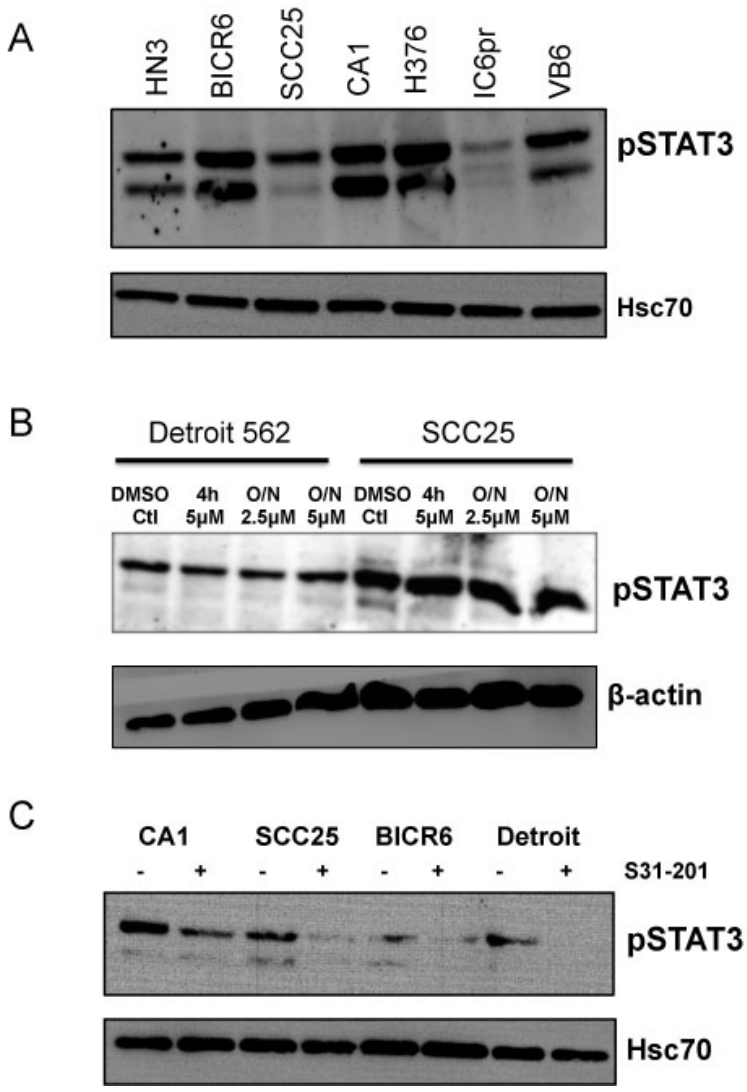

Figure 6.7 pSTAT3 expression in OSCC cell lines.
6.7(A) Western blotting confirmed expression of pSTAT3 in a panel of OSCC cell lines. Lysates were collected at 80-90% confluency. A representative experiment is shown.
6.7(B) Western blotting showing pSTAT3 expression in Detroit and SCC25 cell lines upon treatment with the RTK inhibitor Sunitinib. No change in expression was detected.
6.7(C) Western blotting confirmed inhibition of pSTAT3 upon treatment of cells with the S31-201 inhibitor. Cells were treated overnight with the inhibitor at 200 μM. Negative controls were treated with an equal volume of DMSO. pSTAT3 expression was down-regulated in CA1, SCC25, BICR6 and Detroit cell lines. A representative experiment is shown.

6.7 Effect of pSTAT3 inhibition on β6 expression

Since over-expression of pSTAT3 has been shown to up-regulate β6 expression via binding directly to the ITGB6 promoter in prostate cancer cells (Azare *et al.*, 2007), we next wondered whether inhibiting pSTAT3 would have any inhibitory effect on the expression of αvβ6 in OSCC cell lines. Having confirmed that the STATVI inhibitor (S31-201) successfully inhibited pSTAT3 levels, we repeated the studies in Section 6.6 and then examined β6 gene and protein expression in a panel of OSCC cell lines (Figure 6.8).

Results showed a modest down-regulation of β6 mRNA upon treatment with the inhibitor in four out of five OSCC cell lines (Figure 6.8A). On a protein level, there was a modest down-regulation of β6 total and surface levels upon treatment with S31-201 by flow cytometry and Western blotting, respectively (Figure 6.8B and Figure 6.8C, respectively.) These results suggested that the regulation of β6 expression is possibly multi-factorial and involves other factors and pathways in addition to the JAK/STAT pathway and pSTAT3.

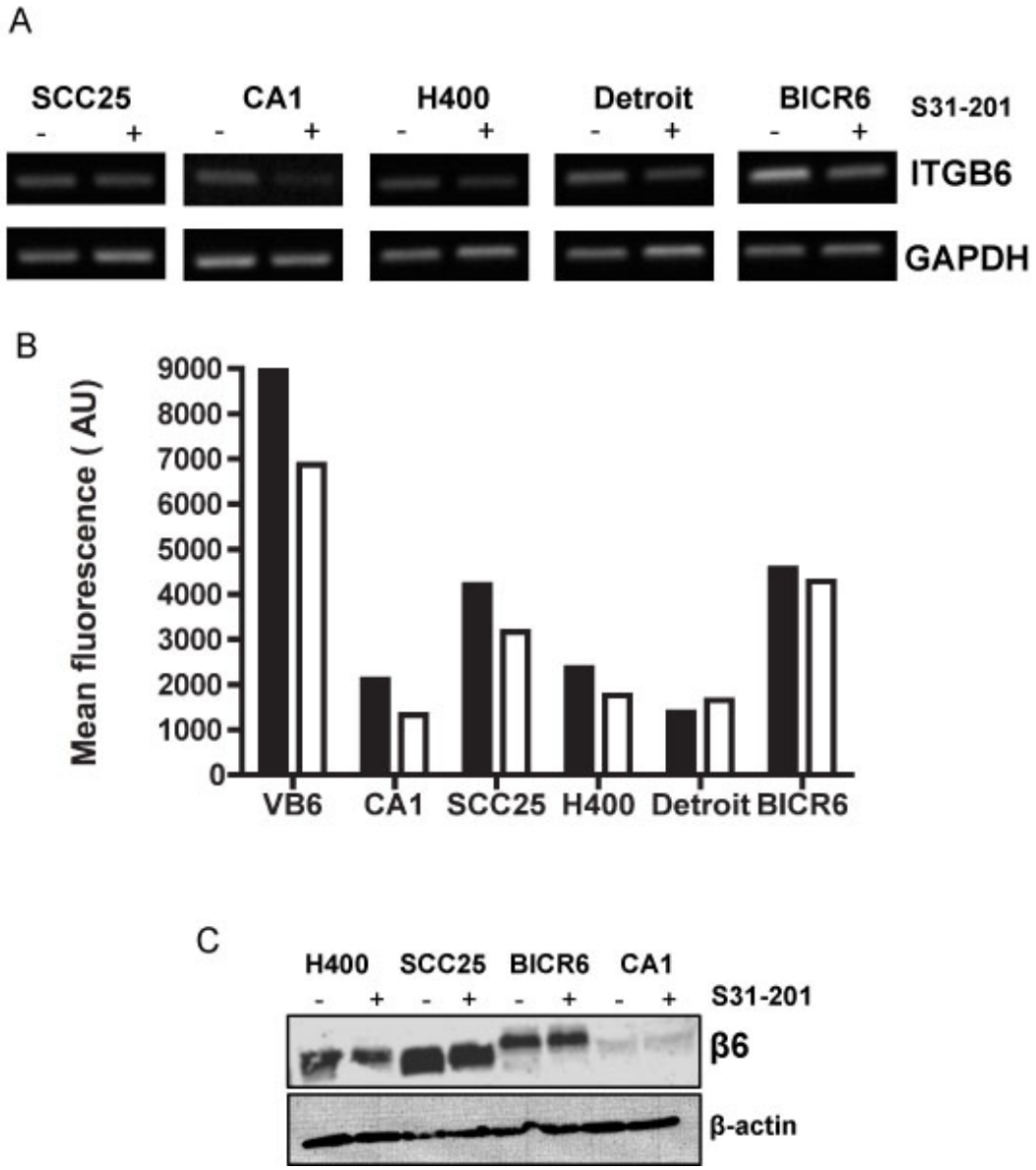

Figure 6.8 S31-201 effect on β6 expression in OSCC cell lines. 2x10^5 cells were plated overnight, serum-starved for 8 h and then treated with S31-201 (STAT3 inhibitor VI) at 200 μM overnight. Control wells were treated with DMSO. Cells were then stained for flow cytometric analysis, lysed for Western blotting or RNA was extracted for RT-PCR. All experiments were carried out in duplicate.

6.8(A) RT-PCR shows down-regulation of β6 mRNA in H400, CA1, Detroit and BICR6 cell lines and a modest reduction in SCC25 cell line. A representative experiment is shown.

6.8(B) FACS analysis for β6 a modest down-regulation of surface β6 protein on S31-201 treatment across all OSCC cell lines, apart from Detroit. Black bars represent control wells; white bars represent STAT3 inhibitor VI treated wells. A representative experiment is shown.

6.8(C) Western blotting showing minimal β6 down-regulation on S31-201 treatment in OSCC cell lines. A representative experiment is shown.

6.8 Effect of TGF-β1 inhibition on β6 expression

As outlined earlier in this thesis, αvβ6 integrin and TGF-β1 have an intimate, bidirectional relationship: the integrin is a key activator of TGF-β1, whilst conversely, TGF-β1 has been shown to induce β6 expression on mRNA and protein level (Zambruno *et al.*, 1995; Sullivan *et al.*, 2011). Furthermore, the ITGB6 promoter contains multiple SMAD binding elements. Given that the results of the previous section suggested that pSTAT3 is unlikely to be the only factor involved in the regulation of β6 expression, we carried out similar inhibitor treatment experiments using a TGF-β Receptor I Kinase inhibitor (ALK5 Inhibitor IV). Upon treatment of the OSCC cell lines H400, Detroit, SCC25 and BICR6 with ALK5, we found that there was aninhibition of β6 expression in the Detroit and H400 cell lines but not in SCC25 and BICR6 (Figure 6.9). This may be due to BICR6 and SCC25 cell lines being refractory to TGF-β1. Furthermore, the data from these experiments suggested a multi-factorial regulatory mechanism for αvβ6 expression.

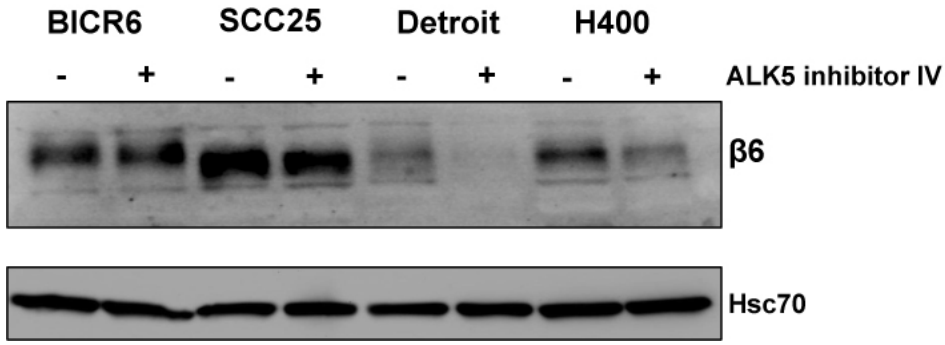

Figure 6.9 ALK5 inhibitor IV effect on β6 expression in OSCC cell lines. $2x10^5$ cells were plated overnight, serum-starved for 8 h and then treated with ALK5 inhibitor IV (TGF-βRI Kinase Inhibitor IV) at 1 μg/ml overnight. Control wells were treated with DMSO. Cells were then lysed for Western blotting. Figure shows down-regulation of total β6 protein in Detroit and H400 cell lines, with little to no effect on β6 expression in BICR6 and SCC25 cell lines. A representative experiment is shown.

6.9 Effect of combinatorial TGF-β1 and pSTAT3 inhibition on β6 expression

The results of the previous section showed that the inhibition of pSTAT3 and TGF-β1 on their own had modest effects on inhibiting β6 expression, suggesting that the regulation of β6 possibly involves both pathways acting in concert. Thus, we next carried out preliminary co-treatment studies using both inhibitors on the SCC25 and CA1 OSCC cell lines. The initial results from these pilot studies showed a down-regulation of β6 total protein on Western blotting (Figure 6.10). These data suggest that the regulation of β6 expression appears to be multifactorial.

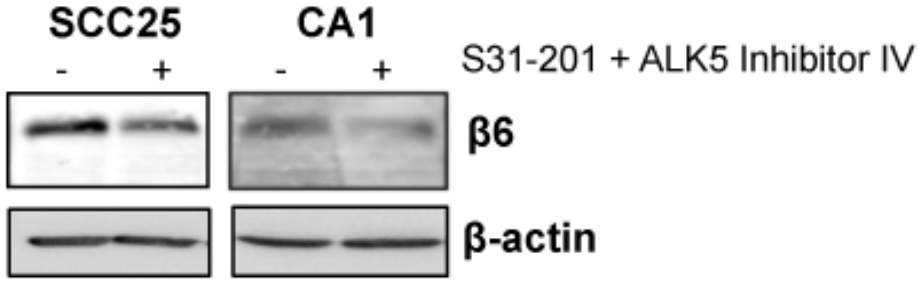

Figure 6.10 S31-201 and ALK5 Inhibitor IV combinational treatment effect on β6 expression. 2x10^5 cells were plated overnight, serum-starved for 8 h and then treated with S31-201 at 200 μM and ALK5 inhibitor IV at 1 μg/ml overnight. Control wells were treated with DMSO. Western blotting showing some β6 total protein down-regulation on combinatorial treatment in the SCC25 and CA1 cell lines. A representative experiment is shown.

6.10 Discussion

Integrin αvβ6 is a heterodimeric cell surface receptor that is unique amongst the integrin superfamily in humans in that it is solely expressed by epithelia (Thomas *et al.*, 2006). αvβ6 is not normally expressed by healthy tissues, but is up-regulated during remodeling processes, including wound healing and fibrosis. Additionally, expression of αvβ6 has been reported in a number of solid tumours, including carcinomas of the head and neck, breast, pancreas and colon (Thomas *et al.*, 2006). Since αvβ6 is exclusively expressed by keratinocytes, it presents itself as an attractive therapeutic target both in cancer and fibrosis. The expression of the integrin is constitutive in diseased states, and as such, inhibiting or downregulating its expression and subsequent functions may be of great value in therapy.

The exact mechanisms by which αvβ6 expression is induced in wound keratinocytes and is then subsequently down-regulated are unknown. Keratinocytes become 'activated' when they are isolated from oral or cutaneous epithelium, where they then begin to resemble wound keratinocytes in culture (Grinnell, 1992). When keratinocytes are freshly isolated, they do not express αvβ6 – however, the integrin is then constitutively expressed and detectable from the first passage onwards. We have found that cultured primary keratinocytes from oral, epidermal and oesophageal biopsies all expressed αvβ6 at high levels (unpublished data). This makes studying the induction of αvβ6 expression difficult *in vitro*.

High cell density has been shown to enhance αvβ6 expression in colon cancer (Niu *et al.*, 2001). We have also observed that confluency up-regulated αvβ6 expression in oral and pancreatic cancer cells (unpublished data). Niu and colleaguges further went on to show that removing the terminal 11 amino acids in the β6 cytoplasmic domain prevented this density-dependent αvβ6 expression induction, replacing it with αvβ5 (Niu *et al.,* 2002), suggesting perhaps that the expression of these two integrins is related.

Another approach to understand the induction of β6 expression is to study the transcriptional regulation of its expression. In this chapter, we cloned a ~1500 bp fragment of genomic DNA corresponding to the ITGB6 promoter. This sequence contained consensus STAT, Ets and SMAD binding sites, and a potential binding site

for Gli1, which we had shown in Chapter 5 of this thesis to down-regulate αvβ6 expression and function in skin keratinocytes.

Azare and colleagues showed that the overexpression of the activated phosphorylated form of STAT3 (pSTAT3) in prostate epithelial cells was tumourigenic, and that it up-regulated αvβ6 protein expression (Azare *et al.*, 2007). They next showed that ITGB6 promoter was transcriptionally activated by pSTAT3 in Luciferase assays. Finally, they showed that pSTAT3 was capable of binding to the ITGB6 promoter in chromatin immunoprecipitation assays (ChIP). In this chapter, we showed that inhibiting pSTAT3 partially inhibited αvβ6 protein expression in OSCC cells. We also showed in Dual Luciferase assays that ITGB6 promoter activation was significantly reduced when deletion constructs were made lacking the STAT binding sites that Azare and colleagues had examined. Our data suggests that pSTAT3 may have a role in regulating αvβ6 expression in the context of HNSCC. Given that pSTAT3 has been shown to be expressed in HNSCC, it would be worthwhile to examine in more detail the correlation, if any, between αvβ6 and pSTAT3 expression in OSCC. Further studies to show the functional correlation of the two molecules would also be of value.

The Ets1 proto-oncogene is a member of the Ets transcription factors, which share a unique DNA binding domain (Dittmer, 2003). Aberrant expression of Ets1 has been reported in a number of solid tumours, including prostate, breast and colorectal cancer (Dittmer, 2003). There has been one study showing that Ets1 may have a role in modulating αvβ6 expression in colorectal cancer (Bates *et al.*, 2005), in which ITGB6 promoter was transactivated by the Ets1 transcription factor, and electrophoretic mobility shift assays were used to show modulation of the ITGB6 promoter by Ets1. Whether or not Ets1 has a role to play in regulating αvβ6 in OSCC remains to be elucidated. Studies have examined expression of Ets1 in OSCC using immunohistochemistry and attempted to link it with disease prognosis. Thus, it may be worthwhile to examine correlation between Ets1 and αvβ6 expression. More importantly, however, showing that Ets1 binds to the ITGB6 promoter may be of value, especially since the study by Bates and colleagues showed modulation of the promoter by EMSA, a less robust technique than ChIP assay.

The cytokine TGF-β1 and αvβ6 integrin have an intimate, often reciprocal relationship. The integrin is one of the main mechanisms of activating TGF-β1. And in turn, TGF-β1

has been shown to induce the *de novo* expression of αvβ6 in human keratinocytes and bile duct epithelial cells (Zambruno *et al.*, 1995; Sullivan *et al.*, 2011). When we inhibited TGF-β1 signaling by using the TGF-βRI kinase inhibitor ALK5 Inhibitor IV, we observed a discernible inhibition of αvβ6 protein expression in three out of four OSCC cell lines. The most pronounced inhibition was in the Detroit OSCC cell line, consistent with a study by Van Aarsen and colleagues, where inhibition of TGF-β1 signaling by inhibiting the TGF-βRII in this particular cell line led to reduced tumour xenografts *in vivo* and, importantly, inhibition of αvβ6 expression *in vitro* (Van Aarsen *et al.*, 2008). Whether or not TGF-β1 signaling influences β6 gene transcription directly via the Smad TFs binding the ITGB6 promoter remains to be seen, and further studies dissecting this mechanism would be of value.

In this chapter, we also treated OSCC keratinocytes with a TGF-βRI kinase inhibitor in addition to a STAT3 inhibitor and found a more pronounced inhibition of αvβ6 expression than when each inhibitor was used on its own. The data confirm that TGF-β1 has a role in modulating αvβ6 expression, but also that this mechanism is possibly multi-factorial in addition to other factors, like the STATs and possibly Ets-1. Since there was a considerable degree of variation in our results, the data suggest that there may be a degree of cell line variation. It is not uncommon for OSCC cells to become refractory to TGF-β1 signalling in oncogenesis (Prime *et al.*, 2004), and this is a particular limitation to these experiments. Further studies characterising TGF-β1 signalling pathways in these cell lines would be of value.

Another cytokine that may have a role in modulating αvβ6 expression is tumour necrosis factor-α (TNF-α). Using TNF-$\alpha^{-/-}$ mice, Scott *et al.* (2004) showed that αvβ6 was up-regulated when exogenous TNF-α was administered. Interestingly, Bates *et al*.'s aforementioned study, which examined the modulation of αvβ6 by Ets-1, showed that TGF-β functioned synergistically with TNF-α, upregulating αvβ6 through Ets1. Since TGF-β1 and TNF-α are commonly found in epithelial wounds, they may play a role in modulating αvβ6 expression induction. Again, these data support the notion that the regulation and induction of αvβ6 expression is possibly a multifactorial mechanism involving TGF-β1, TNF-α, Ets1 and pSTAT3 through multiple, possibly converging, signaling pathways.

6.11 Summary

In this chapter, we successfully cloned the full-length ITGB6 promoter and two additional deletion constructs. We examined ITGB6 promoter activity, and confirmed that the transcriptional activity of the promoter is dependent on the presence of a DNA sequence containing consensus STAT and Ets binding sites. We showed that the inhibition of pSTAT3 on its own had little effect on the expression of β6, but that combinatorial inhibition of the JAK/STAT and the TGF-β pathway downregulated αvβ6 expression to a certain extent in a number of cell lines. These data suggest that the regulation of β6 expression is possibly multifactorial, and involves a number of factors in different signaling pathways. These data also imply that there is cell line variability in terms of TGF-β1 signalling and further studies examining these pathways would be of value. These data have implications on both the understanding of the regulation of β6 expression in normal physiology; and also on developing targeted therapies for solid tumours in which αvβ6 integrin is highly expressed.

Chapter 7
Final Discussion and Future Work

7.1 Overview of the Study

The main premise of this study was first to examine the expression of αvβ6 in a number of pathogenic states of the head neck, and then to dissect its functions. This led us to investigate the mechanisms regulating the expression of the integrin in health and in disease.

Specific objectives included:

- Examining the expression of αvβ6 in clinical specimens of OSF, OSCC and BCC.
- Dissecting the functions of αvβ6 *in vitro*, namely the activation of TGF-β1, the promotion of keratinocyte motility and its role in EMT.
- Studying the potential utility of αvβ6 as a prognostic marker for disease progression in OSCC.
- Generating the tools to investigate the regulation of αvβ6 expression and performing pilot studies on candidate molecules and pathways implicated in these processes.

7.2 Discussion and Future Work

The αvβ6 integrin is expressed exclusively by epithelial cells in humans (Thomas *et al.*, 2006). Although generally undetectable in healthy tissues, it is upregulated during tissue remodeling. In wound healing, expression of the integrin is tightly controlled and, following wound resolution, expression is quickly downregulated. In contrast, the integrin is constitutively expressed in a number of pathologic processes, particularly cancer and organ fibrosis (Thomas *et al.*, 2006). αvβ6 has several functions during tumourigenesis and fibrosis, including the promotion of cell migration and invasion and the activation of TGF-β1, through which epithelial-to-mesenchymal transition (EMT) may be promoted. Several of these functions were examined in this thesis, and will be discussed in this section. Additionally, the fact that αvβ6 is highly expressed in numerous cancer types, as well as fibrotic processes, makes it an attractive target for therapy; however, the mechanisms regulating its expression are remain to be fully elucidated.

In this thesis, we examined the expression and function of αvβ6 in several pathogenic states in the head and neck, including oral submucous fibrosis, oral squamous cell carcinoma and basal cell carcinoma of the skin. We found that the integrin was expressed in the majority of these conditions, and that its expression correlated generally with disease severity. We then went on to dissect αvβ6 functions within the specific contexts of these conditions.

One of the major functions of αvβ6 in wound healing, tumourigenesis and fibrosis is its promotion of keratinocyte migration. In Chapter 3 of this thesis, we showed that the betel quid alkaloid arecoline modulated αvβ6-dependent keratinocyte migration both in Transwell® assays and in the more physiologically relevant organotypic assays. The alkaloid is an agonist of the muscarinic receptor pathway, acting on the M group of receptors. We found that treatment of immortalised, normal oral keratinocytes with arecoline up-regulated αvβ6 expression, suggesting that M receptor signalling may be involved in the regulation of αvβ6 expression during physiological and pathological processes. Interestingly, previous work by Chernyavsky and colleagues has shown that the M_4 muscarinic receptor activation up-regulated 'pro-migratory' integrins αvβ6 and αvβ5 through Rho/RhoA Kinase activation (Chernyavsky *et al.*, 2004). Subsequent studies by Jenkins and colleagues have shown that the Rho/RhoA Kinase pathway is implicated in signalling to the cytoplasmic domain of β6 and modulating its activation of TGF-β1 (Xu *et al.*, 2009; Jenkins *et al.*, 2006). Our findings here are consistent with these studies; showing that arecoline, through the M_4 receptor pathway, upregulates αvβ6 expression and possibly modulates its functions in OSF. Interestingly, the antimuscarinic drug tropicamide inhibited arecoline-dependent αvβ6 upregulation. Further studies examining the effect of tropicamide and other antimuscarinic reagents may be useful in dissecting αvβ6 signalling in health and in disease.

The role of αvβ6 in the epithelial to mesenchymal transition (EMT) has recently been investigated, but there is limited data as to its role in this process. We have touched upon this potential role in the Chapters 3 and 4 of this thesis. The oncogene *Ras* is frequently mutated in OSCC in the Asian population, and together with TGF-β1 has been shown to modulate EMT (Janda *et al.*, 2002). *Ras* mutations have also been described in OSF (Kuo *et al.*, 1994), and it is possible that the combination of αvβ6-dependent TGF-β1 activation and *Ras* signalling promotes malignant transformation of OSF through inducing EMT. Further work examining αvβ6 expression in OSF and

OSCC cases that have transformed on a background of OSF with genetic analysis of *Ras* mutations and expression of TGF-β1 pathway signalling molecules (e.g. pSmad2/3) would be of value.

In Chapter 4 of this thesis, we examined the interactions of αvβ6 integrin with components of the Sonic Hedgehog pathway, specifically Gli1 in the pathogenesis of basal cell carcinoma. Our results showed that αvβ6, highly expressed in the aggressive morphoeic variant of the disease, exerted a pro-EMT effect on immortalized skin keratinocytes in culture when cells were stimulated with epidermal growth actor (EGF), an activator of the *Ras* pathway and a known EMT inducer (Weinberg and Hanahan, 2011). We also found that morphoeic BCC showed higher expression of EGFR *in vivo* compared with the nodular variant. These results are consistent with the finding that αvβ6 and EGFR co-expression in OSCC is associated with more aggressive disease (Professor Gareth Thomas – personal communication).

The interaction of αvβ6 with Gli1 in the context of EMT is particularly interesting, given that Gli1 itself has been shown to exert pro-EMT effects in development and in disease, particularly in colorectal cancer (Varnat *et al.*, 2009). Our findings suggest that the role of Gli1 in EMT is more tissue-specific, as its expression appeared to be down-regulated in the majority of morphoeic BCC. These data suggest that Gli1 actually exerts a more epithelioid phenotype in BCC, through downregulation of αvβ6 and suppression TGF-β1 activation and EMT. Further studies examining the expression of known EMT inducers Snail, Twist and Zeb both on BCC clinical specimens and *in vitro* may be informative. Again, investigating the EGFR signalling pathway interaction with αvβ6 would also be imperative to further validate these findings.

αvβ6 has been shown to be prognostic in colorectal carcinomas (Bates *et al.*, 2005), and there is emerging data that αvβ6 expression can be useful in identifying a subset of aggressive breast adenocarcinomas (Professor Louise Jones - personal communication). In this thesis, we performed a comprehensive retrospective analysis of a 282-case OSCC clinico-pathological database, and found that αvβ6 expression was not in itself a useful prognostic factor for OSCC. There may be several possible reasons for this finding. Firstly, the integrin is usually expressed by the majority OSCC cases, making it difficult to use it to identify a particular subset of the disease. It may be that αvβ6 within individual tumour islands is present on the cell surface but is not being

actively internalised within the cell, thereby rendering it not functional – thus, even though the majority of tumours 'express' the integrin, it may not be fully functional. Interestingly, however, we found that αvβ6 was not expressed by basaloid and verrucous SCCs, two SCC subtypes which generally present with an overall better prognosis than classic OSCC. One can thus speculate that the integrin either plays no role in the pathogenesis of these subtypes, or it may serve as a marker of the more aggressive phenotypes in these tumours.

Studying the regulation of αvβ6 expression is of particular importance given its functional roles in the pathogenesis of cancer and fibrosis. The results of Chapters 3 and 4 of this thesis led us to further investigate these mechanisms. Firstly, we observed that arecoline, through the muscarinic receptor pathway, played a role in upregulating αvβ6 expression in OSF; and secondly, we found that activation of the Sonic Hedgehog pathway suppressed αvβ6 expression in keratinocytes. Having identified a potential Gli binding site in the ITGB6 promoter, we proceeded to clone the ITGB6 promoter and carried out pilot studies investigating the transcriptional regulation of the integrin in Chapter 6 of this thesis.

The pilot studies performed in Chapter 6 showed that the candidate molecules implicated in regulating αvβ6 expression; namely pSTAT3 and TGF-β1, possibly act in concert to promote expression of the integrin. These findings were supported by studies of ITGB6 transcription, in which truncating the ITGB6 promoter to eliminate the consensus STAT and SMAD binding sites resulted in a reduction of promoter transactivation. Future studies examining the expression of pSTAT3 and TGF-β1 signalling components in OSCC clinical specimens, and correlating the expression with αvβ6 and patient survival would be of particular importance. Furthermore, detailed analysis of these signalling pathways and how they converge in regulating αvβ6 expression would also be of value. The TF Ets1 has also been shown to be implicated in regulating αvβ6, as has TNF-α. Studies incorporating these two molecules in addition to STAT3 and TGF-β1, both *in vitro* and *in vivo* would further dissect β6 expression regulation. The mechanism by which Gli1 downregulates αvβ6 is of particular interest. Given that Gli1 is a TF, it may be that it binds the ITGB6 promoter directly. However, since the action of this TF is primarily as a promoter transactivator, it would be more likely that it this down-regulation is an indirect effect. Chromatin

immunoprecipitation assays (ChIP) would be carried out in this case to verify these findings.

Future plans include screening chemical libraries to identify molecules that may potentially downregulate the transcription of ITGB6, which would potentially be of considerable therapeutic benefit. However, these assays would be of more relevance physiologically if carried out on keratinocyte cell lines that have been stably transfected with the ITGB6 promoter, rather than the transient transfection method, which does not take into account chromatin organisation.

7.3 Conclusion

Expression of αvβ6 has been reported in numerous carcinomas and tissue fibroses, and there is increasing evidence to suggest that it has an invasion-promoting effect, particularly in OSCC (Yap & Jenei *et al.*, 2009; Thomas *et al*., 2006; Ramos *et al*., 2002; Li *et al*., 2003). Our data confirm that αvβ6 promotes oral fibrosis, OSCC invasion and may also support EMT in BCC.

We have generated a number of tools to study the regulation of αvβ6 expression and performed preliminary work examining these regulatory mechanisms. More detailed studies of the candidate pathways and molecules involved in αvβ6 expression regulation and signalling – namely, STAT3, TGF-β1, Ets1 and TNF-α will be of value, along with the development of specific inhibitors of αvβ6 expression.

Finally, since αvβ6 is expressed on the cell surface and has little or no expression on normal tissues it represents an attractive therapeutic target for monoclonal antibodies or inhibitory peptides. Additional work to fully dissect the mechanisms by which αvβ6 is regulated would be of value not only in understanding the roles of αvβ6 in pathophysiology but also in targeting the integrin in cancer and fibrosis.

8 References

Adachi, M., T. Taki, et al. (2000). "Significance of integrin alpha5 gene expression as a prognostic factor in node-negative non-small cell lung cancer." Clin Cancer Res **6**(1): 96-101.

Adolphe, C., R. Hetherington, et al. (2006). "Patched1 functions as a gatekeeper by promoting cell cycle progression." Cancer Res **66**(4): 2081-2088.

Agrez, M., A. Chen, et al. (1994). "The alpha v beta 6 integrin promotes proliferation of colon carcinoma cells through a unique region of the beta 6 cytoplasmic domain." J Cell Biol **127**(2): 547-556.

Ahmed, N., F. Pansino, et al. (2002a). "Overexpression of alpha(v)beta6 integrin in serous epithelial ovarian cancer regulates extracellular matrix degradation via the plasminogen activation cascade." Carcinogenesis **23**(2): 237-244.

Ahmed, N., J. Niu, et al. (2002b). "Direct integrin alphavbeta6-ERK binding: implications for tumour growth." Oncogene **21**(9): 1370-1380.

Ahmed, N., F. Pansino, et al. (2002c). "Association between alphavbeta6 integrin expression, elevated p42/44 kDa MAPK, and plasminogen-dependent matrix degradation in ovarian cancer." J Cell Biochem **84**(4): 675-686.

Ahmed, N., C. Riley, et al. (2004). "Expression and localization of alphavbeta6 integrin in extraplacental fetal membranes: possible role in human parturition." Mol Hum Reprod **10**(3): 173-179.

Al-Hazmi, N., G. J. Thomas, et al. (2007). "The 120 kDa cell-binding fragment of fibronectin up-regulates migration of alphavbeta6-expressing cells by increasing matrix metalloproteinase-2 and -9 secretion." Eur J Oral Sci **115**(6): 454-458.

AlDahlawi, S., A. Eslami, et al. (2006). "The alphavbeta6 integrin plays a role in compromised epidermal wound healing." Wound Repair Regen **14**(3): 289-297.

Allen, M. D., R. Vaziri, et al. (2011). "Clinical and functional significance of alpha9beta1 integrin expression in breast cancer: a novel cell-surface marker of the basal phenotype that promotes tumour cell invasion." J Pathol **223**(5): 646-658.

Annes, J. P., Y. Chen, et al. (2004). "Integrin alphaVbeta6-mediated activation of latent TGF-beta requires the latent TGF-beta binding protein-1." J Cell Biol **165**(5): 723-734.

Annes, J. P., D. B. Rifkin, et al. (2002). "The integrin alphaVbeta6 binds and activates latent TGFbeta3." FEBS Lett **511**(1-3): 65-68.

Argiris, A., M. V. Karamouzis, et al. (2008). "Head and neck cancer." Lancet **371**(9625): 1695-1709.

Arihiro, K., M. Kaneko, et al. (2000). "Significance of alpha 9 beta 1 and alpha v beta 6 integrin expression in breast carcinoma." Breast Cancer **7**(1): 19-26.

Armstrong, B. K. and A. Kricker (2001). "The epidemiology of UV induced skin cancer." J Photoch Photob B **63**(1-3): 8-18.

Arora, S., J. Kaur, et al. (2005). "Stromelysin 3, Ets-1, and vascular endothelial growth factor expression in oral precancerous and cancerous lesions: correlation with microvessel density, progression, and prognosis." Clin Cancer Res **11**(6): 2272-2284.

Azare, J., K. Leslie, et al. (2007). "Constitutively activated Stat3 induces tumorigenesis and enhances cell motility of prostate epithelial cells through integrin beta 6." Mol Cell Biol **27**(12): 4444-4453.

Bai, C. B., D. Stephen, et al. (2004). "All mouse ventral spinal cord patterning by hedgehog is Gli dependent and involves an activator function of Gli3." Dev Cell **6**(1): 103-115.

Bandyopadhyay, A. and S. Raghavan (2009). "Defining the role of integrin alphavbeta6 in cancer." Curr Drug Targets **10**(7): 645-652.

Baraldi, A., G. Zambruno, et al. (1995). "Beta 1 and beta 3 integrin upregulation in rapidly progressive glomerulonephritis." Nephrol Dial Transpl **10**(7): 1155-1161.

Bartelt, M. A. and J. L. Duncan (1978). "Adherence of group A streptococci to human epithelial cells." Infect Immun **20**(1): 200-208.

Bates, R. C., D. I. Bellovin, et al. (2005). "Transcriptional activation of integrin beta6 during the epithelial-mesenchymal transition defines a novel prognostic indicator of aggressive colon carcinoma." J Clin Invest **115**(2): 339-347.

Bello, L., G. Carrabba, et al. (2001). "Low-dose chemotherapy combined with an antiangiogenic drug reduces human glioma growth in vivo." Cancer Res **61**(20): 7501-7506.

Berryman, S., S. Clark, et al. (2005). "Early events in integrin alphavbeta6-mediated cell entry of foot-and-mouth disease virus." J Virol **79**(13): 8519-8534.

Blanco-Mezquita, J. T., A. E. Hutcheon, et al. (2011). "{alpha}V{beta}6 Integrin Promotes Corneal Wound Healing." Invest Ophthalmol Vis Sci **52**(11):8505-13.

Boukamp, P., R. T. Petrussevska, et al. (1988). "Normal keratinization in a spontaneously immortalized aneuploid human keratinocyte cell line." J Cell Biol **106**(3): 761-771.

Brennan, J. A., J. O. Boyle, et al. (1995). "Association between cigarette smoking and mutation of the p53 gene in squamous-cell carcinoma of the head and neck." New Engl J Med **332**(11): 712-717.

Breuss, J. M., J. Gallo, et al. (1995). "Expression of the beta 6 integrin subunit in development, neoplasia and tissue repair suggests a role in epithelial remodeling." J Cell Sci **108 (Pt 6)**: 2241-2251.

Breuss, J. M., N. Gillett, et al. (1993). "Restricted distribution of integrin beta 6 mRNA in primate epithelial tissues." J Histoch Cytoch **41**(10): 1521-1527.

Bringuier, P. P., M. McCredie, et al. (1998). "Carcinomas of the renal pelvis associated with smoking and phenacetin abuse: p53 mutations and polymorphism of carcinogen-metabolising enzymes." Int J Cancer **79**(5): 531-536.

Bryne, M., Koppang, H. S., et al. (1992). “Malignancy grading of the deep invasive margins of oral squamous cell carcinoma has high prognostic value.” J Pathol **166**(4):375-81.

Brown, J. K., S. M. McAleese, et al. (2006). "Integrin-alphavbeta6, a putative receptor for foot-and-mouth disease virus, is constitutively expressed in ruminant airways." J Histochem Cytochem **54**(7): 807-816.

Busk, M., R. Pytela, et al. (1992). "Characterization of the integrin alpha v beta 6 as a fibronectin-binding protein." J Bio Chem **267**(9): 5790-5796.

Cass, D. L., K. M. Bullard, et al. (1998). "Epidermal integrin expression is upregulated rapidly in human fetal wound repair." J Paed Surg **33**(2): 312-316.

Chen, R., O. Kim, et al. (2001). "Regulation of the PH-domain-containing tyrosine kinase Etk by focal adhesion kinase through the FERM domain." Nat Cell Biol **3**(5): 439-444.

Chen, Y. K., H. C. Huang, et al. (1999). "Primary oral squamous cell carcinoma: an analysis of 703 cases in southern Taiwan." Oral Oncol **35**(2): 173-179.

Chernyavsky, A. I., J. Arredondo, et al. (2004). "Novel signaling pathways mediating reciprocal control of keratinocyte migration and wound epithelialization through M3 and M4 muscarinic receptors." J Cell Biol **166**(2): 261-272.

Chiu, C. J., C. P. Chiang, et al. (2001). "Association between genetic polymorphism of tumor necrosis factor-alpha and risk of oral submucous fibrosis, a pre-cancerous condition of oral cancer." J Dent Res **80**(12): 2055-2059.

Christenson, L. J., T. A. Borrowman, et al. (2005). "Incidence of basal cell and squamous cell carcinomas in a population younger than 40 years." JAMA **294**(6): 681-690.

Clark, R. A., G. S. Ashcroft, et al. (1996). "Re-epithelialization of normal human excisional wounds is associated with a switch from alpha v beta 5 to alpha v beta 6 integrins." Br J Derm **135**(1): 46-51.

Cosset, E. C., J. Godet, et al. (2011). "Involvement of TGFbeta pathway in the regulation of alpha(5) beta(1) integrins by caveolin-1 in human glioblastoma." Int J Cancer.

Coughlan, L., S. Vallath, et al. (2009). "In vivo retargeting of adenovirus type 5 to alphavbeta6 integrin results in reduced hepatotoxicity and improved tumor uptake following systemic delivery." J Virol **83**(13): 6416-6428.

Cox, D., M. Brennan, et al. (2010). "Integrins as therapeutic targets: lessons and opportunities." Nat Rev Drug Disc **9**(10): 804-820.

Crowson, A. N. (2006). "Basal cell carcinoma: biology, morphology and clinical implications." Mod Pathol **19 Suppl 2**: S127-147.

D'Souza, G., A. R. Kreimer, et al. (2007). "Case-control study of human papillomavirus and oropharyngeal cancer." New Engl J Med **356**(19): 1944-1956.

Dahmane, N., J. Lee, et al. (1997). "Activation of the transcription factor Gli1 and the Sonic hedgehog signalling pathway in skin tumours." Nature **389**(6653): 876-881.

Dalton, S. L. (1999). "American Academy of Dermatology 1999 Awards for Young Investigators in Dermatology. Alphavbeta6 integrin mediates latent TGF-beta activation: implications for cutaneous fibrosis." J Am Acad Dermatol **41**(3 Pt 1): 457-458.

Dalvi, N., G. J. Thomas, et al. (2004). "Modulation of the urokinase-type plasminogen activator receptor by the beta6 integrin subunit." Biochem Biophys Res Commun **317**(1): 92-99.

Danen, E. H., P. J. Ten Berge, et al. (1994). "Emergence of alpha 5 beta 1 fibronectin- and alpha v beta 3 vitronectin-receptor expression in melanocytic tumour progression." Histopathology **24**(3): 249-256.

Davies, M., M. Robinson, et al. (2005). "Induction of an epithelial to mesenchymal transition in human immortal and malignant keratinocytes by TGF-beta1 involves MAPK, Smad and AP-1 signalling pathways." J Cell Biol **95**(5): 918-931.

De Wever, O., P. Demetter, et al. (2008). "Stromal myofibroblasts are drivers of invasive cancer growth." Int J Cancer **123**(10): 2229-2238.

Defilles, C., J. C. Lissitzky, et al. (2009). "alphavbeta5/beta6 integrin suppression leads to a stimulation of alpha2beta1 dependent cell migration resistant to PI3K/Akt inhibition." Exp Cell Res **315**(11): 1840-1849.

Dennler, S., J. Andre, et al. (2007). "Induction of sonic hedgehog mediators by transforming growth factor-beta: Smad3-dependent activation of Gli2 and Gli1 expression in vitro and in vivo." Cancer Res **67**(14): 6981-6986.

Derynck, R. and Y. E. Zhang (2003). "Smad-dependent and Smad-independent pathways in TGF-beta family signalling." Nature **425**(6958): 577-584.

Desgrosellier, J. S., L. A. Barnes, et al. (2009). "An integrin alpha(v)beta(3)-c-Src oncogenic unit promotes anchorage-independence and tumor progression." Nature Med **15**(10): 1163-1169.

Desgrosellier, J. S. and D. A. Cheresh (2010). "Integrins in cancer: biological implications and therapeutic opportunities." Nature Rev Cancer **10**(1): 9-22.

Dicara, D., A. Burman, et al. (2008). "Foot-and-mouth disease virus forms a highly stable, EDTA-resistant complex with its principal receptor, integrin alphavbeta6: implications for infectiousness." J Virol **82**(3): 1537-1546.

Dickson, M. A., W. C. Hahn, et al. (2000). "Human keratinocytes that express hTERT and also bypass a p16(INK4a)-enforced mechanism that limits life span become immortal yet retain normal growth and differentiation characteristics." Mol Cell Biol **20**(4): 1436-1447.

Dittmer, J. (2003). "The biology of the Ets1 proto-oncogene." Mol Canc **2**: 29.

Dixit, R. B., A. Chen, et al. (1996). "Identification of a sequence within the integrin beta6 subunit cytoplasmic domain that is required to support the specific effect of alphavbeta6 on proliferation in three-dimensional culture." J Biol Chem **271**(42): 25976-25980.

Dosanjh, A., T. Ikonen, et al. (2004). "Respiratory epithelial expression of integrin alphaVbeta6 in chronic progressive allograft rejection." J Heart Lung Transplant **23**(4): 456-460.

Dvorak, H. F. (1986). "Tumors: wounds that do not heal. Similarities between tumor stroma generation and wound healing." New Engl J Med **315**(26): 1650-1659.

Elayadi, A. N., K. N. Samli, et al. (2007). "A peptide selected by biopanning identifies the integrin alphavbeta6 as a prognostic biomarker for nonsmall cell lung cancer." Cancer Res **67**(12): 5889-5895.

Elliott, R. L. and G. C. Blobe (2005). "Role of transforming growth factor Beta in human cancer." J Clin Onc **23**(9): 2078-2093.

Endo, H., A. Oikawa, et al. (2004). "Plexiform neurofibromas express the transcription factor Gli1." Dermatology **209**(4): 284-287.

Eslami, A., C. L. Gallant-Behm, et al. (2009). "Expression of integrin alphavbeta6 and TGF-beta in scarless vs scar-forming wound healing." J Histochem Cytochem **57**(6): 543-557.

Ferris, N. P., N. G. Abrescia, et al. (2005). "Utility of recombinant integrin alpha v beta6 as a capture reagent in immunoassays for the diagnosis of foot-and-mouth disease." J Virol Methods **127**(1): 69-79.

Fiaschi, M., B. Rozell, et al. (2007). "Targeted expression of GLI1 in the mammary gland disrupts pregnancy-induced maturation and causes lactation failure." J Biol Chem **282**(49): 36090-36101.

Fontana, L., Y. Chen, et al. (2005). "Fibronectin is required for integrin alphavbeta6-mediated activation of latent TGF-beta complexes containing LTBP-1." FASEB J **19**(13): 1798-1808.

Forsyth, N. R., V. Morrison, et al. (2002). "Functional evidence for a squamous cell carcinoma mortality gene(s) on human chromosome 4." Oncogene **21**(33): 5135-5147.

Fouchier, F., C. Penel, et al. (2007). "Integrin alphavbeta6 mediates HT29-D4 cell adhesion to MMP-processed fibrinogen in the presence of Mn2+." Eur J Cell Biol **86**(3): 143-160.

Freytag, J., C. E. Wilkins-Port, et al. (2010). "PAI-1 mediates the TGF-beta1+EGF-induced "scatter" response in transformed human keratinocytes." J Investig Dermatol **130**(9): 2179-2190.

Friedrichs, K., P. Ruiz, et al. (1995). "High expression level of alpha 6 integrin in human breast carcinoma is correlated with reduced survival." Cancer Res **55**(4): 901-906.

Ganter, M. T., J. Roux, et al. (2008). "Interleukin-1beta causes acute lung injury via alphavbeta5 and alphavbeta6 integrin-dependent mechanisms." Circ Res **102**(7): 804-812.

Gao, S. D., H. Y. Chang, et al. (2008). "[Preparation and characterization of the polyclonal antibody against pig integrin beta6 subunit LBD as FMDV receptor]." Xi Bao Yu Fen Zi Mian Yi Xue Za Zhi **24**(10): 975-978.

Gewin, L., N. Bulus, et al. (2010). "TGF-beta receptor deletion in the renal collecting system exacerbates fibrosis." J Amer Nephrol **21**(8): 1334-1343.

Ghali, L., S. T. Wong, et al. (1999). "Gli1 protein is expressed in basal cell carcinomas, outer root sheath keratinocytes and a subpopulation of mesenchymal cells in normal human skin." J Invest Dermatol **113**(4): 595-599.

Ghannad, F., D. Nica, et al. (2008). "Absence of alphavbeta6 integrin is linked to initiation and progression of periodontal disease." Am J Pathol **172**(5): 1271-1286.

Goel, H. L., J. M. Underwood, et al. (2010). "Beta1 integrins mediate cell proliferation in three-dimensional cultures by regulating expression of the sonic hedgehog effector protein, GLI1." J Cell Physiol **224**(1): 210-217.

Goh, K. L., J. T. Yang, et al. (1997). "Mesodermal defects and cranial neural crest apoptosis in alpha5 integrin-null embryos." Development **124**(21): 4309-4319.

Gonzalez-Moles, M. A., C. Scully, et al. (2008). "Oral lichen planus: controversies surrounding malignant transformation." Oral Dis **14**(3): 229-243.

Goodwin, A. and G. Jenkins (2009). "Role of integrin-mediated TGFbeta activation in the pathogenesis of pulmonary fibrosis Biochem Soc Trans **37**(Pt 4): 849-854.

Gordon, K. J. and G. C. Blobe (2008). "Role of transforming growth factor-beta superfamily signaling pathways in human disease." Bioch Biophy Acta **1782**(4): 197-228.

Grachtchouk, M., R. Mo, et al. (2000). "Basal cell carcinomas in mice overexpressing Gli2 in skin." Nature Genetics **24**(3): 216-217.

Grimbaldeston, M. A., A. Green, et al. (2003). "Susceptibility to basal cell carcinoma is associated with high dermal mast cell prevalence in non-sun-exposed skin for an Australian populations." Photochem Photobiol **78**(6): 633-639.

Grimbaldeston, M. A., L. Skov, et al. (2000). "Communications: high dermal mast cell prevalence is a predisposing factor for basal cell carcinoma in humans." J Invest Dermatol **115**(2): 317-320.

Grinnell, F. (1992). "Wound repair, keratinocyte activation and integrin modulation." J Cell Sci **101 (Pt 1)**: 1-5.

Gruber, G., J. Hess, et al. (2005). "Correlation between the tumoral expression of beta3-integrin and outcome in cervical cancer patients who had undergone radiotherapy." Br J Cancer **92**(1): 41-46.

Gu, X., J. Niu, et al. (2002). "Integrin alpha(v)beta6-associated ERK2 mediates MMP-9 secretion in colon cancer cells." Br J Cancer **87**(3): 348-351.

Guan, J. L. and D. Shalloway (1992). "Regulation of focal adhesion-associated protein tyrosine kinase by both cellular adhesion and oncogenic transformation." Nature **358**(6388): 690-692.

Gumbiner, B. M. (2005). "Regulation of cadherin-mediated adhesion in morphogenesis." Nature Rev Mol Cell Biol **6**(8): 622-634.

Gupta, P. C. and S. Warnakulasuriya (2002). "Global epidemiology of areca nut usage." Addict Biol **7**(1): 77-83.

Haapasalmi, K., K. Zhang, et al. (1996). "Keratinocytes in human wounds express alpha v beta 6 integrin." J Invest Dermatol **106**(1): 42-48.

Hahm, K., M. E. Lukashev, et al. (2007). "Alphav beta6 integrin regulates renal fibrosis and inflammation in Alport mouse." Am J Pathol **170**(1): 110-125.

Hakkinen, L., H. C. Hildebrand, et al. (2000). "Immunolocalization of tenascin-C, alpha9 integrin subunit, and alphavbeta6 integrin during wound healing in human oral mucosa." J Histochem Cytochem **48**(7): 985-998.

Hakkinen, L., L. Koivisto, et al. (2004). "Increased expression of beta6-integrin in skin leads to spontaneous development of chronic wounds." Am J Pathol **164**(1): 229-242.

Hamidi, S., T. Salo, et al. (2000). "Expression of alpha(v)beta6 integrin in oral leukoplakia." Br J Cancer **82**(8): 1433-1440.

Hanahan, D. and R. A. Weinberg (2000). "The hallmarks of cancer." Cell **100**(1): 57-70.

Hanahan, D. and R. A. Weinberg (2011). "Hallmarks of cancer: the next generation." Cell **144**(5): 646-674.

Haque, M. F., M. Harris, et al. (1998). "Immunolocalization of cytokines and growth factors in oral submucous fibrosis." Cytokine **10**(9): 713-719.

Hato, T., J. Yamanouchi, et al. (2006). "Identification of critical residues for regulation of integrin activation in the beta6-alpha7 loop of the integrin beta3 I-like domain." J Thromb Haemost **4**(10): 2278-2280.

Hausner, S. H., C. K. Abbey, et al. (2009). "Targeted in vivo imaging of integrin alphavbeta6 with an improved radiotracer and its relevance in a pancreatic tumor model." Cancer Res **69**(14): 5843-5850.

Hausner, S. H., D. DiCara, et al. (2007). "Use of a peptide derived from foot-and-mouth disease virus for the noninvasive imaging of human cancer: generation and evaluation of 4-[18F]fluorobenzoyl A20FMDV2 for in vivo imaging of integrin alphavbeta6 expression with positron emission tomography." Cancer Res **67**(16): 7833-7840.

Hazarey, V. K., D. M. Erlewad, et al. (2007). "Oral submucous fibrosis: study of 1000 cases from central India." J Oral Pathol Med **36**(1): 12-17.

Hazelbag, S., G. G. Kenter, et al. (2007). "Overexpression of the alpha v beta 6 integrin in cervical squamous cell carcinoma is a prognostic factor for decreased survival." J Pathol **212**(3): 316-324.

Hecht, J. L., B. M. Dolinski, et al. (2008). "Overexpression of the alphavbeta6 integrin in endometrial cancer." Appl Immunohistochem Mol Morphol **16**(6): 543-547.

Heikkila, O., P. Susi, et al. (2009). "Integrin alphaVbeta6 is a high-affinity receptor for coxsackievirus A9." J Gen Virol **90**(Pt 1): 197-204.

Heo, J. S., M. Y. Lee, et al. (2007). "Sonic hedgehog stimulates mouse embryonic stem cell proliferation by cooperation of Ca2+/protein kinase C and epidermal growth factor receptor as well as Gli1 activation." Stem Cells **25**(12): 3069-3080.

Hogmalm, A., D. Sheppard, et al. (2010). "beta6 Integrin subunit deficiency alleviates lung injury in a mouse model of bronchopulmonary dysplasia." Am J Respir Cell Mol Biol **43**(1): 88-98.

Holmstrup, P., P. Vedtofte, et al. (2006). "Long-term treatment outcome of oral premalignant lesions." Oral Oncol **42**(5): 461-474.

Horan, G. S., S. Wood, et al. (2008). "Partial inhibition of integrin alpha(v)beta6 prevents pulmonary fibrosis without exacerbating inflammation." Am J Respir Crit Care Med **177**(1): 56-65.

Hosotani, R., M. Kawaguchi, et al. (2002). "Expression of integrin alphaVbeta3 in pancreatic carcinoma: relation to MMP-2 activation and lymph node metastasis." Pancreas **25**(2): e30-35.

Hsu, M. Y., D. T. Shih, et al. (1998). "Adenoviral gene transfer of beta3 integrin subunit induces conversion from radial to vertical growth phase in primary human melanoma." Am J Pathol **153**(5): 1435-1442.

Huang, C., K. Jacobson, et al. (2004). "MAP kinases and cell migration." J Cell Sci **117**(Pt 20): 4619-4628.

Huang, X., J. Wu, et al. (1998). "The integrin alphavbeta6 is critical for keratinocyte migration on both its known ligand, fibronectin, and on vitronectin." J Cell Sci **111 (Pt 15)**: 2189-2195.

Huang, X., J. Wu, et al. (1998). "Expression of the human integrin beta6 subunit in alveolar type II cells and bronchiolar epithelial cells reverses lung inflammation in beta6 knockout mice." Am J Respir Cell Mol Biol **19**(4): 636-642.

Huang, X. Z., J. F. Wu, et al. (1996). "Inactivation of the integrin beta 6 subunit gene reveals a role of epithelial integrins in regulating inflammation in the lung and skin." The Journal of cell biology **133**(4): 921-928.

Hunter, K. D., E. K. Parkinson, et al. (2005). "Profiling early head and neck cancer." Nature Rev Cancer **5**(2): 127-135.

Hynes, R. O. (1987). "Integrins: a family of cell surface receptors." Cell **48**(4): 549-554.

Hynes, R. O. (2002). "Integrins: bidirectional, allosteric signaling machines." Cell **110**(6): 673-687.

Hynes, R. O. (2004). "The emergence of integrins: a personal and historical perspective." Matrix Biol **23**(6): 333-340.

Ikram, M. S., G. W. Neill, et al. (2004). "GLI2 is expressed in normal human epidermis and BCC and induces GLI1 expression by binding to its promoter." J Invest Dermatol **122**(6): 1503-1509.

Ikushima, H. and K. Miyazono (2010). "TGFbeta signalling: a complex web in cancer progression." Nature Rev Cancer **10**(6): 415-424.

Impola, U., V. J. Uitto, et al. (2004). "Differential expression of matrilysin-1 (MMP-7), 92 kD gelatinase (MMP-9), and metalloelastase (MMP-12) in oral verrucous and squamous cell cancer." J Pathol **202**(1): 14-22.

Inaguma, S., K. Kasai, et al. (2011). "GLI1 facilitates the migration and invasion of pancreatic cancer cells through MUC5AC-mediated attenuation of E-cadherin." Oncogene **30**(6): 714-723.

Isaac, U., J. S. Issac, et al. (2008). "Histopathologic features of oral submucous fibrosis: a study of 35 biopsy specimens." Oral Surg Oral Med Oral Radiol Oral Pathol Endodont **106**(4): 556-560.

Isohata, N., K. Aoyagi, et al. (2009). "Hedgehog and epithelial-mesenchymal transition signaling in normal and malignant epithelial cells of the esophagus." Int J Cancer **125**(5): 1212-1221.

Jackson, T., D. Sheppard, et al. (2000). "The epithelial integrin alphavbeta6 is a receptor for foot-and-mouth disease virus." J Virol **74**(11): 4949-4956.

Jacobsen, J. N., B. Steffensen, et al. (2010). "Skin wound healing in diabetic beta6 integrin-deficient mice." Acta Pathol Microbiol Immunol Scand **118**(10): 753-764.

Janda, E., K. Lehmann, et al. (2002). "Ras and TGF[beta] cooperatively regulate epithelial cell plasticity and metastasis: dissection of Ras signaling pathways." J Cell Biol **156**(2): 299-313.

Janes, S. M. and F. M. Watt (2004). "Switch from alphavbeta5 to alphavbeta6 integrin expression protects squamous cell carcinomas from anoikis." J Cell Biol **166**(3): 419-431.

Jefferies, S., S. M. Edwards, et al. (2001). "No germline mutations in CDKN2A (p16) in patients with squamous cell cancer of the head and neck and second primary tumours." Br J Cancer **85**(9): 1383-1386.

Jeng, J. H., Y. J. Wang, et al. (2003). "Roles of keratinocyte inflammation in oral cancer: regulating the prostaglandin E2, interleukin-6 and TNF-alpha production of oral epithelial cells by areca nut extract and arecoline." Carcinogenesis **24**(8): 1301-1315.

Jenkins, R. G., X. Su, et al. (2006). "Ligation of protease-activated receptor 1 enhances alpha(v)beta6 integrin-dependent TGF-beta activation and promotes acute lung injury." J Clin Invest **116**(6): 1606-1614.

Joberty, G., C. Petersen, et al. (2000). "The cell-polarity protein Par6 links Par3 and atypical protein kinase C to Cdc42." Nature Cell Biol **2**(8): 531-539.

J., M. Sugiyama, et al. (1996). "Restoration of alpha v beta 5 integrin expression in neoplastic keratinocytes results in increased capacity for terminal differentiation and suppression of anchorage-independent growth." Oncogene **12**(1): 119-126.

Jones, J., F. M. Watt, et al. (1997). "Changes in the expression of alpha v integrins in oral squamous cell carcinomas." J Oral Pathol Med **26**(2): 63-68.

Jovanovic, J., J. Takagi, et al. (2007). "alphaVbeta6 is a novel receptor for human fibrillin-1. Comparative studies of molecular determinants underlying integrin-rgd affinity and specificity." J Biol Chem **282**(9): 6743-6751.

Kalluri, R. and R. A. Weinberg (2009). "The basics of epithelial-mesenchymal transition." J Clin Invest **119**(6): 1420-1428.

Karlstrom, R. O., O. V. Tyurina, et al. (2003). "Genetic analysis of zebrafish gli1 and gli2 reveals divergent requirements for gli genes in vertebrate development." Development **130**(8): 1549-1564.

Kasai, K., S. Inaguma, et al. (2008). "SCL/TAL1 interrupting locus derepresses GLI1 from the negative control of suppressor-of-fused in pancreatic cancer cell." Cancer Res **68**(19): 7723-7729.

Katoh, Y. and M. Katoh (2009). "Integrative genomic analyses on GLI1: positive regulation of GLI1 by Hedgehog-GLI, TGFbeta-Smads, and RTK-PI3K-AKT signals, and negative regulation of GLI1 by Notch-CSL-HES/HEY, and GPCR-Gs-PKA signals." Int J Oncol **35**(1): 187-192.

Kawashima, A., S. Tsugawa, et al. (2003). "Expression of alphav integrin family in gastric carcinomas: increased alphavbeta6 is associated with lymph node metastasis." Pathol Res Pract **199**(2): 57-64.

Kinzler, K. W., S. H. Bigner, et al. (1987). "Identification of an amplified, highly expressed gene in a human glioma." Science **236**(4797): 70-73.

Koth, L. L., B. Alex, et al. (2007). "Integrin beta6 mediates phospholipid and collectin homeostasis by activation of latent TGF-beta1." Am J Respir Cell Mol Biol **37**(6): 651-659.

Kracklauer, M. P., C. Schmidt, et al. (2003). "TGFbeta1 signaling via alphaVbeta6 integrin." Mol Cancer **2**: 28.

Kraft, S., B. Diefenbach, et al. (1999). "Definition of an unexpected ligand recognition motif for alphav beta6 integrin." J Biol Chem **274**(4): 1979-1985.

Kuo, M. Y., J. H. Jeng, et al. (1994). "Mutations of Ki-ras oncogene codon 12 in betel quid chewing-related human oral squamous cell carcinoma in Taiwan." J Oral Pathol Med **23**(2): 70-74.

Lai, S. Y. and F. M. Johnson (2010). "Defining the role of the JAK-STAT pathway in head and neck and thoracic malignancies: implications for future therapeutic approaches." Drug Res Update **13**(3): 67-78.

Lamb, L. E., J. C. Zarif, et al. (2011). "The androgen receptor induces integrin alpha6beta1 to promote prostate tumor cell survival via NF-kappaB and Bcl-xL Independently of PI3K signaling." Cancer Res **71**(7): 2739-2749.

Landen, C. N., T. J. Kim, et al. (2008). "Tumor-selective response to antibody-mediated targeting of alphavbeta3 integrin in ovarian cancer." Neoplasia **10**(11): 1259-1267.

Larjava, H., K. Haapasalmi, et al. (1996). "Keratinocyte integrins in wound healing and chronic inflammation of the human periodontium." Oral Dis **2**(1): 77-86.

Larjava, H., L. Koivisto, et al. (2011). "Epithelial Integrins with Special Reference to Oral Epithelia." J Dent Res **90**(12):1367-76.

Lee, J., K. A. Platt, et al. (1997). "Gli1 is a target of Sonic hedgehog that induces ventral neural tube development." Development **124**(13): 2537-2552.

Lewis, M. P., K. A. Lygoe, et al. (2004). "Tumour-derived TGF-beta1 modulates myofibroblast differentiation and promotes HGF/SF-dependent invasion of squamous carcinoma cells." Br J Cancer **90**(4): 822-832.

Li, H., D. Huang, et al. (2010). "Scutellarin inhibits cell migration by regulating production of alphavbeta6 integrin and E-cadherin in human tongue cancer cells." Oncol Rep **24**(5): 1153-1160.

Li, X., W. Deng, et al. (2007). "Gli1 acts through Snail and E-cadherin to promote nuclear signaling by beta-catenin." Oncogene **26**(31): 4489-4498.

Li, X., W. Deng, et al. (2006). "Snail induction is an early response to Gli1 that determines the efficiency of epithelial transformation." Oncogene **25**(4): 609-621.

Li, X., Y. Yang, et al. (2003). "Alphavbeta6-Fyn signaling promotes oral cancer progression." J Biol Chem **278**(43): 41646-41653.

Liotta, L. A., K. Tryggvason, et al. (1980). "Metastatic potential correlates with enzymatic degradation of basement membrane collagen." Nature **284**(5751): 67-68.

Ludlow, A., K. O. Yee, et al. (2005). "Characterization of integrin beta6 and thrombospondin-1 double-null mice." J Cell Mol Med **9**(2): 421-437.

Luettich, K. and C. Schmidt (2003). "TGFbeta1 activates c-Jun and Erk1 via alphaVbeta6 integrin." Mol Cancer **2**: 33.

Ma, L. J., H. Yang, et al. (2003). "Transforming growth factor-beta-dependent and -independent pathways of induction of tubulointerstitial fibrosis in beta6(-/-) mice." Am J Pathol **163**(4): 1261-1273.

Macha, M. A., A. Matta, et al. (2011). "Guggulsterone (GS) inhibits smokeless tobacco and nicotine-induced NF-kappaB and STAT3 pathways in head and neck cancer cells." Carcinogenesis **32**(3): 368-380.

Mackenzie, I. C. (2004). "Growth of malignant oral epithelial stem cells after seeding into organotypical cultures of normal mucosa." J Oral Pathol Med **33**(2): 71-78.

Mandal, P. K., P. A. Heard, et al. (2007). "Solid-phase synthesis of Stat3 inhibitors incorporating O-carbamoylserine and O-carbamoylthreonine as glutamine mimics." Bioorg Med Chem Letters **17**(3): 654-656.

Mao, L., W. K. Hong, et al. (2004). "Focus on head and neck cancer." Cancer Cell **5**(4): 311-316.

Margadant, C. and A. Sonnenberg (2010). "Integrin-TGF-beta crosstalk in fibrosis, cancer and wound healing." EMBO Rep **11**(2): 97-105.

Marsh, A., C. Wicking, et al. (2005). "DHPLC analysis of patients with Nevoid Basal Cell Carcinoma Syndrome reveals novel PTCH missense mutations in the sterol-sensing domain." Hum Mutat **26**(3): 283.

Marsh, D., S. Dickinson, et al. (2008). "alpha vbeta 6 Integrin promotes the invasion of morphoeic basal cell carcinoma through stromal modulation." Cancer Res **68**(9): 3295-3303.

Marsh, D., K. Suchak, et al. (2011). "Stromal features are predictive of disease mortality in oral cancer patients." J Pathol **223**(4): 470-481.

Marur, S., G. D'Souza, et al. (2010). "HPV-associated head and neck cancer: a virus-related cancer epidemic." Lancet Oncol **11**(8): 781-789.

Marur, S. and A. A. Forastiere (2010). "Challenges of integrating chemotherapy and targeted therapy with radiation in locally advanced head and neck squamous cell cancer." Cur Opin Oncol **22**(3): 206-211.

McCabe, N. P., S. De, et al. (2007). "Prostate cancer specific integrin alphavbeta3 modulates bone metastatic growth and tissue remodeling." Oncogene **26**(42): 6238-6243.

McKinney, M., J. H. Miller, et al. (1991). "Interactions of agonists with M2 and M4 muscarinic receptor subtypes mediating cyclic AMP inhibition." Mol Pharmacol **40**(6): 1014-1022.

Miller, L. C., W. Blakemore, et al. (2001). "Role of the cytoplasmic domain of the beta-subunit of integrin alpha(v)beta6 in infection by foot-and-mouth disease virus." J Virol **75**(9): 4158-4164.

Mogi, S., D. Dang, et al. (2005). "The expression of integrin alpha(v)beta6 promotes the epithelial cell morphology and suppresses invasive behavior in transformed oral keratinocytes." Anticancer Res **25**(2A): 751-755.

Monaghan, P., S. Gold, et al. (2005). "The alpha(v)beta6 integrin receptor for Foot-and-mouth disease virus is expressed constitutively on the epithelial cells targeted in cattle." J Gen Virol **86**(Pt 10): 2769-2780.

Morgan, M. R., M. Jazayeri, et al. (2011). "Psoriasin (S100A7) associates with integrin beta6 subunit and is required for alphavbeta6-dependent carcinoma cell invasion." Oncogene **30**(12): 1422-1435.

Morgan, M. R., G. J. Thomas, et al. (2004). "The integrin cytoplasmic-tail motif EKQKVDLSTDC is sufficient to promote tumor cell invasion mediated by matrix metalloproteinase (MMP)-2 or MMP-9." J Biol Chem **279**(25): 26533-26539.

Morita, K., C. Lo Celso, et al. (2006). "HAN11 binds mDia1 and controls GLI1 transcriptional activity." J Dermatol Sci **44**(1): 11-20.

Morris, D. G., X. Huang, et al. (2003). "Loss of integrin alpha(v)beta6-mediated TGF-beta activation causes Mmp12-dependent emphysema." Nature **422**(6928): 169-173.

Moutasim, K. A., V. Jenei, et al. (2010). "Betel-derived alkaloid up-regulates keratinocyte alphavbeta6 integrin expression and promotes oral submucous fibrosis." J Pathol.

Mu, D., S. Cambier, et al. (2002). "The integrin alpha(v)beta8 mediates epithelial homeostasis through MT1-MMP-dependent activation of TGF-beta1."J Cell Biol **157**(3): 493-507.

Munger, J. S., X. Huang, et al. (1999). "The integrin alpha v beta 6 binds and activates latent TGF beta 1: a mechanism for regulating pulmonary inflammation and fibrosis." Cell **96**(3): 319-328.

Murillo, M. M., G. del Castillo, et al. (2005). "Involvement of EGF receptor and c-Src in the survival signals induced by TGF-beta1 in hepatocytes." Oncogene **24**(28): 4580-4587.

Nadendla, S. K., A. Hazan, et al. (2011). "GLI1 confers profound phenotypic changes upon LNCaP prostate cancer cells that include the acquisition of a hormone independent state." PLoS One **6**(5): e20271.

Nadler, E. P., D. Patterson, et al. (2009). "Integrin alphavbeta6 and mediators of extracellular matrix deposition are up-regulated in experimental biliary atresia." J Surg Res **154**(1): 21-29.

Nair, J., H. Ohshima, et al. (1985). "Tobacco-specific and betel nut-specific N-nitroso compounds: occurrence in saliva and urine of betel quid chewers and formation in vitro by nitrosation of betel quid." Carcinogenesis **6**(2): 295-303.

Natsuizaka, M., S. Ohashi, et al. (2010). "Insulin-like growth factor-binding protein-3 promotes transforming growth factor-{beta}1-mediated epithelial-to-mesenchymal transition and motility in transformed human esophageal cells." Carcinogenesis **31**(8): 1344-1353.

Ndoye, A., R. Buchli, et al. (1998). "Identification and mapping of keratinocyte muscarinic acetylcholine receptor subtypes in human epidermis." J Invest Dermatol **111**(3): 410-416.

Neill, G. W., L. R. Ghali, et al. (2003). "Loss of protein kinase Calpha expression may enhance the tumorigenic potential of Gli1 in basal cell carcinoma." Cancer Res **63**(15): 4692-4697.

Neill, G. W., W. J. Harrison, et al. (2008). "GLI1 repression of ERK activity correlates with colony formation and impaired migration in human epidermal keratinocytes." Carcinogenesis **29**(4): 738-746.

Neville, B. W. and T. A. Day (2002). "Oral cancer and precancerous lesions." CA Cancer J Clin **52**(4): 195-215.

Nguyen, V. T., A. I. Chernyavsky, et al. (2004). "Synergistic control of keratinocyte adhesion through muscarinic and nicotinic acetylcholine receptor subtypes." Exp Cell Res **294**(2): 534-549.

Nikitakis, N. G., H. Siavash, et al. (2004). "Targeting the STAT pathway in head and neck cancer: recent advances and future prospects." Curr Cancer Drug Targets **4**(8): 637-651.

Nilsson, M., A. B. Unden, et al. (2000). "Induction of basal cell carcinomas and trichoepitheliomas in mice overexpressing GLI-1." Proc Natl Acad Sci USA **97**(7): 3438-3443.

Niu, J., D. J. Dorahy, et al. (2002). "Integrin expression in colon cancer cells is regulated by the cytoplasmic domain of the beta6 integrin subunit." Int J Cancer **99**(4): 529-537.

Niu, J., X. Gu, et al. (2001). "The alphaVbeta6 integrin regulates its own expression with cell crowding: implications for tumour progression." Int J Cancer **92**(1): 40-48.

Nystrom, M. L., D. McCulloch, et al. (2006). "Cyclooxygenase-2 inhibition suppresses alphavbeta6 integrin-dependent oral squamous carcinoma invasion." Cancer Res **66**(22): 10833-10842.

Nystrom, M. L., G. J. Thomas, et al. (2005). "Development of a quantitative method to analyse tumour cell invasion in organotypic culture." J Pathol **205**(4): 468-475.

Ohashi, S., M. Natsuizaka, et al. (2010). "Epidermal growth factor receptor and mutant p53 expand an esophageal cellular subpopulation capable of epithelial-to-mesenchymal transition through ZEB transcription factors." Cancer Res **70**(10): 4174-4184.

Ohta, H., K. Aoyagi, et al. (2009). "Cross talk between hedgehog and epithelial-mesenchymal transition pathways in gastric pit cells and in diffuse-type gastric cancers." Br J Cancer **100**(2): 389-398.

Oikawa, T. and T. Yamada (2003). "Molecular biology of the Ets family of transcription factors." Gene **303**: 11-34.

Parkin, D. M. (2001). "Global cancer statistics in the year 2000." Lancet Oncol **2**(9): 533-543.

Paterson, I. C., J. W. Eveson, et al. (1996). "Molecular changes in oral cancer may reflect aetiology and ethnic origin." Eur J Cancer **32B**(3): 150-153.

Patsenker, E., Y. Popov, et al. (2008). "Inhibition of integrin alphavbeta6 on cholangiocytes blocks transforming growth factor-beta activation and retards biliary fibrosis progression." Gastroenterology **135**(2): 660-670.

Patsenker, E., L. Wilkens, et al. (2010). "The alphavbeta6 integrin is a highly specific immunohistochemical marker for cholangiocarcinoma." J Hepatol **52**(3): 362-369.

Peinado, H., D. Olmeda, et al. (2007). "Snail, Zeb and bHLH factors in tumour progression: an alliance against the epithelial phenotype?" Nat Rev Cancer **7**(6): 415-428.

Pindborg, J. J. and S. M. Sirsat (1966). "Oral submucous fibrosis." Oral Surg Oral Med Oral Pathol **22**(6): 764-779.

Popov, Y., E. Patsenker, et al. (2008). "Integrin alphavbeta6 is a marker of the progression of biliary and portal liver fibrosis and a novel target for antifibrotic therapies." J Hepatol **48**(3): 453-464.

Powell, D. W., R. C. Mifflin, et al. (1999). "Myofibroblasts. I. Paracrine cells important in health and disease." Am J Physiol **277**(1 Pt 1): C1-9.

Powles, T., S. Chowdhury, et al. (2011). "Sunitinib and other targeted therapies for renal cell carcinoma." Br J Cancer **104**(5): 741-745.

Prieto, A. L., G. M. Edelman, et al. (1993). "Multiple integrins mediate cell attachment to cytotactin/tenascin." Proc Natl Acad Sci USA **90**(21): 10154-10158.

Prime, S. S., M. Davies, et al. (2004). "The role of TGF-beta in epithelial malignancy and its relevance to the pathogenesis of oral cancer (part II)." Crit Rev Oral Biol Med **15**(6): 337-347.

Prime, S. S., S. V. Nixon, et al. (1990). "The behaviour of human oral squamous cell carcinoma in cell culture." J Pathol **160**(3): 259-269.

Puthawala, K., N. Hadjiangelis, et al. (2008). "Inhibition of integrin alpha(v)beta6, an activator of latent transforming growth factor-beta, prevents radiation-induced lung fibrosis." Am J Respir Crit Care Med **177**(1): 82-90.

Quandt, K., K. Frech, et al. (1995). "MatInd and MatInspector: new fast and versatile tools for detection of consensus matches in nucleotide sequence data." Nucl Acid Res **23**(23): 4878-4884.

Ramos, D. M., M. But, et al. (2002). "Expression of integrin beta 6 enhances invasive behavior in oral squamous cell carcinoma." Matrix Biol **21**(3): 297-307.

Ramos, D. M., D. Dang, et al. (2009). "The role of the integrin alpha v beta6 in regulating the epithelial to mesenchymal transition in oral cancer." Anticancer Res **29**(1): 125-130.

Ramsay, A. G., M. D. Keppler, et al. (2007). "HS1-associated protein X-1 regulates carcinoma cell migration and invasion via clathrin-mediated endocytosis of integrin alphavbeta6." Cancer Res **67**(11): 5275-5284.

Ramsay, A. G., J. F. Marshall, et al. (2007). "Integrin trafficking and its role in cancer metastasis." Cancer Mets Rev **26**(3-4): 567-578.

Regezi, J. A., D. M. Ramos, et al. (2002). "Tenascin and beta 6 integrin are overexpressed in floor of mouth in situ carcinomas and invasive squamous cell carcinomas." Oral Oncol **38**(4): 332-336.

Regl, G., G. W. Neill, et al. (2002). "Human GLI2 and GLI1 are part of a positive feedback mechanism in Basal Cell Carcinoma." Oncogene **21**(36): 5529-5539.

Reichart, P. A. and H. P. Philipsen (2005). "Oral erythroplakia--a review." Oral Oncol **41**(6): 551-561.

Reszka, A. A., Y. Hayashi, et al. (1992). "Identification of amino acid sequences in the integrin beta 1 cytoplasmic domain implicated in cytoskeletal association." J Cell Biol **117**(6): 1321-1330.

Rogers, S. N., J. S. Brown, et al. (2009). "Survival following primary surgery for oral cancer." Oral Oncol **45**(3): 201-211.

Ruiz i Altaba, A., C. Mas, et al. (2007). "The Gli code: an information nexus regulating cell fate, stemness and cancer." Trends Cell Biol **17**(9): 438-447.

Saha, A., D. Ellison, et al. (2010). "High-resolution in vivo imaging of breast cancer by targeting the pro-invasive integrin alphavbeta6." J Pathol **222**(1): 52-63.

Saharinen, J., M. Hyytiainen, et al. (1999). "Latent transforming growth factor-beta binding proteins (LTBPs)--structural extracellular matrix proteins for targeting TGF-beta action." Cytokine Growth Factor Rev **10**(2): 99-117.

Saranath, D., S. E. Chang, et al. (1991). "High frequency mutation in codons 12 and 61 of H-ras oncogene in chewing tobacco-related human oral carcinoma in India." Br J Cancer **63**(4): 573-578.

Sawada, T., M. Abe, et al. (2004). "beta6 integrin is up-regulated in chronic renal allograft dysfunction." Clin Transplant **18**(5): 525-528.

Schmidt, C. (2004). "Retraction: TGFbeta1 signaling via alphaVbeta6 integrin." Mol Cancer **3**: 2.

Scott, K. A., C. H. Arnott, et al. (2004). "TNF-alpha regulates epithelial expression of MMP-9 and integrin alphavbeta6 during tumour promotion. A role for TNF-alpha in keratinocyte migration?" Oncogene **23**(41): 6954-6966.

Scrivener, Y., E. Grosshans, et al. (2002). "Variations of basal cell carcinomas according to gender, age, location and histopathological subtype." Br J Dermatol **147**(1): 41-47.

Scully, C., J. Langdon, et al. (2010). "Marathon of eponyms: 7 Gorlin-Goltz syndrome (Naevoid basal-cell carcinoma syndrome)." Oral Dis **16**(1): 117-118.

Secretan, B., K. Straif, et al. (2009). "A review of human carcinogens--Part E: tobacco, areca nut, alcohol, coal smoke, and salted fish." Lancet Oncol **10**(11): 1033-1034.

Shah, J. P. (1990). "Patterns of cervical lymph node metastasis from squamous carcinomas of the upper aerodigestive tract." Am J Surg **160**(4): 405-409.

Shahi, M. H., P. Schiapparelli, et al. (2011). "Expression and epigenetic modulation of sonic hedgehog-GLI1 pathway genes in neuroblastoma cell lines and tumors." Tumour Biol **32**(1): 113-127.

Sheppard, D. (2006). "Transforming growth factor beta: a central modulator of pulmonary and airway inflammation and fibrosis." Proc Amer Thorac **3**(5): 413-417.

Shi, M., J. Zhu, et al. (2011). "Latent TGF-beta structure and activation." Nature **474**(7351): 343-349.

Shida, T., M. Furuya, et al. (2006). "Sonic Hedgehog-Gli1 signaling pathway might become an effective therapeutic target in gastrointestinal neuroendocrine carcinomas." Cancer Biol Ther **5**(11): 1530-1538.

Siavash, H., N. G. Nikitakis, et al. (2004). "Signal transducers and activators of transcription: insights into the molecular basis of oral cancer." Crit Rev Oral Biol Med **15**(5): 298-307.

Singh, A. and J. Settleman (2010). "EMT, cancer stem cells and drug resistance: an emerging axis of evil in the war on cancer." Oncogene **29**(34): 4741-4751.

Sipos, B., D. Hahn, et al. (2004). "Immunohistochemical screening for beta6-integrin subunit expression in adenocarcinomas using a novel monoclonal antibody reveals strong up-regulation in pancreatic ductal adenocarcinomas in vivo and in vitro." Histopathology **45**(3): 226-236.

Slack-Davis, J. K., K. A. Atkins, et al. (2009). "Vascular cell adhesion molecule-1 is a regulator of ovarian cancer peritoneal metastasis." Cancer Res **69**(4): 1469-1476.

Sloan, E. K., N. Pouliot, et al. (2006). "Tumor-specific expression of alphavbeta3 integrin promotes spontaneous metastasis of breast cancer to bone." Breast Cancer Res **8**(2): R20.

Smythe, W. R., E. LeBel, et al. (1995). "Integrin expression in non-small cell carcinoma of the lung." Cancer Mets Rev **14**(3): 229-239.

Song, Y., J. F. Pittet, et al. (2008). "Role of integrin alphav beta6 in acute lung injury induced by Pseudomonas aeruginosa." Infect Immun **76**(6): 2325-2332.

Sood, A. K., J. E. Coffin, et al. (2004). "Biological significance of focal adhesion kinase in ovarian cancer: role in migration and invasion." Am J Pathol**165**(4): 1087-1095.

Sponer, U., S. Pieh, et al. (2005). "Upregulation of alphavbeta6 integrin, a potent TGF-beta1 activator, and posterior capsule opacification." J Cataract Refract Surg **31**(3): 595-606.

Stecca, B., C. Mas, et al. (2007). "Melanomas require HEDGEHOG-GLI signaling regulated by interactions between GLI1 and the RAS-MEK/AKT pathways." Proc Natl Acad Sci U S A **104**(14): 5895-5900.

Stecca, B. and A. Ruiz i Altaba (2009). "A GLI1-p53 inhibitory loop controls neural stem cell and tumour cell numbers." EMBO J **28**(6): 663-676.

Stecca, B. and I. A. A. Ruiz (2010). "Context-dependent regulation of the GLI code in cancer by Hedgehog and non-Hedgehog signals." J Mol Cell Biol **2**(2): 84-95.

Sullivan, B. P., P. H. Weinreb, et al. (2010). "The coagulation system contributes to alphaVbeta6 integrin expression and liver fibrosis induced by cholestasis." Am J Pathol **177**(6): 2837-2849.

Sume, S. S., A. Kantarci, et al. (2010). "Epithelial to mesenchymal transition in gingival overgrowth." Am J Pathol **177**(1): 208-218.

Symons, M., J. M. Derry, et al. (1996). "Wiskott-Aldrich syndrome protein, a novel effector for the GTPase CDC42Hs, is implicated in actin polymerization." Cell **84**(5): 723-734.

Tabata, T., H. Kawakatsu, et al. (2008). "Induction of an epithelial integrin alphavbeta6 in human cytomegalovirus-infected endothelial cells leads to activation of transforming growth factor-beta1 and increased collagen production." Am J Pathol **172**(4): 1127-1140.

Tafolla, E., S. Wang, et al. (2005). "JNK1 and JNK2 oppositely regulate p53 in signaling linked to apoptosis triggered by an altered fibronectin matrix: JNK links FAK and p53." J Biol Chem **280**(20): 19992-19999.

Takeuchi, Y., M. Suzawa, et al. (1997). "Differentiation and transforming growth factor-beta receptor down-regulation by collagen-alpha2beta1 integrin interaction is mediated by focal adhesion kinase and its downstream signals in murine osteoblastic cells." J Biol Chem **272**(46): 29309-29316.

Tamkun, J. W., D. W. DeSimone, et al. (1986). "Structure of integrin, a glycoprotein involved in the transmembrane linkage between fibronectin and actin." Cell **46**(2): 271-282.

Teh, M. T., S. T. Wong, et al. (2002). "FOXM1 is a downstream target of Gli1 in basal cell carcinomas." Cancer Res **62**(16): 4773-4780.

Testaz, S., A. Jarov, et al. (2001). "Sonic hedgehog restricts adhesion and migration of neural crest cells independently of the Patched- Smoothened-Gli signaling pathway." Proc Natl Acad Sci USA **98**(22): 12521-12526.

Thiery, J. P. (2003). "Epithelial-mesenchymal transitions in development and pathologies." Curr Opin Cell Biol **15**(6): 740-746.

Thiery, J. P., H. Acloque, et al. (2009). "Epithelial-mesenchymal transitions in development and disease." Cell **139**(5): 871-890.

Thomas, G. J., I. R. Hart, et al. (2002). "Binding of TGF-beta1 latency-associated peptide (LAP) to alpha(v)beta6 integrin modulates behaviour of squamous carcinoma cells." Br J Cancer **87**(8): 859-867.

Thomas, G. J., M. P. Lewis, et al. (2001a). "Expression of the alphavbeta6 integrin promotes migration and invasion in squamous carcinoma cells." J Invest Dermatol **117**(1): 67-73.

Thomas, G. J., M. P. Lewis, et al. (2001b). "AlphaVbeta6 integrin promotes invasion of squamous carcinoma cells through up-regulation of matrix metalloproteinase-9." Int J Cancer **92**(5): 641-650.

Thomas, G. J., M. L. Nystrom, et al. (2006). "Alphavbeta6 integrin in wound healing and cancer of the oral cavity." J Oral Pathol Med **35**(1): 1-10.

Tilakaratne, W. M., M. F. Klinikowski, et al. (2006). "Oral submucous fibrosis: review on aetiology and pathogenesis." Oral Oncol **42**(6): 561-568.

Tilghman, R. W., J. K. Slack-Davis, et al. (2005). "Focal adhesion kinase is required for the spatial organization of the leading edge in migrating cells." J Cell Sci **118**(Pt 12): 2613-2623.

van der Waal, I. (2009). "Potentially malignant disorders of the oral and oropharyngeal mucosa; terminology, classification and present concepts of management." Oral Oncol **45**(4-5): 317-323.

Varnat, F., I. Siegl-Cachedenier, et al. (2010). "Loss of WNT-TCF addiction and enhancement of HH-GLI1 signalling define the metastatic transition of human colon carcinomas." EMBO Mol Med **2**(11): 440-457.

Vermeer, B. J., M. C. Wijsman, et al. (1986). "Binding and internalization of low-density lipoproteins in SCC25 cells and SV40 transformed keratinocytes. A morphologic study." J Invest Dermatol **86**(2): 195-200.

Vincent-Salomon, A. and J. P. Thiery (2003). "Host microenvironment in breast cancer development: epithelial-mesenchymal transition in breast cancer development." Breast Cancer Res **5**(2): 101-106.

Wagstaff, J. L., S. Vallath, et al. (2010). "Two-dimensional heteronuclear saturation transfer difference NMR reveals detailed integrin alphavbeta6 protein-peptide interactions." Chem Commun (Camb) **46**(40): 7533-7535.

Wang, B., B. M. Dolinski, et al. (2007). "Role of alphavbeta6 integrin in acute biliary fibrosis." Hepatology **46**(5): 1404-1412.

Wang, L., N. Raikwar, et al. (2002). "Induction of alpha-catenin, integrin alpha3, integrin beta6, and PDGF-B by 2,8-dihydroxyadenine crystals in cultured kidney epithelial cells." Exp Nephrol **10**(5-6): 365-373.

Wang, T., G. Niu, et al. (2004). "Regulation of the innate and adaptive immune responses by Stat-3 signaling in tumor cells." Nature Med **10**(1): 48-54.

Warnakulasuriya, S. (2009). "Global epidemiology of oral and oropharyngeal cancer." Oral Oncol **45**(4-5): 309-316.

Weaver, S. R., G. R. Blackshaw, et al. (2004). "Comparison of special interest computed tomography, endosonography and histopathological stage of oesophageal cancer." Clin Radiol **59**(6): 499-504.

Webb, D. J., K. Donais, et al. (2004). "FAK-Src signalling through paxillin, ERK and MLCK regulates adhesion disassembly." Nature Cell Biol **6**(2): 154-161.

Weinacker, A., A. Chen, et al. (1994). "Role of the integrin alpha v beta 6 in cell attachment to fibronectin. Heterologous expression of intact and secreted forms of the receptor." J Biol Chem **269**(9): 6940-6948.

Weinacker, A., R. Ferrando, et al. (1995). "Distribution of integrins alpha v beta 6 and alpha 9 beta 1 and their known ligands, fibronectin and tenascin, in human airways." Am J Resp Cell Mol Biol **12**(5): 547-556.

Weinreb, P. H., K. J. Simon, et al. (2004). "Function-blocking integrin alphavbeta6 monoclonal antibodies: distinct ligand-mimetic and nonligand-mimetic classes." J Biol Chem **279**(17): 17875-17887.

Wendt, M. K., J. A. Smith, et al. (2010). "Transforming growth factor-beta-induced epithelial-mesenchymal transition facilitates epidermal growth factor-dependent breast cancer progression." Oncogene **29**(49): 6485-6498.

Westwick, J. K., C. Weitzel, et al. (1994). "Tumor necrosis factor alpha stimulates AP-1 activity through prolonged activation of the c-Jun kinase." J Biol Chem **269**(42): 26396-26401.

Williams, C. H., T. Kajander, et al. (2004). "Integrin alpha v beta 6 is an RGD-dependent receptor for coxsackievirus A9." J Virol **78**(13): 6967-6973.

Wipff, P. J. and B. Hinz (2008). "Integrins and the activation of latent transforming growth factor beta1 - an intimate relationship." Eur J Cell Biol **87**(8-9): 601-615.

Wong, C. S., R. C. Strange, et al. (2003). "Basal cell carcinoma." Brit Med J **327**(7418): 794-798.

Wong, V. A., J. A. Marshall, et al. (2002). "Management of periocular basal cell carcinoma with modified en face frozen section controlled excision." Ophthal Plast Reconstr Surg **18**(6): 430-435.

Woolgar, J. A. (2006). "Histopathological prognosticators in oral and oropharyngeal squamous cell carcinoma." Oral Oncol **42**(3): 229-239.

Worthington, J. J., B. I. Czajkowska, et al. (2011). "Intestinal Dendritic Cells Activate Transforming Growth Factor beta and Induce Foxp3(+) T Regulatory Cells via Integrin alphavbeta8." Gastroenterology **141**(5):1802-12.

Wynn, T. A. (2008). "Cellular and molecular mechanisms of fibrosis." J Pathol **214**(2): 199-210.

Xia, L., L. Tian-You, et al. (2009). "Arecoline and oral keratinocytes may affect the collagen metabolism of fibroblasts." J Oral Pathol Med **38**(5): 422-426.

Xie, Y., K. Gao, et al. (2009). "Mice lacking beta6 integrin in skin show accelerated wound repair in dexamethasone impaired wound healing model." Wound Repair Regen **17**(3): 326-339.

Xu, M. Y., J. Porte, et al. (2009). "Lysophosphatidic acid induces alphavbeta6 integrin-mediated TGF-beta activation via the LPA2 receptor and the small G protein G alpha(q)." Am J Pathol **174**(4): 1264-1279.

Xu, X. F., C. Y. Guo, et al. (2009). "Gli1 maintains cell survival by up-regulating IGFBP6 and Bcl-2 through promoter regions in parallel manner in pancreatic cancer cells." J Carcinogen **8**: 13.

Xue, H., A. Atakilit, et al. (2001). "Role of the alpha(v)beta6 integrin in human oral squamous cell carcinoma growth in vivo and in vitro." Biochem Biophys Res Commun **288**(3): 610-618.

Yamazaki, D., S. Kurisu, et al. (2005). "Regulation of cancer cell motility through actin reorganization." Cancer Sci **96**(7): 379-386.

Yang, G. Y., K. S. Xu, et al. (2008). "Integrin alpha v beta 6 mediates the potential for colon cancer cells to colonize in and metastasize to the liver." Cancer Sci **99**(5): 879-887.

Yang, Z., Z. Mu, et al. (2007). "Absence of integrin-mediated TGFbeta1 activation in vivo recapitulates the phenotype of TGFbeta1-null mice." J Cell Biol **176**(6): 787-793.

Yokosaki, Y., H. Monis, et al. (1996). "Differential effects of the integrins alpha9beta1, alphavbeta3, and alphavbeta6 on cell proliferative responses to tenascin. Roles of the beta subunit extracellular and cytoplasmic domains." J Biol Chem **271**(39): 24144-24150.

Yoon, J. W., Y. Kita, et al. (2002). "Gene expression profiling leads to identification of GLI1-binding elements in target genes and a role for multiple downstream pathways in GLI1-induced cell transformation." J Biol Chem **277**(7): 5548-5555.

Yu, H. and R. Jove (2004). "The STATs of cancer--new molecular targets come of age." Nat Rev Cancer **4**(2): 97-105.

Yurchenco, P. D. and W. G. Wadsworth (2004). "Assembly and tissue functions of early embryonic laminins and netrins." Curr Opinion Cell Biol **16**(5): 572-579.

Zambruno, G., P. C. Marchisio, et al. (1995). "Transforming growth factor-beta 1 modulates beta 1 and beta 5 integrin receptors and induces the de novo expression of the alpha v beta 6 heterodimer in normal human keratinocytes: implications for wound healing." J Cell Biol **129**(3): 853-865.

Zbinden, M., A. Duquet, et al. (2010). "NANOG regulates glioma stem cells and is essential in vivo acting in a cross-functional network with GLI1 and p53." EMBO J **29**(15): 2659-2674.

Zeisberg, M., C. Bottiglio, et al. (2003). "Bone morphogenic protein-7 inhibits progression of chronic renal fibrosis associated with two genetic mouse models." Am J Physiol **285**(6): F1060-1067.

Zhang, L., Z. J. Sun, et al. (2010). "Immunohistochemical expression of SHH, PTC, SMO and GLI1 in glandular odontogenic cysts and dentigerous cysts." Oral Dis **16**(8): 818-822.

Zhang, S., J. Han, et al. (1995). "Rho family GTPases regulate p38 mitogen-activated protein kinase through the downstream mediator Pak1." J Biol Chem **270**(41): 23934-23936.

Zhang, Z. Y., K. S. Xu, et al. (2008). "Integrin alphanvbeta6 acts as a prognostic indicator in gastric carcinoma." Clin Oncol **20**(1): 61-66.

Zhao, R., X. Q. Liu, et al. (2010). "Vascular endothelial growth factor (VEGF) enhances gastric carcinoma invasiveness via integrin alpha(v)beta6." Cancer Lett **287**(2): 150-156.

Zhao-Yang, Z., X. Ke-Sen, et al. (2008). "Signaling and regulatory mechanisms of integrin alphavbeta6 on the apoptosis of colon cancer cells." Cancer Lett **266**(2): 209-215.

Zhou, H. and R. H. Kramer (2005). "Integrin engagement differentially modulates epithelial cell motility by RhoA/ROCK and PAK1." J Biol Chem **280**(11): 10624-10635.

9 Appendices

9.1 Media, solutions and buffers

Phosphate buffered saline (PBS), 10x

NaCl	80 g
KCl	2.5 g
Na_2HPO_4	2.5 g
KH_2PO_4	2.5 g

Made up to 1 litre with distilled H_2O, titrated to pH 7.2 and autoclaved.

Tris buffered saline (TBS), 10x

Tris base	24.2 g
NaCl	80g

Made up to 1litre with distilled H_2O, titrated to pH 7.6.

Oral keratinocyte growth medium (o-KGM)

α-MEM (Gibco)

10% heat-irradiated foetal calf serum (BioSera)

1.8x10-4M adenine (Sigma)

0.5 mg/ml hydrocortisone (Sigma)

10 ng/ml epidermal growth factor (Sigma)

2 mM L-glutamine (PAA)

Epidermal keratinocyte growth medium (e-KGM)

DMEM : Hams F12 (1:1) (PAA)

10% heat-irradiated foetal calf serum (BioSera)

0.5 mg/ml hydrocortisone (Sigma)

2 mM L-glutamine (PAA)

Fibroblast growth medium (for HFFF2 cells)

DMEM (PAA)

10% heat-irradiated foetal calf serum (BioSera)

2 mM L-glutamine (PAA)

Primary fibroblast growth medium

DMEM (PAA)

10% heat-irradiated foetal calf serum (BioSera)

2 mM L-glutamine (PAA)

100 IU/l penicillin / 100 mg/l streptomycin (PAA)

2.5 mg/l amphotericin B (Gibco)

Recipe for SDS-polyacrylamide gels

Resolving gels (15 ml)

	8%	**10%**	**12%**
Distilled H_2O	6.9 ml	5.9	4.9
30% acrylamide mix	4 ml	5	6
1.5 M Tris (pH 8.8)	3.8 ml	3.8	3.8
10% SDS	150 µl	150	150
10% ammonium persulphate (APS)	150 µl	150	150
TEMED	9 µl	6	6

Stacking gel (4 ml)

Distilled H_2O	2.7 ml
30% acrylamide mix	670 µl
1M Tris (pH 6.8)	500 µl
10% SDS	40 µl
10% APS	40 µl
TEMED	4 µl

Running buffer (10x) (1L)

Tris base	29 g
Glycine	144 g
SDS	10 g
Distilled H_2O to 1 litre	

Lysis buffer (10 ml)

1M HEPES (pH 7.8)	200 µl
10% NP40	1 ml
5M NaCl	100 µl
1M $MgCl_2$	30 µl
1M $CaCl_2$	10 µl
1M sucrose	3 ml
Distilled H_2O	5.66 ml

Western blot transfer buffer

Tris base	1.4 g
Glycine	7.2 g
Ethanol	200 ml
Distilled H_2O to 1 litre	

Western blot blocking buffer (100ml)

10% Tween	1 ml
Marvel skimmed milk powder	5 g
PBS to 100 ml	

Western blot blocking buffer for phosphorylated proteins (100ml)

10% Tween	100 µl
Bovine serum albumin (BSA)	5 g
TBS to 100 ml	

Western blot wash buffer (500 ml)

10% Tween	5 ml
PBS or TBS up to 100 ml	

9.2 Antibodies and reagents

Antibodies

Primary antibody	Species	Supplier	IHC/IF dilution	WB/FACS dilution
Hsc-70	Mouse	Santa Cruz	N/A	1:10,000
β-actin	Rabbit	Sigma-Aldrich	N/A	1:5,000
6.2G2 (β6)	Mouse	Biogen Idec	1:1,000	N/A
6.3G9 (β6)	Mouse	Biogen Idec	N/A	1:500
10D5 (β6)	Mouse	Calbiochem	N/A	1:1,000
6.2A1 (β6)	Mouse	Biogen Idec	1:500	N/A
6.20w (β6)	Rat	In-house	N/A	1:500
53a.2 (β6)	Rat	In-house	1:500	N/A
7.2 (α4)	Rat	In-house	N/A	1:500
Smad4	Mouse	Santa Cruz	1:100	N/A
pSmad2 (Ser465/467)	Rabbit	Cell Signaling	1:100	N/A
α-SMA	Mouse	Dako	1:100	1:1,000
Gli-1	Mouse	Cell Signaling	1:100	1:1,000
Gli-1	Rabbit	Santa Cruz	1:50	N/A
pStat3 (Tyr705)	Mouse	Cell Signaling	N/A	1:1,000
pStat3 (Tyr705)	Rabbit	Cell Signaling	1:100	N/A
E-Cadherin	Mouse	Abcam	1:50	1:1,000
E-Cadherin	Mouse	Dako	1:50	N/A
N-Cadherin	Rabbit	Cell Signaling	N/A	1:1,000
Vimentin	Rabbit	Cell Signaling	1:50	1:1,000
Vimentin	Mouse	Dako	1:50	N/A
Snail	Mouse	In-house	N/A	1:1,000
Twist	Mouse	Abcam	N/A	1:1,000
Zeb1	Rabbit	Santa Cruz	N/A	1:1,000
CK5/6	Mouse	Dako	N/A	1:1,000

Reagents and inhibitors

All reagents and inhibitors were maintained at -20° C for long-term storage.

Reagent	Supplier	Diluent	Concentration
Arecoline hydrobromide	Sigma-Aldrich®	dH_2O	5 – 25 μg/ml
ALK5 inhibitor IV (TGF-β RI kinase inhibitor IV)	Calbiochem	DMSO	1 μg/ml
S31-201 (Stat3 inhibitor VI)	Santa Cruz Biotechnology	DMSO	200 μM
Sunitinib malate	Sigma-Aldrich®	DMSO	2.5 – 10 μM
Tropicamide	Sigma-Aldrich®	Ethanol	400 μM

9.3 Primer sequences

RT-PCR primers

Gene ID	Sequence	Product size (bp)
Col1A1	F CCCACCAATCACCTGCGTACAGA R TTCTTGGTCGGTGGGTGACTCTGA	214
TIMP1	F GACGGCCTTCTGCAATTC R GTATAAGGTGTCTGGTTGACTTCTG	78
CHRM1	F AGACGCCAGGCAAAGGGGGTGG R CACGGGGCTTCTGGCCCTTGCC	348
CHRM2	F ACAAGAAGGAGCCTGTTGCCAACC R CAATCTTGCGGGCTACAATATTCTG	438
CHRM3	F GACAGAAAACTTTGTCCACCCCAC R AGAAGTCTTAGCTGTGTCCACGGC	496
CHRM4	F TCCTCAAGAGCCCACTAATGAAGC R TTCTTGCGCACCTGGTTGCGAGC	433
CHRM5	F CTCACCACCTGTAGCAGCTACCC R CTCTCTTTCGTTTGGTCATTTGATG	397
ITGB6	F CTCTTTCCAGTGTGGGGTGT R CTCTCTTTCGTTTGGTCATTTGATG	199
GAPDH	F CTCTTTCCAGTGTGGGGTGT R CTCTCTTTCGTTTGGTCATTTGATG	195

Cloning primers

Cloning oligonucleotides	**Sequence**
-1325/+208	F *GCTC*ACGCGTCGCAAAATTCTTGCCATGTT R*CGTG*CTCGAGCTTGCTGTGCAGACCGATTA
-600/+208	F *GCTC*ACGCGTGGGCACCATCATTTCTGTTT R*CGTG*CTCGAGCTTGCTGTGCAGACCGATTA
-81/+208	F *GCTC*ACGCGTCCCACCTTCTTGGTGATTGT R*GCTC*CTCGAGCTTGCTGTGCAGACCGATTA
Sequencing Primers	Sequencing primers were designed flanking the pGL3-Basic multiple cloning site (MCS), where the *ITGB6* promoter (and various deletion constructs) was inserted between the *Mlu*I and *Xho*I sites.

9.4 Publications

- **KA Moutasim**, V Jenei, K Sapienza, D Marsh, PH Weinreb, SM Violette, MP Lewis, JF Marshall, F Fortune, WM Tilakaratne, IR Hart, GJ Thomas. Betel-derived alkaloid up-regulates keratinocyte alphavbeta6 integrin and promotes oral submucous fibrosis. *J Pathol* (2011); 233(3):366-77.

- D Marsh, K Suchak, **KA Moutasim**, S Vallath, C Hopper, W Jerjes, T Upile, N Kalavrezos, SM Violette, PH Weinreb, KA Chester, JS Chana, JF Marshall, AK Hackshaw, K Piper, GJ Thomas. Stromal features are predictive of disease mortality in oral cancer patients. *J Pathol* (2011); 233(4):470-81.

- **KA Moutasim**, ML Nystrom, GJ Thomas. Cell migration and invasion assays. *Methods Mol Biol* (2011); 731:333-43.

Journal of Pathology
J Pathol 2011; **223:** 366–377
Published online 25 October 2010 in Wiley Online Library (wileyonlinelibrary.com) DOI: 10.1002/path.2786

ORIGINAL PAPER

Betel-derived alkaloid up-regulates keratinocyte alphavbeta6 integrin expression and promotes oral submucous fibrosis

Karwan A Moutasim,[1] Veronika Jenei,[1] Karen Sapienza,[2,3] Daniel Marsh,[2] Paul H Weinreb,[4] Shelia M Violette,[5] Mark P Lewis,[6] John F Marshall,[2] Farida Fortune,[3] Waninayaka M Tilakaratne,[3,7] Ian R Hart[2] and Gareth J Thomas[1]*

[1] *Southampton Cancer Research UK Centre, University of Southampton Faculty of Medicine, Southampton, UK*
[2] *Centre for Tumour Biology, Barts and The London School of Medicine and Dentistry, London, UK*
[3] *Clinical and Diagnostic Oral Sciences, Barts and The London School of Medicine and Dentistry, London, UK*
[4] *Biogen Idec, Cambridge, MA, USA*
[5] *Stromedix, Cambridge, MA, USA*
[6] *Department of Sport and Exercise Sciences, University of Bedfordshire, Luton, UK*
[7] *Faculty of Dental Sciences, University of Peradeniya, Sri Lanka*

**Correspondence to: Gareth J Thomas, Southampton Cancer Research UK Centre, Somers Building, Mail Point 824, Southampton General Hospital, Southampton SO16 6YD, UK e-mail: g.thomas@soton.ac.uk*

Abstract

Oral submucous fibrosis (OSF) is a premalignant, fibrosing disorder of the mouth, pharynx, and oesophagus, with a malignant transformation rate of 7–13%. OSF is strongly associated with areca (betel) nut chewing and worldwide, over 5 million people are affected. As αvβ6 integrin is capable of promoting both tissue fibrosis and carcinoma invasion, we examined its expression in fibroepithelial hyperplasia and OSF. αvβ6 was markedly up-regulated in OSF, with high expression detected in 22 of 41 cases ($p < 0.001$). We investigated the functional role of αvβ6 using oral keratinocyte-derived cells genetically modified to express high αvβ6 (VB6), and also NTERT-immortalized oral keratinocytes, which express low αvβ6 (OKF6/TERT-1). VB6 cells showed significant αvβ6-dependent activation of TGF-β1, which induced transdifferentiation of oral fibroblasts into myofibroblasts and resulted in up-regulation of genes associated with tissue fibrosis. These experimental *in vitro* findings were confirmed using human clinical samples, where we showed that the stroma of OSF contained myofibroblasts and that TGF-β1-dependent Smad signalling was detectable both in keratinocytes and in myofibroblasts. We also found that arecoline, the major alkaloid of areca nuts, up-regulated keratinocyte αvβ6 expression. This was modulated through the M_4 muscarinic acetylcholine receptor and was suppressed by the M_4 antagonist, tropicamide. Arecoline-dependent αvβ6 up-regulation promoted keratinocyte migration and induced invasion, raising the possibility that this mechanism may support malignant transformation. Over 80% of OSF-related oral cancers examined had moderate/high αvβ6 expression. These data suggest that the pathogenesis of OSF may be epithelial-driven and involve arecoline-dependent up-regulation of αvβ6 integrin.

Keywords: arecoline; betel; integrin; myofibroblast; oral submucous fibrosis; TGF-β1

Received 2 August 2010; Revised 7 September 2010; Accepted 15 September 2010

No conflicts of interest were declared.

Introduction

Oral submucous fibrosis (OSF) is a chronic, premalignant disease characterized by progressive submucosal fibrosis of the oral cavity, pharynx, and, occasionally, the upper oesophagus [1,2]. It is especially common in people of South Asian origin, with an estimated 5 million patients affected worldwide [3]. The main aetiological factor associated with the disease is the chewing of areca (betel) nut, practised by approximately 10–20% of the world's population, particularly in the Indian subcontinent and Far East [4], and recent studies have demonstrated a clear dose-dependent relationship between the use of areca nut and the development of OSF [2]. The chemical constituents of areca nut appear to play a major role in the pathogenesis of OSF, particularly the alkaloids arecoline, arecaidine, guvacine, and guvacoline [2]. Approximately 7–13% of OSF cases have been reported to progress to oral squamous cell carcinoma (OSCC) [2], and there is accumulating evidence that implicates areca nut in the development of other gastrointestinal malignancies, including oesophageal and liver carcinoma [5].

The progression of OSF involves fibrosis and hyalinization of the sub-epithelial oral tissues, which accounts for most of the clinical features of the disease (trismus, dysguesia, dysphagia, and dysarthria). The mechanisms initiating OSF development and progression, however,

have yet to be determined. Research has focused primarily on fibroblasts, examining mechanisms regulating ECM synthesis and degradation [2]. It appears that the main pathological change in OSF is increased accumulation of type I collagen within the sub-epithelial tissues. This is thought to result from an imbalance between matrix deposition and degradation, and studies have found increased levels of fibrogenic cytokines such as bFGF (FGF2), PDGF, and TGF-β1 in OSF tissues [6]. Additionally, decreased proteolytic activity has been described, as a result of both down-regulation of matrix metalloproteinases and up-regulation of protease inhibitors such as TIMPs [2].

The multifunctional cytokine TGF-β1 regulates many cell processes and is regarded as having a central role in promoting ECM deposition and tissue fibrosis through inducing the transdifferentiation of fibroblasts, and other cell types, into smooth muscle actin (SMA)-positive myofibroblasts [7,8]. TGF-β1 is secreted as an inactive complex with its latency-associated peptide (LAP) and requires activation before binding to its receptors [9]. Latent TGF-β1 may be activated through cleavage of LAP by plasmin and metalloproteinases [8,10]. Additionally, activation may occur through binding to thrombospondin or the integrins αvβ6 and αvβ8 [11].

The integrin αvβ6 is epithelial-specific and usually not detectable on normal adult epithelia, but is up-regulated during tissue remodelling, including wound healing and carcinogenesis [12,13]. Binding of αvβ6 to the LAP of both TGF-β1 and TGF-β3 results in activation of the cytokines, and several studies have shown that αvβ6-dependent TGF-β1 activation promotes pathogenic organ fibrosis [14–17]. Recently, Horan *et al* showed that antibody blockade of αvβ6 suppressed murine pulmonary fibrosis, thus suggesting that αvβ6 may be an attractive target in the therapy of fibrotic diseases [18].

Building on preliminary results [19], we show here that αvβ6 is markedly up-regulated in OSF *in vivo* and is strongly expressed in around 50% of cases. In order to determine the possible functional role of αvβ6 in OSF, we used a keratinocyte-derived cell line genetically modified to express high levels of αvβ6 (VB6), and also NTERT-immortalized human oral keratinocytes with low αvβ6 expression (OKF6/TERT-1). The VB6 cells showed αvβ6-dependent activation of TGF-β1, which induced transdifferentiation of human fibroblasts into myofibroblasts. Myofibroblasts significantly up-regulated genes associated with tissue fibrosis including collagen 1 and TIMP-1. These experimental *in vitro* findings were confirmed using human clinical samples where we showed that the lamina propria of OSF contained SMA-positive myofibroblasts and that TGF-β1-dependent SMAD signalling could be identified in both keratinocytes and myofibroblasts. We found that arecoline, the major alkaloid of areca nuts, induces αvβ6 expression in oral keratinocytes. This was modulated through the M_4 muscarinic acetylcholine receptor and could be suppressed by the M_4 antagonist tropicamide. Increased αvβ6 expression promoted keratinocyte migration and induced invasion, suggesting that the integrin may play a role in malignant transformation. Indeed, over 80% of OSCCs arising on a background of OSF had moderate/high αvβ6 expression. These data suggest that OSF development may be driven by activation of TGF-β1 by epithelial cells, a process that involves alkaloid-dependent up-regulation of αvβ6 expression on keratinocytes.

Materials and methods

Antibodies and reagents

The monoclonal antibodies (mAbs) used were as follows: 6.2G2 and 6.3G9, anti-human anti-αvβ6 (Stromedix, Cambridge, MA, USA); 620 w and 53a2, rat mAbs against human αvβ6 that were produced in-house; mAbs to smooth muscle actin (SMA; 1A4; Dako, Cambridgeshire, UK), phospho-Smad2 (3101; Cell Signalling), and Smad4 (sc-7966, Santa Cruz Biotechnology, CA, USA) were purchased commercially. Rat-tail type I collagen and Matrigel were from BD Biosciences (Oxford, UK). Arecoline hydrobromide and tropicamide were obtained from Sigma (Dorset, UK).

Immunohistochemistry

The antibodies used were anti-αvβ6 (6.2G2; 0.5 μg/ml), anti-SMA (1A4; 1 : 100), anti-Smad4 (sc-7966; 1 : 100), and anti-phosphoSmad2 (3101; 1 : 50). Antigen retrieval varied according to the primary antibody: Digest-All 3 Pepsin Solution (Zymed Laboratories, CA, USA) for 5 min at 37 °C (6.2G2) or microwave treatment for 25 min in 0.01 mol/l citrate buffer (pH 6; Smad4, pSmad2). No antigen retrieval was required for SMA. Endogenous peroxidase was neutralized with 0.45% hydrogen peroxidase in methanol for 15 min, and primary antibodies were applied in 0.1% BSA in PBS for 1 h at 37 °C (6.2G2, 1A4) or overnight at 4 °C (sc-7966, 3101). Anti-mouse IgG biotinylated secondary antibody (Vectastain Elite ABC Reagent, Vector Laboratories, CA, USA) was applied for 30 min, followed by peroxidase-labelled streptavidin (Vectastain Elite ABC Reagent, Vector Laboratories) for 30 min. Peroxidase was visualized using DAB+ (Dako) for 5 min and counterstained in Mayer's haematoxylin (Sigma).

Forty-one OSF and 14 fibroepithelial hyperplasia cases were selected from archival material and stained for αvβ6, SMA, pSmad2, and Smad4. Staining for αvβ6 was then scored according to the Quickscore method, as previously described [20]. Appropriate ethical approval was obtained.

Cell culture

Using cDNA transfection techniques, we had previously created an oral keratinocyte (OSCC) cell line

expressing high levels of αvβ6 [21]. An αvβ6-negative cell line containing the vector controls was also generated (IC6pr). Immortalized oral keratinocytes with low endogenous levels of αvβ6 (OKF6/TERT-1) [22] were also used (purchased from Harvard Institute of Medicine). Cells were maintained in keratinocyte growth medium [21]. Primary oral fibroblasts (POFs) were isolated from tissue of patients undergoing routine biopsy and cultured as previously described [23]. Ethical approval was obtained (REC No 09/H0501/90). Human fetal foreskin fibroblasts (HFFF2, American Type Culture Collection) were maintained in fibroblast growth medium (DMEM supplemented with 10% FCS) at 37 °C in a humidified atmosphere.

Flow cytometry

Flow cytometry [22] was performed using anti-αvβ6 (620 w) and Alexafluor 488-conjugated secondary antibody (Molecular Probes, Invitrogen, Paisley, UK). Negative controls used secondary antibody only. Labelled cells were scanned on a FACSCalibur cytometer (BD Biosciences) and analysed using CellQuest software, acquiring 1×10^4 events. Results show mean fluorescence (arbitrary units).

TGF-β1 bioassay

Mink lung epithelial reporter cells (MLECs) stably expressing a TGF-β1-responsive luciferase reporter construct [24] were plated overnight in 96-well plates in DMEM, 10% FCS (5×10^4 cells per well). The medium was changed to serum-free α-MEM, and VB6, IC6pr or OKF6/TERT-1 cells (2.5×10^4 cells per well) were added to each well in serum-free α-MEM containing anti-αvβ6 antibody (10 μg/ml, 6.3G9; Stromedix, MA, USA) or control antibody (10 μg/ml, mouse monoclonal anti-α4 integrin, mAb7.2; produced in-house). The cells were co-cultured overnight, washed once in PBS, and lysed in reporter lysis buffer (Promega, Southampton, UK). Luciferase assay substrate (Promega) was added to the supernatant and the luminescence measured using a Wallac plate reader.

Co-culture experiments

Fibroblasts were cultured with keratinocytes, as described previously [20]. The cells were either lysed for analysis by western blotting or fixed and processed for immunofluorescence.

Western blot analysis

Cells were lysed in NP40 buffer (Biosource, Invitrogen, Paisley, UK). Samples containing equal amounts of protein were electrophoresed under reducing conditions in 8–10% SDS-PAGE gels. Protein was electroblotted to PVDF membranes (Amersham Biosciences, Buckinghamshire, UK). Blots were probed with antibodies against αvβ6 (620W) or SMA. Horseradish peroxidase-conjugated anti-rat or anti-mouse (Dako) was used as secondary antibodies. Bound antibodies were detected with the enhanced chemiluminescence western blotting detection kit system (Amersham). Blots were probed for Hsc-70 (Santa Cruz Biotechnology) as a loading control. Exposures of blots in the linear range were quantified by densitometry software (ImageJ).

Confocal microscopy

Cells were grown on 13 mm coverslips, fixed in 4% formaldehyde in cytoskeletal buffer, and permeabilized with 0.2% Triton X-100 [20]. Non-specific staining was blocked by incubation in 5% normal goat serum. Cells were then incubated with anti-SMA (1A4) and anti-αvβ6 (53a2) for 1 h, and binding was detected by incubation with secondary antibodies conjugated with Alexafluor 488 or Alexafluor 546 (Invitrogen) for 45 min. Nuclei were visualized using 4′,6-diamidino-2-phenylindole (Invitrogen, Paisley, UK). Images were recorded and processed with a confocal laser scanning microscope (Zeiss LSM510, Zeiss, Welwyn, Garden City, UK).

RT-PCR

Total RNA was extracted using an RNeasy Mini Kit (Qiagen, West Sussex, UK) according to the manufacturer's recommendations. Template cDNA was obtained by reverse transcription of 1 μg of total RNA using a High Capacity cDNA Reverse Transcription Kit (Applied Biosystems, CA, USA). Semi-quantitative RT-PCR was performed using *GoTaq*® Hot Start Polymerase (Promega) as previously described [25] and the primers shown in the Supporting information, Supplementary methods. TGF-β1 ELISA method is shown in the Supporting Information, Supplementary Methods.

Keratinocyte treatments

To knockdown β6 integrin, pre-designed siRNA oligonucleotides were used as previously described (Dharmacon Products, Thermo Scientific, Northumberland, UK) [25]. Arecoline-treated OKF6/TERT-1 were seeded into six-well plates at a density of 10^4 cells per well, cultured for 16 h, and transfected with β6 or control siRNA (30 nM) using Oligofectamine (Invitrogen). OKF6/TERT-1 cells were plated at a density of 2.5×10^5 in six-well dishes and treated for 48 h with 5–10 μg/ml arecoline with or without 350 μM tropicamide. Control wells were treated with vehicle (PBS and/or ethanol, respectively).

Cell migration assays

OKF6/TERT-1 cells were treated with arecoline (5–10 μg/ml) with or without tropicamide (350 μM) for 48 h prior to the assay. Haptotactic migration assays were carried out using LAP-coated (0.5 μg/ml) polycarbonate filters (8 mm pore size, Transwell, Costar, Scientific Laboratory Supplies, Yorkshire, UK) and were performed as previously described [26]. Cells migrating to the lower chamber were trypsinized and counted on a Casy 1 counter (Shärfe System GmbH,

Reutlingen, Germany). For blocking experiments, anti-αvβ6 antibody (6.3G9, 10 μg/ml) was added to the cells for 30 min before plating and was present throughout the assay.

Collagen gel contraction assays

POFs or HFFF2 cells were co-cultured with VB6 cells ± antibodies (as above) prior to seeding in type I collagen at a final concentration of 1×10^6 cells/ml and 2 mg collagen/ml. The mixture was poured into 24-well tissue culture plates (1 ml per well) and allowed to polymerize at 37 °C for 1 h. 1 ml of 10% DMEM was then added and the gels were manually detached from the wells. Gel contraction was observed at 24 h and gels were weighed.

Organotypic culture

Organotypic cultures with an air–tissue interface were prepared as previously described [27]. Gels comprised a 50:50 mixture of Matrigel and type I collagen containing 5×10^5 per ml of fibroblasts, to which 1×10^6 OKF6/TERT-1 cells were added. The cell suspension was treated with 5 μg/ml or 10 μg/ml arecoline, and this was present for the duration of the experiment. Control cells were treated with PBS. The medium was changed every 2 days. After 7 days, the gels were bisected, fixed in formal saline, and processed to paraffin.

Statistical analysis

Data are expressed as the mean ± SD of a given number of observations. Where appropriate, one-way ANOVA was used to compare multiple groups. Comparisons between groups were made with Student's *t*-test. A p value of less than 0.05 was considered to be significant. Figures show representative examples of independent repeats, with error bars representing SD.

Results

αvβ6 is significantly up-regulated in OSF

Given that αvβ6 is implicated in the pathological fibrosis of several organs, we examined the expression and distribution of the integrin in OSF using immunohistochemistry. The results are summarized in Table 1. Of 41 OSF cases examined, strong expression (+++) of αvβ6 was present in 54% of cases (Figures 1B–1F). In contrast, no strong αvβ6 staining was observed in fibroepithelial hyperplasia (Figure 1A; $p < 0.001$).

αvβ6 expression is significantly higher in VB6 cells than in OKF6/TERT-1 cells

To determine the functional role of αvβ6 in OSF, we first examined the TERT-immortalized oral keratinocyte cell line OKF6/TERT-1 for αvβ6 expression. Although normal oral keratinocytes express αvβ6 *in vitro* [26], OKF6/TERT-1 cells expressed αvβ6 at relatively low levels (Figure 2A). We therefore used the VB6 cell line, which we had previously generated to express high levels of αvβ6 along with IC6pr control cells, which are αvβ6-negative [21]. We confirmed, using flow cytometry, western blotting, and confocal microscopy, that αvβ6 expression was significantly higher in VB6 cells than in OKF6/TERT-1 and IC6pr cells (Figure 2A). Thus, we used VB6 as a model for the high αvβ6-expressing keratinocytes identified in our OSF clinical samples.

αvβ6 modulates TGF-β1 activation and myofibroblast transdifferentiation

The activation of stromal fibroblasts into contractile myofibroblasts is commonly seen in tissue fibrosis [28–30], and TGF-β1 is considered to be a major cytokine in inducing this myofibroblastic phenotype [7,29]. We confirmed that treatment of POFs and HFFF2 with TGF-β1 induced myofibroblastic transdifferentiation, shown by up-regulation of SMA (Figure 2B). Myofibroblastic transdifferentiation was accompanied by up-regulation of genes associated with tissue fibrosis, including collagen I and TIMP-1 (Figure 2B). Primary oesophageal fibroblasts behaved similarly (data not shown). Up-regulation of TIMP-1 was more pronounced in HFFF2 and oesophageal fibroblasts compared with oral fibroblasts.

Several cell functions, including activation of TGF-β1, are modulated by αvβ6. To investigate whether activation of this cytokine by oral keratinocytes is αvβ6-dependent, we carried out a TGF-β1 bioassay as described previously [20]. Consistent with their lower level of αvβ6 expression, TGF-β1 activation was significantly less with OKF6/TERT-1 cells than VB6 cells ($p = 0.0006$) and similar to the αvβ6-negative IC6pr cells (Figure 3A). Inhibition of αvβ6 reduced TGF-β1 activation by VB6 cells (41% reduction, $p =$

Table 1. αvβ6 expression in oral submucous fibrosis

	Cases	Negative	Low	High
Fibroepithelial hyperplasia	14	3	11	0
Oral submucous fibrosis	41	9	10	22 (54%)

Forty-one OSF and 14 fibroepithelial hyperplasia cases were selected from archival material and stained for αvβ6 as previously described [19]. Briefly, the staining intensity of αvβ6 was scored on a scale of 1–3 (1, weak; 2, moderate; and 3, strong), and the proportion of keratinocytes staining positively was scored on a scale of 1–4 (1, focal staining confined to basal layer; 2, diffuse staining confined to basal layer; 3, diffuse staining of basal and suprabasal layers; and 4, diffuse staining of full thickness of epithelium). The score for intensity was added to the score for proportion to give a score in the range of 0–7 and grouped as negative (score = 0), low (score = 1–4), or high (score = 5–7). No strong expression was detected in hyperplastic oral mucosa; however, there was significantly higher expression in OSF, with high expression seen in 22 cases (54%; $p < 0.001$).

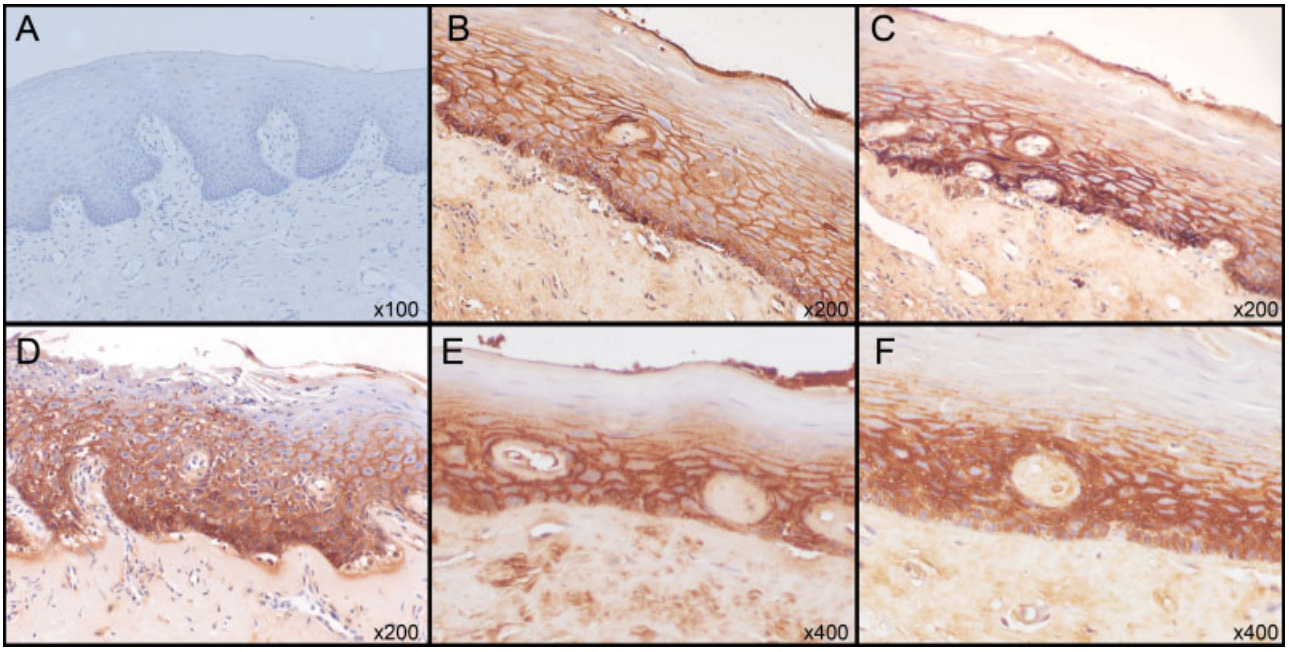

Figure 1. Immunohistochemistry showing representative αvβ6 expression in fibroepithelial hyperplasia (A) and individual cases of OSF (B–F). αvβ6 expression was significantly higher in OSF ($p \leq 0.001$).

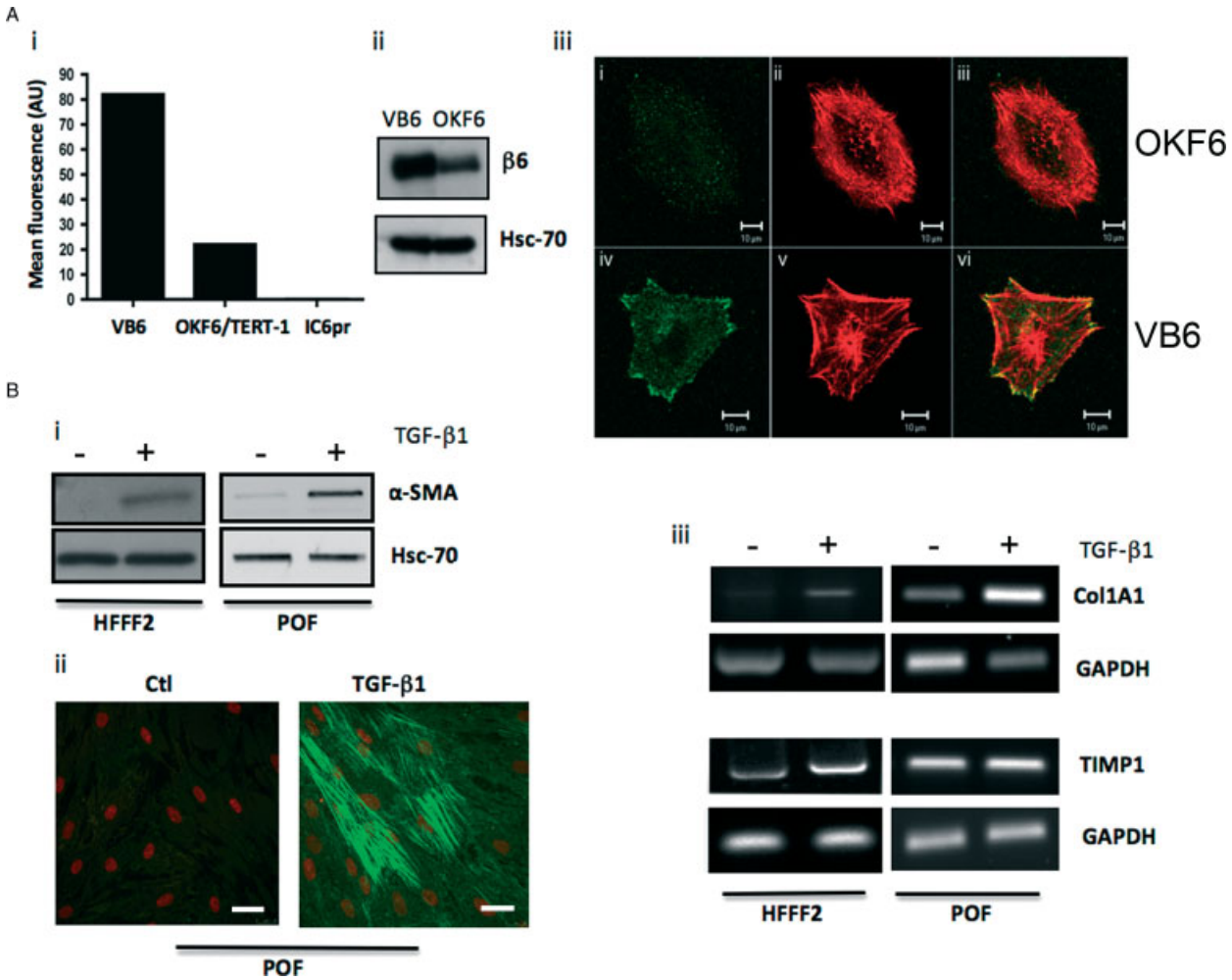

Figure 2. (A) Flow cytometry (i), western blotting (ii), and confocal microscopy (iii) showed that VB6 cells [20] expressed relatively higher levels of αvβ6 compared with OKF6/TERT-1 and IC6pr cells. (B) Western blotting (i) and confocal microscopy (ii) confirmed that treatment of HFFF2 cells and primary oral fibroblasts (POF) with TGF-β1 resulted in myofibroblastic transdifferentiation, shown by up-regulation of SMA. This transdifferentiation was associated with up-regulation of genes associated with tissue fibrosis, including collagen 1 and TIMP1 shown by RT-PCR (iii).

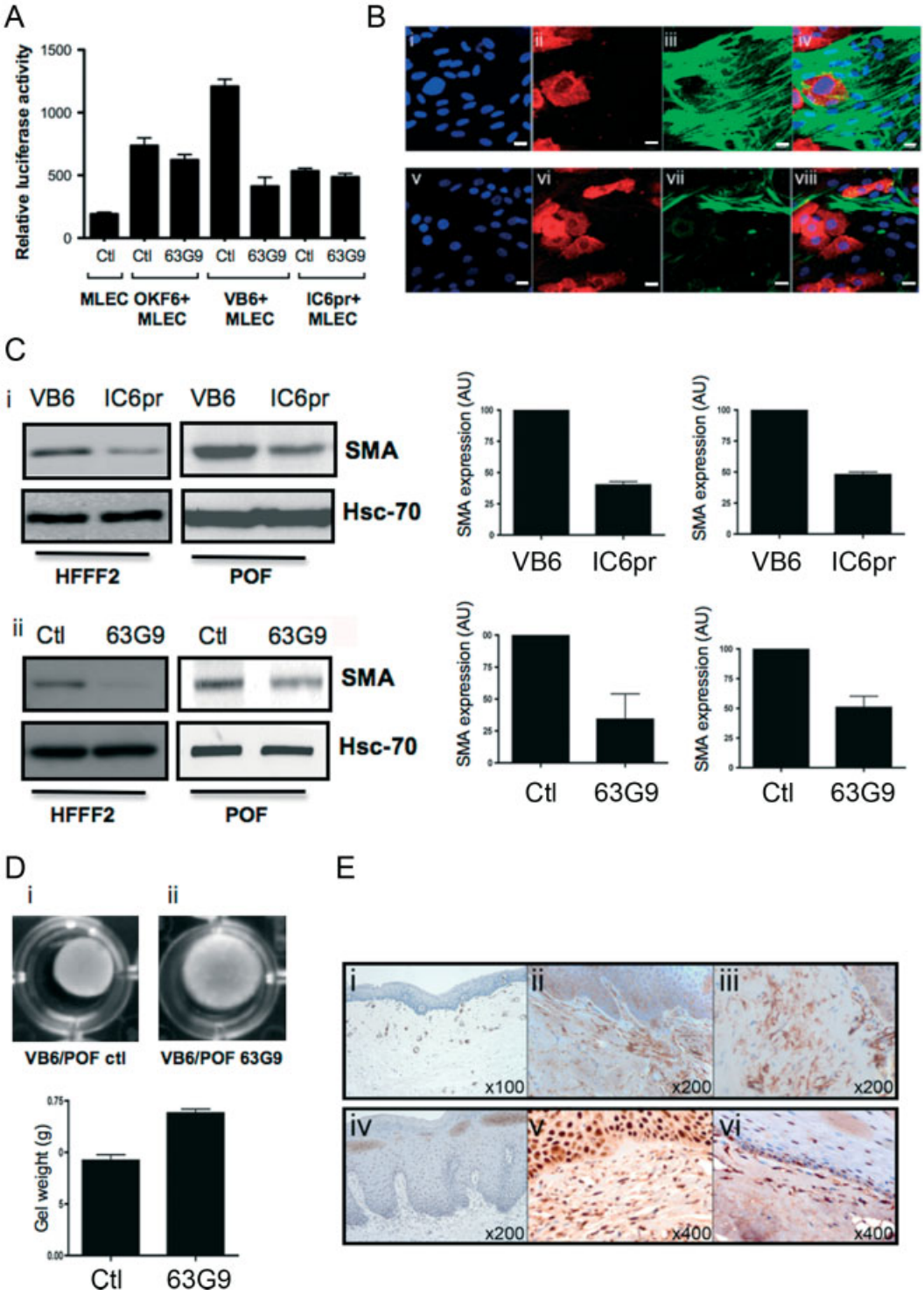

Figure 3. (A) TGF-β1 activation assay. Co-culture of VB6 cells with mink lung epithelial reporter cells (MLEC) promoted TGF-β1 activation, which was suppressed by antibody blockade of αvβ6 integrin (6.3G9). TGF-β1 activation was significantly higher in VB6 cells than in OKF6/TERT-1 and IC6pr cells. (B) HFFF2 cells and VB6 cells were co-cultured on glass coverslips and treated with control (7.2; i–iv) or anti-αvβ6 (6.3G9; v–viii) antibodies. Confocal micrograph shows cell nuclei (blue; i and v), αvβ6-positive VB6 cells (red; ii and vi), SMA-positive myofibroblasts (green; iii and vii), or the combined images (right; iv and viii). When co-cultured with VB6, HFFF2 cells up-regulated SMA indicating myofibroblastic transdifferentiation (i–iv). The transdifferentiation was suppressed by inhibiting αvβ6 (v–viii). Scale bar = 50 μM. (Ci) Western blotting showing that high-αvβ6-expressing VB6 cells induce myofibroblast transdifferentiation more effectively than IC6pr control cells, which are αvβ6-negative. VB6-dependent myofibroblastic transdifferentiation was suppressed by an αvβ6 inhibitory antibody (ii). Histograms represent the combined densitometric analyses from three sets of experiments. (D) Collagen gel contraction assay. Co-culture of VB6 cells and POF promoted myofibroblast-dependent gel contraction (i). This was αvβ6-dependent and suppressed by an αvβ6 inhibitory antibody (ii). Histograms represent the combined gel weights from four independent experiments. (E) SMA and Smad immunohistochemistry. SMA-positive myofibroblasts were not detectable in fibroepithelial hyperplasia (i), but were prominent within the lamina propria of OSF cases (ii, iii). pSmad2- and Smad4-positive nuclei (v and vi, respectively) were prominent in both keratinocytes and myofibroblasts in OSF, compared with fibroepithelial hyperplasia (iv), confirming activated TGF-β1 signalling.

0.0006; Figure 3A), but had little effect on low αvβ6-expressing OKF6/TERT-1 or IC6pr cells.

To determine whether VB6 cells could induce myofibroblast differentiation, we carried out co-culture experiments with POFs and HFFF2 fibroblasts. Co-culture of fibroblasts with VB6 cells induced myofibroblast transdifferentiation, producing a significant increase in SMA expression (Figures 3B and 3C), which was associated with cytoplasmic stress fibres (Figure 2B). Co-cultures of IC6pr and POFs or HFFF2 fibroblasts showed significantly less SMA expression (Figure 3Ci; $p = 0.003$ and $p = 0.002$, respectively). To confirm that myofibroblast generation was αvβ6-dependent, we repeated the assays in the presence of an αvβ6 inhibitory antibody (Figure 3Cii). When the αvβ6 antibody was included, SMA expression was inhibited significantly (Figure 3B). This was confirmed by western blotting ($p = 0.003$ and $p = 0.006$; Figure 3*C*ii).

To address whether αvβ6-dependent myofibroblastic transdifferentiation produced a functional effect, we carried out collagen gel contraction assays using co-cultures of VB6 cells and POFs. Inhibition of keratinocyte αvβ6 significantly inhibited gel contraction, demonstrating that this myofibroblast-dependent process can be promoted by epithelial cells (Figure 3D; $p = 0.02$). Similar results were obtained with HFFF2 cells (data not shown).

SMA-positive myofibroblasts are present in OSF

Our *in vitro* data predicted that the lamina propria of OSF would contain collagen-producing myofibroblasts, which may be responsible for the fibrosis that characterizes the disease. To determine whether the lamina propria contained myofibroblasts, we immunostained OSF samples to detect SMA expression (Figure 3E). SMA-positive myofibroblasts were more pronounced in the superficial lamina propria adjacent to the epithelium (Figure 3Eii), but were also detected in the deeper submucosa (Figure 3Eiii). To further confirm that the TGF-β1 signalling pathway is activated in OSF, we immunostained OSF samples for pSmad2, and found pSmad2- and Smad4-positive nuclei in both myofibroblasts and basal and suprabasal keratinocytes (Figures 3 Ev and 3Evi).

Arecoline up-regulates αvβ6 expression in keratinocytes, modulated through the M_4 muscarinic acetylcholine receptor

The alkaloid arecoline is a potentially carcinogenic constituent of areca nut [2,31] and concentrations as high as 100 μg/ml of the alkaloid have been reported in saliva isolated from OSF patients [32]. To determine whether arecoline had an effect on αvβ6 expression, we treated OKF6/TERT-1 cells, which express low levels of αvβ6, with 5–10 μg/ml arecoline for 48 h and found a significant up-regulation of αvβ6 protein expression at this physiologically relevant concentration ($p = 0.006$; Figure 4A). RT-PCR showed increased levels of *β6* mRNA following arecoline treatment, indicating transcriptional regulation (Figure 4A).

Arecoline is a known agonist of acetylcholine muscarinic receptors [33], and it has been shown previously that overexpression of the M_4 muscarinic receptor is associated with up-regulation of keratinocyte migratory integrins [34]. We confirmed using RT-PCR that OKF6/TERT-1 cells expressed M_4 (Figure 4B), and examined whether arecoline-dependent up-regulation of αvβ6 was modulated through this receptor, using the M_4 antagonist tropicamide [35]. Culture of OKF6/TERT-1 cells with tropicamide suppressed arecoline-induced up-regulation of αvβ6 (Figure 4C; $p = 0.04$). We confirmed this finding by confocal microscopy and flow cytometry (Figure 4C and data not shown, respectively).

Since OKF6/TERT-1 cells express low levels of αvβ6, they spread poorly on the αvβ6 ligand LAP, producing a spindled morphology (Figure 4C ii; top panel). Treatment of cells with arecoline promoted cell spreading and the formation of ruffling membranes, with cells having a more rounded, epithelioid appearance, while tropicamide suppressed this morphological change (Figure 4C ii; middle and bottom panels, respectively).

Arecoline-dependent up-regulation of αvβ6 promotes myofibroblast transdifferentiation, keratinocyte migration, and invasion

We confirmed that arecoline-dependent up-regulation of αvβ6 in OKF6/TERT-1 cells promoted the transdifferentiation of oral fibroblasts into myofibroblasts in co-culture and that this was inhibited by tropicamide (Figure 5A; $p = 0.005$ and $p = 0.027$). In the absence of keratinocytes, arecoline-treated fibroblasts did not up-regulate SMA expression (data not shown), nor did arecoline significantly increase endogenous TGF-β1 secretion by keratinocytes or fibroblasts (Supporting information, Supplementary Figure 1). Around 7–13% of OSF patients develop invasive malignancy, and so we also examined the effect of arecoline on keratinocyte motility. We found that although OKF6/TERT-1 cells migrated poorly towards the αvβ6 substrate LAP, migration was promoted significantly by arecoline. This was αvβ6-dependent and was also suppressed by tropicamide (Figure 5B). To investigate the effect of arecoline on keratinocyte invasion, we used organotypic culture, which we have shown previously to be a physiologically relevant method for studying tumour cell invasion [20,25,26,36]. Using this technique, we found similarly that arecoline promoted αvβ6-dependent OKF6/TERT-1 invasion, and this was suppressed by tropicamide (Figure 5C).

αvβ6 is up-regulated in OSF-associated OSCC

Since up-regulated αvβ6 expression promoted keratinocyte invasion, we examined the expression of the

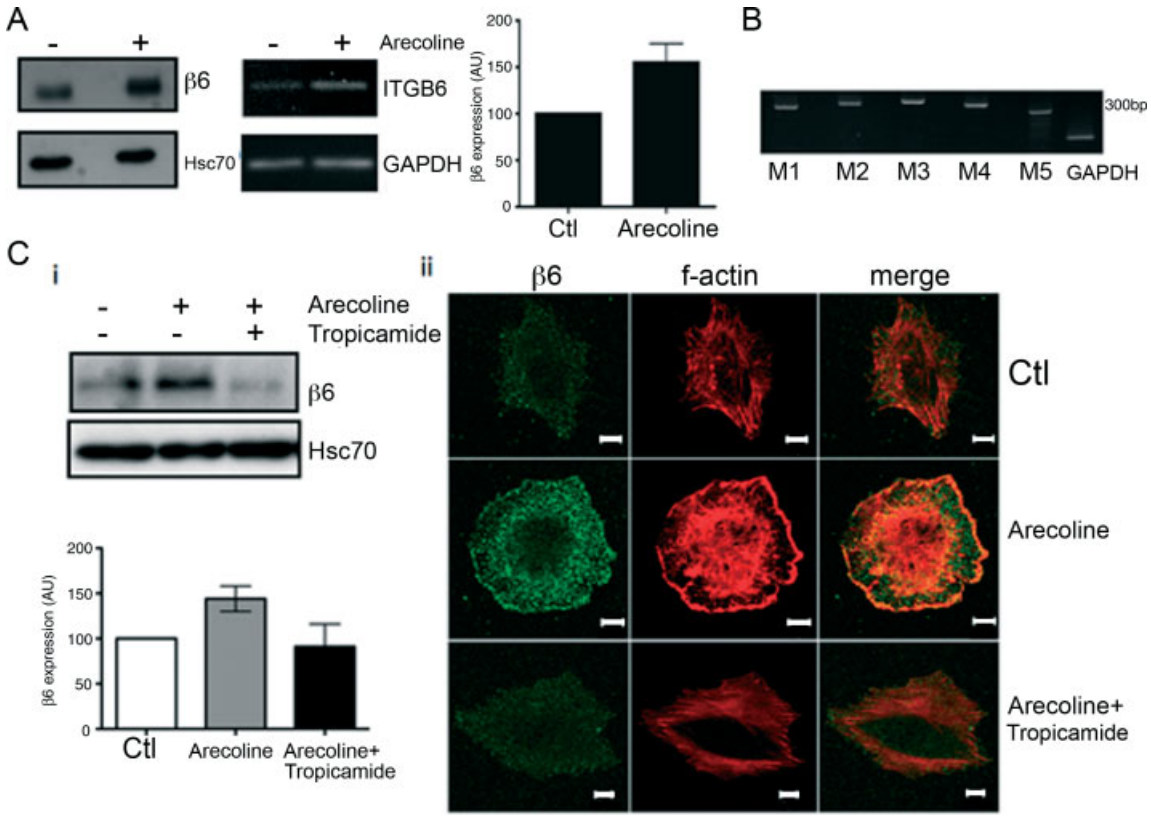

Figure 4. (A) Western blotting and RT-PCR showing up-regulation of αvβ6 expression in OKF6/TERT-1 cells following treatment with 5 μg/ml arecoline for 48 h. Histogram represents the combined results of western blot densitometric analysis from three individual experiments. (B) RT-PCR confirming that OKF6/TERT-1 cells express M_{1-5} receptors. (Ci) Western blotting showing that arecoline-dependent up-regulation of αvβ6 expression in OKF6/TERT-1 cells is suppressed by the selective M_4 receptor antagonist tropicamide. Histogram represents the combined results of western blot densitometric analysis from three individual experiments. (Cii) Confocal microscopy of OKF6/TERT-1 cells plated on the αvβ6 ligand LAP showing αvβ6 expression (green), f-actin (red), and merged images. Up-regulation of αvβ6 expression was seen in arecoline-treated cells (middle panel). This allowed the cells to spread more effectively on LAP, resulting in a rounded, more epithelioid appearance (middle panel). The arecoline-dependent up-regulation of αvβ6 was suppressed by tropicamide, with cell morphology reverting to a more spindled phenotype (lower panel). Scale bar = 10 μM.

integrin in six cases of OSCC arising on a background of OSF. Five of six cases (83%) showed moderate/strong expression of the integrin (Figure 5D). We also immunostained four biopsies from OSF patients that subsequently developed SCC. Three of the four cases of OSF expressed the integrin at moderate/high levels.

Discussion

OSF is a debilitating disease of the oral cavity and oropharynx, with substantial morbidity and a potential for malignant transformation into OSCC [2]. Given its close association with betel quid chewing, the condition is prevalent within the Indian subcontinent and Far East, but it is now also being increasingly seen in the Western world in Asian immigrant communities [37]. Furthermore, the incidence is rising amongst young individuals, which is of particular concern given the chronic course of the disease. The pathogenesis of the disease involves increased accumulation of collagen within the lamina propria of the oral mucosa, eventually leading to scarring of underlying muscle [2,38]. Research has focused primarily on the role of fibroblasts in regulating ECM turnover, examining levels of fibrogenic cytokines, proteases, and protease inhibitors [2]. However, the mechanisms initiating and promoting OSF remain to be elucidated.

The expression of αvβ6 has been increasingly described in numerous carcinoma types, including oral cancer [12,13], and also several fibrotic conditions [14,16,39]. However, the mechanisms regulating its expression are yet to be fully determined. The cytokines tumour necrosis factor-α (TNF-α), TGF-β1 (mediated by the transcription factor Ets-1), and high cell density have previously been reported to up-regulate αvβ6 [40–42]. Here we show that treatment of immortalized normal oral keratinocytes with the areca nut alkaloid arecoline induces up-regulation of the integrin and promotes αvβ6-dependent cell functions, including motility. Keratinocytes express muscarinic acetylcholine receptors M_1–M_5 [43], for which arecoline is an agonist, particularly of the M_4 receptor [33]. Interestingly, Chernyavsky *et al* found that M_4 receptor expression in keratinocytes up-regulated expression of migratory integrins and promoted cell migration [34]. Consistent with these findings, we

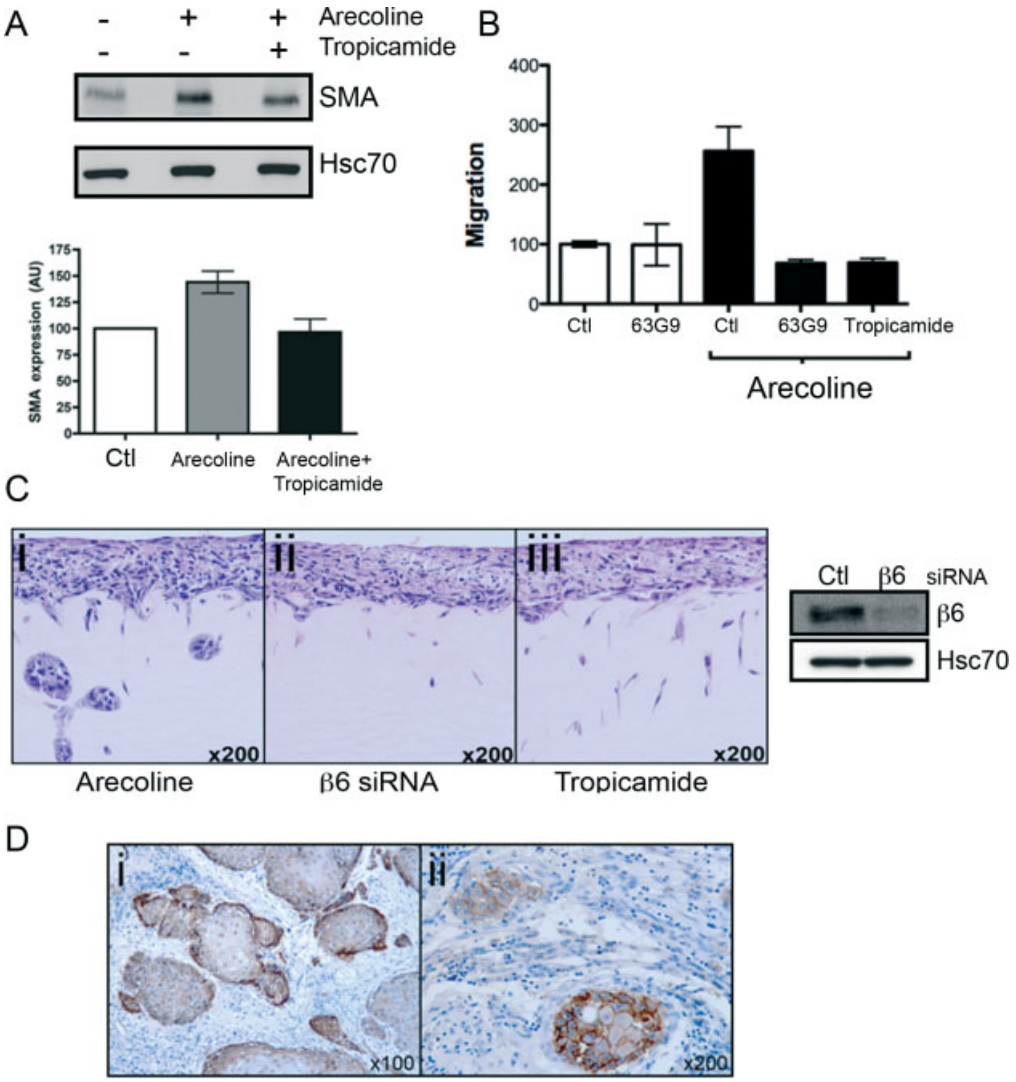

Figure 5. (A) Western blotting showing that tropicamide suppresses POF SMA up-regulation in co-cultures with arecoline-treated OKF6/TERT-1 cells. Histogram represents the combined results of western blot densitometric analysis from three individual experiments. (B) Transwell migration assay showing enhanced migration of OKF6/TERT-1 cells towards the αvβ6 ligand LAP when treated with arecoline. This was inhibited by an αvβ6-blocking antibody and tropicamide. (C) Arecoline-treated OKF6/TERT-1 cells invaded into organotypic cultures (i). Invasion was suppressed by siRNA knockdown of β6 (ii) and tropicamide (iii). (D) Immunohistochemistry showing representative αvβ6 expression in OSCC arising from OSF (i, ii). 83% of cases (five of six) showed moderate/strong αvβ6 expression.

found that treatment of OKF6/TERT-1 keratinocytes with a selective M_4 receptor antagonist prevented arecoline-dependent αvβ6 up-regulation. Arecoline has also been shown to up-regulate *TNF*-α production by keratinocytes; indeed, polymorphisms of the *TNF*-α gene have been reported as a significant risk factor for OSF [44,45]. Since this cytokine has been shown to modulate αvβ6 expression [42], it is possible then that TNF-α may form part of the downstream arecoline/M_4 signalling pathway.

TGF-β1 is regarded as the principal modulator of tissue fibrosis, as it is considered to have a central role in inducing myofibroblast transdifferentiation [7]. Although increased levels of TGF-β1 in OSF have been reported previously, the mechanism by which the latent cytokine is activated has not been investigated [6]. Since latent TGF-β1 is concentrated at high levels within the ECM, activation rather than increased production often regulates this cytokine's function [46,47]. Integrin αvβ6 may activate TGF-β1; indeed, αvβ6-dependent activation of TGF-β1 results in the pathological fibrosis of several epithelial organs. β6-null mice are resistant to pulmonary and renal fibrosis [14,16,20], and inhibition of αvβ6 function retards biliary fibrosis [39]. Interestingly, we also found up-regulation of the integrin in 60% of lichen sclerosus cases (three of five cases; data not shown), raising the possibility that a similar mechanism may modulate mucocutaneous fibrosis. We found, in co-culture assays, that VB6 cells modulated fibroblast-to-myofibroblast transdifferentiation through αvβ6-dependent activation of TGF-β1. Myofibroblasts are the principal modulators of tissue fibrosis, facilitating matrix accumulation both by increasing the deposition and by decreasing the degradation of matrix proteins [7]. We confirmed that

myofibroblasts up-regulated collagen I, the principal matrix protein deposited in OSF, and also the matrix metalloproteinase inhibitor TIMP-1. We also carried out immunochemistry on human OSF samples, demonstrating that the fibrosing lamina propria contained SMA-positive myofibroblasts, which showed nuclear positivity for phosphorylated Smad2 and Smad4, confirming activation of the TGF-β1 signalling pathway. Myofibroblasts were most obvious in the earlier stages of OSF and as the disease progressed, the lamina propria became increasingly acellular. TGF-β1 is also a potent inhibitor of epithelial growth. A characteristic feature of advanced OSF is pronounced epithelial atrophy, and it is possible that this also is mediated through TGF-β1, since pSmad2 nuclear positivity likewise was detected in lesional keratinocytes.

Areca nut is implicated in the development of oesophageal and liver carcinoma, as well as OSCC [5]. We, and others, have shown previously that αvβ6 promotes migration and invasion in several cancers [20,21,36,40]. Consistent with this, we found that arecoline up-regulated αvβ6-dependent keratinocyte migration. Additionally, arecoline-treated OKF6/TERT-1 cells invaded organotypic cultures. Given that 7–13% of OSF patients develop OSCC, it is possible that expression of αvβ6 may contribute, in part, to this malignant transformation. Both OSF and non-OSF OSCCs express αvβ6 at high levels (83% and 85%, respectively [36]), and the integrin is also expressed in premalignant oral epithelial dysplasia [36], supporting a role in OSCC progression. Interestingly, TGF-β1 and *Ras* may modulate epithelial-to-mesenchymal transition (EMT), a process that contributes to tumour cell invasion [48]. In OSCC, *Ras* mutations show great geographical variation, being rare in the Western world, but relatively common in India and South-East Asia, with a similar distribution to areca nut chewing [49]. Indeed, OSCCs in OSF patients have a higher incidence of *Ras* mutations [50,51]. Thus, we will examine whether αvβ6-expressing OSF lesions transform on acquiring mutated *Ras* and then undergo EMT.

In summary, we suggest a possible role for αvβ6 integrin in the pathogenesis of OSF. We found marked up-regulation of αvβ6 in OSF tissue samples and showed that αvβ6-dependent TGF-β1 activation induces myofibroblast transdifferentiation and leads to matrix accumulation. We showed that the areca nut alkaloid arecoline up-regulates αvβ6 expression in oral keratinocytes and that this is modulated through the M_4 muscarinic receptor. We also demonstrated that the lamina propria of OSF contains myofibroblasts and confirmed TGF-β-dependent SMAD signalling. These observations support the suggestion that the paracrine interactions observed *in vitro* between keratinocytes and fibroblasts may also occur *in vivo*. Although previous studies have concentrated on the role of the fibroblasts in the development of OSF, our data suggest that this disease initially is epithelial-driven and also raise the possibility that this mechanism may play a role in the development of OSF-related OSCC.

Acknowledgment

This work was funded by The Health Foundation, Cancer Research UK (CR-UK), the British Association of Oral and Maxillofacial Surgeons (BAOMS), and the British Society for Oral and Maxillofacial Pathology (BSOMP). KAM is a CR-UK Clinical Research Fellow.

Author contribution statement

KAM, VJ, KS, GJT, JFM, MPL, and DM carried out the studies; GJT and WMT assessed the histology; PHW and SMV provided expert guidance and experimental design; IRH, FF, and GJT supported the study through grant funding; GJT project-led the study and wrote the manuscript.

References

1. Pindborg JJ, Sirsat SM. Oral submucous fibrosis. *Oral Surg Oral Med Oral Pathol* 1966; **22**: 764–779.
2. Tilakaratne WM, Klinikiowski MF, Saku T, *et al*. Oral submucous fibrosis: review on aetiology and pathogenesis. *Oral Oncol* 2006; **42**: 561–568.
3. Hazarey VK, Erlewad DM, Mundhe KA, *et al*. Oral submucous fibrosis: study of 1000 cases from central India. *J Oral Pathol Med* 2007; **36**: 12–17.
4. Gupta PC, Warnakulasuriya. Global epidemiology of areca nut usage. *Addict Biol* 2002; **7**: 77–83.
5. Secretan B, Straif K, Baan R, *et al*. A review of human carcinogens—part E: tobacco, areca nut, alcohol, coal smoke, and salted fish. *Lancet Oncol* 2009; **10**: 1033–1034.
6. Haque MF, Harris M, Meghji S, *et al*. Immunolocalization of cytokines and growth factors in oral submucous fibrosis. *Cytokine* 1998; **10**: 713–719.
7. De Wever O, Demetter P, Mareel M, *et al*. Stromal myofibroblasts are drivers of invasive cancer growth. *Int J Cancer* 2008; **123**: 2229–2238.
8. Gordon KJ, Blobe GC. Role of transforming growth factor-β superfamily signalling pathways in human disease. *Biochim Biophys Acta* 2008; **1782**: 197–228.
9. Hyytiäinen M, Penttinen C, Keski-Oja J. Latent TGF-beta binding proteins: extracellular matrix association and roles in TGF-beta activation. *Crit Rev Clin Lab Sci* 2004; **41**: 233–264.
10. Prime SS, Pring M, Savies M, *et al*. TGF-β signal transduction in oro-facial health and non-malignant disease (part I). *Crit Rev Oral Biol Med* 2004; **15**: 324–336.
11. Sheppard D. Integrin-mediated activation of latent transforming growth factor beta. *Cancer Metastasis Rev* 2005; **24**: 395–402.
12. Thomas GJ, Nystrom ML, Marshall JF. αvβ6 integrin in wound healing and cancer of the oral cavity. *J Oral Pathol Med* 2006; **35**: 1–10.
13. Van Aarsen LA, Leone DR, Ho S, *et al*. Antibody-mediated blockade of αvβ6 inhibits tumour progression *in vivo* by a transforming growth factor-β-regulated mechanism. *Cancer Res* 2008; **62**: 561–570.
14. Munger JS, Huang X, Kawakatsu H, *et al*. The integrin αvβ6 binds and activates latent TGF-β1: a mechanism for regulating pulmonary inflammation and fibrosis. *Cell* 1999; **96**: 319–328.

15. Ma LJ, Yang H, Gaspert A, *et al*. Transforming growth factor-β-dependent and -independent pathways of induction of tubulointerstitial fibrosis in β6(−/−) mice. *Am J Pathol* 2003; **163**: 1261–1273.
16. Hahm K, Lukashev ME, Luo Y, *et al*. αvβ6 integrin regulates renal fibrosis and inflammation in Alport mouse. *Am J Pathol* 2007; **170**: 110–125.
17. Wang B, Dolinski BM, Kikuchi N, *et al*. Role of αvβ6 integrin in acute biliary fibrosis. *Hepatology* 2007; **46**: 1404–1412.
18. Horan GS, Wood S, Ona V, *et al*. Partial inhibition of integrin αvβ6 prevents pulmonary fibrosis without exacerbating inflammation. *Am J Respir Crit Care Med* 2008; **177**: 56–65.
19. Moutasim KA, Mirza, D, Marsh D, *et al*. Integrin αvβ6 promotes TGF-β1-dependent myofibroblastic transdifferentiation in oral submucous fibrosis. *Head Neck Oncol* 2009; **I**(Suppl I): P14 (abstract).
20. Marsh D, Dickinson S, Neill GW, *et al*. αvβ6 integrin promotes the invasion of morphoeic basal cell carcinoma through stromal modulation. *Cancer Res* 2008; **68**: 3295–3303.
21. Thomas GJ, Lewis MP, Whawell SA, *et al*. αvβ6 integrin promotes invasion and migration in squamous carcinoma cells. *J Invest Dermatol* 2001; **117**: 67–73.
22. Dickson MA, Hahn WC, Ino Y, *et al*. Human keratinocytes that express hTERT and also bypass a p16INK4a-enforced mechanism that limits life span become immortal yet retain normal growth and differentiation characteristics. *Mol Cell Biol* 2000; **20**: 1436–1447.
23. Saczko J, Dominiak M, Kulbacka J, *et al*. A simple and established method of tissue culture of human gingival fibroblasts for gingival augmentation. *Folia Histochem Cytobiol* 2008; **46**: 117–119.
24. Abe M, Harpel JG, Metz CN, *et al*. An assay for transforming growth factor-β using cells transfected with a plasminogen activator inhibitor-1 promoter-luciferase construct. *Anal Biochem* 1994; **216**: 276–284.
25. Yap LF, Jenei V, Robinson CM, *et al*. Upregulation of Eps8 in oral squamous cell carcinoma promotes cell migration and invasion through integrin-dependent Rac1 activation. *Oncogene* 2009; **28**: 2524–2534.
26. Thomas GJ, Poomsawat S, Lewis MP, *et al*. αvβ6 integrin upregulates matrix metalloproteinase 9 and promotes migration of normal oral keratinocytes. *J Invest Dermatol* 2001; **116**: 898–904.
27. Nystrom ML, Thomas GJ, Stone M, *et al*. Development of a quantitative method to analyse tumour cell invasion in organotypic culture. *J Pathol* 2005; **205**: 468–475.
28. Powell DW, Mifflin RC, Valentich JD, *et al*. Myofibroblasts. I. Paracrine cells important in health and disease. *Am J Physiol* 1999; **277**: C1–C9.
29. Powell DW, Mifflin RC, Valentich JD, *et al*. Myofibroblasts. II. Intestinal subepithelial myofibroblasts. *Am J Physiol* 1999; **277**: C183–C201.
30. Wynn TA. Cellular and molecular mechanisms of fibrosis. *J Pathol* 2008; **214**: 199–210.
31. Lee P, Chang MC, Chang WH, *et al*. Prolonged exposure to arecoline arrested human KB epithelial cell growth: regulatory mechanisms of cell cycle and apoptosis. *Toxicology* 2006; **220**: 81–89.
32. Nair J, Oshima H, Friesen M, *et al*. Tobacco-specific and betel nut-specific N-nitroso compounds: occurrence in saliva and urine of betel quid chewers and formation *in vitro* by nitrosation of betel quid. *Carcinogenesis* 1985; **6**: 295–303.
33. McKinney M, Miller JH, Gibson VA, *et al*. Interactions of agonists with M2 and M4 muscarinic receptor subtypes mediating cyclic AMP inhibition. *Mol Pharmacol* 1991; **40**: 1014–1022.
34. Chernyavsky AI, Arredondo J, Wess J, *et al*. Novel signaling pathways mediating reciprocal control of keratinocyte migration and wound epithelialization through M3 and M4 muscarinic receptors. *J Cell Biol* 2004; **166**: 261–272.
35. Chernyavsky AI, Nguyen VT, Arredondo J, *et al*. The M4 muscarinic receptor-selective effects on keratinocyte crawling locomotion. *Life Sci* 2003; **72**: 2069–2073.
36. Nystrom ML, McCulloch D, Weinreb PH, *et al*. Cyclooxygenase-2 inhibition suppresses αvβ6 integrin-dependent oral squamous carcinoma invasion. *Cancer Res* 2006; **66**: 10833–10842.
37. *IARC Monographs on the Evaluation of Carcinogenic Risks to Humans, Betel-Quid and Areca-Nut Chewing and Some Areca-nut-derived Nitrosamines*, vol 85. *World Health Organisation*, International Agency for Research on Cancer: Lyon, 2004; 39–48.
38. Isaac U, Isaac JS, Khoso NA. Histopathologic features of oral submucous fibrosis: a study of 35 biopsy specimens. *Oral Surg Oral Med Oral Pathol Oral Radiol Endodont* 2008; **106**: 556–560.
39. Patsenker E, Popov Y, Stickel F, *et al*. Inhibition of integrin alphavbeta6 on cholangiocytes blocks transforming growth factor-beta activation and retards biliary fibrosis progression *Gastroenterology* 2008; **135**: 660–670.
40. Bates RC, Bellovin DI, Brown C, *et al*. Transcriptional activation of integrin β6 during the epithelial–mesenchymal transition defines a novel prognostic indicator of aggressive colon carcinoma. *J Clin Invest* 2005; **115**: 339–347.
41. Niu J, Gu X, Ahmed N, *et al*. The alphaVbeta6 integrin regulates its own expression with cell crowding: implications for tumour progression. *Int J Cancer* 2001; **92**: 40–48.
42. Scott KA, Arnott CH, Robinson SC, *et al*. TNF-alpha regulates epithelial expression of MMP-9 and integrin alphavbeta6 during tumour promotion. A role for TNF-alpha in keratinocyte migration. *Oncogene* 2004; **23**: 6954–6966.
43. Ndoye A, Buchli R, Greenberg B, *et al*. Identification and mapping of keratinocyte muscarinic acetylcholine receptor subtypes in human epidermis. *J Invest Dermatol* 1998; **111**: 410–416.
44. Jeng JH, Wang YJ, Chiang BL, *et al*. Roles of keratinocyte inflammation in oral cancer: regulating the prostaglandin E2, interleukin-6 and TNF-alpha production of oral epithelial cells by areca nut extract and arecoline. *Carcinogenesis* 2003; **24**: 1301–1315.
45. Chiu CJ, Chiang CP, Chang ML. Association between genetic polymorphism of tumor necrosis factor alpha and risk of oral submucous fibrosis, a precancerous condition of oral cancer. *J Dent Res* 2001; **80**: 2055–2059.
46. Saharinen J, Hyytiäinen M, Taipale J, *et al*. Latent transforming growth factor-beta binding proteins (LTBPs)—structural extracellular matrix proteins for targeting TGF-beta action. *Cytokine Growth Factor Rev* 1999; **10**: 99–117.
47. Sheppard D. Transforming growth factor beta: a central modulator of pulmonary and airway inflammation and fibrosis. *Proc Am Thorac Soc* 2006; **3**: 413–417.
48. Janda E, Lehmann K, Killisch I, *et al*. *Ras* and TGF-beta cooperatively regulate epithelial cell plasticity and metastasis: dissection of *Ras* signaling pathways. *J Cell Biol* 2002; **156**: 299–313.
49. Paterson IC, Eveson JW, Prime SS. Molecular changes in oral cancer may reflect aetiology and ethnic origin. *Eur J Cancer B Oral Oncol* 1996; **32B**: 150–153.
50. Saranath D, Chang SE, Bhoite LT, *et al*. High frequency mutation in codons 12 and 61 of H-*ras* oncogene in chewing tobacco-related human oral carcinoma in India. *Br J Cancer* 1991; **63**: 573–578.
51. Kuo MY, Jeng JH, Chiang CP, *et al*. Mutations of Ki-*ras* oncogene codon 12 in betel quid chewing-related human oral squamous cell carcinoma in Taiwan. *J Oral Pathol Med* 1994; **23**: 70–74.

SUPPORTING INFORMATION ON THE INTERNET

The following supporting information may be found in the online version of this article.

Supplementary methods. Primer sequences and ELISA method.

Figure S1. TGF-β1 ELISA.

Journal of Pathology
J Pathol 2011; **223:** 470–481
Published online 5 January 2011 in Wiley Online Library
(wileyonlinelibrary.com) DOI: 10.1002/path.2830

ORIGINAL PAPER

Stromal features are predictive of disease mortality in oral cancer patients

Daniel Marsh,[1,2] Krishna Suchak,[3] Karwan A Moutasim,[4] Sabarinath Vallath,[1] Colin Hopper,[5] Waseem Jerjes,[5] Tahwinder Upile,[6] Nicholas Kalavrezos,[5] Shelia M Violette,[7] Paul H Weinreb,[8] Kerry A Chester,[2] Jagdeep S Chana,[9] John F Marshall,[1] Ian R Hart,[1] Allan K Hackshaw,[10] Kim Piper[3] and Gareth J Thomas[4]*

[1] *Centre for Tumour Biology, Bart's and The London School of Medicine and Dentistry, London, UK*
[2] *UCL Cancer Institute, University College London, London, UK*
[3] *Department of Cellular Pathology, Bart's and The London School of Medicine and Dentistry, London, UK*
[4] *Cancer Sciences Division, University of Southampton, Faculty of Medicine, Southampton, UK*
[5] *Oral and Maxillofacial Surgery Unit, University College London, London, UK*
[6] *Department of Surgery, University College London, London, UK*
[7] *Stromedix, Cambridge, MA, USA*
[8] *Biogen Idec, Cambridge, MA, USA*
[9] *Royal Free Hospital, London, UK*
[10] *Cancer Research UK & UCL Cancer Trials Centre, University College London, London, UK*

**Correspondence to: Gareth J Thomas, Cancer Sciences Division, University of Southampton, Faculty of Medicine, Tremona Road, Southampton S016 6YD, UK. e-mail: g.thomas@soton.ac.uk*

Abstract

Worldwide, approximately 405 000 cases of oral cancer (OSCC) are diagnosed each year, with a rising incidence in many countries. Despite advances in surgery and radiotherapy, which remain the standard treatment options, the mortality rate has remained largely unchanged for decades, with a 5-year survival rate of around 50%. OSCC is a heterogeneous disease, staged currently using the TNM classification, supplemented with pathological information from the primary tumour and loco-regional lymph nodes. Although patients with advanced disease show reduced survival, there is no single pathological or molecular feature that identifies aggressive, early-stage tumours. We retrospectively analysed 282 OSCC patients for disease mortality, related to clinical, pathological, and molecular features based on our previous functional studies [EGFR, αvβ6 integrin, smooth muscle actin (SMA), p53, p16, EP4]. We found that the strongest independent risk factor of early OSCC death was a feature of stroma rather than tumour cells. After adjusting for all factors, high stromal SMA expression, indicating myofibroblast transdifferentiation, produced the highest hazard ratio (3.06, 95% CI 1.65–5.66) and likelihood ratio (3.6; detection rate: false positive rate) of any feature examined, and was strongly associated with mortality, regardless of disease stage. Functional assays showed that OSCC cells can modulate myofibroblast transdifferentiation through αvβ6-dependent TGF-β1 activation and that myofibroblasts promote OSCC invasion. Finally, we developed a prognostic model using Cox regression with backward elimination; only SMA expression, metastasis, cohesion, and age were significant. This model was independently validated on a patient subset (detection rate 70%; false positive rate 20%; ROC analysis 77%, $p < 0.001$). Our study highlights the limited prognostic value of TNM staging and suggests that an SMA-positive, myofibroblastic stroma is the strongest predictor of OSCC mortality. Whether used independently or as part of a prognostic model, SMA identifies a significant group of patients with aggressive tumours, regardless of disease stage.

Keywords: oral cancer; SMA; stroma; myofibroblasts; invasion; survival; prognosis

Received 20 October 2010; Revised 22 November 2010; Accepted 22 November 2010

No conflicts of interest were declared.

Introduction

Oral squamous cell carcinoma (OSCC) is the eleventh most common solid tumour worldwide, representing about 4% of all malignancies [1], with approximately 5500 new cases in the UK annually [1,2]. Rising trends of OSCC in young and middle-aged men, particularly tongue cancer, have been reported in European countries and the USA, and while the rising incidence of oropharyngeal cancer is HPV-related, the cause of the increased OSCC incidence is unclear [1–4]. OSCC incidence is strongly related to social and economic deprivation, with the highest rates occurring in the most disadvantaged sections of society [5], and while the incidence of many cancers is predicted to fall over the next decade, it is estimated that OSCC rates will continue to rise significantly [6,7]. OSCC is often difficult to treat and despite improvements in

surgery and radiotherapy, which remain the standard treatments, the mortality rate has remained largely unchanged for decades, with a 5-year survival rate of around 50% [1,2].

Although various biological and molecular markers have been suggested as having utility for determining treatment and predicting prognosis, post-operative management of the patient is determined primarily through detailed pathological examination of the tumour resection specimen and is based on the tumour, node, and metastasis (TNM) classification, which stages the patient according to the size of the primary tumour and the presence of loco-regional and distant metastases [8]. Additional prognostic histopathological information includes tumour depth, grade, and surgical margin status, as well as cohesiveness (pattern of invasion) and presence of perineural or lymphovascular invasion [8]. There is no clear consensus regarding the relative importance of these features and although attempts have been made to combine various parameters into defined scoring systems, their use has produced unsatisfactory inter-observer agreement [8]. The importance of metastasis to loco-regional lymph nodes is well recognized, with the location, number of nodes involved, and, in particular, the spread beyond the lymph node into the soft tissues of the neck (extranodal spread) all reported to be prognostic [8]. Although patients with advanced disease (large tumours with metastases) show decreased survival, particularly if extranodal spread is present, there is, as yet, no single pathological feature or molecular marker that allows the identification of early-stage aggressive tumours within the heterogeneous OSCC population.

Molecular features thought to influence prognosis usually relate to features of the carcinoma cells. For example, we have shown previously that αvβ6 integrin is expressed at moderate-to-high levels in around 85% of OSCCs and promotes tumour invasion, modulated through PGE_2-dependent activation of the small GTP-ase Rac1 [9]. Additionally, αvβ6 activates TGF-β1; this also may promote invasion directly, by promoting tumour cell epithelial-to-mesenchymal transition (EMT) [10], and indirectly, through modulating myofibroblast transdifferentiation, and producing a pro-invasive tumour stroma [11]. Studies have shown that αvβ6 is prognostic in numerous tumour types, including colorectal, gastric, and lung carcinomas [10–13]. Similarly, up-regulation of the epidermal growth factor receptor (EGFR) is commonly found in tumours, and the use of EGFR-targeted inhibitors has increased considerably in recent years [14]. EGFR is overexpressed in up to 72% of OSCCs, although there are conflicting reports as to its prognostic significance [15]. We have recently observed that EGFR signalling potentiates αvβ6-dependent tumour cell function (unpublished data).

It has become increasingly apparent, however, that the 'normal' components of the tumour stroma (including fibroblasts, inflammatory cells, and endothelial cells) play an important role in promoting tumour progression [16,17]. Many types of solid tumour contain smooth muscle actin (SMA)-positive myofibroblasts ('activated' fibroblasts, peritumour fibroblasts, carcinoma-associated fibroblasts) within the stroma [18]. Myofibroblastic transdifferentiation is modulated mainly through TGF-β1 signalling and may be induced in a number of different cell types, including fibroblasts, pericytes, circulating fibrocytes, and mesenchymal stem cells [19]. Additionally, in recent years the concept of EMT has received much attention, with suggestions that apparent stromal cells actually may be derived from epithelial tumour cells [19]. Myofibroblasts have been reported to be associated with poor prognosis in several carcinoma types [20–22]. We have shown previously that myofibroblasts promote the invasion of OSCC cells [23] and that aggressive variants of basal cell carcinoma of the skin contain a prominent, myofibroblastic stroma, which modulates keratinocyte motility through secretion of hepatocyte growth factor (HGF) [11].

Here we show that the strongest independent risk factor of early OSCC death is a feature of the stroma rather than tumour cells. High stromal SMA expression produced the highest hazard ratio and likelihood ratio of any feature examined, and was strongly associated with mortality, regardless of disease stage. Functional assays showed that OSCC cells can promote fibroblast-to-myofibroblast transdifferentiation through αvβ6-dependent activation of TGF-β1 and that myofibroblasts, in turn, promote OSCC invasion. Finally, we developed a prognostic model using Cox regression with backward elimination; only SMA expression, metastasis, cohesion, and age were significant. This model was independently validated on a patient subset. These data suggest that high stromal SMA expression can be used to identify aggressive OSCC, regardless of disease stage, and may be important for the treatment and follow-up of OSCC patients.

Materials and methods

We conducted a retrospective study based on 282 consecutive patients (1992–2005), identified from medical records at two London teaching hospitals. They were included in the study if survival data and archival pathological material were available: 107 from University College Hospital/Eastman Dental Hospital (UCL), and 175 from Barts and the London Hospital (BLT). All patients were treated with primary surgery with or without radiotherapy. Patients did not receive chemotherapy. Ethical approval was obtained (REC reference 07/Q0405/1).

Histology and immunochemistry

Tumour histology was reviewed blindly by pathologists (GJT and KP), according to 1998 UK Royal College of Pathologist Guidelines, and a suitable paraffin block was selected. Data were obtained on age, sex, tumour

stage (I–IV), lymph node (LN) metastasis (yes or no) with or without extranodal spread, grade (well, moderately, poorly differentiated), surgical margins (positive = ≤1 mm, close = >1 to <5 mm, clear = ≥5 mm) [8], tumour depth (in mm), and pattern of invasion (cohesive or discohesive). Tumours were classified as cohesive (Bryne patterns 1 and 2) or discohesive (Bryne patterns 3 and 4) according to their pattern of invasion [24]. The inflammatory infiltrate was scored as high (diffuse), moderate (patchy) or low (weak/absent).

Immunochemistry was performed (αvβ6, EGFR, SMA, p53, p16, EP4) on 4 mm, formalin-fixed, paraffin-embedded serial sections of tumour blocks, according to the manufacturers' or previously published protocols [9,11]. A standard avidin–biotin complex technique was employed, with citrate buffer microwave antigen retrieval (except for αvβ6 [9] and SMA [11]). The antibodies used were EGFR, SMA, p53, p16, (Dako, Ely, UK), EP4 (Cambridge Bioscience, Cambridge, UK), and αvβ6 (Stromedix, Cambridge, USA).

Staining for EGFR, αvβ6, p53, and p16 was evaluated, using a semi-quantitative scoring system described previously, as low, moderate or high [9,11]. EP4 expression was scored as positive or negative. SMA was scored, according to the extent of stromal positivity, as low/negative (<5% stroma positive), moderate (patchy/focal expression, 5–50% stroma positive) or high (diffuse expression throughout tumour, >50% stroma positive). Scoring was carried out by two histopathologists (GJT and KP) independently. Concordance was greater than 95%, confirming the objectivity of the scoring method. Remaining cases were re-analysed and a consensus score was agreed.

Statistical analysis

The primary endpoint was death from OSCC. Survival time was measured from the date of diagnosis until the date of death from OSCC or the date last seen alive. Those who died from causes other than OSCC were censored at the date of death. Cox proportional hazards regression was used to examine the association between the risk of dying from OSCC and each of the factors taken separately and together.

To evaluate the prognostic performance of each factor (ie the 1- and 3-year OSCC death rates), we calculated the detection rate (DR; also known as sensitivity) and false-positive rate (FPR; also known as 1 minus specificity). DR is the proportion of patients who died from OSCC with marker-positive results; FPR is the proportion of patients who did not die from OSCC with marker-positive results. Likelihood ratios (DR/FPR) were obtained, which indicate the strength of a marker (ie maximizing the DR whilst minimizing the FPR) [25].

To examine the factors in combination and allow for associations between them, we developed a prognostic model using Cox regression, in which the dataset of 282 patients was divided into two groups in a 2:1 ratio [26]. Group 1, which was used as the 'training' set to develop the prognostic model, included patients diagnosed up to 9 October 2002 and contained the first two-thirds of OSCC deaths. Group 2 contained patients diagnosed after 9 October 2002, ie the last third of OSCC deaths, and these formed the 'validation' set in which we independently examined the prognostic model. A Cox regression with backward selection and 5% level of statistical significance [26] was applied to group 1, and the parameter estimates were used as scores based on the group of factors that together had the most efficient prognostic ability. These scores were applied to patients in group 2, in which the performance of the model was evaluated by estimating DR and FPR for censored time-to-event data with 3-year mortality as the time point [27,28]. The receiver operating characteristic (ROC) curve analysis also produced an estimate of the area under the curve.

Cell culture

VB6 and CA1 OSCC cells were maintained in keratinocyte growth medium [20]. Primary oral fibroblasts (POFs) were isolated and cultured as described previously [22]. Ethical approval was obtained (REC No 09/H0501/90). POFs were co-cultured with OSCC cells as described previously [11].

TGF-β1 bioassay

OSCC TGF-β1 activation assays were carried out [11] using mink lung epithelial reporter cells (MLECs) with anti-αvβ6 (63G9; Stromedix) or control antibody (anti-α 4 integrin, mAb7.2; produced in-house). Cells were co-cultured overnight and lysed in reporter lysis buffer (Promega, Southampton, UK). Luciferase assay substrate (Promega) was added to the supernatant and luminescence measured using a Wallac plate reader.

Western blot analysis

Samples were electrophoresed in 8–10% SDS-PAGE gels and electroblotted to PVDF membranes (Amersham Biosciences, Little Chalfont, UK). Blots were probed with αvβ6 (62oW; produced in-house) or SMA antibody (Dako), with horseradish peroxidase-conjugated anti-rat or anti-mouse (Dako) as secondary antibodies. Bound antibodies were detected using a chemiluminescence system (Amersham). Blots were probed for Hsc-70 and β-actin (Santa Cruz Biotechnology) as loading controls.

Confocal microscopy

Cells were prepared as described previously [11] and then incubated with anti-SMA (1A4; Dako) and anti-αvβ6 (53a2; produced in-house) antibodies. Secondary antibodies were conjugated with Alexafluor 488 or Alexafluor 546 (Invitrogen). Nuclei were visualized using 4′,6-diamidino-2-phenylindole (Invitrogen).

Images were recorded and processed with a confocal laser scanning microscope (Zeiss LSM510).

Collagen gel contraction assays

POFs were co-cultured with VB6 cells ± antibodies (as above) prior to seeding in type I collagen at a final concentration of 1×10^6 cells/ml and 2 mg collagen/ml. The mixture was poured into 24-well tissue culture plates (1 ml per well) and allowed to polymerize at 37 °C for 1 h. One millilitre of 10% DMEM was then added and the gels were manually detached from the wells. Gel contraction was observed at 24 h.

Transwell invasion assays

Cell invasion assays were performed over 72 h using Matrigel-coated (diluted 1 : 2 in α-MEM) polycarbonate filters (Transwell®, BD Biosciences, Oxford, UK) [11]. Conditioned medium was prepared as described previously [23]. Cells invading the lower chamber were trypsinized and counted on a Casy 1 counter (Sharfe System GmbH, Germany).

Organotypic culture

Organotypic cultures with an air–tissue interface were prepared as described previously [26]. Gels comprised a 50 : 50 mixture of Matrigel and type I collagen with or without 5×10^5 per ml of fibroblasts, to which 5×10^5 OSCC cells were added. The medium was changed every 2 days. After 12 days, the gels were bisected, fixed in formal saline, and processed to paraffin.

Results

Clinical, pathological and immunochemical features at the time of diagnosis are shown in the Supporting information, Supplementary Table 1. Immunochemistry was initially performed on a test set of ~100 cases. p53, p16, and EP4 were not prognostic and were not investigated further (Supporting information, Supplementary Table 2). Immunostaining is shown in Figure 1A and in the Supporting information, Supplementary Figure 1A. The median follow-up was 6.4 years (25th–75th centile 4.4–8.2 years), with a total of 14 714 person-years. The minimum patient follow-up was 3.7 years. Of the 282 patients, 120 were known to have died from OSCC.

Association of risk factors with mortality

Table 1 shows the hazard ratios for OSCC mortality for each factor separately. The death rate was associated with advanced disease stage, close or involved surgical margins, prior radiotherapy, moderately or poorly differentiated tumour grade, metastatic disease, extranodal spread, discohesive pattern of invasion, increasing depth of invasion, low inflammation, and moderate or high SMA expression. There was a suggestion of an effect for age and EGFR. There was insufficient evidence of an association with sex, cancer site, and αvβ6 integrin expression. However, when a multivariate analysis was performed, only surgical margins, metastatic disease, pattern of invasion, and SMA expression remained as statistically significant independent markers of OSCC mortality.

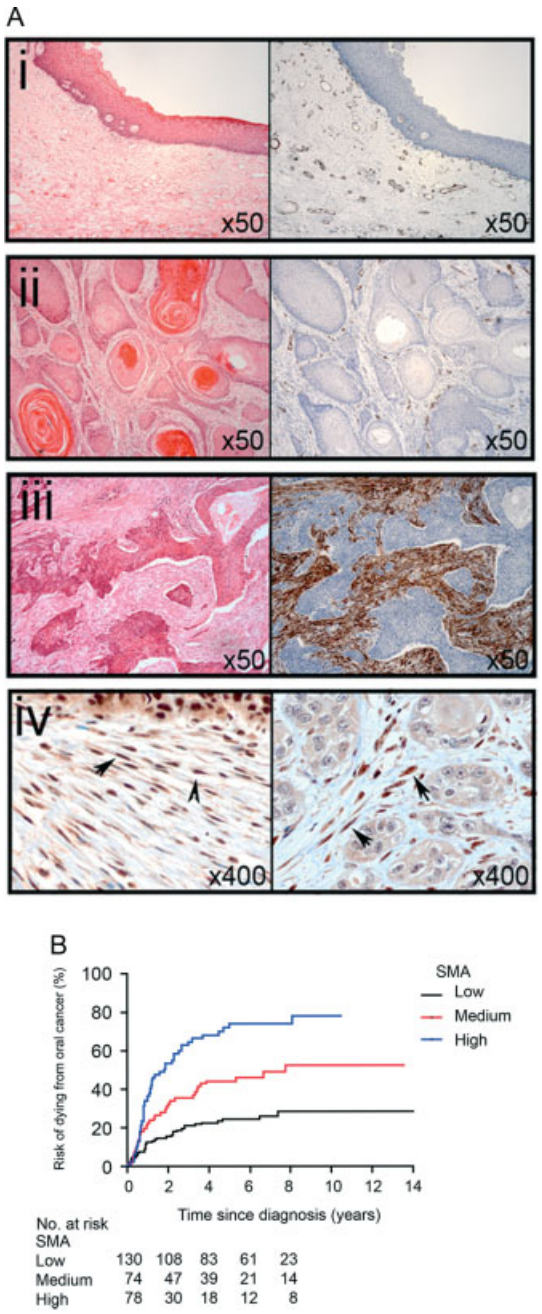

Figure 1. SMA immunochemistry and SMA Kaplan–Meier curves for OSCC mortality.(A) Figure shows paired H+E-stained and SMA-immunostained sections of oral mucosa (i), OSCC with negative/low SMA stroma (ii), and OSCC with strongly positive SMA stroma (iii). Myofibroblast nuclear positivity for phosphorylated Smad2/3 and Smad4, respectively (arrows), is shown in iv, confirming TGF-β-signalling. (B) Kaplan–Meier curves for OSCC mortality according to SMA expression (log-rank test $p < 0.001$).

Table 1. Hazard ratios for each potential prognostic factor in the retrospective cohort (based on 282 patients and 120 deaths from OSCC)

Characteristic	Unadjusted hazard ratio (95% CI)	Adjusted hazard ratio (95% CI)*	*p* value (adjusted model)
Age			
For increase of 5 years	1.04 (0.97–1.11)	1.08 (0.99–1.16)	0.07
Sex			
Male	1.0	1.0	
Female	0.96 (0.66–1.40)	1.43 (0.94–2.18)	0.10
Cancer site			
Buccal	1.0	1.0	0.93
Floor of mouth	0.95 (0.46–1.95)	0.83 (0.38–1.80)	
Tongue	1.01 (0.55–1.88)	0.99 (0.50–1.94)	
Lip	0.48 (0.18–1.26)	0.71 (0.26–1.93)	
Other	1.30 (0.68–2.35)	0.98 (0.50–1.94)	
Disease stage			
I	1.0	1.0	0.20
II	2.61 (1.41–4.82)	1.90 (0.99–3.66)	
III	3.02 (1.34–6.82)	1.62 (0.65–4.03)	
IV	3.64 (2.24–5.94)	1.21 (0.62–2.33)	
Radiotherapy			
No	1.0	1.0	0.41
Yes	1.94 (1.35–2.78)	1.18 (0.80–1.75)	
Grade			
Well differentiated	1.0	1.0	0.94
Moderately differentiated	1.82 (1.03–3.22)	1.07 (0.51–2.21)	
Poorly differentiated	2.96 (1.59–5.52)	1.11 (0.58–2.12)	
Surgical margins			
Clear (>5 mm)	1.0	1.0	0.04
Close (1–5 mm)	1.81 (1.07–3.05)	1.98 (1.16–3.38)	
Involved (<1 mm)	2.58 (1.60–4.17)	1.68 (0.97–2.93)	
Metastases			
No	1.0	1.0	0.05
Yes	2.31 (1.61–3.32)	1.76 (1.00–3.11)	
Extranodal spread			
No	1.0	1.0	0.70
Yes	2.54 (1.63–3.96)	1.12 (0.63–1.98)	
Pattern of invasion			
Cohesive	1.0	1.0	0.001
Discohesive	2.46 (1.71–3.54)	2.07 (1.33–3.24)	
Depth of invasion			
For increase of 5 mm	1.40 (1.23–1.59)	0.96 (0.78–1.19)	0.71
Inflammation			
Low	1.0	1.0	0.55
Medium	0.58 (0.38–0.88)	0.88 (0.55–1.42)	
High	0.32 (0.18–0.57)	0.69 (0.36–1.35)	
SMA			
Low	1.0	1.0	0.002
Medium	2.18 (1.35–3.51)	2.01 (1.14–3.52)	
High	4.26 (2.74–6.61)	3.06 (1.65–5.66)	
αvβ6 integrin			
Low	1.0	1.0	0.074
Medium	0.76 (0.44–1.35)	0.67 (0.37–1.21)	
High	1.51 (0.97–2.35)	1.19 (0.71–1.92)	
EGFR			
Low	1.0	1.0	0.97
Medium	1.29 (0.80–2.07)	1.021 (0.61–1.70)	
High	1.72 (1.11–2.66)	0.96 (0.59–1.57)	

*Adjusted for all the other factors with hazard ratio estimates in this column except for αvβ6 and EGFR.

Table 2. OSCC death rates (95% confidence intervals) according to SMA expression

	SMA expression		
	Low	Medium	High
1 year	12% (7–18)	22% (12–32)	37% (26–48)
2 years	21% (14–28)	36% (25–47)	65% (54–76)
3 years	26% (18–34)	44% (32–56)	74% (63–85)
Median survival (95% CI)	Not reached	93 months (40–not estimable)	22 months (13–22)

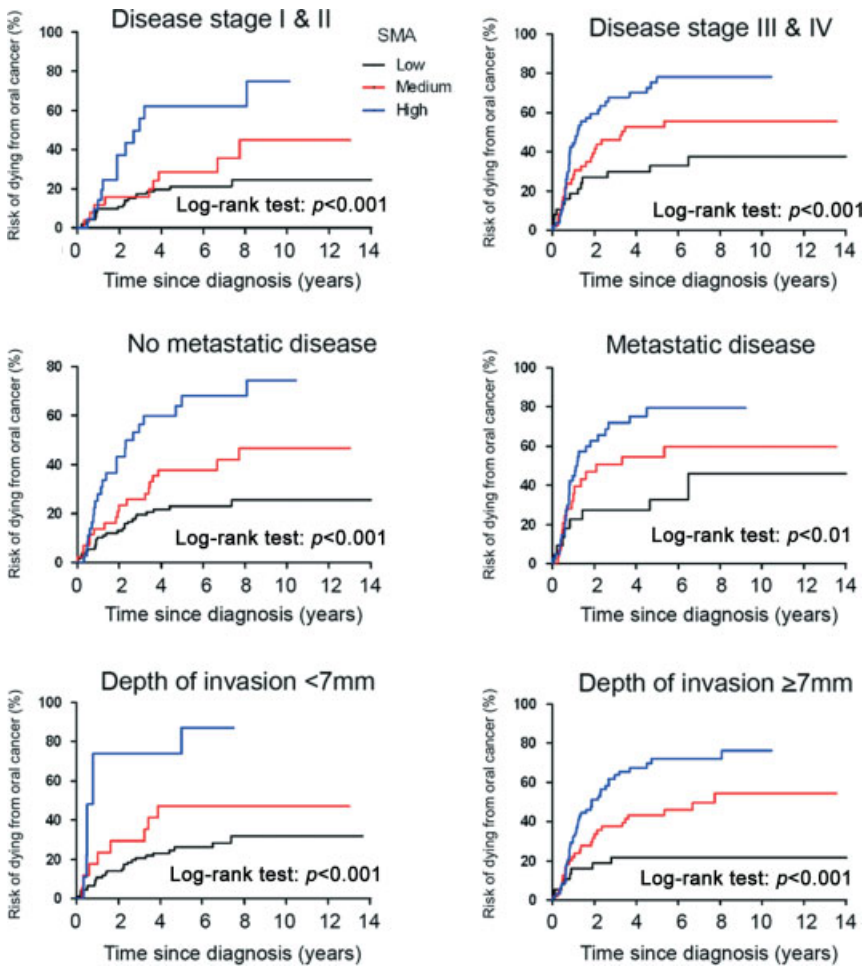

Figure 2. Kaplan–Meier curves for SMA expression for disease stage, metastatic disease, and depth of invasion. SMA was strongly associated with OSCC mortality regardless of whether patients had advanced disease or not.

Figure 1A shows typical examples of tumours with negative/low and high SMA expression. The percentage of patients with low, medium, and high SMA expression was 46%, 26%, and 28%, respectively (Supporting information, Supplementary Table 1). The hazard ratios for medium and high SMA expression indicated a two- and three-fold increase in OSCC mortality compared with low expression (hazard ratios 2.01 and 3.06, respectively; $p = 0.002$). Furthermore, high SMA expression had the highest hazard ratio out of any factor (3.06, 95% CI 1.65–5.66). SMA expression was still statistically significant when multivariate analyses were performed including all other factors (Table 1). SMA expression was also correlated with depth of invasion and extranodal metastatic spread ($p < 0.001$ for each). There was no correlation with patient age or tumour site ($p = 0.29$, $p = 0.12$ respectively).

There was a highly significant difference between the Kaplan–Meier curves for OSCC mortality according to SMA expression ($p < 0.001$; Figure 1B). Table 2 shows the 1-, 3-, and 5-year OSCC death rates. High SMA expression was associated with a poor prognosis, with 74% of patients dying from OSCC by 3 years (95% CI 63–85%). The median survival was not reached in patients with low SMA expression, but it was 93 and 22 months in those with medium and high SMA expression, respectively. Indeed, high SMA expression had the lowest median survival of all the factors except extranodal spread (15 months); the medians for other factors were 25 months (metastatic disease), 26 months (discohesive invasion), 28 months (poorly differentiated grade), 32 months (stage IV), and 43 months (involved margins). Figure 2 shows that SMA was strongly associated with OSCC mortality regardless of whether patients had advanced disease or not.

Prognostic performance of each factor individually

Table 3 shows the prognostic performance of each factor (using DR and FPR). The likelihood ratio for 3-year mortality only exceeds 3 for two factors: extranodal spread (3.4) and high SMA expression (3.6). Although several factors on their own can identify a high proportion of patients who died from OSCC by 3 years (high DR), they also identify too many patients who did not die from OSCC (high FPR). For example, the DR at 3 years for stage IV disease was 62% but the FPR was 34%. However, high SMA expression was seen in almost half (DR = 47%) of patients who died from OSCC by 3 years, but the FPR was only 13%. It

Table 3. Prognostic value of each baseline patient characteristic (for the death rate at 1 and 3 years)

	1-year status			3-year status		
Characteristic and definition of test-positive	DR % (60 deaths)	FPR % (214 alive)	Likelihood ratio	DR % (99 deaths)	FPR % (164 alive)	Likelihood ratio
Age, years						
≥45	95	90	1.05	95	88	1.1
≥50	85	82	1.04	87	79	1.1
≥55	73	69	1.06	74	67	1.1
≥60	57	56	1.02	58	55	1.05
Sex						
Male	68	63	1.1	64	64	1.0
Disease stage						
≥ II, III, IV	93	57	1.6	88	52	1.7
≥ III, IV	75	43	1.7	69	39	1.8
IV	71	37	1.9	62	34	1.8
Radiotherapy						
Yes	50	39	1.3	53	35	1.5
Grade						
Moderate; poor	88	79	1.1	90	76	1.2
Poor	33	17	1.9	31	15	2.1
Surgical margins						
Close; involved	87	66	1.3	83	62	1.3
Involved	62	35	1.8	54	32	1.7
Metastases						
Yes	55	36	1.5	48	23	2.1
Extranodal spread						
Yes	27	10	2.7	24	7	3.4
Pattern of invasion						
Discohesive	72	35	2.1	66	30	2.2
Depth of invasion, mm						
≥4.0	88	75	1.2	89	71	1.2
≥5.0	85	65	1.3	85	60	1.4
≥6.0	73	59	1.2	76	52	1.5
≥10.0	60	30	2.0	59	23	2.6
Inflammation						
Low; medium	92	75	1.2	90	71	1.3
Low	63	43	1.5	65	37	1.8
SMA						
Medium; high	73	47	1.6	73	40	1.8
High	47	22	2.1	47	13	3.6
αvβ6 integrin						
Medium; high	88	51	1.7	93	72	1.3
High	65	46	1.4	71	41	1.7
EGFR						
Medium; high	67	66	1.0	72	42	1.7
High	38	30	1.3	43	21	2.0

DR = detection rate (sensitivity) — the percentage of those who have died with the specified characteristic. FPR = false-positive rate (1 — specificity) — the percentage of those who are still alive with the specified characteristic. Likelihood rate = DR ÷ FPR (the higher the number, the more powerful the marker).

was therefore the best predictor of mortality out of all the factors considered.

Functional role of myofibroblasts *in vitro*

In order to examine the functional role of myofibroblasts *in vitro*, we generated myofibroblasts by treating primary oral fibroblasts (POFs) with TGF-β1, which is considered to be the major cytokine inducing the myofibroblastic phenotype [17]. We confirmed that treatment of POFs with TGF-β1 induced myofibroblastic transdifferentiation, shown by up-regulation of SMA (Figure 3Aii). Co-culture of VB6 and CA1 OSCC cells with POFs also promoted myofibroblastic transdifferentiation (Figure 3Aiii and data not shown, respectively).

TGF-β1 is secreted in latent form and may be activated through several mechanisms; in keratinocytes, we have shown previously that αvβ6 is a major mechanism for activation of the cytokine [11]. VB6 cells express markedly higher levels of αvβ6 than CA1 cells (Figure 3B). Consistent with this, inhibition of αvβ6 significantly suppressed TGF-β1 activation in VB6 cells (Figure 3Ci) but not in CA1 cells (Figure 3Cii; $p = 0.21$).

To determine whether induction of myofibroblast transdifferentiation by VB6 cells was αvβ6-dependent, we performed co-culture assays using POFs. Co-culture of POF with VB6 cells induced myofibroblast transdifferentiation, producing a significant increase in SMA expression, which was suppressed

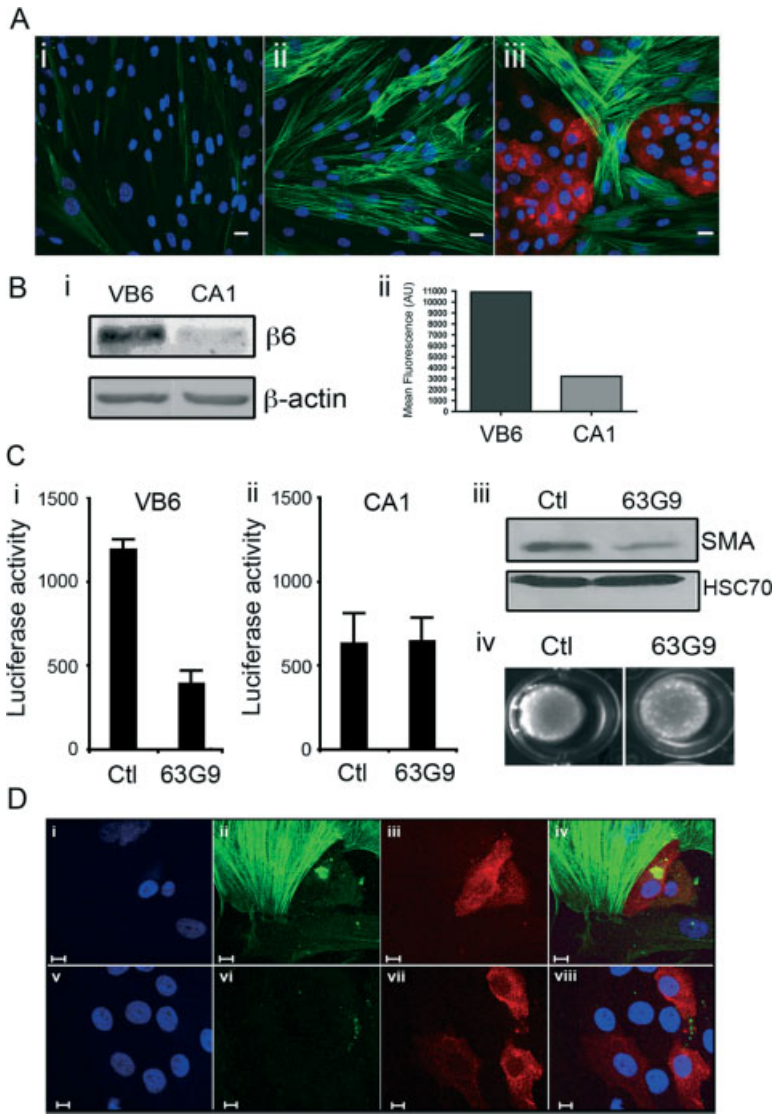

Figure 3. (A) Primary oral fibroblasts (POFs) were grown on glass coverslips and treated with TGF-β1 (ii) or co-cultured with VB6 OSCC cells (iii). Confocal micrograph shows cell nuclei (blue), SMA-positive myofibroblasts (green), and αvβ6-positive VB6 OSCC cells (red). When treated with TGF-β1 (ii) or co-cultured with VB6 (iii), POFs up-regulated SMA, indicating myofibroblastic transdifferentiation. Scale bar = 50 μM. (B) Western blotting (i) and flow cytometry (ii) showed that VB6 cells [9] expressed relatively higher levels of αvβ6 compared with CA1 cells. (C) TGF-β1 activation assay (i and ii). Co-culture of VB6 (i) and CA1 (ii) cells with mink lung epithelial reporter cells (MLECs). VB6 cells activated TGF-β1, which was suppressed by antibody blockade of αvβ6 integrin (6.3G9). CA1 cells did not show αvβ6-dependent activation of TGF-β1. (iii) Western blotting of VB6 and POFs co-cultures showing that myofibroblast transdifferentiation of POFs was suppressed by an αvβ6 inhibitory antibody. (iv) Collagen gel contraction assay. Co-culture of VB6 cells and POFs promoted myofibroblast-dependent gel contraction, which was suppressed by an αvβ6 inhibitory antibody, 63G9. (D) POF and VB6 cells were co-cultured on glass coverslips and treated with control (7.2; i–iv) or anti-αvβ6 (6.3G9; v–viii) antibodies. Confocal micrograph shows cell nuclei (blue; i and v), αvβ6-positive VB6 cells (red; ii and vi), SMA-positive myofibroblasts (green; iii and vii), or the combined images (right; iv and viii). When co-cultured with VB6, POF cells up-regulated SMA, indicating myofibroblastic transdifferentiation (i–iv). The transdifferentiation was suppressed by inhibiting αvβ6 (v–viii). Scale bar = 50 μM.

by αvβ6 inhibition (Figures 3Ciii and 3D). To address whether αvβ6-dependent myofibroblastic transdifferentiation produced a functional effect, we carried out collagen gel contraction assays using co-cultures of VB6 cells and POFs. Inhibition of αvβ6 significantly inhibited gel contraction, demonstrating that this myofibroblast-dependent process can be promoted by epithelial cells (Figure 3Civ).

To determine whether myofibroblasts secrete factors which stimulate the invasion of OSCC cells, we carried out Transwell assays using myofibroblast-conditioned medium (MCM) as a chemoattractant in the lower chamber of the Transwell. Primary fibroblast-conditioned medium (FCM) was used for comparison. We found that MCM significantly promoted the invasion of VB6 and CA1 cells compared with FCM (Figure 4A; $p \leq 0.0001$, $p \leq 0.0001$).

To further investigate the effect of myofibroblasts on OSCC invasion, we used organotypic cultures, which we have shown previously to be a physiologically relevant method for studying tumour cell invasion [9,11]. Using this technique, we found that if fibroblasts were excluded from the gel, no invasion occurred. When POFs were included with OSCC cells in the

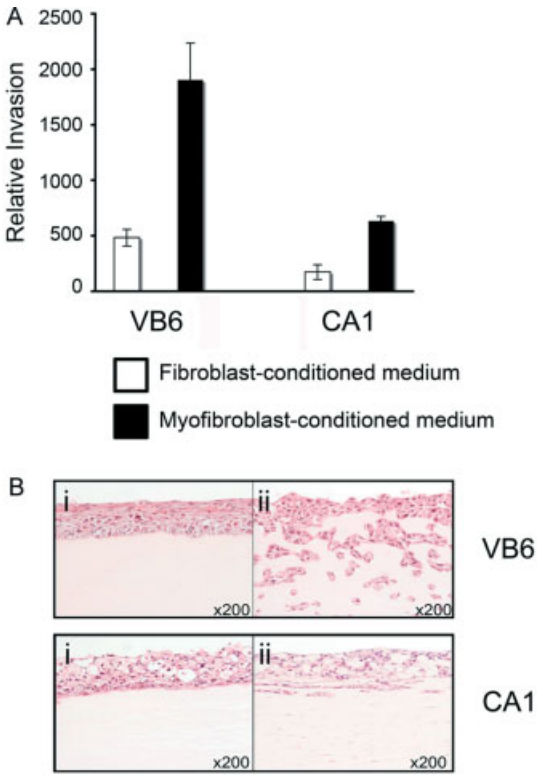

Figure 4. (A) Transwell invasion assay using fibroblast-conditioned (FCM) or myofibroblast-conditioned medium (MCM) as a chemoattractant. Invasion of VB6 and CA1 OSCC cells was promoted significantly by MCM. (B) Organotypic invasion assay using VB6 and CA1 OSCC cells with and without (myo)fibroblasts. Fibroblasts transdifferentiated into myofibroblasts when co-cultured in the assay and promoted invasion (ii). When fibroblasts were omitted from the gel, no invasion occurred (i).

assay, they transdifferentiated into myofibroblasts and promoted tumour invasion (Figure 4B).

Performance of a prognostic model (several factors together)

Finally, we used Cox regression with backward elimination on a training set of patients (group 1; 163 patients and 80 OSCC deaths) to select the most efficient group of OSCC prognostic factors. The final model only contained SMA expression, age, metastatic disease status, and tumour cohesion. The regression parameter estimates were 0.0226 (age), 0.585 (metastatic disease), 0.899 (discohesive pattern of invasion), and 0.731 and 1.186 for medium and high SMA expression, respectively. These parameter estimates were used to derive a score for each patient in the independent validation dataset (group 2; 116 patients and 40 OSCC deaths), and a ROC analysis was performed using time-to-event data with censoring. These four factors were together highly predictive of OSCC mortality at 3 years, with an area under the curve of 77% (Figure 5; $p < 0.001$). Around 70% of patients who died from OSCC by 3 years were classified as test-positive (DR = 70%) based on these factors, but only 20% of those who had not died were classified as test-positive (FPR = 20%; Figure 5).

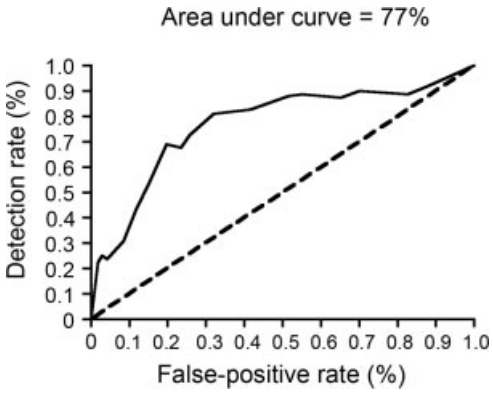

Figure 5. Receiver operating characteristic (ROC) curve for 3-year OSCC mortality. ROC curve for 3-year OSCC mortality derived using a model containing SMA, age, metastatic disease status, and tumour cohesion, and applied to the independent validation dataset. The line of no effect is also shown (dashed; AUC 50%). This prognostic model was highly predictive of OSCC mortality, with an area under the curve of 77% ($p < 0.001$). Around 70% of patients who died from OSCC by 3 years were classified as test-positive (DR = 70%) based on these factors, but only 20% of those who had not died were classified as test-positive (FPR = 20%).

Discussion

Oral cancer is a heterogeneous disease and, at present, classification and prognostic indices are based solely on tumour morphology. Patient management is influenced by the tumour–node–metastasis (TNM) system, supplemented with additional pathological information from the tumour and lymph nodes [8]. Although patients with advanced disease commonly show poor survival, this is not invariably so, and there is no single pathological or molecular feature that identifies aggressive tumours at an early stage.

In our large study, we examined several molecular markers. The pathology features were typical of those generally seen in OSCC patients. Consistent with previous large studies, tumour stage, grade, depth, discohesive pattern of invasion, positive surgical margins, metastatic disease, and extranodal spread were statistically significant risk factors for OSCC mortality [8,29–31]. The failure of the majority of the molecular markers to predict prognosis was unexpected. The selection of the biomarkers was based on those molecules that we had identified in our laboratory-based studies as potentially OSCC-promoting [9,11,23]. However, stromal SMA expression was the most significant independent prognostic marker of all clinical, pathological or molecular features examined and was highly predictive of mortality. The likelihood ratio for 3-year mortality (DR/FPR) exceeded 3 for only two factors: extranodal spread (3.4) and high SMA expression (3.6), confirming that SMA was the best predictor of mortality out of all the factors considered. Extranodal spread is usually a feature of advanced disease, whereas SMA was strongly associated with OSCC mortality regardless of disease stage, i.e. also in small tumours prior to metastasis. Furthermore, high SMA expression was identifiable on initial

diagnostic biopsy, thus identifying aggressive tumours prior to definitive therapy.

A myofibroblastic stroma has been reported to correlate with poor prognosis in several tumour types, including breast, colorectal, and oesophageal carcinoma [20–22,32], and the presence of a myofibroblastic stroma has been reported to be associated with local recurrence and metastasis in tongue carcinomas [21,33]. SMA stromal positivity may possibly serve as a general marker of carcinoma aggressiveness, although it is not yet clear why certain tumours develop this stroma. TGF-β1 is the most potent cytokine driving myofibroblast transdifferentiation [17]. In OSCC, we found that myofibroblasts usually showed nuclear positivity for phosphorylated Smad2 and Smad4 (Figure 1A), confirming activation of the TGF-β1 signalling pathway. It is likely that a supportive SMA-positive stroma is generated because a subset of tumours is particularly effective at activating TGF-β1 (and probably refractory to its growth-suppressive effect). SMA expression correlated significantly with αvβ6 ($p = 0.011$), and we have also shown that OSCC cells may promote myofibroblast transdifferentiation through αvβ6-dependent activation of TGF-β1 *in vitro*. This suggests that αvβ6 may be a major TGF-β1 activation mechanism in OSCC, similar to our previous findings in morphoeic basal cell carcinoma of the skin [11]. Another possibility is that stromal cells from different individuals vary in their ability to transdifferentiate into myofibroblasts.

Further understanding of the biological mechanisms regulating this stromal response may give some indication as to why the tumours behave aggressively and may also allow the development of new therapeutic strategies [34]. Myofibroblasts have been shown to promote cell motility in several tumour types, by up-regulating the secretion of growth factors and matrix proteins, and also by remodelling the extracellular matrix [17]. We have shown that myofibroblasts promote OSCC invasion *in vitro* and have demonstrated previously that this may be modulated through the secretion of HGF, a growth factor that promotes cell scattering and migration [11,23]. Since tumour cell motility is critical for the development and progression of the primary tumour, as well as the metastatic process, similar mechanisms may be disease-promoting *in vivo*, and SMA correlated significantly with tumour depth and extranodal metastatic spread (both $p < 0.001$). Metastatic tumour deposits within lymph nodes, and extranodal spread from lymph nodes into the soft tissues of the neck, were invariably surrounded by a prominent myofibroblastic stroma (Supporting information, Supplementary Figure 1B). Conceivably, SMA-positive cells within lymph nodes may represent tumour cell EMT, which has been shown to promote metastasis in other tumour types [18]. However, from the appearance of the nuclear architecture in SMA-positive myofibroblasts and the lack of stromal p53 staining in p53-positive tumours, there is little reason to suspect that these are carcinoma cells that have undergone EMT. It is more likely that myofibroblasts are generated from local, or circulating, mesenchymal cells and support disease progression by generating a supportive environment conducive to disease dissemination.

Several limitations must be considered in interpreting our findings. Patients lost to follow-up were excluded from the study, as were cases with insufficient archival material for full immunochemical analysis; if these were characteristically different to those who were included, there may have been some bias. Additionally, although the BLT cohort contains a significant number of patients of South-East Asian extraction, both cohorts in this study came from the same city, and these findings may not be generalizable to other settings with different genetic or ethnic influences.

Our study does highlight the limited predictive value of the TNM system, which is used currently to stage OSCC and plan patient therapy. We identified four prognostic factors that together had a good performance in identifying OSCC mortality: SMA expression, metastasis, tumour cohesion, and age. Of these, only metastatic disease is included in the current TNM classification. Prospective analysis of this prognostic model will be informative and allow detailed observation of the natural disease progression in this patient group, perhaps suggesting how treatment may be altered to improve survival. We are currently developing a prospective multicentre study to validate these findings.

In summary, we have shown that high stromal SMA expression is an effective predictor of OSCC patient mortality. Whether used independently or as part of a prognostic model, SMA identifies a significant group of patients with aggressive tumours, regardless of disease stage, and on diagnostic biopsy. These results might be relevant for the clinical evaluation and treatment of OSCC patients.

Acknowledgment

This study was supported by The Health Foundation, Restoration of Appearance Trust (RAFT), Royal College of Surgeons of England, Cancer Research UK, British Association of Head and Neck Oncologists (BAHNO), and British Association of Oral and Maxillofacial Surgeons (BAOMS).

Abbreviations

CI	confidence interval
HR	hazard ratio
OSCC	oral squamous cell carcinoma
SMA	smooth muscle actin

Author contribution statement

DM, KS, KAM, SV, CH, WJ, NK, TU, GJT, and JFM carried out the studies; GJT and KP performed

the pathology; AKH carried out the statistical analysis; PHW and SMV provided expert guidance and experimental design; IRH, KC, JSC, and GJT obtained funding for the study. GJT project-led the study and wrote the manuscript.

References

1. Stewart BW, Kleihues P (eds). *World Cancer Report*. WHO International Agency for Research on Cancer: Lyon, 2003.
2. Office for National Statistics. *Cancer Statistics Registrations: Registrations of Cancer Diagnosed in 2006, England*. Series MB1, No 37, 2009.
3. Macfarlane GJ, Boyle P, Evstifeeva TV, *et al*. Rising trends of oral cancer mortality among males worldwide: the return of an old public health problem. *Cancer Causes Control* 1994; **5**: 259–265.
4. Schantz SP, GP Yu. Head and neck cancer incidence trends in young Americans, 1973–1997, with a special analysis for tongue cancer. *Arch Otolaryngol Head Neck Sur* 2002; **128**: 268–274.
5. Conway D, Petticrew M, Marlborough H, *et al*. Socioeconomic inequalities and oral cancer risk: a systematic review and meta-analysis of case–control studies. *Int J Cancer* 2008; **122**: 2811–2819.
6. Moller H, Fairley L, Coupland V, *et al*. The future burden of cancer in England: incidence and numbers of new patients in 2020. *Br J Cancer* 2007; **96**: 1484–1488.
7. Smith BD, Smith GL, Hurria A, *et al*. Future of cancer incidence in the United States: burdens upon an aging, changing nation. *J Clin Oncol* 2009; **27**: 2758–2765.
8. Woolgar J. Histopathological prognosticators in oral and oropharyngeal squamous cell carcinoma. *Oral Oncol* 2006; **42**: 229–239.
9. Nystrom ML, McCulloch D, Weinreb PH, *et al*. Cyclooxygenase-2 inhibition suppresses alphavbeta6 integrin-dependent oral squamous carcinoma invasion. *Cancer Res* 2006; **66**: 10833–10842.
10. Bates RC, Bellovin DI, Brown C, *et al*. Transcriptional activation of integrin β6 during the epithelial–mesenchymal transition defines a novel prognostic indicator of aggressive colon carcinoma. *J Clin Invest* 2005; **115**: 339–347.
11. Marsh D, Dickinson S, Neill GW, *et al*. Alphavbeta6 integrin promotes invasion of morphoeic basal cell carcinoma through stromal modulation. *Cancer Res* 2008; **68**: 3295–3303.
12. Elayadi AN, Samli KN, Prudkin L, *et al*. A peptide selected by biopanning identifies the integrin αvβ6 as a prognostic biomarker for non-small cell lung cancer. *Cancer Res* 2007; **67**: 5889–5895.
13. Hazelbag S, Kenter GG, Gorter A, *et al*. Overexpression of the αvβ6 integrin in cervical squamous cell carcinoma is a prognostic factor for decreased survival. *J Pathol* 2007; **212**: 316–324.
14. Cardiello F, Tortora G. EGFR antagonists in cancer treatment. *N Engl J Med* 2008; **358**: 1160–1174.
15. Forastiere A. Head and neck cancer: recent advances and new standards of care. *J Clin Oncol* 2006; **24**: 2603–2605.
16. Liotta LA, Kohn EC. The microenvironment of the tumour–host interface. *Nature* 2001; **411**: 375–379.
17. De Wever O, Demetter P, Mareel M, *et al*. Stromal myofibroblasts are drivers of invasive cancer growth. *Int J Cancer* 2008; **123**: 2229–2238.
18. Radisky DC, Kenny PA, Bissell MJ. Fibrosis and cancer: do myofibroblasts come also from epithelial cells via EMT? *J Cell Biochem* 2007; **101**: 830–839.
19. Xu J, Lamouille S, Derynck R. TGF-beta-induced epithelial to mesenchymal transition. *Cell Res* 2009; **19**: 156–172.
20. Tsujino T, Seshimo I, Yamamoto H, *et al*. Stromal myofibroblasts predict disease recurrence for colorectal cancer. *Clin Cancer Res* 2007; **13**: 2082–2090.
21. Kellermann MG, Sobral LM, da Silva SD, *et al*. Myofibroblasts in the stroma of oral squamous cell carcinoma are associated with poor prognosis. *Histopathology* 2007; **51**: 849–853.
22. Surowiak P, Murawa D, Materna V, *et al*. Occurrence of stromal myofibroblasts in the invasive ductal breast cancer tissue is an unfavourable prognostic factor. *AntiCancer Res* 2007; **27**: 2917–2924.
23. Lewis MP, Lygoe K, Nystrom ML, *et al*. SCC-derived TGF-β1 promotes myofibroblast differentiation and modulates scatter factor-dependent tumour invasion. *Br J Cancer* 2004; **90**: 822–832.
24. Bryne M, Koppang HS, Lilleng R, *et al*. Malignancy grading of the deep invasive margins of oral squamous cell carcinomas has high prognostic value. *J Pathol* 1992; **166**: 375–381.
25. Deeks J, Altman D. Diagnostic tests 4: likelihood ratios. *Br Med J* 2004; **329**: 168–169.
26. Royston P, Moons KG, Altman DG, *et al*. Prognosis and prognostic research: developing a prognostic model. *Br Med J* 2009; **338**: 1373–1377.
27. Lu L, Liu C. Using the time dependent ROC curve to build a better survival model in SAS [Internet]. North East SAS Users group (NESUG) 2006; http://www.nesug.org/Proceedings/nesug06/an/da29.pdf.
28. Heagerty PJ, Lumley T, Pepe MS. Time dependent ROC curves for censored survival data and a diagnostic marker. *Biometrics* 2000; **56**: 337–344.
29. Shah JP. Patterns of cervical lymph node metastasis from squamous carcinomas of the upper aerodigestive tract. *Am J Surg* 1990; **160**: 405–409.
30. Chen YK, Huang HC, Lin LM, *et al*. Primary oral squamous cell carcinoma: an analysis of 703 cases in southern Taiwan. *Oral Oncol* 1999; **35**: 173–179.
31. Rogers SN, Brown JS, Woolgar JA, *et al*. Survival following primary surgery for oral cancer. *Oral Oncol* 2009; **45**: 201–211.
32. Saadi A, Shannon NB, Lao-Sirieix P. Stromal genes discriminate preinvasive from invasive disease, predict outcome, and highlight inflammatory pathways in digestive cancers. *Proc Natl Acad Sci U S A* 2010; **107**: 2177–2182.
33. Vered M, Dayan D, Yahalom R, *et al*. Cancer-associated fibroblasts and epithelial–mesenchymal transition in metastatic oral tongue squamous cell carcinoma. *Int J Cancer* 2010; **127**: 1356–1362.
34. Hofmeister V, Schrama D, Becker JC. Anti-cancer therapies targeting the tumour stroma. *Cancer Immunol Immunother* 2008; **57**: 1–17.

SUPPORTING INFORMATION ON THE INTERNET

The following supporting information may be found in the online version of this article.

Table S1. Baseline characteristics of patients in the retrospective cohort (ie at the time of diagnosis).

Table S2. p53, p16, and EP4 analysis.

Figure S1. OSCC immunochemistry.

Chapter 27

Cell Migration and Invasion Assays

Karwan A. Moutasim, Maria L. Nystrom, and Gareth J. Thomas

Abstract

A number of *in vitro* assays have been developed to study tumor cell motility. Historically, assays have been mainly monocellular, where carcinoma cells are studied in isolation. Scratch assays can be used to study the collective and directional movement of populations of cells, whereas two chamber assays lend themselves to the analysis of chemotactic/haptotactic migration and cell invasion. However, an inherent disadvantage of these assays is that they grossly oversimplify the complex process of invasion, lacking the tumor structural architecture and stromal components. Organotypic assays, where tumor cells are grown at an air/liquid interface on gels populated with stromal cells, are a more physiologically relevant method for studying 3-dimensional tumor invasion.

Key words: Invasion, Migration, Scratch assay, Transwell, Matrix, Organotypic culture

1. Introduction

Tumor cell migration and invasion *in vivo* is a complex process, and many *in vitro* assays have been developed in an attempt to recapitulate these processes. Historically, migration/invasion assays have been mainly monocellular, where carcinoma cells have been studied in isolation. Such single cell movement may be mesenchymal or amoeboid, and cells may switch rapidly between the different types of motility. Cells using mesenchymal motility are typically elongated and spindle-shaped, forming actin-rich filopodia or lamellipodia at the leading edge. This process is modulated by Rho GTPases, particularly Rac and cdc42, and involves integrins and proteolytic enzymes such as matrix metalloproteinases. Amoeboid invasion is characterized by cycles of expansion and contraction of the cell body, which allows the cell to squeeze through gaps in the extracellular matrix. Amoeboid invasion is promoted by the Rho/Rock signaling pathway and mediated by

Ian A. Cree (ed.), *Cancer Cell Culture: Methods and Protocols, Second Edition*, Methods in Molecular Biology, vol. 731,
DOI 10.1007/978-1-61779-080-5_27,

cortically located myosin and actin. Additionally, cells may move collectively, sprouting, branching, streaming, or moving as a sheet, and maintaining cell–cell contacts. Collective migration allows coordination of many cells and is a more complex process to study *in vitro*.

It is reported increasingly that tumor stroma has an invasion promoting effect. More physiologically relevant assays should, therefore, incorporate stromal components such as fibroblasts, endothelial cells, macrophages etc. and also reproduce 3-D characteristics of the relevant organ. This chapter aims to cover a range of different techniques that are used to assess tumor cell migration and invasion.

1.1. In Vitro Scratch Assay

This is a simple and inexpensive method to study cell migration *in vitro*. In this assay, a "wound" is created in a cell monolayer and the ability of cells to migrate, and thus, "close" the wound, is assessed by capturing images at different time points (Fig. 1).

The major advantages of this technique are its simplicity and relative low cost and also the ability to visualize cell movement in real time using time-lapse microscopy. Classically, it has been used to study the collective movement of populations of cells, for example, skin wound healing, where to some extent it mimics the migration of keratinocytes as an epithelial sheet. It is useful for studying cell–cell and cell–matrix interactions, and the role of gene overexpression or suppression can be investigated using standard transfection techniques, including microinjection. Analysis of directional migration can be carried out with fluorescently labeled cells using time-lapse microscopy and image analysis software. Cell signaling events can also be investigated by microscopic visualization of specific fluorescently labeled intracellular proteins.

The technique is not suitable for studying chemotaxis, but its relative simplicity and low cost, combined with the lack of need for specialist equipment, still make a popular method for studying cell movement.

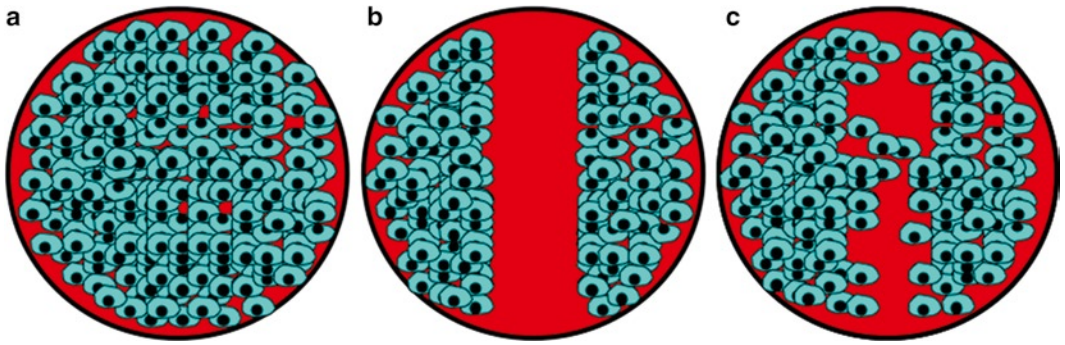

Fig. 1. Scratch assay, in which (**a**) represents a confluent culture, (**b**) the scratch on the surface, and (**c**) the healing scratch.

1.2. Modified Boyden Chamber Assay

In this assay, cells are added to an upper chamber from where they are allowed to invade through a cell permeable membrane toward an attractant placed in the lower chamber (1). Different types of stimuli can be investigated using this system; chemotaxis (movement toward a soluble gradient, e.g., growth factor in the lower chamber), haptotaxis [movement toward a gradient of substratum-bound attractant (e.g., matrix protein coated on the undersurface of the membrane)], or random migration (chemokinesis). After a defined period of time, the cells that have invaded through the membrane into the lower chamber may be counted, making this assay easily quantifiable (2).

Originally designed to study the migration of nonadherent inflammatory cells, the Boyden chamber has been modified in several ways to make it suitable to study invasion of adherent carcinoma cells (1). Firstly, the cell-permeable membrane was coated with a proteinaceous matrix or "basement membrane equivalent" (BME) to replicate the basement membrane through which carcinoma cells must invade *in vivo* (3). Secondly, since invaded carcinoma cells are adherent and remain attached to the undersurface of the cell permeable membrane, invasion cannot be quantified simply by counting the cells in the medium in the lower chamber using a spectrophotometer or a hemocytometer (1, 4). Instead, the cells fixed to the undersurface of the membrane must be either detached from the membrane with trypsin and counted or stained *in situ* in the membrane and counted using a microscope and eyepiece graticule (1, 5). Other methods to quantify this assay include fluorescence, radiolabeling, or colorimetric analysis using various cell dyes or cell viability markers (1, 6, 7). Modified Boyden chambers are commercially available and a widely used example is the Transwell® assay (Fig. 2) (8), which is available with filters of various pore sizes (reflecting the cell type under investigation) and benefits from being highly reproducible (8).

The methods described above examine cell migration. To investigate tumor cell invasion, a physical protein barrier is required. Transwell assays can also be used to study tumor cell invasion, by coating the upper surface of the cell-permeable membrane with an ECM protein gel (Fig. 2b). The protein composition of the gel may vary, but a substrate that has enjoyed widespread use is Matrigel®, isolated from the Englebreth-Holm-Swarm mouse sarcoma, a tumor rich in ECM proteins (9, 10). Matrigel® largely is composed of laminin, Type IV collagen, and heparan sulfate proteoglycans, which are the main constituents of basement membrane, which forms the initial barrier to carcinoma invasion (10). At high concentrations, Matrigel® will polymerise when warmed to 37°C such that it forms a barrier similar in composition to basement membrane. The concentration of Matrigel® should be sufficiently high to provide a physical barrier that will differentiate between invasive and noninvasive cells, but not so

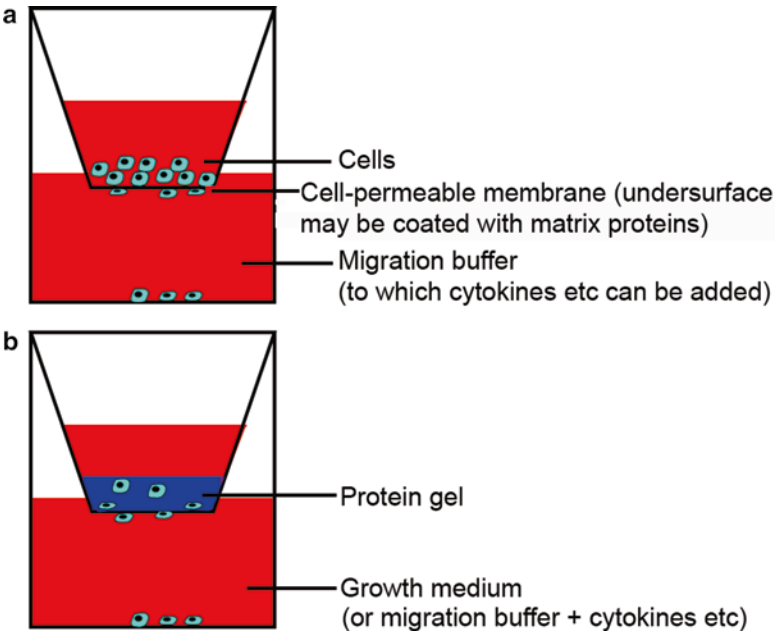

Fig. 2. Transwell migration and invasion assays.

high that it impedes penetration of even the most invasive cells (10). A dilution of 1 part Matrigel:2 parts base medium is usually sufficient (11).

1.3. Three-Dimensional Methods of Studying Invasion

The assays described previously in this chapter have "traded" physiological relevance for ease of repetition and their inherent disadvantage is that they grossly oversimplify the complex process of invasion. Transwell assays lack structural architecture and the cells are added as a single cell suspension. Another inherent disadvantage of these monocellular assays is the absence of stromal cells, which are of fundamental importance in carcinoma invasion. Although stromal paracrine influence can be studied in these simple monocellular assays, for example, by using fibroblast-conditioned medium (12, 13), it is recognized that tumors have a complex architecture with cells of different types in close juxtaposition and this direct physical contact between different cell types may be important. Multicellular invasion assays have been developed which yield information of greater clinical relevance to their monocellular counterparts.

1.4. Organotypic Cultures

Organotypic culture has been especially successful in the field of skin biology (11), but has also been developed to recapitulate other sites such as breast (14), lung (15), oral cavity (16) and pancreas (17). In this assay, epithelial cells are grown at an air/liquid interface on collagen matrices populated with fibroblasts (Fig. 3). Such models have allowed study of cell interactions, whether in the context of normal epithelial growth and differentiation, or between

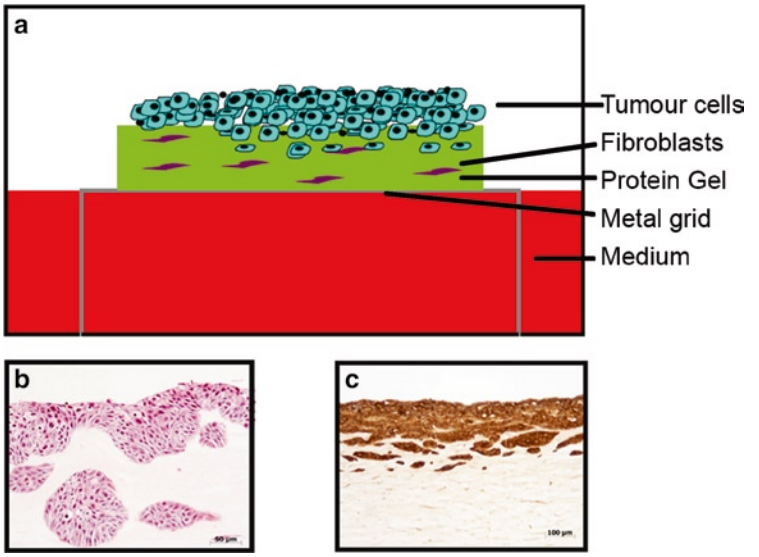

Fig. 3. Organotypic culture. (**a**) Schematic representation of an organotypic culture. (**b**) H+E-stained section of basal cell carcinoma organotypic culture. Note the surface epithelium and the invading islands of tumor. (**c**) A squamous carcinoma organotypic culture immunostained for cytokeratins to highlight the tumor cells.

tumor cells and fibroblasts (16, 18). Additionally, organotypic cultures can be transplanted into immunocompromised mice to study invasion *in vivo* (16).

2. Materials

2.1. In Vitro Scratch Assay

1. Tissue culture medium (e.g., DMEM) with supplements (fetal bovine serum, glutamine, antibiotics).
2. Trypsin/versene (EDTA).
3. Phosphate-buffered saline (PBS).
4. Tissue culture dishes (e.g. 60 mm).
5. Scalpel.
6. p200 pipette tips.
7. Phase-contrast microscope.

Additional materials:

1. Plasmid-encoding GFP or other markers.
2. CO_2-independent medium.
3. Stage incubator.
4. CO_2 supply.
5. Video camera.
6. Image analysis software.

2.2. Transwell® Migration Assay

1. Polycarbonate filters (Transwell®, 8-μm pore size, Becton Dickinson).
2. Attractant of choice [e.g., growth factor (chemotaxis), extracellular matrix protein (haptotaxis)].
3. PBS.
4. Migration buffer (tissue culture medium containing 0.1% BSA, adenine, and glutamine).
5. Tissue culture medium (e.g. DMEM).
6. Trypsin/versene.

2.3. Transwell® Invasion Assays

1. Polycarbonate filters (Transwell®, 8-μm pore size, Becton Dickinson).
2. Matrigel (BD Biosciences).
3. PBS.
4. Tissue culture medium (e.g. DMEM) with and without supplements.
5. Trypsin/versene.

2.4. Three-Dimensional Invasion Assays

1. Collagen type I (rat-tail, BD Biosciences).
2. Matrigel (BD Biosciences).
3. FBS.
4. 10× DMEM.
5. Fibroblast growth medium (e.g., DMEM supplemented with 10% FBS, glutamine with/without Pen/Strep).
6. 25% Glutaraldehyde.
7. Steel grids.
8. Nylon mesh (100-μm pore size).

3. Methods

3.1. In Vitro Scratch Assay

1. An appropriate tissue culture dish (e.g., 60 mm) is coated with the extracellular matrix substrate of choice (e.g. fibronectin), and an appropriate control (e.g., poly-D-lysine) and dishes are incubated for 2 h at 37°C.
2. Unbound is ECM is removed by washing with PBS.
3. Cells that have previously been grown to subconfluency are trypsinized and plated onto dish to create a confluent layer.
4. Plates are incubated for 6 h at 37°C to allow attachment and spreading over the substrate.
5. A "scratch" is created using a p200 pipette tip by scraping the monolayer in a neat, straight line. The plate is washed with

the growth medium to remove the debris, and fresh medium is added.

6. Reference points on the outer surface of the dish are placed using a scalpel, at the approximate areas of the scratch.
7. The dish is placed under a phase-contrast microscope (see Note 1) and the first image is acquired.
8. The dish is returned to the incubator at 37°C for 8–18 h. Examine the dish periodically and capture images at different time points to determine the rate of cell migration. It is critical to match the reference points each time the dish is placed at the microscope.
9. Further analysis and quantification is done using a computer software (e.g., Image Pro-Plus, Media Cybernetics) (19).

3.2. Transwell® Migration Assay (Haptotactic Migration)

1. 200 µL protein solution (e.g., fibronectin 10 µg/mL is added to the lower chamber and incubated for 1 h at 37°C).
2. The protein solution is removed and replaced with 200 µL migration buffer for 30 min at 37°C.
3. Cells are plated in the upper chamber of quadruplicate wells at a density of 5×10^4 in 50 µL of migration buffer for 8–24 h (depending on the cell line).
4. After 8–24 h, the cells in the lower chamber (including those attached to the undersurface of the membrane) are trypsinized (500 µL trypsin/versene is added to the lower well) and counted.

3.3. Transwell® Invasion Assays

1. 70 µL Matrigel (diluted 1:2 in serum-free growth medium) is added to the upper chamber and allowed to gel for 1 h at 37°C.
2. To act as a chemoattractant, 500 µL of complete (serum-containing) tissue culture medium is placed in the lower chamber.
3. Cells are plated in the upper chamber of quadruplicate wells at a density of 5×10^4 in 200 µL of serum-free medium and incubated at 37°C for 72 h.
4. After 72 h, the cells in the lower chamber (including those attached to the undersurface of the membrane) are trypsinized (500 µL trypsin/versene per well) and counted.

3.4. Three-Dimensional Invasion Assays

Day 1 – Gel Preparation

1. A fibroblast cell suspension is prepared at 500,000 cells/gel in FGM.
2. Gels are mixed on ice in the following ratios:

Collagen: matrigel (1:1)	7 volumes (3.5 collagen: 3.5 matrigel)
10× DMEM	1 volume
FBS	1 volume
Fibroblasts	1 volume

3. 1 mL of the above mix is aliquoted into each well of a 24-well plate and incubated at 37°C for 1 h.
4. After gel polymerisation, 1 mL of FGM is added per well and gels are left for 18 h at 37°C to equilibrate.

Day 2 – Plating out cells on top of gels

1. Medium is aspirated from the top of the gels.
2. Keratinocytes are plated out at 500,000 cells per gel in keratinocyte medium supplemented with 10% FCS and glutamine.
3. Gels are incubated overnight at 37°C.

Day 2 – Preparation of nylon sheets

1. Sterile nylon sheets (one sheet per each gel) are placed in a sterile dish.
2. Fibroblast-free gel solution is made in the following ratios:

Collagen	7 volumes
10× DMEM	1 volume
FCS	1 volume
10% DMEM	1 volume

3. The solution is mixed well, and if yellow, is neutralized with sterile NaOH 0.1 M until it turns pink.
4. 250 µL is added to each nylon sheet and incubated at 37°C for 15–30 min.
5. Fix in 10 mL 1% glutaraldehyde (in PBS). Incubate at 4°C for 1 h.
6. Gels are washed three times with PBS, once in FGM and then left in FGM at 4°C overnight.

Day 3 – Raising gels on to grids

1. A steel grid is placed into each well of a 6-well plate and a gel-coated nylon sheet is laid on top of it. Steel grids are made from 2.5 cm^2 of stainless steel mesh with the edges bent down to form 4- to 5-mm high legs.
2. Organotypic gels are removed from the 24-well plate using a sterile spatula and then placed on the collagen-coated nylon sheet that is resting on the steel grid (see Note 2).

3. The well with complete keratinocyte growth medium, such that it reaches the undersurface of the grid, thus allowing the epithelial layer to grow at an air–liquid interface, and incubated at 37°C (see Note 3).
4. Medium is replaced every 2 days.
5. Gels are harvested after 7–14 days of culture.

3.4.1. Processing of Gels

1. The organotypic culture is removed from the well *in toto* and cut in half with a sterile scalpel.
2. Both halves are fixed in a Universal tube containing 10% formol saline for 24 h.
3. Formol saline is replaced with 70% ethanol left overnight.
4. Gels can then be processed to paraffin blocks and sectioned for staining and/or immunochemistry.

3.4.2. Quantifying Invasion from Organotypic Cultures

Although organotypic cultures recapitulate the morphology of SCC *in vivo*, analysis generally has been subjective and restricted to description of the invasive appearance in stained sections. Some authors have attempted to quantify tumor cell invasive activity in three-dimensional assays. For example, confocal microscopy has been used to determine depth of invasion of fluorescently labeled cells into a gel (20). Consecutive images at increasing depths of focus (Z-sectioning) have been used to reconstruct three-dimensional images and the number of cells at each level determined by using computer software to count pixel number per slice.

Others have quantified invasion in three-dimensional cocultures by measuring the infiltration distance, i.e., the maximum distance between the epithelium-tumor frontier and the most distant tumor cells, in serial sections (15). However, this measurement does not take into account the pattern or amount of tumor invasion.

More recently, digital image analysis methods that assess tumor infiltration objectively have been developed (21). For example, Nystrom and colleagues analyzed the degree of invasion by generating an "Invasion Index" which was the product of the depth of invasion, and the number and area of invading tumor islands (21); such methods give an accurate representation of tumor invasiveness and are also applicable to analyzing tumor invasion *in vivo*.

4. Notes

1. Cells transfected with a marker plasmid (e.g., GFP) can be observed under a fluorescence microscope. If a time-lapse microscope is used, particular attention should be paid to the

growth medium if the stage incubator is equipped with a temperature control only, in which case cells should be kept in CO_2-independent (HEPES-buffered) medium (19).

2. Critical step: particular care should be taken when raising the gels onto the steel grids to avoid misorientation and destruction of the gel.
3. Note that it is this initial time point that is defined as day 1 of the organotypic culture.

References

1. Shaw, L. M. (2005) Tumour cell invasion assays. *Methods Mol. Biol.* **294**, 97–105.
2. Brown, N. S. & Bicknell, R. (2001) *Cell Migration and the Boyden Chamber,* Totowa, New Jersey, Humana Press Inc.
3. Iwamoto, Y. & Sugioka, Y. (1992) Use of a reconstituted basement membrane to study the invasiveness of tumour cells. *Adv. Exp. Med. Biol.* **324**, 141–149.
4. Grotendorst, G. R. (1987) Spectrophotometric assay for the quantitation of cell migration in the Boyden chamber chemotaxis assay. *Methods Enzymol.* **147**, 144–152.
5. Terranova, V. P., Hujanen, E. S., Loeb, D. M., Martin, G. R., Thornburg, L. & Glushko, V. (1986) Use of a reconstituted basement membrane to measure cell invasiveness and select for highly invasive tumour cells. *Proc. Natl. Acad. Sci. U.S.A.* **83**, 465–469.
6. Saito, K., Oku, T., Ata, N., Miyashiro, H., Hattori, M., & Saiki, I. (1997) A modified and convenient method for assessing tumour cell invasion and migration and its application to screening for inhibitors. *Biol. Pharm. Bull.* **20**, 345–348.
7. Albini, A. (1998) Tumour and endothelial cell invasion of basement membranes. The Matrigel chemoinvasion assay as a tool for dissecting molecular mechanisms. *Pathol. Oncol. Res.* **4**, 230–241.
8. Thomas, G. J., Lewis, M. P., Hart, I. R., Marshall, J. F., & Speight, P. M. (2001). Alphavbeta6 integrin promotes invasion of squamous carcinoma cells through upregulation of matrix metalloproteinase-9. *Int. J. Cancer* **92**, 641–650.
9. Kleinman, H. K., McGarvey, M. L., Liota, L. A., Robey, P. G., Martin, G. R. (1982). Isolation and characterization of type IV collagen, laminin and heparan sulfate proteoglycan from the EHS sarcoma. *Biochemistry*, **21**, 6188–6193.
10. Kleinman, H. K., Martin, G. R. (2005). Matrigel: basement membrane matrix with biological activity. *Semin. Cancer Biol.* **15**, 378–386.
11. Marsh D, Dickinson S, Neill GW, Marshall JF, IR Hart, Thomas GJ (2008). αvβ6 integrin promotes the invasion of morphoeic basal cell carcinoma through stromal modulation. *Cancer Res.* **68,** 3295–303.
12. De Wever, O., Nguyen, Q. D., Van Hoorde, L., Bracke, M., Bruyneel, E., Gespach, C. & Mareel, M. (2004). Tenascin-C and SF/HGF produced by myofibroblasts *in vitro* provide convergent pro-invasive signals to human colon cancer cells through RhoA and Rac. *FASEB J.* **18**, 1016–1018.
13. Lewis, M. P., Lygoe, K. A., Nystrom, M. L., Anderson, W. P., Speight, P. M., Marshall, J. F., & Thomas G. J. (2004) Tumour-derived TGF-beta1 modulates myofibroblast differentiation and promotes HGF/SF-dependent invasion of squamous carcinoma cells. *Br. J. Cancer*, **90**, 822–832.
14. Kim, J. B., Stein, R., & O'Hare, M. J. (2004) Three-dimensional in vitro tissue culture models of breast cancer – a review. *Breast Cancer Res. Treat.* **85**, 281–291.
15. Al-Batran, S. E., Astner, S. T., Supthut, M., Gamarra, F., Brueckner, K., Welsch, U., Knuechel, R. & Huber, R. M. (1999). Three-dimensional *in vitro* cocultivation of lung carcinoma cells with human bronchial organ culture as a model for bronchial carcinoma. *Am. J. Respir. Cell Mol. Biol.* **21**, 200–208.
16. Nystrom ML, McCullogh D, Weinreb P, Violette S, Speight PM, Marshall JF, Hart IR, Thomas GJ (2006). COX-2 inhibition suppresses αvβ6 integrin-dependent oral squamous carcinoma invasion. *Cancer Res.* **66,** 10833–42.
17. Froeling, F. E., Mirza, T. A., Feakins, R. M., Seedhar, A., Elia, G., Hart, I. R., Kocher, H. M. (2009) Organotypic culture model of pancreatic

cancer demonstrates that stromal cells modulate E-cadherin, beta-catenin and Ezrin expression in tumour cells. *Am. J. Pathol.* **175**, 636–648.

18. Boukamp, P., Breitkreutz, D., Stark, H. J. & Fusenig, N. E. (1990) Mesenchyme-mediated and endogenous regulation of growth and differentiation of human skin keratinocytes derived from different body sites. *Differentiation* **44**, 150–161.
19. Liang, C., Park A. Y., and Guan J. (2007) *In vitro* scratch assay: a convenient and inexpensive method for analysis of cell migration *in vitro*. *Nat. Prot.* **2**, 329–333.
20. Vial, E., Sahai, E., Marshall, C. J. (2003) ERK-MAPK signalling co-ordinately regulates activity of Rac1 and RhoA for tumour cell motility. *Cancer Cell* **4**, 67–79.
21. Nystrom, M. L., Thomas, G. J., Stone, M. L., Mackenzie, I. C., Marshall, J. F. (2005) Development of a quantitative method to analyse tumour cell invasion in organotypic culture. *J. Pathol.* **205**, 468–475.